UNIVERSITÉ D'AIX-MARSEILLE

ÉCOLE DOCTORALE DES SCIENCES DE LA VIE ET DE LA SANTÉ 62

Unité de recherche des maladies infectieuses et tropicales émergentes (URMITE)

Thèse présentée pour obtenir le grade universitaire de docteur

Discipline : Biologie

Spécialité : Biochimie structurale

Pauline JACQUET

Amélioration d'une enzyme hyperthermostable pour la dégradation des organophosphorés

---

Soutenue le 19/12/2017 devant le jury composé de :

Dr. Isabelle ANDRÉ	Rapporteur
Dr. Rachid BAATI	Rapporteur
Pr. Pierre DOUMENQ	Examinateur
Dr. David DAUDÉ	Examinateur
Pr. Éric CHABRIÈRE	Directeur de thèse

La science est surtout une prise de conscience de plus en plus complète de ce qui peut et doit être découvert.

Boris Vian

Remerciements

Je remercie chaleureusement toutes les personnes qui m'ont aidée et soutenue au cours de ma thèse.

Plus particulièrement, je remercie Eric Chabrière et David Daudé, pour m'avoir donné cette opportunité de thèse et de m'avoir fait confiance pour la réaliser.

Un énorme merci aussi à l'équipe pour l'aide au cours de ces années de thèse, avec l'excellente ambiance et leur présence au quotidien : Laure Plener, Benjamin Rémy (a.k.a. Dieu de la dance), Laetitia Poirier (et Gaston un peu quand même), Sonia Mion, Lucile Pinault, Magali Richez, Marielle Bedotto, Sylvain Buffet, Nicholas Armstrong et Philippe Decloquement.

Je remercie également Mikael Elias et Céline Bergonzi pour les travaux de cristallographie réalisés à Minneapolis et le formidable stage de cristallographie que j'ai fait avec eux.

Evidemment je tiens à remercie ma famille, mes parents Agnès et François, mes sœurs Émilie, Charlotte et Daphné, mes beaux-frères Matthieu et Alexis, mon neveu Gaspard ainsi que le reste de ma famille. Je ne les remercierai jamais assez de me supporter et surtout de leur soutien constant au fil des ans, ainsi que leurs incessantes questions au cours de ces trois ans : « et ta thèse, ça avance ? »… Merci !

De même, je remercie mes amies Florence et Anne pour leurs conseils et soutien.

Je remercie la DGA et l'AMU pour le financement de ma thèse.

Pour finir, je remercie les membres du jury d'avoir évalué avec objectivité mes travaux de thèse.

Publications

Revues

Jacquet P, Daudé D, Bzdrenga J, Masson P, Elias M, and Chabrière E. Current and emerging strategies for organophosphate decontamination: special focus on hyperstable enzymes. *Environmental Science and Pollution Research* 2016.

Bzdrenga J, Daudé D, Rémy B, **Jacquet P**, Plener L, Elias M, and Chabrière E. Biotechnological applications of quorum quenching enzymes. *Chemico-Biological Interactions* 2016.

Poirier L, **Jacquet P**, Elias M, Daudé D, and Chabrière E. La décontamination des organophosphorés : vers de nouvelles alternatives. *Annales Pharmaceutiques Françaises* 2017.

Articles

Jacquet P, Hiblot J, Daudé D, Bergonzi C, Gotthard G, Armstrong N, Chabrière E, and Elias M. Rational engineering of a native hyperthermostable lactonase into a broad spectrum phosphotriesterase. *Scientific Reports* 2017.

Poirier L, Brun L, **Jacquet P**, Lepolard C, Armstrong N, Torre C, Daudé D, Ghigo E, and Chabrière E. Enzymatic degradation of organophosphorus insecticides decreases toxicity in planarians and enhances survival. *Scientific Reports* 2017.

Guendouze A, Plener L, Bzdrenga J, **Jacquet P**, Rémy B, Elias M, Lavigne J-P, Daudé D, and Chabrière E. Effect of quorum quenching lactonase in clinical isolates of *Pseudomonas aeruginosa* and comparison with quorum sensing inhibitors. *Frontiers in Microbiology* 2017.

Article en préparation

Jacquet P, Daudé D, Bergonzi C, Chabrière E, and Elias M. Turning a promiscuous hyperthermostable lactonase into a proficient phosphotriesterase.

Posters

Jacquet P, Daudé D, Elias M, and Chabrière E. Structure-based approach for enzyme engineering against organophosphorus chemicals. *Congrès de l'Association Française de Cristallographie*, Marseille, July 4th-7th 2016.

Jacquet P, Daudé D, Elias M, and Chabrière E. Improvement of hyperthermostable enzyme for organophosphorus degradation by directed evolution. *25th Annual Meeting of Doctoral School*, Marseille, June 1st-2nd 2017.

Présentation orale

Jacquet P, Daudé D, Poirier L, Elias M, and Chabrière E. Improvement of hyperthermostable enzyme for external decontamination of organophosphorus chemicals. *The 2nd International Conference CBRNE*, Lyon, May 29th-June 1st 2017

Abréviations

5-FU : **5-f**luoro**u**racil

AChE : **A**cetyl**ch**olin**e**sterase

ACh : **A**cetyl**ch**oline

AHL : **A**cyl**h**omoserine **l**actone

AI : **A**uto**i**nducer

AIP : **A**uto**i**nducer **p**eptide

APR : **A**ncestral **p**rotein **r**econstruction

BChE : **B**utyryl**ch**olin**e**sterase

***Bd*PTE** : ***B**revundimonas **d**iminuta* **p**hospho**t**ri**e**sterase

CC : **C**losed **c**onformation

CWA : **C**hemical **w**arfare **a**gent

DOC : **D**e**o**xy**c**holic acid

DSF : **D**ifferential **s**canning **f**luorimetry

DSF : **D**iffusible **s**ignal **f**actor

GC/MS : **G**as **c**hromatography / **m**ass **s**pectrometry

***Hs*-AChE** : ***H**omo **s**apiens*-**a**cetyl**ch**olin**e**sterase

IAS : **I**nfections **a**ssociées aux **s**oins

IQS : **I**ntegrated **Q**S **s**ignal

NOEC : **N**o **o**bserved **e**ffect **c**oncentration

OC : **O**pen **c**onformation

OP : **O**rgano**p**hosphate

OPAA : **O**rgano**p**hosphate **a**cide **a**nhydrolase

OPH : **O**rgano**p**hosphate **h**ydrolase

PEG : **P**oly**e**thylene **g**lycol

PMSF : **P**henyl**m**ethyl**s**ulfonyl **f**luoride

***p*NP acetate** : ***para*-n**itro**p**henol **acetate**

PQS : ***P**seudomonas* **q**uinolone **s**ignal

PLL : **P**hosphotriesterase-**l**ike **l**actonase

PTE : **P**hospho**t**ries**t**erase

QQ : **Q**uorum **q**uenching

QS : **Q**uorum **s**ensing

QSI : **Q**uorum **s**ensing **i**nhibitor

rAChE : **r**ecombinant **a**cetyl**ch**olin**e**sterase

RI : Kovats **r**etention **i**ndex

SDS : **S**odium **d**odecyl **s**ulfate

SDS-PAGE : **S**odium **d**odecyl **s**ulfate-**p**oly**a**crylamide **g**el **e**lectrophoresis

***Smed*-AChE** : ***S**chmidtea **med**iterranea*-**a**cetyl**ch**olin**e**sterase

***Sso*Pox** : ***S**ulfolobus **so**lfataricus* **P**ara**ox**onase

$\mathbf{T_m}$: **M**elting **t**emperature

Sommaire

Abréviations 9

Introduction 15

I. Synthèse bibliographique 23

1. Décontamination des organophosphorés 23
2. Des enzymes pour bloquer la communication bactérienne 49

II. Projet de recherche 67

Objectifs de la thèse 67

Partie 1 : Ingénierie rationnelle d'une lactonase native hyperthermostable en phosphotriestérase à large spectre 71

1.1. Introduction 73

1.2. Results and Discussion 74

1.3. Materials and Methods 88

Partie 2 : Transformation d'une lactonase hyperthermostable en une phosphotriestérase hautement active 95

2.1. Introduction 97

2.2. Materials and methods 99

2.3. Results 102

2.4. Discussion 112

Partie 3 : La dégradation enzymatique des insecticides organophosphorés diminue la toxicité et améliore la régénération chez les planaires 117

3.1. Introduction 119

3.2. Results 120

3.3. Discussion 130

3.4. Materials and Methods 132

Partie 4 : Evaluation de l'efficacité du quorum quenching par une lactonase sur des isolats cliniques de *Pseudomonas aeruginosa* et comparaison avec des inhibiteurs du quorum sensing. 137

4.1. Introduction 138

4.2. Materials and Methods 139

4.3. Results 141

4.4. Discussion 147

III. Conclusions et perspectives 153

Conclusions 153

Perspectives 155

IV. Annexes 159

1. Données supplémentaires du projet de recherche 159

1.1. **Partie 1** : Ingénierie rationnelle d'une lactonase native hyperthermostable en phosphotriestérase à large spectre 159

1.2. **Partie 2** : Transformation d'une lactonase hyperthermostable en une phosphotriestérase hautement active 169

1.3. **Partie 3** : La dégradation enzymatique des insecticides organophosphorés diminue la toxicité et améliore la régénération chez les planaires 171

1.4. **Partie 4** : Evaluation de l'efficacité du quorum quenching par une lactonase sur des isolats cliniques de *Pseudomonas aeruginosa* et comparaison avec des inhibiteurs du quorum sensing 176

2. Publication annexe 185

V. Références 207

Introduction

Introduction

Les protéines sont des biomolécules naturelles présentes dans tous les organismes et assurant une multitude de fonctions, depuis la catalyse de réactions biochimiques, la régulation de l'expression génique, la constitution des membranes cellulaires ou des tissus et bien d'autres encore[1]. Parmi les protéines, les enzymes sont des catalyseurs biologiques qui permettent d'accélérer les réactions chimiques en diminuant l'énergie d'activation de la réaction[2]. Les contraintes imposées par l'environnement et la compétition entre les espèces ont permis de sélectionner, au cours du temps, les enzymes les plus efficaces en accumulant progressivement les mutations bénéfiques conférant un avantage sélectif (i.e. améliorant le succès reproducteur ou fitness). Au cours de l'évolution, de nouveaux biocatalyseurs ont divergés des enzymes originelles (ou ancestrales) pour catalyser plus spécifiquement une réaction d'intérêt. En parallèle de la réaction optimisée par évolution, des activités dites de promiscuité qui sont le plus souvent l'héritage de l'enzyme ancestrale, permettent à de nombreuses enzymes d'avoir une activité alternative ou de reconnaitre des substrats alternatifs[3]. Ces activités de promiscuité sont des phénomènes très répandus parmi les enzymes et peuvent constituer un avantage adaptatif pour l'évolution lorsque de nouvelles pressions de sélection apparaissent[4]. La promiscuité joue donc un rôle primordial dans les processus évolutifs et peut constituer des points de divergence pour l'apparition de nouvelles enzymes[1,4–6]. Si l'évolution est un processus lent à l'échelle humaine, il peut cependant être plus ou moins rapide en fonction de la pression de sélection et des espèces. Les contraintes environnementales et la compétition entre les espèces à reproduction rapide accélèrent le processus d'évolution. Par exemple, chez les bactéries ou les insectes des phénomènes de résistance pouvant impliquer des enzymes ont pu être observés suite à l'utilisation massive d'antibiotiques ou d'insecticides (e.g. β-lactamases pour les antibiotiques et phosphotriestérases pour les insecticides)[7]. Ainsi la diversité des enzymes associée à leur promiscuité catalytique joue le plus souvent un rôle important dans l'évolution des espèces.

Parmi les contraintes environnementales pouvant influencer les trajectoires évolutives, la température joue un rôle primordial sur les processus biologiques. En effet, ce facteur essentiel de l'environnement affecte l'ensemble des organismes vivants et les relations entre la température de croissance des organismes et les propriétés biophysiques de leurs enzymes (et des protéines en général) ont été particulièrement étudiées. Ainsi, les bactéries et les enzymes associées, peuvent être classées en fonction de la température optimale de croissance du microorganisme, classiquement : psychrophiles (-5 à 15°C), mésophiles (15 à 45°C), thermophiles (45 à 80°C), et hyperthermophiles (>80°C)[8]. De ce fait, les enzymes issues d'organismes thermophiles ou hyperthermophiles sont généralement thermostables et ont une stabilité intrinsèque bien plus grande que leurs équivalents mésophiles et psychrophiles. L'adaptation des enzymes à la température repose principalement sur la capacité des enzymes à maintenir leur repliement et l'organisation de leur site actif[9]. Les enzymes thermostables ont suscité un vif intérêt pour des applications biotechnologiques de par leur capacité à résister à de nombreuses contraintes physico-chimiques[10]. En effet, elles ont des avantages biotechnologiques prometteurs : ces enzymes sont compatibles avec les températures élevées utilisées dans les procédés industriels, elles ont une haute résistance aux agents dénaturants comme les solvants ou les détergents et elles supportent de plus hautes concentrations en substrat[11,12]. En outre, cette stabilité à la température confère des avantages pour des approches d'évolution par biologie moléculaire comme l'évolution dirigée qui consiste à reproduire en laboratoire et en accéléré

les processus d'évolution naturelle. Ces enzymes sont le plus souvent capables de tolérer un plus grand nombre de mutations avant la déstabilisation de leur structure[12].

Parmi les enzymes hyperthermostables avec une activité de promiscuité on retrouve les phosphotriesterase-like lactonases (PLLs). Ces dernières, ont été identifiées pour la première fois chez les archées hyperthermoacidophiles *Sulfolobus solfataricus* et *Sulfolobus acidocaldarius*[13,14]. Les PLLs sont des lactonases natives avec une activité de promiscuité phosphotriestérase. Ces enzymes sont étroitement liées aux phosphotriestérases (PTEs, EC 3.1.8.1), des enzymes bactériennes qui sont capables d'hydrolyser les organophosphorés (OPs). PLLs et PTEs partagent le même ancêtre commun mais elles ont divergé **(Figure 1A)** ; l'activité de promiscuité phosphotriestérase devenant ainsi l'activité majoritaire pour les PTEs avec des vitesses de dégradation des OPs approchant la limite de diffusion, montrant que les PTEs ont été parfaitement optimisées pour ce type de substrat. L'origine des PTEs a très certainement été causée par des mutations induites suite à une exposition prolongée aux OPs et constitue un formidable exemple d'évolution adaptative[15]. PLLs et PTEs appartiennent à la superfamille des amidohydrolases (EC 3.5.1 et 3.5.2). Leurs structures se caractérisent par une construction en tonneau $(\alpha/\beta)_8$ et un site actif pourvu de deux cations métalliques coordonnés par quatre histidines et impliqués dans la catalyse comme acide de Lewis, activant une molécule d'eau en anion hydroxyde qui va agir comme un nucléophile pour réagir avec le substrat **(Figure 1B** et **Figure 2A)**.

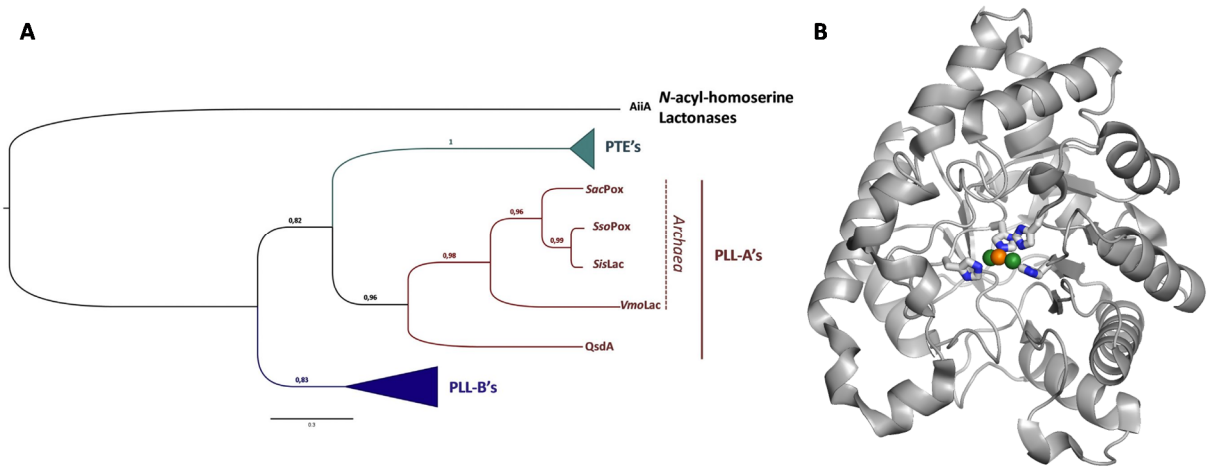


Figure 1 : Evolution et structure des PLLs.
(A) Arbre phylogénétique des PLLs (adapté de Bzdrenga (2016)[16]). **(B)** Structure de *Sso*Pox (PDB : 2VC5), la molécule d'eau catalytique est représentée par une sphère orange, les métaux par des sphères vertes et les quatre histidines sont représentées en sticks gris et bleus, le reste de la structure est en représentation cartoon (image réalisée sur PyMOL[17]).

Les PLLs sont composées de deux sous-familles, PLL-A et PLL-B. Les PLL-A sont capables de dégrader les acylhomosérines lactones (AHLs) et les oxo-lactones, au contraire des PLL-B qui hydrolysent seulement les oxo-lactones **(Figure 2A)**[18,19]. La dégradation des AHLs a été particulièrement étudiée durant la dernière décennie car ces molécules sont synthétisées par les bactéries Gram négatif et sont impliquées dans un système de communication bactérien complexe mieux connu sous le nom de quorum sensing. Ces molécules permettent ainsi aux bactéries de se signaler les unes aux autres proportionnellement à la densité de population et induisent un changement de comportement global au-delà d'une certaine concentration. La communauté change alors de comportement pour adopter un mode de vie collectif. Dans certains cas, les bactéries peuvent adopter un état virulent associé à la sécrétion de nombreux facteurs (e.g. toxines, sidérophores, protéases) ou à la formation d'un biofilm, véritable barrière derrière laquelle les bactéries se protègent des agents antimicrobiens et du système immunitaire de l'hôte. L'activité phosphotriestérase, quant à elle, repose sur l'habilité à dégrader les organophosphorés qui sont des composés neurotoxiques utilisés comme pesticides et agents neurotoxiques de guerre **(Figure 2A)**. L'origine de la promiscuité entre l'activité phosphotriestérase et lactonase vient de la ressemblance géométrique entre la conformation des phosphotriesters et l'état de transition tétraédrique de l'hydrolyse des lactones, cette similarité serait aussi à l'origine de la divergence des PTEs **(Figure 2B)**[20]. La dégradation des OPs, qui sont capables de perturber le développement et le système nerveux central humain à de très faibles concentrations, constitue un enjeu sociétal et environnemental majeur.

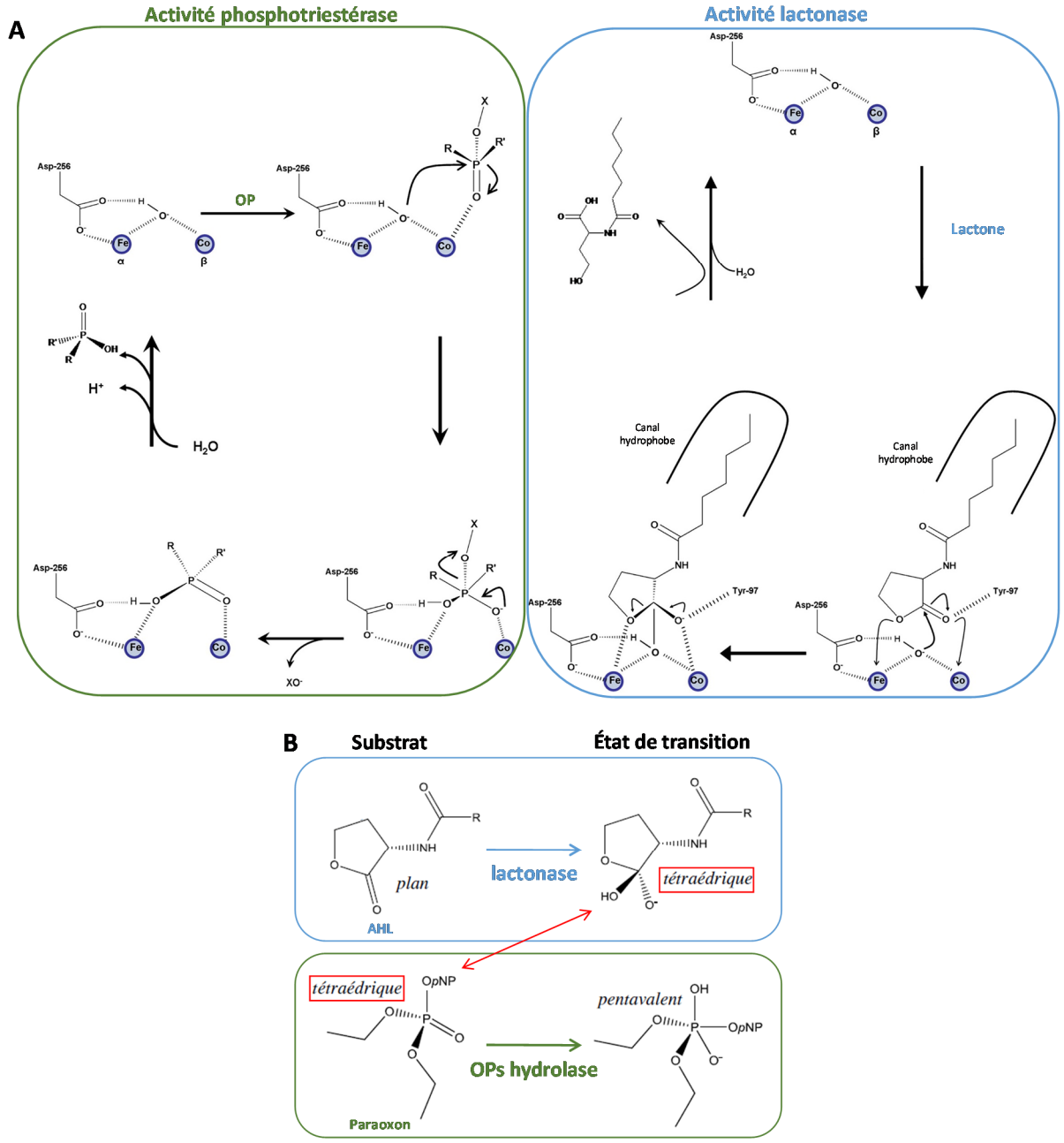


Figure 2 : Activités des PLLs.

(A) Mécanismes de réaction des activités phosphotriestérase et lactonase (adapté de Elias et al (2008)[18]). **(B)** Ressemblance géométrique entre l'état de transition de l'hydrolyse des lactones et la configuration des organophosphorés (adaptation à partir de Gotthard (2013)[20]).

Parmi les PLLs-A, l'enzyme hyperthermostable *Sso*Pox (*Sulfolobus solfataricus* Paraoxonase), issue de l'archée *Sulfolobus solfataricus* isolée des sources chaudes du Vésuve, est particulièrement intéressante de par ses doubles activité lactonase/phosphotriestérase et sa haute stabilité thermique (T_m=106°C)[18]. *Sso*Pox est efficace pour hydrolyser un certain nombre de lactones (k_{cat}/K_M~10^3-10^4 $M^{-1}.s^{-1}$ sur les C8-AHL et 3-oxo-C10-AHL notamment) et possède une activité de promiscuité phosphotriestérase moins développée (k_{cat}/K_M~10^2-10^3 $M^{-1}.s^{-1}$ sur éthyl-paraoxon et méthyl-paraoxon). L'enzyme sauvage est active sur une large gamme de pH de 5.0 à 9.0 et son activité peut

être accrue en présence de certains détergents comme le dodécylsulfate de sodium (SDS) ou le désoxycholate de sodium (DOC)[21–23].

Les enzymes thermostables étant généralement de bons candidats pour l'évolution en laboratoire, des stratégies de mutagénèse ont été considérées et ont permis d'améliorer ses performances pour des applications industrielles. Le variant *Sso*Pox-W263I montrant des propriétés biotechnologiques extrêmement intéressantes a ainsi été obtenu. Ses activités lactonase et phosphotriestérase sont améliorées (k_{cat}/K_M~10^3 $M^{-1}.s^{-1}$ sur l'éthyl-paraoxon et ~10^5 $M^{-1}.s^{-1}$ sur le 3-oxo-C12-AHL), il est capable de résister à de hautes températures (jusqu'à 150°C pour l'enzyme lyophilisée), au contact avec des solvants organiques (comme l'acétone, le chloroforme, le toluène, l'éther diéthylique,…), à la stérilisation (autoclave, oxyde d'éthylène et radiations β), au stockage (l'enzyme reste active pendant au moins 9 mois) et à l'immobilisation (réticulation avec du glutaraldéhyde dans des billes d'alginate)[10]. De plus, contrairement au dogme affirmant que les enzymes thermostables ne sont pas actives à basse température, *Sso*Pox-W263I conserve une activité très significative à -18°C. L'ensemble de ses impressionnantes capacités démontre bien que *Sso*Pox est un outil biotechnologique avec un énorme potentiel pour un vaste champ d'applications allant de la décontamination des composés organophosphorés à l'inhibition de la virulence bactérienne. Ces propriétés font également de *Sso*Pox une excellente base pour de l'évolution dirigée afin d'obtenir des variants améliorés plus diversifiés, par exemple sur l'hydrolyse des lactones ou encore des organophosphorés.

Fort des résultats obtenus par le laboratoire pour l'amélioration de l'activité lactonase de *Sso*Pox, l'objectif de ma thèse a consisté à améliorer les performances de l'enzyme *Sso*Pox par évolution dirigée, plus particulièrement son activité phosphotriestérase pour la dégradation des composés organophosphorés, insecticides et agents neurotoxiques de guerre. Dans un premier temps, un état de l'art exhaustif répertoriant les différentes stratégies de décontamination des OPs avec une emphase particulière sur les méthodes enzymatiques a été réalisé. Compte tenu des nombreuses propriétés de l'enzyme, un deuxième travail bibliographique a permis de dresser un bilan des différentes perspectives liées à la perturbation du quorum sensing grâce à son activité lactonase. Dans un deuxième temps, les résultats majeurs obtenus pour l'amélioration de l'activité phosphotriestérase de *Sso*Pox à travers deux stratégies d'évolution sont reportés dans les deux premières parties. Par la suite, un variant amélioré de *Sso*Pox pour la décontamination d'insecticides obtenu par la première stratégie a été plus particulièrement étudié et l'impact de la dégradation enzymatique a été évaluée sur un modèle *in vivo* original : la planaire. Ces résultats sont reportés dans une troisième partie. Pour finir, le potentiel du variant *Sso*Pox-W263I, pour l'inhibition de la communication bactérienne chez des souches cliniques a été évalué et les résultats sont reportés dans une quatrième, et dernière, partie.

I. Synthèse bibliographique

1. Décontamination des organophosphorés

I. Synthèse bibliographique

1. Décontamination des organophosphorés

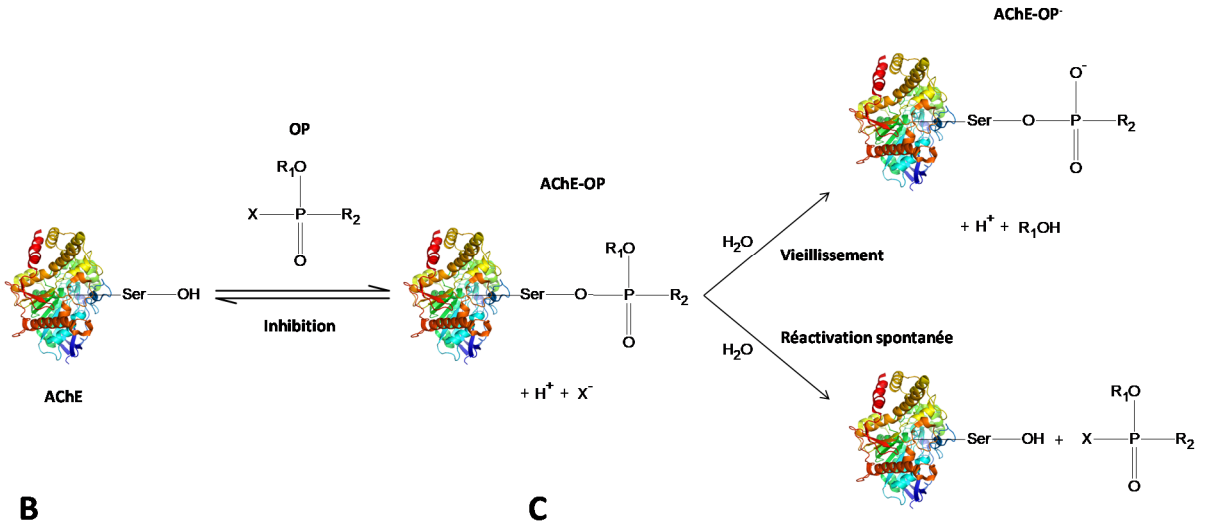
Les organophosphorés (OPs) sont des composés créés au milieu du XIXème siècle. En 1848 Voegeli produit le premier acide phosphorique d'ester : le triéthyl phosphate[24]. Quelques années plus tard, en 1854, le tetraéthylpyrophosphate est synthétisé par De Clermont et Moschnin. Ce composé est le premier organophosphoré avec un effet inhibiteur pour les cholinestérases[24]. Ces découvertes marquent l'accélération du développement des organophosphorés, ils seront d'abord optimisés comme pesticides ; puis rapidement, au vu de leur haute toxicité, comme agents neurotoxiques de guerre (Chemical warfare agents, CWAs)[25]. De 1934 à 1944, un chimiste allemand Schrader et ses collaborateurs travaillant dans la société I. G. Farben ont synthétisé plus de 2 000 organophosphorés incluant le parathion comme pesticide et le tabun, le sarin et le soman comme agents neurotoxiques de guerre. Bien que développés, en partie, pendant la seconde guerre mondiale, les agents neurotoxiques de guerre ont été utilisés principalement à partir de l'après-guerre, par exemple avec l'utilisation du sarin et du tabun pendant la guerre Iran-Irak (1980-1988)[26]. En 1993, les CWAs ont été classés comme arme de destruction massive dans un traité signé par plus de 200 pays (UN Resolution 678)[27]. Cependant, leur utilisation reste encore d'actualité, notamment avec l'emploi du sarin lors des attentats de Matsumoto et Tokyo (1994-1995), ou encore l'utilisation du sarin en Syrie (en 2013 et 2017) et récemment, début 2017, avec l'utilisation du VX pour l'assassinat de Kim Jong-nam[26]. Les pesticides de type OPs ont largement été employés dans l'agriculture, par exemple aux États-Unis en 1990 ils représentaient 70% des pesticides utilisés toute utilisation confondue. En raison de leur toxicité leur utilisation a fortement diminué mais représentait toujours 35% des pesticides utilisés aux États-Unis en 2007 (« Pesticides industry sales and usage », 2006 and 2007, United States Environmental Protection Agency). De nos jours, les OPs restent encore les insecticides les plus utilisés dans le monde, comme le chlorpyrifos encore utilisé en Europe (Reg. (EU) No 762/2013), ils ont une large gamme d'emploi de nématocides, acaricides à fongicides[26]. En parallèle, de manière anecdotique, les OPs sont aussi utilisés comme additifs au niveau des fluides hydrauliques et des huiles moteurs dans les systèmes hydrauliques des avions, en raison de leurs propriétés anti-usure, lubrifiante, anticorrosion et ignifuge (tricresyl phosphate, tributyl phosphate, triphenyl phosphate…)[28,29].

Suite au bannissement des insecticides organochlorés dans les années 70, l'utilisation des OPs a explosé. Ainsi, à cause de leur forte utilisation comme pesticides, les OPs sont responsables de nombreuses pollutions environnementales (des eaux et des sols) et d'intoxication chaque année. En effet, environ 3 millions d'intoxications sont reportées annuellement, dues à une exposition accidentelle ou intentionnelle, 20% de ces intoxications vont mener à une issue fatale[26]. L'importante toxicité des OPs vient du fait qu'ils sont des inhibiteurs de l'acétylcholinestérase (AChE, EC 3.1.1.7) humaine, une enzyme clé du système nerveux central[30,31]. L'AChE est une sérine hydrolase, elle permet de terminer les signaux synaptiques en hydrolysant l'acétylcholine (ACh), le neurotransmetteur. L'AChE se compose d'une triade catalytique (Ser200, His440 et Glu327) ainsi qu'un trou oxyanion (groupes NH de Gly118, Gly119, et Ala201), des éléments caractéristiques des sérines hydrolases[32,33]. L'hydrolyse de l'ACh est initiée par une attaque nucléophile du résidu Ser200 sur le carbonyle de l'ACh, s'en suit une succession d'acylation et de désacylation[30,32,34]. Le résidu catalytique (Ser200) est crucial

pour le mécanisme catalytique, cependant ce résidu est aussi réactif envers des inhibiteurs covalents tels que les pesticides et les CWAs[27,35,36].

Ces inhibiteurs agissent par phosphylation au niveau de la sérine catalytique (Ser200), bloquant ainsi l'hydrolyse de l'ACh. Les produits phosphylés vont soit se réactiver spontanément (ou par l'utilisation de réactivateurs tels que les oximes), soit se désalkyler (processus de « vieillissement ») résultant sur un complexe enzyme-OP impossible à réactiver. Ce processus de « vieillissement » est plus ou moins rapide en fonction de l'inhibiteur[27,34,37] **(Figure 3A et 3B)**. Cette inhibition de l'AChE conduit à une accumulation de l'ACh au niveau de la fente synaptique, entrainant une hyperstimulation des récepteurs muscariniques et nicotiniques[27,38]. Cela affecte le système cholinergique, qui englobe le système nerveux central et végétatif. Ainsi, les intoxications aux OPs vont être responsables d'un large spectre de signes cliniques **(Figure 3C)**.

A



B

CWA	Soman	Sarin	Tabun	VX
Temps d'apparition du vieillissement	Quelques minutes	5-6 heures	> 46 heures	> 48 heures

C

Symptômes	Intoxication aux OPs
Miosis / Larmoiement	Légère
Fasciculations locales	Légère
Hypersalivation / Sudation	Légère
Nausée	Légère
Vomissement / Défécation / Miction	Modérée
Bronchoconstriction / Bronchorrhée	Modérée
Bradycardie	Modérée
Détresse respiratoire	Modérée
Arythmie / Insuffisance veineuse	Aigüe
Convulsions	Aigüe
Coma / Arrêt respiratoire / Mort	Aigüe

Figure 3 : Intoxication aux OPs.
(A) Mécanisme d'inhibition de l'AChE par un OP. **(B)** Délai d'apparition du phénomène de « vieillissement » pour différents CWAs (adapté de Vonescha et al, 2011[39]). **(C)** Symptômes possibles après intoxication aux OPs (adapté de Worek et al, 2016[25]).

En cas d'intoxication aux OPs, des contre-mesures médicales existent telles que l'utilisation de réactivateurs permettant de réactiver l'AChE inhibée avant « vieillissement », les principaux réactivateurs sont les oximes (comme la pralidoxime et l'asoxime)[39–41]. En prévention d'une intoxication, des techniques de prophylaxie existent également telles que les biocatalyseurs stœchiométriques l'AChE et la butyrylcholinestérase (BChE) qui sont les plus étudiés[42,43]. L'efficacité

de l’ensemble de ces techniques reste cependant modérée d'où la nécessité de mettre au point des techniques de décontamination externe pour limiter l’intoxication. Ainsi, la décontamination externe des OPs est un enjeu majeur à bien des niveaux ; environnemental, agroalimentaire, ou encore militaire. Des méthodes de décontamination existent mais elles ne sont pas totalement satisfaisantes, c’est pourquoi les méthodes émergentes ont un fort potentiel.

Ces recherches ont fait l’objet d’une revue sur les méthodes actuelles et émergentes de décontamination. Cette revue regroupe les principales méthodes pour la décontamination externe des OPs avec un focus tout particulier porté sur les enzymes. Actuellement différents types de décontamination externe existent : à grande échelle, à l’échelle individuelle et pour la destruction des stocks. Ces méthodes sont efficaces mais elles ne sont pas polyvalentes, pour certaines agressives et responsables de pollutions secondaires. Parmi les méthodes émergentes, l'utilisation de cyclodextrines s'avère particulièrement douce mais leur mode d’action stœchiométrique limite leur efficacité. D'autres stratégies, telles que les méthodes photochimiques sont quant à elles compatibles avec une utilisation au niveau des sols, des eaux ou encore des atmosphères contaminées. Cependant l’efficacité de ces méthodes est extrêmement variable et dépend de nombreux paramètres (comme la concentration des contaminants présents au niveau des zones à décontaminer).

Pour pallier aux limitations des méthodes précédemment citées, des biocatalyseurs comme les enzymes constituent une alternative polyvalente, efficace et douce. Ces dernières années des biocatalyseurs, extrêmement efficaces pour la dégradation des OPs, ont été intensivement explorés. En effet, de nombreuses enzymes sont capables d’hydrolyser efficacement les OPs. Parmi ces dernières, un biocatalyseur prometteur, l’enzyme hyperthermostable *Sso*Pox s’avère particulièrement intéressante pour des applications de décontamination externe grâce à ses propriétés catalytiques et son impressionnante stabilité qui la rend compatible avec une utilisation industrielle.

J'ai participé activement à la réalisation de cette synthèse bibliographique, depuis sa structuration, la rédaction de la partie sur les méthodes émergentes, la création de figures, mais également les processus de dépôt et de révision.

Environ Sci Pollut Res
DOI 10.1007/s11356-016-6143-1

Current and emerging strategies for organophosphate decontamination: special focus on hyperstable enzymes

Pauline Jacquet[1] · **David Daudé**[2] · **Janek Bzdrenga**[1] · **Patrick Masson**[3] · **Mikael Elias**[4] · **Eric Chabrière**[1]

Received: 1 July 2015 / Accepted: 20 January 2016
© Springer-Verlag Berlin Heidelberg 2016

Abstract Organophosphorus chemicals are highly toxic molecules mainly used as pesticides. Some of them are banned warfare nerve agents. These compounds are covalent inhibitors of acetylcholinesterase, a key enzyme in central and peripheral nervous systems. Numerous approaches, including chemical, physical, and biological decontamination, have been considered for developing decontamination methods against organophosphates (OPs). This work is an overview of both validated and emerging strategies for the protection against OP pollution with special attention to the use of decontaminating enzymes. Considerable efforts have been dedicated during the past decades to the development of efficient OP degrading biocatalysts. Among these, the promising biocatalyst *Sso*Pox isolated from the archaeon *Sulfolobus solfataricus* is emphasized in the light of recently published results. This hyperthermostable enzyme appears to be particularly attractive for external decontamination purposes with regard to both its catalytic and stability properties.

Responsible editor: Philippe Garrigues

Pauline Jacquet and David Daudé contributed equally to this work.

✉ Eric Chabrière
eric.chabriere@univ-amu.fr

[1] Aix Marseille Université, URMITE, UM63, CNRS 7278, IRD 198, INSERM 1095, Marseille, France

[2] Gene&GreenTK, Faculté de Médecine, 27 boulevard Jean Moulin, Cedex 5, Marseille 13385, France

[3] Neuropharmacology Laboratory, Kazan Federal University, Kazan 420008, Russia

[4] Department of Biochemistry, Molecular Biology and Biophysics & Biotechnology Institute, University of Minnesota, St. Paul, MN 55108, USA

Keywords Bioremediation · Phosphotriesterase · Organophosphorus · Pesticide · Chemical warfare agent · SsoPox · Enzyme · Decontamination

Introduction

Man-made organophosphorus compounds (OPs) are highly-toxic chemicals that were produced as chemical warfare nerve agents (CWNAs) to harm, kill, or neutralize the opponent in a war strategy. The first massive production of OPs was developed by German scientists before and during the 2nd world war, with several molecules, dubbed agents G (for Germany), such as tabun (in 1936), sarin (in 1937), and soman (in 1944; Szinicz 2005). After the 2nd world war, other toxic molecules, dubbed agents V (for Victory, Venomous, or Viscuous), were developed by other nations, such as VX (USA), RVX (Russia), or CVX (China; Fig. 1). Massive stocks of these compounds had been accumulated during the cold war (Gupta 2009). In 1993, the international convention, signed by some 200 countries, called for the arrested development of these chemical weapons, and planned for the destruction of existing stocks before 2007 (Organisation for the Prohibition of Chemical Weapons 2005; Gupta 2009). Large stocks, however, still exist today, partly because of the lack of low-cost, rapid, environmental friendly and safe solutions to destroy these chemicals. Additionally, such nerve agents (e.g., sarin) have been used during terrorist attacks in Matsumoto and Tokyo subway (Japan) in 1994 and 1995. Furthermore, organophosphate-based pesticides also constitute a serious threat as they are both highly toxic and widespread and could be fraudulently used for terrorist attacks or asymmetric conflicts.

OP compounds, and particularly V-agent derivatives, were also commercialized as insecticides, during the

Published online: 02 February 2016

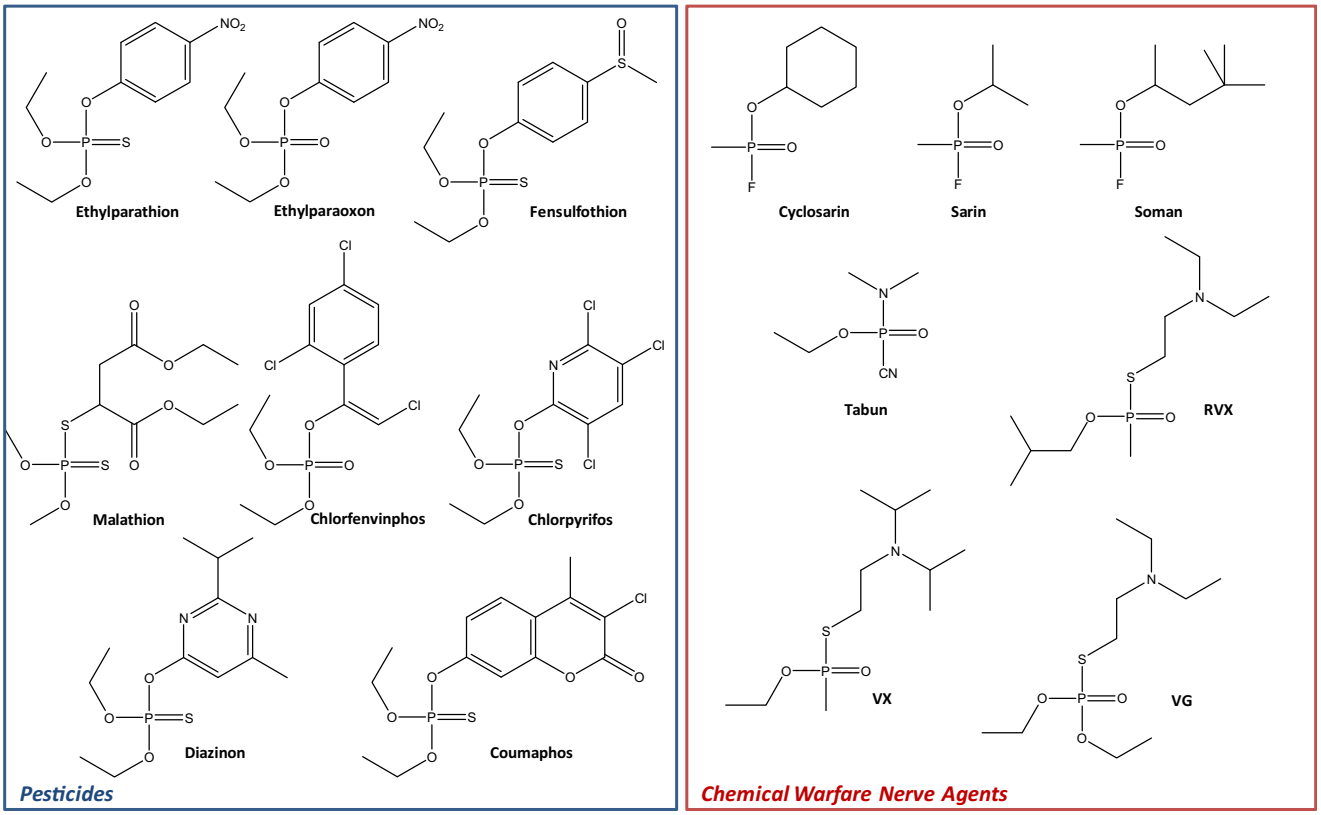


Fig. 1 Chemical structures of main organophosphate pesticides and chemical warfare nerve agents

1950s. They progressively replaced the insecticide Dichlorodiphenyltrichloroethane (DDT), an organochlorine banned in the 1970s. Being less persistent in the environment than DDT, the use of OPs have, nevertheless, been restricted in Europe and USA. However, they remain massively used in other parts of the world in intensive agriculture. The most commonly used OP insecticides are malathion, ethyl- or methylparathion, and chlorpyrifos (Fig. 1). OPs comprise major environmental (soils and water) pollutants (Jaipieam et al. 2009), and their use is estimated to lead to 3 million intoxications, yielding to 300,000 deaths in the world every year, the main part of these being ascribable to suicides due to deliberate ingestion of pesticides (Gunnell et al. 2007; Patel et al. 2012).

The extreme toxicity of OPs stems from their ability to irreversibly inhibit acetylcholinesterase (AChE), a key enzyme in the nervous system. Indeed, AChE terminates the degradation of the neurotransmitter acetylcholine in synaptic clefts and neuromuscular junctions. When AChE is inhibited, acetylcholine accumulates and saturates the cholinergic receptors. Acute intoxication by OPs results in apparition of various symptoms, abbreviated SLUDGEM, for salivation, lacrimation, urination, diaphoresis, gastrointestinal upset, emesis, and miosis (Zwiener and Ginsburg 1988; Lessenger and Reese 1999). Mechanistically, OPs react with the catalytic serine (Ser 200) of Human AChE, via phosphylation, forming a covalent phosphoenzyme (Beauregard et al. 1981). This OP-AChE intermediate can subsequently, depending on the OP nature, undergo an aging process (i.e., dealkylation occurs on the adduct). This process prevents reactivation of the phosphoenzyme. The aging kinetics is a very important parameter to account for while treating OP poisoning.

Due to the health threat presented by OPs both from acute and chronic intoxications, special attention has been dedicated to the development of decontamination strategies. Ideally, a decontamination solution would offer high efficiency, broad spectrum of action, smooth utilization compatible with skin or material treatment, no environmental impact, no secondary contamination, and low price. Hereafter is presented an overview of both current and emerging decontamination methods either physical, chemical, or biological. Their respective characteristics are summarized, and further developments and future perspectives are discussed.

Existing methods for decontamination of OP intoxications

Current methods of decontaminating pesticides and CWNAs can be separated into three categories:

(i) Physical decontamination: It encompasses all passive methods aimed at removing the contaminating agent

from any given surface, be it biotic or abiotic. It relies on mechanical action to absorb, remove, or flush the agent away, but does not usually destroy it.

(ii) Chemical decontamination: It refers to any given method that allows neutralization of the agent by chemical reactions, such as: hydrolysis, oxidation, or reduction.

(iii) Enzymatic decontamination: This method relates to the use of enzymes that are capable of hydrolyzing pesticides or CWNAs.

A possibly ideal decontamination device would use several methods that belong to the aforementioned categories, allowing for a surface cleaning combined with a rapid, efficient neutralization and/or destruction of the contaminating agent, thus, maximizing the effects and reducing the health and environmental hazards.

Large-scale decontamination

Large-scale decontamination is performed on surfaces after a massive OP exposure. The objectives are both to eliminate the contamination in situ as well as to reduce the potential of cross contamination, for example between the victim and the treating personnel. Currently available techniques are well suited for material decontamination; however, they often are aggressive and lack the ability to be fully safe for treating the victims. The solutions presented here are a non-exhaustive panel of available solutions.

– Hypochlorite

  Decontamination with a sodium hypochlorite solution may be used at the concentration of 0.5 % for personnel and 5 % for equipment (Tuorinsky et al. 2009). This solution proves to be useful both at removing the nerve agent from the surface and neutralizing it by oxidation. Be it for material and personnel, this method is still quite aggressive, due to its strong corroding potential towards eyes, skin, open wounds, and materials.

– Sodium hydroxide

  Sodium hydroxide is used to perform alkaline hydrolysis of OPs by a nucleophilic attack of the hydroxide ion on the phosphorus atom of OPs. It allows for the degradation of large amounts of nerve agents into their corresponding, non-toxic phosphonic acid.
  Combination of both aforementioned products, called super tropical bleach with 93 % calcium hypochlorite and 7 % sodium hydroxide, is used with high efficiency for material decontamination, with hypochlorite ion acting as a catalyst in the hydrolysis reaction (Singh et al. 2010). However, this method is highly corrosive and may neither be used for sensitive material nor personnel decontamination.

– DS2

  DS2 or "Decontamination solution 2" is used for material decontamination. It contains 70 % diethylenetriamine (DETA), 28 % 2-methoxyethanol, and 2 % sodium hydroxide. The active ingredient, 2-methoxyethanol, is highly effective against sulfur mustard and acts by elimination reaction, thus, forming divinyl sulfide. The mode of action against CWNAs is somewhat different as 2-methoxyethanol acts as a nucleophile and reacts with G- and V-agents (Singh et al. 2010). However, it is toxic and aggressive to treated surfaces as it even tends to degrade paints (Fielding 1964; Firmin 2003).

– BX-24 and BX-29

  These decontamination solutions, used in NATO forces, act by oxidation and hydrolysis. Personnel decontamination solution is composed of amphoteric compounds, amides, and a surfactant. It is advertised to be a safe decontamination solution. The BX-24 is a non-corrosive product designed for material decontamination.

– Decontamination formulation DF-200

  This product is used as foam in order to decontaminate toxic chemical warfare material. An enhancement over the previous DF-100 product, DF-200 is composed of nucleophilic compounds and oxidizing products, a bleaching activator, a sorbent, and an inorganic base, dissolved in water. It is in three distinct parts to be mixed together prior to use, with part one being a proprietary mix of quaternary ammonium compounds and surfactants, part two is composed of 8 % hydrogen peroxide, and part three is composed of glycerol diacetate, which catalyzes the oxidation process (Tucker and Comstock 2004; Tucker and Engler 2005; Tucker 2014). It is active against G- and V-agents with a 99 % decontamination of the treated surface after 30 min (Tucker 2014). The fact that this product is divided into three parts might cause logistical difficulties on the onset of a massive event.

Personal-scale decontamination

The kinetics of nerve agent penetration in the body is so fast that decontamination and treatment have to be performed on site and as soon as possible, at the individual level. Indeed, transportation time to proper medical facilities without prior application of topical solutions would greatly reduce the

chances of a patient's survival and would threaten medical personnel by spreading secondary contaminations. Currently available methods dealing with nerve agent exposure rely on external decontamination followed by medical treatment of the personnel exposed.

Ready-to-use kits for personal decontamination are primarily used by armies around the world. They have to comply with operational requirements and find the best trade-off in terms of size, weight, easiness of use, and of course efficiency.

– M291 SDK (Skin Decontamination Kit)

  Adopted by US Army in 1989, the M291 SDK is a ready-to-use, non-woven fiber pad, filled with an absorbent and a resin. The absorbent is a high-contact surface carbonaceous compound, in order to remove the agent from the skin. The resin itself is composed of two ion exchange resins, an anionic and a cationic one, able to neutralize the contaminant through hydrolysis (Khan et al. 2013). This technology was in use by the US Army until its progressive replacement by the Reactive Skin Decontamination Lotion (RSDL) around 2007. Its efficacy is very low on VX and very limited against soman as compared to other decontamination methods, such as 1 % soapy water and 0.5 % bleach (Braue Jr. et al. 2010a, b). It is not suitable for eye and wound decontamination.

– RSDL (Reactive Skin Decontamination Lotion)

  The RSDL is the current solution provided to soldiers and civilian security personnel in order to deal with topical exposure to OPs. It consists of an individually packed sponge, impregnated with a solution containing Diacetylmonoxime (DAM) and Dekon 139—a proprietary mix—dissolved in polyethylene glycol monomethyl ether (Bannard et al. 1991). This formulation allows for desorption of the agent from the skin and its chemical degradation via a nucleophilic reaction. The time required to achieve decontamination is less than 3 min for G- and V-agents (Elsinghorst et al. 2015). Its efficacy outperforms the one of M291 towards agents such as VX and soman (Braue Jr. et al. 2010a, b). The protective ratio (defined as the ratio between the LD_{50} of treated versus untreated group) of RSDL on guinea pigs is about 60 times higher than the one of M291 against VX (66.4 and 1.1, respectively; Braue Jr. et al. 2010a). Regarding soman, the protective ratio of RSDL still is five times better than the one of M291 (14 and 2.7, respectively; Braue Jr. et al. 2010b). The RSDL is efficient at decontaminating the skin as long as it is applied within minutes post-exposure. Like the M291 SDK, RSDL is not compatible with eye and wound cleaning.

– Fuller's earth

  Used by several NATO countries, pads impregnated with Fuller's earth purely rely on a physical and passive absorbance of the contaminating OP. It is mainly composed of fine aluminum silicate powder that confers a high-surface area, allowing for a good topical absorbance of contaminants (Taysse et al. 2007). The major drawback of using such a pad comes from the generation of contaminated dusts presenting an inhalation hazard.

  There is a current lack of non-corrosive solutions that would prove to be adequate both for sensitive material and personnel decontamination. Indeed, oxidative and corrosive solutions for decontamination are harmful and destructive to most military and civilian equipment and basic supplies. They may eliminate the threat of CWNAs but will leave behind a chemical contamination that is disastrous. Moreover, it should be noted that personnel decontamination using surfactant containing solutions (i.e., soapy water) represents a risk of spreading the agent over a wider skin surface. Even though it helps solubilize the chemicals, it may negatively affect the very aim of decontamination. It is, thus, of uttermost importance to opt for methods enabling sequestration and/or swift destruction of said nerve agents.

Stockpile destruction

In order to comply the Chemical Weapon Convention, the means of disposal were studied that could lead to destruction of stockpiles without harmful effect on environment and associated health hazards, as previous dumping at sea and burying method were problematic (US National Research Council 1996). It encompasses large hydrolysis systems and incineration used by western countries. Russia uses another method for destruction of G-agents, relying on neutralization followed by bitumination (Pearson and Magee 2002).

– Incineration

  The destruction by two-stage incineration is a process in use since the 1980s for the destruction of CWNA ammunitions, bulk agents, effluents, and equipment associated with stockpile disposal (US National Research Council 1994). First stage allows for the pulverization of the liquid agents and their heating to 1,480 °C. The subsequent gases serve as a fuel for processing by the second stage, an afterburner maintained at a lower, 1,100 °C temperature (English II 1974; Pearson and Magee 2002). The incinerator is equipped with a pollution abatement system that mixes the gases with sodium hydroxide and water to

remove acid gases and particles to reach safe standards (Pearson and Magee 2002).

– Hydrolysis

OPs are hydrolyzed using sodium hydroxide. However, the way hydrolysis is performed depends on the nature of the agent. While G-agents can be hydrolyzed safely at ambient temperature, VX hydrolysis has to be performed at 90 °C, temperature at which P–S hydrolysis is favored over P–O bond (Yang 1999; Pearson and Magee 2002; Kim et al. 2011).

– Neutralization–bitumination

Mainly used by Russia, neutralization–bitumination is a two-stage method that allows for the destruction of G-nerve agents. CWNAs are first mixed with 80 % monoethanolamine for 1 h at 110 °C (neutralization), followed by a reaction with bitumen and calcium hydroxide for 1 h at 200 °C (bitumination). Russian VX (RVX) is disposed of by a reaction with potassium isobutylate dissolved in isobutanol and *N*-methylpyrrolidinone. This solution is heated at 95 °C for 30 min before being added in bitumen (Pearson and Magee 2002).

Emerging chemical and physical alternatives for OPs decontamination

Cyclodextrins (CDs)

CDs are cyclic oligosaccharides composed of six to eight D-glucopyranoside units. They form a hydrophobic cavity able to host hydrophobic and apolar molecules (Sambrook and Notman 2013). This biomimetic catalysis capacity allows CDs to scavenge OPs.

Native CDs (α-CD, β-CD, and γ-CD) were first demonstrated to inactivate CWNAs. Among these, β-CD was shown to be the most efficient (Désiré and Saint-André 1986; Désiré and Saint-André 1987). Then, starting from β-CD as a precursor, substituted CDs such as iodosobenzoate-β-CD (IBA-β-CD) were developed and showed the ability to hydrolyze pesticides and CWNAs (Hoskin et al. 1999). The importance of the presence of an α-nucleophile such as IBA was underlined (Masurier et al. 2005; Wille et al. 2009; Müller et al. 2011; Rougier et al. 2011). Other derivatives were synthesized such as O-benzyl-β-CD, fully methylated β and α-CD (TRIMEB and TRIMEA, respectively), partially methylated β-CD (DIMEB), depicting a better solubility in water and organic solvents. CDs are promising compounds which could be used for skin, mucosa, wound, and also for material decontamination (Letort et al. 2015). Notwithstanding these benefits, some limitations have to be pointed out that circumvent the use of CDs, as a high-molecular weight (1, 134 $g.mol^{-1}$ for β-CD) and a low turnover. Additionally, none of the current CDs are able to degrade VX and possibly any OP containing a P–S bond due to the remarkable stability of such a linkage (Wille et al. 2009; Kalakuntla et al. 2013). Furthermore, *p*-nitrophenol (degradation product of paraoxon) inhibits the degradation process efficiency of paraoxon by β-CD (Masurier et al. 2005; Estour et al. 2013). Presumably, other OPs degradation products could lead to the same effect. Moreover, CDs rate for P–F degradation is very low (Hoskin et al. 1999).

Photochemical methods

Photochemical methods are based on light radiation to degrade OPs and organic substances in general. These methodologies have been well-reviewed elsewhere by Reddy and Kim (2015). Photochemical methods are part of advanced oxidation processes (AOPs), which use the high reactivity of HO radicals to degrade pollutants (Hossain et al. 2013). Briefly, photochemical-based techniques include five classes used for OPs degradation in soil, water, or air:

– Photolysis

Photolytic degradation of targeted compound consists in the absorption of radiation in both direct and indirect ways, leading to the destruction of the compound. Several examples of OP photolysis (diazinon, methylparathion, or quinalphos) have been reported to date in both direct (Wan et al. 1994; Sinderhauf and Schwack 2003; Gonçalves et al. 2006; Segal-Rosenheimer and Dubowski 2010; Muñoz et al. 2011) and indirect manner (Lam et al. 2003; Garbin et al. 2007).

– Photolysis with an oxidant

The association of classical photolysis with chemical oxidants like H_2O_2 and O_3 enhances the efficiency of the process and seems to prevent formation of unfavorable products (Wu and Linden 2010).

– Photo-Fenton method

This method involves photo-Fenton process, relying on the photoreduction of dissolved Fe(III) complexes into Fe(II) ions, followed by the Fenton reaction and the oxidation of organic compounds (Kim and Vogelpohl 1998; Ikehata and El-Din 2006).

– Photocatalysis

It refers to the photo-excitation of a semiconductor such as titanium dioxide (TiO_2), zinc oxide (ZnO), or tungsten trioxide (WO_3). Semiconductors are intermediates to reduction or oxidation of the OPs. This technique shows certain limits like electronic recombination (Balkaya 1999; Konstantinou et al. 2001; Jonidi-Jafari et al. 2004; Li et al. 2005; Evgenidou et al. 2006; Chen et al. 2011).

– Photosensitized-induced process

This process uses sensitizers able to absorb light radiation, then transfering the excess energy to a targeted compound. This technique is useful for OPs with a low absorption efficiency (Kamiya and Kameyama 2001; Nowakowska et al. 2005).

Photochemical methods have been mainly used for water decontamination (Reddy and Kim 2015). A few studies on air and solid surface decontamination of CWNAs have been reported to date (Zuo et al. 2007; Kim et al. 2007). Photochemical methods are easy to handle and rather inexpensive. However, the efficiency of those methods depends on numerous variables such as effluent flow rate, types, and concentrations of contaminants (like inorganic ions).

Others

Other techniques for OP decontamination exist. These methods remain marginal and would require further development. Hereafter is a non-exhaustive list of these techniques.

– Metal–Organic Framework (MOF)

MOFs are crystalline materials, composed of metal ions or clusters linked together by polydentate organic linkers. Based on metal nodes, MOF could be tailored to work as an artificial enzyme (Lee et al. 2009). For example, it could be used for CWNAs degradation through hydrolysis by adsorbed water using Cu-BTC (HKUST-1, $Cu_3(C_9H_3O_6)_2$) or NU-1000 ($Zr_6(\mu_3\text{-}O)_4(\mu_3\text{-}OH)_4(H_2O)_4(OH)_4$) (DeCoste and Peterson 2014; Mondloch et al. 2015).

– Degradation by non-thermal plasma (NTP)

NTP (also called dielectric barrier discharge plasma) is able to destroy a broad spectrum of OPs as well as other chemicals and biological pathogens (Kim et al. 2007). When OPs are exposed to plasma, their chemical bonds are effectively broken; subsequently, generated products seem harmless (Bai et al. 2010). This technique is mainly used for wastewater decontamination (Hu et al. 2013).

– Gamma irradiation process

Gamma irradiation process is used for degradation of numerous pollutants. It is also part of AOPs such as photochemical methods. Gamma irradiation is used to degrade OPs such as chlorpyrifos, diazinon, or malathion in water. This technique is mainly used for water decontamination (Basfar et al. 2007; Mohamed et al. 2009; Hossain et al. 2013).

Organophosphate neutralizing enzymes

Organophosphate hydrolase (OPH)

OPHs belong to the aryltriphosphate dialkylphosphohydrolase (EC 3.1.8.1) and are part of the amidohydrolase superfamily (Schomburg and Stephan 1998; Seibert and Raushel 2005). They are encoded by the OP degradation (*opd*) genes and have been initially found in *Brevundimonas diminuta* MG (previously *Pseudomonas diminuta*) and *Sphingobium fuliginis* ATCC 27551 (previously *Flavobacterium sp.*; Sethunathan and Yoshida 1973; Serdar et al. 1982; Mulbry et al. 1986; Harper et al. 1988). Another enzyme, encoded by a gene closely related to *opd*, namely *opd*A, was isolated from *Agrobacterium radiobacter* P230 (Horne et al. 2002; Horne et al. 2003). Extensive efforts have been devoted to the characterization and engineering of these enzymes (Theriot and Grunden 2010; Wales and Reeves 2012). Relevant works are summarized hereafter.

– OPH from *Brevundimonas diminuta*

B. diminuta carrying the plasmid pCMS1 was found to hydrolyze the pesticide parathion (Serdar et al. 1982). From this plasmid, the gene *opd* coding for a 35-kDa phosphotriesterase was cloned and sequenced (McDaniel et al. 1988). This enzyme was purified and characterized against a wide panel of OP-based insecticides (Dumas et al. 1989). The catalytic efficiency (k_{cat}/K_M) against paraoxon was found to be particularly high: 4.0×10^7 M^{-1} s^{-1}. Efficacy against sarin and soman was further highlighted, albeit with lower k_{cat}/K_M values as compared to paraoxon, 8.0×10^4 M^{-1} s^{-1} and 9.3 x 10^3 M^{-1} s^{-1}, respectively (Dumas et al. 1990). The 3D-structure of the apoenzyme was shown to consist of an $(\beta/\alpha)_8$ fold (Benning et al. 1994). The holoenzyme reconstituted with cadmium and a complex with the substrate analog diethyl 4-methylbenzylphosphate were also obtained (Benning et al. 1995; Vanhooke et al. 1996). Protein engineering strategies were further considered to increase OPH activity (Iyer and Iken 2015). Variants at positions W131,

F132, and F306 with enhanced activity against diisopropylfluorophosphate (DFP) were obtained demonstrating for the first time that mutagenesis was relevant to increase the hydrolysis of P–F linkages (Watkins et al. 1997). Three hydrophobic binding pockets were identified in the structure and 14 residues forming these subsites were targeted for mutagenesis purposes (Chen-Goodspeed et al. 2001a). The role of G60 residue on stereoselectivity was emphasized as G60A substitution drastically altered R_P-enantiomers recognition leading to a 13000-fold greater k_{cat}/K_M in favor of methyl phenyl *p*-nitrophenyl phosphate S_P- compared to R_P-enantiomer. Substitution H257Y was then associated with a reversal of chiral specificity with an increase by up to 500-fold regarding R_P-enantiomers for a variant harboring 4 substitutions I106G/F132G/H257Y/S308G (Chen-Goodspeed et al. 2001b). DNA shuffling coupled with a bacterial cell surface display based screening, led to the isolation of variant 22A11 (A14T/A80V/K185R/H257Y/I274N) and a 25-fold increase in methylparathion hydrolysis (Cho et al. 2002). A similar strategy led to the variant B3561 (A14T/L17P/A80V/V116I/K185R/A203T/I274N/P342S) that exhibited a 725-fold increase in k_{cat}/K_M for chlorpyrifos and a 39-fold improvement in paraoxon hydrolysis (Cho et al. 2004). K185R and I274N substitutions were shown to increase overall hydrolysis rate by being involved in the formation of hydrogen bonds with surrounding residues leading to beneficial structural changes (Cho et al. 2006). Directed evolution of the phosphotriesterase from *B. diminuta* was also investigated and resulted in the selection of variant S5 (K185R/D208G/R319S) with a 20-fold enhancement in functional expression in *E. coli* (Roodveldt and Tawfik 2005). The degradation of V-type nerve agents was recently investigated through computationally focused library screening and two-site mutagenesis (Cherny et al. 2013; Bigley et al. 2013). The first study led to various improved variants, among these C23 (K77A/A80V/F132E/T173N/G208D/H254G/I274N) was particularly relevant with a k_{cat}/K_M value for the toxic S_p isomer of VX of 8.3 x 10^4 M^{-1} s^{-1} (Cherny et al. 2013). In the second study, 12 active-site residues were targeted and led to a 26-fold improvement for the hydrolysis of the VX analogue DEVX as compared to the wild-type protein and a 230-fold improvement for the racemic nerve agent VX with catalytic efficiency up to 7 x 10^4 M^{-1} s^{-1} (Bigley et al. 2013). Very recently, PTE was engineered into a functional trimer showing enhanced activity when displayed onto semiconductor quantumdot (Breger et al. 2015). Altogether, these results underline that phosphotriesterase from *B. diminuta* is a good candidate for catalytic decontamination of organophosphorus chemicals that can be enhanced with enzyme engineering strategies.

– OPH from *Sphingobium fuliginis*.

S. fuliginis (ATCC 27551) was isolated from paddy water and shown to degrade both diazinon and parathion (Sethunathan and Yoshida 1973). An enzymatic extract partially purified from *S. fuliginis* was further shown to possess a phosphotriesterase activity for the degradation of various OPs (Brown 1980). The production of parathion hydrolase in *S. fuliginis* strain ATCC 2751 was associated to a 43-kb plasmid harboring a gene closely related with the *opd* sequence from *B. diminuta* (Mulbry et al. 1986), the encoded proteins sharing 99 % sequence identity. The recombinant expression of OPH from *S. fuliginis* was investigated (Rowland et al. 1991). *Streptomyces lividans* was targeted for this purpose as it expresses the enzyme as a secreted soluble enzyme at a milligram scale (Steiert et al. 1989). The production yield was further optimized by investigating the effect of signal sequences (Rowland et al. 1992). Preparation of OP-decontaminating solutions were considered and the enzyme was found to be stable for long term storage after freeze-drying in the presence of trehalose and its activity was enhanced with 0.01% sodium carboxyl polyoxyethylene tridecylether (Sode and Nakamura 1997). The influence of cobalt and zinc on both activity and expression of the enzyme was evaluated using *opd-lacZ* fusions (Manavathi et al. 2005).

The capacity of the native enzyme to discriminate enantiomers was considered using various OPs and found to be limited (Ohuchi et al. 1997). Protein engineering was thus considered to enhance its efficiency (Iyer and Iken 2015). Variant H254G/H257W/L303T was able to catalyze the hydrolysis of a chromogenic analogue of the most toxic stereoisomer of soman nearly 3 orders of magnitude faster than the native enzyme (Hill et al. 2003). Further mutagenesis enhanced the hydrolysis of VX and pesticides (Gopal et al. 2000). Variant L136Y displayed a 33% increase in VX hydrolysis rate. Rate hydrolysis of mutants W131F and F132Y was enhanced by 4-fold and 5.8-fold with demeton-S methyl and DFP respectively. Further optimization lead to 25-fold increased in k_{cat}/K_M compared to the wild-type with demeton-S methyl for variant with nine mutations (A80V/I106V/F132D/K185R/D208G/H257W/I274N/S308L/R319S) and up to 18-fold increase against malathion for variant harboring 10 amino-acid substitutions (G60V/A80V/I106V/F132D/K185R/D208G/H257W/I274N/F306V/R319S) (Schofield and DiNovo 2010). Protein engineering was also considered for enhancing CWNAs degradation. Position 254 was proved to be crucial for VX hydrolysis (Nakayama et al. 2014), and catalytic efficiency of variant L271/Y309A was enhanced up to 150-fold compared to the wild-type enzyme (Jeong et al. 2014).

– OPH from *Agrobacterium radiobacter* (OpdA)

The bacterial strain *Agrobacterium radiobacter* P230 was found capable of hydrolyzing OP-based pesticides. The gene, namely *opdA*, involved in OP hydrolysis was thus cloned and sequenced and was found closely related to the *opd* gene from *Flavobacterium* sp. strain ATCC 27551 (Horne et al. 2002).

OpdA shares 91% identity with OPH from *Flavobacterium* sp. strain ATCC 27551. The structure of OpdA was solved and complexes with ethylene glycol and dimethyl thiophosphate revealed similarities between OpdA mechanism and other previously reported metallophosphoesterases (Jackson et al. 2005). This enzyme showed 10-fold enhancement compared to homologous phosphotriesterase from *Flavobacterium* sp. strain ATCC 27551 for the degradation of dimethyl organophosphate based insecticides. Substitutions Y257H and F272L were mainly responsible for this difference (Horne et al. 2006).

Protein engineering was used to enhance the degradation of OP-based pesticides. Rational design enabled to identify two successive residues, namely F131 and W132, involved in stereospecificity. Variant W131H/F132A displayed 480-fold and 8-fold enhancement in catalytic efficiency for stereoisomers *Z* and *E* of chlorfenvinphos respectively (Jackson et al. 2009). Combinatorial active site mutagenesis was also applied to OpdA and led to the selection of variant S308L/Y309A resulting in a 5000-fold increase in k_{cat}/K_M for the hydrolysis of malathion (Naqvi et al. 2014).

The potential of OpdA for degrading CWNAs was also considered. The hydrolysis of both G- and V-type nerve agents by OpdA was investigated. The enzyme hydrolyzed cyclosarin and soman with catalytic efficiencies of 3.9 x 10^2 M^{-1} s^{-1} and 5.8 x 10^2 M^{-1} s^{-1}, respectively. The activities towards V-agents were lower by two orders of magnitude when compared to agents from G-series. Regarding VX, a k_{cat}/K_M value of 4.5 M^{-1} s^{-1} was measured (Wille et al. 2012). Three OpdA variants were investigated and shown k_{cat}/K_M values up to 1.7 x 10^5 M^{-1} s^{-1} for tabun. Conversely, soman was poorly hydrolyzed (Dawson et al. 2008).

– Examples of applications of OPH for OP decontamination

Insofar as OPH are efficient biocatalysts for OP hydrolysis, they have been considered for decontamination purposes. In order to promote the use of these enzymes and to address their stability limitations, immobilization strategies were envisaged. Trityl agarose was used for the immobilization of a phosphotriesterase in a fixed bed reactor maintaining its ability to hydrolyze organophosphate pesticides (Caldwell and Raushel 1991a). The thermostability of the immobilized enzyme was moreover enhanced compared to the free form with a 6-fold increase in half-life at 55°C. A process for the immobilization onto nylon was also described (Caldwell and Raushel 1991b). The K_M was increased by 5-6 times compared to the soluble enzyme but reduced the maximum rate against paraoxon to less than 10%. Long term storage was also enhanced for the immobilized enzyme. The enzyme was immobilized into a decontaminating sponge (Havens and Rase 1993), and covalently linked within polyurethane foams (LeJeune and Russell 1996). The stability of the enzyme was tremendously enhanced and enzymatic foams became attractive for large scale nerve agents decontamination (LeJeune et al. 1997; LeJeune et al. 1998; LeJeune and Russell 1999). However, limitations of the technology were due to insufficient activity of OPH for the most toxic organophosphorus chemicals (Donarski et al. 1989). Surface-expression coupled with immobilization was further considered to develop low-cost decontamination systems (Richins et al. 1997; Chen et al. 2000; Richins et al. 2000; Cho et al. 2002; Mansee et al. 2005). Recently, covalent immobilization of OpdA onto polyester textiles was reported offering various perspectives for environmental decontamination (Gao et al. 2014). Other examples of OPH immobilization on amyloid fibril nanoscaffold or amphiphilic block copolymer were also described (Raynes et al. 2011; Suthiwangcharoen and Nagarajan 2014) as well as an original approach consisting in the immobilization of OPH onto carbon nanotube paper (Mechrez et al. 2014).

DFPase from *Loligo vulgaris*

A special attention was raised to the Diisopropylfluorophosphate fluorohydrolase (DFPase, EC 3.1.8.2) from *Loligo vulgaris*. This squid-type enzyme was initally found to efficiently hydrolyze DFP and tabun (Hoskin 1971; Hoskin and Roush 1982). Its catalytic mechanism was considered and the 3D-structure was solved and described as a 6-fold β propeller (Scharff et al. 2001a; Scharff et al. 2001b). Kinetics studies and site-directed mutagenesis were performed to decipher the reaction mechanism of the enzyme and identify the essential residues in the active site (Hartleib and Rüterjans 2001a; Scharff et al. 2001a; Scharff et al. 2001b; Katsemi et al. 2005). Residue H287 was shown to act as a general base catalyst whereas two other histidine residues, namely H181 and H274, appeared to have a stabilizing effect. Roles of the two high-affinity Ca^{2+}-binding sites were also described as being strongly involved in the overall stabilization of the DFPase structure and probably in the catalysis (Hartleib et al. 2001). The heterelogous production of the enzyme was considered using an *E. coli* expression system and yielded to large amounts of active and soluble protein that could be further purified using an His-tag and appeared to be stable for 1 year at 4 °C (Hartleib and Rüterjans 2001b).

Organophosphate acid anhydrolase (OPAA) and related prolidases

A moderately halophilic bacterial isolate identified as a species of *Alteromonas* was found able to degrade several OPs (DeFrank and Cheng 1991). From this extract, the main enzyme, OPAA-2, was purified to homogeneity and found to be a 60-kDa polypeptide. This enzyme was shown to hydrolyze DFP ($k_{cat}/K_M = 7.7$ x 10^4 M^{-1} s^{-1}) as well as phosphofluoridate nerve agents including sarin ($k_{cat}/K_M = 2.8$ x 10^5 M^{-1} s^{-1}), soman ($k_{cat}/K_M = 6.1 \times 10^4$ M^{-1} s^{-1})

or cyclosarin ($k_{cat}/K_M = 9.6 \times 10^5$ M^{-1} s^{-1}) and was poorly active with paraoxon (Cheng et al. 1996; Theriot and Grunden 2010). A special attention was thus paid to *Alteromonas* strains that were screened for their OP-hydrolyzing activity (DeFrank et al. 1993; Cheng et al. 1993). Many genes encoding OPAAs were reported and the enzymes were shown to be closely related to prolidases (EC 3.4.13.9). Their promiscuous ability to hydrolyze dipeptides with C-terminal proline (Xaa-Pro) was then underlined (Cheng et al. 1996; Cheng et al. 1997). Nevertheless, OPAAs are particularly efficient for hydrolyzing OP compounds and are also able to degrade G-type CWNAs. Their large-scale production has moreover been demonstrated (Cheng et al. 1998; Cheng et al. 1999; Cheng and Defrank 2000). Both substrate and stereochemical specificity of OPAA from *Alteromonas* sp. JDS6.5 were analyzed and a preference for S_p enantiomers was demonstrated (Hill et al. 2000). The X-ray structure of the enzyme revealed two distinct domains, N- and C-terminus. The C-terminus domain contains Mn^{2+} divalent cations and displayed a "pita-bread" fold (Vyas et al. 2010). This work highlighted relationships between prolidases and OPAAs that were completed by the 3D structure of OPAA from the marine bacterium *Alteromonas macleodii* (Štěpánková et al. 2013). Prolidases from hyperthermophilic sources were also attractive and *Pyrococcus* sp. strains were investigated. Enzymes from *Pyrococcus furiosus* or *Pyrococcus horikoshii* (Maher et al. 2004; Theriot et al. 2009; Theriot et al. 2010), appeared to be good candidates for the development of decontamination solutions and were further considered for random mutagenesis investigations. Improved variants against nerve agents and Xaa-Pro dipeptides over a broad range of temperature were described (Theriot et al. 2010; Theriot et al. 2011). The dual activity prolidase/OPAA was also observed with prolidase from human origin (Wang et al. 2004; Wang et al. 2006; diTargiani et al. 2010; Costante et al. 2012). This is particularly interesting as human enzymes are really appealing for the development of catalytic bioscavengers.

Paraoxonase

Another class of enzyme from human origin, namely paraoxonase (PON, EC 3.1.8.1.), has found considerable interest. Since the earliest report describing the ability of a mammalian serum esterase to degrade paraoxon (Aldridge 1953) and nerve agents (Broomfield and Ford 1991; Davies et al. 1996), numerous data were collected regarding the potential of PON for OP bioscavenging (Rochu et al. 2007). PON is capable of hydrolyzing a wide spectrum of OP pesticides (Mackness et al. 1991; Furlong et al. 1991; Li et al. 1995). PON from rabbit and human serum were purified to homogeneity and were shown to be similar, though differing in the amino terminus sequence (Gan et al. 1991; Furlong et al. 1991). However, human PON remains difficult to purify from plasma or heterologously express in high yield. Baculovirus and adenovirus infections of *Trichoplusia ni* larvae allowed to produce large quantities of functional recombinant HuPON1 (Otto et al. 2010; Hodgins et al. 2013). Enzyme engineering was deeply investigated to generate improved variants. Site-directed mutagenesis and group-selective labeling modifications were applied to decipher the role of molecular determinants of catalysis (Josse et al. 1999a; Josse et al. 1999b). Supplementary essential residues were also identified with a DFPase-like homology model (Yeung et al. 2004). Complete description of PON1's active site was achieved by solving the 3D structure of a recombinant PON1 variant (rePON1-G2E6) expressed in *E. coli* and obtained through directed evolution (Harel et al. 2004; Aharoni et al. 2004). Mammalian paraoxonase PON1 was found to be more efficient for the detoxification of soman and cyclosarin than OPH from *P. diminuta* and DFPase from *Lolio vulgaris*. Variants obtained from PON1 were further improved by about 10-fold against cyclosarin and soman as well as DFP, parathiol, or chlorpyrifios-oxon with up to 380-fold increase (Amitai et al. 2006). An engineered recombinant human PON1 ($rHuPON1_{K192}$) was also generated and highly purified. The stereospecificity of both recombinant and wild-type PON1 were evaluated using fluorogenic surrogates of nerve agents and were shown to be in favor of R_p isomers (Ashani et al. 2010). Directed evolution experiments were, thus, utilized to increase the efficiency of PON1 towards G-agents (Gupta et al. 2011). Rational and random mutagenesis were combined using a high-throughput methodology based on the utilization of fluorogenic analogs in emulsion compartments and a low-throughput plate screening. The activity against the coumarin analog of S_p cyclosarin was enhanced by $\approx 10^5$-fold for variant 4E9 (L69G/S111T/H115W/H134R/F222S/T332) as compared to the wild-type like variant rePON1-G3C9 reaching catalytic efficiency $>10^5$ M^{-1} s^{-1}. Another work led to the isolation of significantly improved variants for degrading G-Agents (Goldsmith et al. 2012). Among these, variant VIID2 (L55I/L69V/H115A/H134R/H197/R/F222M/I291L/T332S) was of special interest. Although significant enhancements for the decontamination of G-agents have been achieved, the hydrolysis of V-type agents still remains critical. Computational experiments were applied to understand the way PONs hydrolyze VX and drew new perspectives for their engineering (Peterson et al. 2011). Double-substituted variants of human PON1 (H115W/Y71A and H115W/F347W) were constructed and showed up to 2-fold increase in catalytic efficiency as compared to the wild-type enzyme (Kirby et al. 2013). Noteworthy, PON were also deeply studied for evolutionary biology considerations. Original strategies including back-to-ancestor/consensus mutations or neutral-genetic drift were employed to evolve PON in non-conventional manners (Amitai et al. 2007; Khersonsky et al. 2009; Alcolombri et al. 2011; Bar-Rogovsky et al. 2013). Although rarely investigated, PON3 paraoxonase was also purified (Draganov et al.

2000; Reddy et al. 2001) and considered for directed evolution purposes. The catalytic efficiency of recombinant variants of PON3 against paraoxon was enhanced by up to 240-fold (Aharoni et al. 2004). Both activity and stability of PON3 were shown to be tunable through combination of family shuffling and phylogeny-based mutagenesis (Khersonsky et al. 2009). Of note, another enzyme, namely, the Senescence marker protein 30 (SMP30), has been showed to display a 3D structure closely related to PON1, although containing a single metal-binding site. SMP30 is a lactonase able to hydrolyze various aldolactones and is also promiscuous towards OPs sush as DFP (Kondo et al. 2004; Scott and Bahnson 2011).

Methylparathion hydrolase

Methylparathion hydrolase (MPH, EC 3.1.8.1) is an aryldialkylphosphatase belonging to metallo-β-lactamase family. Gene *mpd* coding for MPH was first identified in *Plesiomonas* sp. strain M6 (Zhongli et al. 2001). The gene *mpd* was then sequenced, effectively expressed in *E. coli* and further purified as a monomer (Fu et al. 2004). Another closely related gene was identified in *Pseudomonas* sp. strain WBC-3 (Liu et al. 2005). The encoded enzyme was purified and crystallized and the 3D structure revealed a dimeric enzyme each subunit containing a mixed hybrid binuclear zinc center in which the more solvent-exposed β-metal cation was replaced by cadmium (Dong et al. 2005). Interestingly, MPH was shown to be homologous to other metallo-β-lactamases but did not display any similarity with phosphotriesterases. Recombinant MPH expressed in *E. coli* was characterized and was shown to be active on methylparathion as well as other OP pesticides including malathion or dichlorvos (Yang et al. 2008). Another MPH, dubbed OPHC2, was identified in *Pseudomonas pseudoalcaligenes* strain C2-1 (Ningfeng et al. 2004) and *Stenotrophomonas* sp. strain SMSP-1 (Shen et al. 2010). The former was characterized and its 3D structure was solved (Gotthard et al. 2013a; Gotthard et al. 2013b). Recently, an OPHC2 analogue, namely *Po*OPH from *Pseudomonas oleovorans*, was discovered (Luo et al. 2014). This enzyme displays lactonase and arylesterase activities as well as a promiscuous OPH activity. Variant $PoOPH_{M2}$ (H250I/I263W) was designed and found improved by 6,962- and 106-fold against methylparathion and ethylparaoxon, respectively. Random mutagenesis of MPH from *Pseudomonas stutzeri* further led to a 5-fold increase in the hydrolysis of chlorpyrifos (Xie et al. 2014). Additional *mpd* genes harbored by seven strains isolated from methylparathion contaminated sites were subcloned and expressed in *E. coli* (Zhang et al. 2006). Phylogenetic analysis supported by GC-content comparisons between *mpd* genes and respective host's chromosome suggested that horizontal gene transfer may have occurred, playing an important role for bacterial adaptation to methylparathion contamination.

Phosphotriesterase-Like Lactonase

Among the enzymes able to degrade OPs, phosphotriesterase-like lactonases (PLLs) constitute a promising protein family closely related to bacterial phosphotriesterases (Afriat et al. 2006; Draganov 2010). PLLs are natural lactonases catalyzing the hydrolysis of *N*-acyl-homoserine lactones (AHLs) involved in the *quorum* sensing system of bacterial species, and additionally, exhibit a promiscuous OPH activity. Regarding both the predominant metabolic role of lactones in bacterial communication and the relatively recent occurrence of OPs, widely used as pesticides during the last decades, it has been assumed that the phosphotriesterase activity of PLL has emerged from a lactonase template harboring a promiscuous activity for OP hydrolysis. Interestingly, modern phosphotriesterase have probably evolved from a lactonase ancestor that lost its capacity to hydrolyze AHL to the benefit of higher OP-degradation rates. Natural evolution has led to the selection of enzymes with phosphotriesterase activity close to catalytic perfection to the detriment of the natural lactonase activity. Afriat-Jurnou and coworkers have, for example, demonstrated that ancestral reconstruction, starting from OPH from *B. diminuta* restore its lactonase catalytic ability, providing an experimental evidence of the evolutionary linkage between these enzymatic activities (Afriat-Jurnou et al. 2012). PLLs have been isolated from various hosts including hyperthermophile bacteria (Xiang et al. 2009; Zhang et al. 2012), or archaea (Merone et al. 2005; Hiblot et al. 2012a; Gotthard et al. 2013b; Bzdrenga et al. 2014; Kallnik et al. 2014). These enzymes display remarkable stability to temperature, pH, detergent, solvent, or storage, offering good perspectives for utilizations in external decontamination of OPs. The enzyme *Sso*Pox from the archeon *Sulfolobus solfataricus* is particularly interesting and is one of the most promising PLL for OP countermeasures. Major results and perspectives are detailed hereafter.

*Sso*Pox: a highly stable, OP-degrading capable enzyme

An archaeon-sourced enzyme with tremendous stability

The archea *Sulfolobus solfataricus* was discovered within the Vesuvio's sulfatare and found to possess a gene homologous to the *B. diminuta* PTE. The encoded enzyme was expressed and its phosphotriesterase ability, albeit low, was highlighted. Among the hydrolyzed substrates was paraoxon, hence, was it called *Sso*Pox: *Sulfolobus solftataricus* Paraoxonase (Merone et al. 2005). It was also found to efficiently hydrolyze various lactones, including *N*-acyl homoserine lactones, known to be involved in bacterial communication (*quorum* sensing). Actually, the lactonase activity of *Sso*Pox was found to be two orders of magnitude higher than its phosphotriesterase activity, underlining that it is most probably a natural

lactonase, whose capacity to hydrolyze OPs chemicals stemmed from a promiscuous enzymatic template.

Due to its hypertermophilic origin the enzyme exhibits an incredible stability to temperature, being active from 10 to 100 °C, with an impressive denaturation temperature of 106 °C as well as a tremendous resistance to the denaturing effect of urea. Furthermore, *Sso*Pox was active from pH 5.0 to pH 9.0 confirming the unusual properties of this enzyme. *Sso*Pox was crystallized and its 3D structure was solved in both *apo* and complex forms (Elias et al. 2007; Elias et al. 2008). The structure was reported as a distorted $(\beta/\alpha)_8$ barrel-fold and was found to be close to mesophilic OPH from both *B. diminuta* and *A. radiobacter*.

The major structural discrepancies between *Sso*Pox and OPHs consist in the shortening of loop 7 as well as both extremities of the polypeptide chain. The arrangement of loop 8 is also variable between the structures and extra loops are observed within *Sso*Pox structure (Fig. 2). These conformational changes are probably involved in the overall enzyme stability by either rigidifying the structure or favoring dimer formation. An investigation of the structural determinants of *Sso*Pox as compared to its mesophilic counterparts was also performed (Vecchio et al. 2009). Surface salt bridge network and a tight quaternary structure were shown to be involved in complex networks and optimization of dimer subunit interfaces, respectively. From this observation came the idea to benefit from the outstanding structural stability of this enzyme, in order to transfer the efficient *B. diminuta* PTE active site within *Sso*Pox scaffold.

Engineering *Sso*Pox to enhance promiscuous phosphotriesterase activity

Thus, protein engineering strategies have been considered in order to increase its potential for bioremediation. Indeed, protein stability has been proved to promote evolvability by minimizing the effect of destabilizing mutations and buffering their deleterious damages (Tokuriki and Tawfik 2009). Hyperthermophile scaffolds are usually good candidates for evolutionary considerations as their tremendous stability may confer an enhanced tolerance to mutation-induced stability changes. Protein polymorphism may thus be generated without drastic effect on protein fitness. Moreover, substrate promiscuity has been identified as a potential origin of functional divergences that could be used as starting point in evolutionary trajectories (Khersonsky et al. 2006).

The rationale was that mesophilic phosphotriesterases probably emerged from PLLs, so their respective sequences and structures were compared and led to the identification of residues probably involved in the enhancement of OP-degradation. Mutational databases listing potential beneficial substitutions for phosphotriesterase activity were designed (Chabriere et al. 2014; Chabriere et al. 2015). These databases combined with *in silico* analyses were used as starting point for engineering

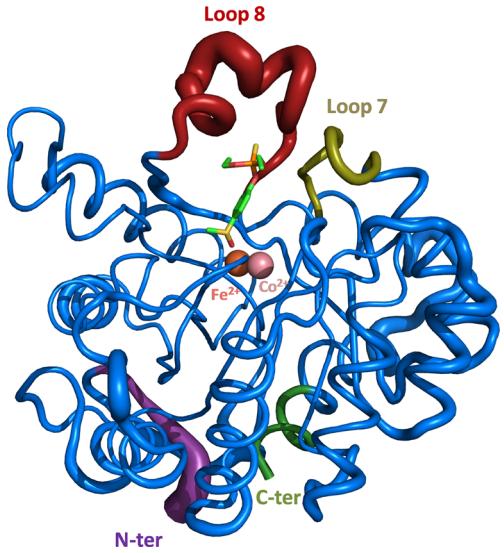


Fig. 2 Overall 3D structure of *Sso*Pox in complex with fensulfothion (PDB ID: 3uf9). Protein backbone is showed as *cartoon*; N- and C-ter are highlighted in *purple* and *green*, respectively. Loop-7 and loop-8 that govern substrate promiscuity are emphasized in *yellow* and *red*. Divalent active-site cations are shown as *spheres*

*Sso*Pox toward OP based pesticide degradation (Fig. 3). Variants with up to 2000-fold increased activity against certain pesticides and enlarged substrate scope were obtained (unpublished results). Mutations R223H and Y97W were first shown to impact phosphotriesterase activity (Elias et al. 2008). Residue W263 was also deeply investigated (Hiblot et al. 2012b). This residue is located in the active site and was shown to be involved in enzyme conformational flexibility, mediating substrate promiscuity. Saturation mutagenesis was performed at this position using NNS-degenerated primers. Two subsets of mutations were distinguished as regard to either their lactonase or phosphotriesterase activity. Within this latter, variants W263F, W263L and W263M were particularly attractive. Catalytic parameters of *Sso*Pox variants towards OPs are reported in Table 1. *Sso*Pox and its variants were shown to be active on a wide range of OPs including pesticides (*e.g.* paraoxon, parathion, malathion) and chemical warfare agent analogs (IMP-, PinP-, and CMP-coumarin). The stimulation of *Sso*Pox activity by anionic detergent at ambient temperature was also demonstrated and is of prime interest for external decontamination purpose as it could help spreading the enzyme on soiled surfaces (Hiblot et al. 2012b). Future engineering experiments on *Sso*Pox are in progress in order to provide a stable, proficient catalyst capable of detoxifying a broad spectrum of toxic OPs.

Concluding remarks

Decontamination methods against OP poisoning have been exhaustively studied during the past decades. Efficient physico-chemical methods including hypochlorite and

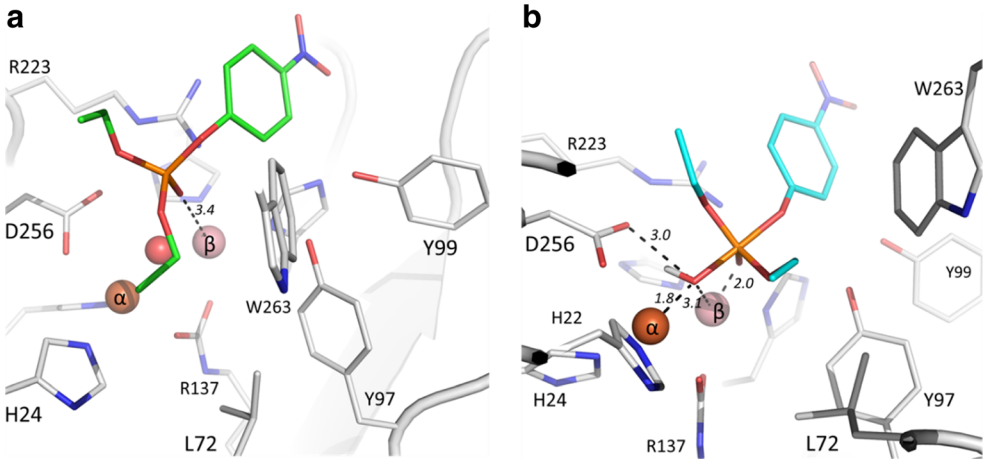


Fig. 3 Molecular docking of paraoxon to *Sso*Pox structure. The docking of paraoxon (ground state, GS; green sticks; **a**) and of its corresponding putative oxyanionic pentavalent hydrolytic transition state (TS; cyan sticks; **b**) was performed in *Sso*Pox (PDB ID: 2vc5). Metal cations and active-site water molecules (in *red*) are shown as *spheres*. Distances are indicated in Ångstroms. Briefly, the molecular docking was performed using torsion and charge parameters generated using ADT 4.2 (http://autodock.scripps.edu/resources/adt) and the Gasteiger method. A single-negative charge was attributed to the oxyanion atom of the pentavalent paraoxon hydrolysis intermediate. Hydrogen atom positions and the atomic partial charges (Gasteiger method) of the receptor protein models were added using ADT 4.2. A +2 charge was attributed to the two-cation ions that comprise the active site of *Sso*Pox. The docking simulations were performed using Autodock 4.0 (Morris et al. 1998; Huey et al. 2007) and the Lamarckian genetic algorithm. Forty runs of genetic algorithm were performed for each couple ligand-receptor pair using the default parameters. The output ligand configurations were clustered and selected by their binding energy scores and their chemical relevance

Table 1 Catalytic parameters of SsoPox wild-type and variants towards organophosphate pesticides and nerve agents with respective reactions conditions (Elias et al. 2008; Hiblot et al. 2012b; Hiblot et al. 2013)

Substrate	Enzyme	Condition	k_{cat} (s^{-1})	K_M (μM)	k_{cat}/K_M ($M^{-1}s^{-1}$)
Ethylparaoxon	WT	70 °C	3.98	3,270	1.22×10^3
		25 °C	12.59	24,250	5.19×10^2
		SDS 0.1 %, 25 °C	40.72	12,340	3.30×10^3
		SDS 0.01%, 25 °C	24.59	3,830	6.42×10^3
		DOC 0.1 %, 25 °C	6.30	570	1.10×10^4
		DOC 0.05 %, 25 °C	4.72	270	1.22×10^3
		DOC 0.01 %, 25 °C	10.51	730	1.72×10^4
	W263F	25 °C	8.47	700	1.21×10^4
		SDS 0.1 %, 25 °C	117.70	2,462	4.78×10^4
		SDS 0.01 %, 25 °C	85.85	1,168	7.35×10^4
	W263M	25 °C	6.82	931	7.33×10^3
	W263L	25 °C	ND	ND	2.37×10^3
	W263I	25 °C	ND	ND	1.21×10^3
	W263V	25 °C	ND	ND	8.83×10^3
	W263T	25 °C	ND	ND	1.06×10^3
Methylparaoxon	WT	25 °C	2.71	2,142	1.27×10^3
Methylparathion	WT	25 °C	1.1×10^{-3}	121	9.09
Malathion	WT	25 °C	8.9×10^{-4}	160	5.56
CMP-coumarin	WT	25 °C	ND	ND	8.13×10^3
	WT	SDS 0.01 %, 25 °C	25.47	137	1.86×10^5
	W263F	25 °C	9.41	114	8.23×10^4
	W263F	SDS 0.01 %, 25 °C	8.64	60	1.44×10^5
IMP-coumarin	WT	25 °C	ND	ND	1.67×10^3
	W263F	25 °C	8.39	95	8.85×10^4
PinP-coumarin	W263F	25 °C	0.11	16	7.08×10^3

sodium hydroxide have emerged for the efficient external decontamination of OPs or stockpile elimination and have already been used for this purpose. These methods usually involve harsh chemical conditions and are not compatible with the decontamination of personnel or sensitive materials. Other methods were developed such as RSDL or Fuller's earth. Whereas RSDL is efficient at decontaminating the skin, it is not compatible with eye and wound cleaning and would be hardly adaptable to a large number of contaminated people. Fuller's earth shows good topical absorbance of contaminants but do not degrade OPs, possibly resulting in large amounts of secondary pollution. Moreover, toxic dusts are generated during the decontamination process, complicating the use of the method at a large scale. Alternatively, photochemical methods are under development for the mineralization of OP chemical in environmental media but would not be relevant for people decontamination. Methods that can be used for both material and personel are under intensive investigations. CDs were proved to be efficient bioscavengers but because of their stoichiometric action, they may not be cost-effective in a case of large scale pollution. Investigations also focus on another promising solution, the use of OP-degrading enzymes. Indeed, the use of enzymes is appealing because they offer a non-corrosive, safe and catalytic way for decontaminating OPs. Protein engineering has been deeply applied for increasing the catalytic efficiencies of recombinant enzymes. Whereas the stability and the production costs of enzymes may be an issue, the discovery of highly thermostable OPs-degrading enzymes such as *Sso*Pox, and their engineering for higher activity is expected to turn them into competitive and economically-attractive OP-biodecontaminants.

Acknowledgments P.J. and J.B. are Ph.D. students granted by Direction Générale de l'Armement (DGA).

References

Afriat L, Roodveldt C, Manco G, Tawfik DS (2006) The latent promiscuity of newly identified microbial lactonases is linked to a recently diverged phosphotriesterase†. Biochemistry (Mosc) 45:13677–13686. doi:10.1021/bi061268r

Afriat-Jurnou L, Jackson CJ, Tawfik DS (2012) Reconstructing a missing link in the evolution of a recently diverged phosphotriesterase by active-site loop remodeling. Biochemistry (Mosc) 51:6047–6055. doi:10.1021/bi300694t

Aharoni A, Gaidukov L, Yagur S et al (2004) Directed evolution of mammalian paraoxonases PON1 and PON3 for bacterial expression and catalytic specialization. Proc Natl Acad Sci USA 101:482–487. doi:10.1073/pnas.2536901100

Alcolombri U, Elias M, Tawfik DS (2011) Directed evolution of sulfotransferases and paraoxonases by ancestral libraries. J Mol Biol 411:837–853. doi:10.1016/j.jmb.2011.06.037

Aldridge WN (1953) Serum esterases. 2. An enzyme hydrolysing diethyl p-nitrophenyl phosphate (E 600) and its identity with the A-esterase of mammalian sera. Biochem J 53:117–124

Amitai G, Gaidukov L, Adani R et al (2006) Enhanced stereoselective hydrolysis of toxic organophosphates by directly evolved variants of mammalian serum paraoxonase. FEBS J 273:1906–1919. doi:10.1111/j.1742-4658.2006.05198.x

Amitai G, Gupta RD, Tawfik DS (2007) Latent evolutionary potentials under the neutral mutational drift of an enzyme. HFSP J 1:67–78. doi:10.2976/1.2739115/10.2976/1

Ashani Y, Gupta RD, Goldsmith M et al (2010) Stereo-specific synthesis of analogs of nerve agents and their utilization for selection and characterization of paraoxonase (PON1) catalytic scavengers. Chem Biol Interact 187:362–369. doi:10.1016/j.cbi.2010.02.039

Bai Y, Chen J, Yang Y et al (2010) Degradation of organophosphorus pesticide induced by oxygen plasma: Effects of operating parameters and reaction mechanisms. Chemosphere 81:408–414. doi:10.1016/j.chemosphere.2010.06.071

Balkaya N (1999) A study of optimal experimental conditions in the photocatalytic degradation of an organophosphorous insecticide. Environ Technol 20:617–623. doi:10.1080/09593332008616856

Bannard RAB, Casselman AA, Purdon JG, Bovenkamp JW (1991) Broad spectrum chemical decontaminant system. Patent US 5:075, 297

Bar-Rogovsky H, Hugenmatter A, Tawfik DS (2013) The evolutionary origins of detoxifying enzymes: the mammalian serum paraoxonases (PONs) relate to bacterial homoserine lactonases. J Biol Chem 288:23914–23927. doi:10.1074/jbc.M112.427922

Basfar AA, Mohamed KA, Al-Abduly AJ et al (2007) Degradation of diazinon contaminated waters by ionizing radiation. Radiat Phys Chem 76:1474–1479. doi:10.1016/j.radphyschem.2007.02.055

Beauregard G, Lum J, Roufogalis BD (1981) Effect of histidine modification on the aging of organophosphate-inhibited acetylcholinesterase. Biochem Pharmacol 30:2915–2920. doi:10.1016/0006-2952(81)90252-5

Benning MM, Kuo JM, Raushel FM, Holden HM (1994) Three-dimensional structure of phosphotriesterase: an enzyme capable of detoxifying organophosphate nerve agents. Biochemistry (Mosc) 33:15001–15007. doi:10.1021/bi00254a008

Benning MM, Kuo JM, Raushel FM, Holden HM (1995) Three-dimensional structure of the binuclear metal center of phosphotriesterase. Biochemistry (Mosc) 34:7973–7978. doi:10.1021/bi00025a002

Bigley AN, Xu C, Henderson TJ et al (2013) Enzymatic neutralization of the chemical warfare agent VX: evolution of phosphotriesterase for phosphorothiolate hydrolysis. J Am Chem Soc 135:10426–10432. doi:10.1021/ja402832z

Braue Jr EH, Smith KH, Doxzon BF, et al (2010a) Evaluation of RSDL, M291 SDK, 0.5% bleach, 1% soapy water and SERPACWA. Part 2. Challenge with soman. DTIC Document: ADA539735, Army Medical Research institute of chemical defense Aberdeen Proving ground MD

Braue Jr EH, Smith KH, Doxzon BF, et al (2010b) Evaluation of RSDL, M291 SDK, 0.5% bleach, 1% soapy water and SERPACWA. Part 1. Challenge with VX. DTIC Document: ADA525186, Army Medical Research institute of chemical defense Aberdeen Proving ground MD

Breger JC, Walper SA, Oh E et al (2015) Quantum dot display enhances activity of a phosphotriesterase trimer. Chem Commun 51:6403–6406. doi:10.1039/C5CC00418G

Broomfield CA, Ford KW (1991) Hydrolysis of nerve gases by plasma enzymes. Proc 3rd Int Meet Cholinesterases Gd-Motte 161.

Brown KA (1980) Phosphotriesterases of flavobacterium sp. Soil Biol Biochem 12:105–112. doi:10.1016/0038-0717(80)90044-9

Bzdrenga J, Hiblot J, Gotthard G et al (2014) SacPox from the thermoacidophilic crenarchaeon Sulfolobus acidocaldarius is a proficient lactonase. BMC Res Notes 7:333. doi:10.1186/1756-0500-7-333

Caldwell SR, Raushel FM (1991a) Detoxification of organophosphate pesticides using an immobilized phosphotriesterase from Pseudomonas diminuta. Biotechnol Bioeng 37:103–109. doi:10.1002/bit.260370203

Caldwell SR, Raushel FM (1991b) Detoxification of organophosphate pesticides using a nylon based immobilized phosphotriesterase fromPseudomonas diminuta. Appl Biochem Biotechnol 31:59–73. doi:10.1007/BF02922126

Chabriere E, Elias M, Hiblot J, Raoult D (2014) Sulfolobal phosphotriesterase-like (pll) lactonases activity having enhanced properties and the uses thereof.

Chabriere E, Elias M, Hiblot J, Raoult D (2015) Vulcanisaetal phosphotriesterase-like lactonases (pll) having enhanced properties and the uses thereof.

Chen W, Richins RD, Mulchandani P et al (2000) Biodegradation Of Organophosphorus Nerve Agents by Surface Expressed Organophosphorus Hydrolase. In: Zwanenburg B, Mikołajczyk M, Kiełbasiński P (eds) Enzymes in action. Springer, The Netherlands, pp 211–221

Chen H, Shen M, Chen R et al (2011) Photocatalytic degradation of commercial methyl parathion in aqueous suspension containing La-doped TiO2 nanoparticles. Environ Technol 32:1515–1522. doi:10.1080/09593330.2010.543927

Cheng T, Liu L, Wang B et al (1997) Nucleotide sequence of a gene encoding an organophosphorus nerve agent degrading enzyme from Alteromonas haloplanktis. J Ind Microbiol Biotechnol 18:49–55. doi:10.1038/sj.jim.2900358

Cheng T-C, Defrank JJ (2000) Hydrolysis of Organophosphorus Compounds by Bacterial Prolidases. In: Zwanenburg B, Mikołajczyk M, Kiełbasiński P (eds) Enzymes in action. Springer, The Netherlands, pp 243–261

Cheng T-C, Harvey SP, Stroup AN (1993) Purification and properties of a highly active organophosphorus acid anhydrolase from Alteromonas undina. Appl Environ Microbiol 59:3138–3140

Cheng TC, Harvey SP, Chen GL (1996) Cloning and expression of a gene encoding a bacterial enzyme for decontamination of organophosphorus nerve agents and nucleotide sequence of the enzyme. Appl Environ Microbiol 62:1636–1641

Cheng T-C, Rastogi VK, Defrank JJ, Sawiris GP (1998) G-type nerve agent decontamination by Alteromonas prolidase. Ann N Y Acad Sci 864:253–258. doi:10.1111/j.1749-6632.1998.tb10316.x

Cheng T, DeFrank JJ, Rastogi VK (1999) Alteromonas prolidase for organophosphorus G-agent decontamination. Chem Biol Interact 119–120:455–462. doi:10.1016/S0009-2797(99)00058-7

Chen-Goodspeed M, Sogorb MA, Wu F et al (2001a) Structural determinants of the substrate and stereochemical specificity of phosphotriesterase†. Biochemistry (Mosc) 40:1325–1331. doi:10.1021/bi001548l

Chen-Goodspeed M, Sogorb MA, Wu F, Raushel FM (2001b) Enhancement, relaxation, and reversal of the stereoselectivity for phosphotriesterase by rational evolution of active site residues†. Biochemistry (Mosc) 40:1332–1339. doi:10.1021/bi001549d

Cherny I, Greisen P, Ashani Y et al (2013) Engineering V-type nerve agents detoxifying enzymes using computationally focused libraries. ACS Chem Biol 8:2394–2403. doi:10.1021/cb4004892

Cho CM-H, Mulchandani A, Chen W (2002) Bacterial cell surface display of organophosphorus hydrolase for selective screening of improved hydrolysis of organophosphate nerve agents. Appl Environ Microbiol 68:2026–2030. doi:10.1128/AEM.68.4.2026-2030.2002

Cho CM-H, Mulchandani A, Chen W (2004) Altering the substrate specificity of organophosphorus hydrolase for enhanced hydrolysis of chlorpyrifos. Appl Environ Microbiol 70:4681–4685. doi:10.1128/AEM.70.8.4681-4685.2004

Cho CM-H, Mulchandani A, Chen W (2006) Functional analysis of organophosphorus hydrolase variants with high degradation activity towards organophosphate pesticides. Protein Eng, Des Sel 19:99–105. doi:10.1093/protein/gzj007

Costante M, Biggemann L, Alamneh Y et al (2012) Hydrolysis potential of recombinant human skin and kidney prolidase against diisopropylfluorophosphate and sarin by in vitro analysis. Toxicol In Vitro 26:182–188. doi:10.1016/j.tiv.2011.11.006

Davies HG, Richter RJ, Keifer M et al (1996) The effect of the human serum paraoxonase polymorphism is reversed with diazoxon, soman and sarin. Nat Genet 14:334–336. doi:10.1038/ng1196-334

Dawson RM, Pantelidis S, Rose HR, Kotsonis SE (2008) Degradation of nerve agents by an organophosphate-degrading agent (OpdA). J Hazard Mater 157:308–314. doi:10.1016/j.jhazmat.2007.12.099

DeCoste JB, Peterson GW (2014) Metal–organic frameworks for air purification of toxic chemicals. Chem Rev 114:5695–5727. doi:10.1021/cr4006473

DeFrank JJ, Cheng TC (1991) Purification and properties of an organophosphorus acid anhydrase from a halophilic bacterial isolate. J Bacteriol 173:1938–1943

DeFrank JJ, Beaudry WT, Cheng T-C et al (1993) Screening of halophilic bacteria and Alteromonas species for organophosphorus hydrolyzing enzyme activity. Chem Biol Interact 87:141–148. doi:10.1016/0009-2797(93)90035-W

Désiré B, Saint-André S (1986) Interaction of soman with beta-cyclodextrin. Fundam Appl Toxicol Off J Soc Toxicol 7:646–657

Désiré B, Saint-André S (1987) Inactivation of sarin and soman by cyclodextrins in vitro. Experientia 43:395–397

diTargiani RC, Chandrasekaran L, Belinskaya T, Saxena A (2010) In search of a catalytic bioscavenger for the prophylaxis of nerve agent toxicity. Chem Biol Interact 187:349–354. doi:10.1016/j.cbi.2010.02.021

Donarski WJ, Dumas DP, Heitmeyer DP et al (1989) Structure-activity relationships in the hydrolysis of substrates by the phosphotriesterase from Pseudomonas diminuta. Biochemistry (Mosc) 28:4650–4655. doi:10.1021/bi00437a021

Dong Y-J, Bartlam M, Sun L et al (2005) Crystal structure of methyl parathion hydrolase from Pseudomonas sp. WBC-3. J Mol Biol 353:655–663. doi:10.1016/j.jmb.2005.08.057

Draganov DI (2010) Lactonases with oragnophosphatase activity: structural and evolutionary perspectives. Chem Biol Interact 187:370–372. doi:10.1016/j.cbi.2010.01.039

Draganov DI, Stetson PL, Watson CE et al (2000) Rabbit serum paraoxonase 3 (PON3) is a high density lipoprotein-associated lactonase and protects low density lipoprotein against oxidation. J Biol Chem 275:33435–33442. doi:10.1074/jbc.M004543200

Dumas DP, Caldwell SR, Wild JR, Raushel FM (1989) Purification and properties of the phosphotriesterase from Pseudomonas diminuta. J Biol Chem 264:19659–19665

Dumas DP, Durst HD, Landis WG et al (1990) Inactivation of organophosphorus nerve agents by the phosphotriesterase from Pseudomonas diminuta. Arch Biochem Biophys 277:155–159. doi:10.1016/0003-9861(90)90564-F

Elias M, Dupuy J, Merone L et al (2007) Crystallization and preliminary X-ray diffraction analysis of the hyperthermophilic *Sulfolobus solfataricus* phosphotriesterase. Acta Crystallograph Sect F Struct Biol Cryst Commun 63:553–555. doi:10.1107/S1744309107023512

Elias M, Dupuy J, Merone L et al (2008) Structural basis for natural lactonase and promiscuous phosphotriesterase activities. J Mol Biol 379:1017–1028. doi:10.1016/j.jmb.2008.04.022

Elsinghorst PW, Worek F, Koller M (2015) Detoxification of organophosphorus pesticides and nerve agents through RSDL: efficacy evaluation by 31P NMR spectroscopy. Toxicol Lett 233:207–213. doi:10.1016/j.toxlet.2014.12.004

English II J (1974) Design aspects of a low emission, two-stage incinerator. In: Proceedings of the 1974 ASME National Incinerator Conference. ASME, New York

Estour F, Letort S, Müller S et al (2013) Functionalized cyclodextrins bearing an alpha nucleophile—a promising way to degrade nerve agents. Chem Biol Interact 203:202–207. doi:10.1016/j.cbi.2012.10.020

Evgenidou E, Konstantinou I, Fytianos K, Albanis T (2006) Study of the removal of dichlorvos and dimethoate in a titanium dioxide mediated photocatalytic process through the examination of intermediates and the reaction mechanism. J Hazard Mater 137:1056–1064. doi:10.1016/j.jhazmat.2006.03.042

Fielding G (1964) Field decontamination studies with chemical warfare decontaminating solution DS2. US Naval Research Laboratory, Washigton DC

Firmin MC (2003) The future of decontamination operations—an analysis of decontamination foam 200. Army Chem Rev 34–36

Fu G, Cui Z, Huang T, Li S (2004) Expression, purification, and characterization of a novel methyl parathion hydrolase. Protein Expr Purif 36:170–176. doi:10.1016/j.pep.2004.04.019

Furlong CE, Richter RJ, Chapline C, Crabb JW (1991) Purification of rabbit and human serum paraoxonase. Biochemistry (Mosc) 30:10133–10140. doi:10.1021/bi00106a009

Gan KN, Smolen A, Eckerson HW, Du BNL (1991) Purification of human serum paraoxonase/arylesterase. Evidence for one esterase catalyzing both activities. Drug Metab Dispos 19:100–106

Gao Y, Truong YB, Cacioli P et al (2014) Bioremediation of pesticide contaminated water using an organophosphate degrading enzyme immobilized on nonwoven polyester textiles. Enzyme Microb Technol 54:38–44. doi:10.1016/j.enzmictec.2013.10.001

Garbin JR, Milori DMBP, Simões ML et al (2007) Influence of humic substances on the photolysis of aqueous pesticide residues. Chemosphere 66:1692–1698. doi:10.1016/j.chemosphere.2006.07.017

Goldsmith M, Ashani Y, Simo Y et al (2012) Evolved stereoselective hydrolases for broad-spectrum G-type nerve agent detoxification. Chem Biol 19:456–466. doi:10.1016/j.chembiol.2012.01.017

Gonçalves C, Dimou A, Sakkas V et al (2006) Photolytic degradation of quinalphos in natural waters and on soil matrices under simulated solar irradiation. Chemosphere 64:1375–1382. doi:10.1016/j.chemosphere.2005.12.020

Gopal S, Rastogi V, Ashman W, Mulbry W (2000) Mutagenesis of organophosphorus hydrolase to enhance hydrolysis of the nerve agent VX. Biochem Biophys Res Commun 279:516–519. doi:10.1006/bbrc.2000.4004

Gotthard G, Hiblot J, Gonzalez D et al (2013a) Crystallization and preliminary X-ray diffraction analysis of the organophosphorus hydrolase OPHC2 from *Pseudomonas pseudoalcaligenes*. Acta Crystallograph Sect F Struct Biol Cryst Commun 69:73–76. doi:10.1107/S174430911205049X

Gotthard G, Hiblot J, Gonzalez D et al (2013b) Structural and enzymatic characterization of the phosphotriesterase OPHC2 from Pseudomonas pseudoalcaligenes. PLoS One 8, e77995. doi:10.1371/journal.pone.0077995

Gunnell D, Eddleston M, Phillips MR, Konradsen F (2007) The global distribution of fatal pesticide self-poisoning: systematic review. BMC Public Health 7:357. doi:10.1186/1471-2458-7-357

Gupta RC (2009) Handbook of toxicology of chemical warfare agents.

Gupta RD, Goldsmith M, Ashani Y et al (2011) Directed evolution of hydrolases for prevention of G-type nerve agent intoxication. Nat Chem Biol 7:120–125. doi:10.1038/nchembio.510

Harel M, Aharoni A, Gaidukov L et al (2004) Structure and evolution of the serum paraoxonase family of detoxifying and antiatherosclerotic enzymes. Nat Struct Mol Biol 11:412–419. doi:10.1038/nsmb767

Harper LL, McDaniel CS, Miller CE, Wild JR (1988) Dissimilar plasmids isolated from Pseudomonas diminuta MG and a Flavobacterium sp. (ATCC 27551) contain identical opd genes. Appl Environ Microbiol 54:2586–2589

Hartleib J, Rüterjans H (2001a) Insights into the reaction mechanism of the diisopropyl fluorophosphatase from Loligo vulgaris by means of kinetic studies, chemical modification and site-directed mutagenesis. Biochim Biophys Acta BBA—Protein Struct Mol Enzymol 1546:312–324. doi:10.1016/S0167-4838(01)00153-4

Hartleib J, Rüterjans H (2001b) High-yield expression, purification, and characterization of the recombinant Diisopropylfluorophosphatase from Loligo vulgaris. Protein Expr Purif 21:210–219. doi:10.1006/prep.2000.1360

Hartleib J, Geschwindner S, Scharff EI, Rüterjans H (2001) Role of calcium ions in the structure and function of thediisopropylfluorophosphatase from Loligo vulgaris. Biochem J 353:579–589

Havens PL, Rase HF (1993) Reusable immobilized enzyme/polyurethane sponge for removal and detoxification of localized organophosphate pesticide spills. Ind Eng Chem Res 32:2254–2258. doi:10.1021/ie00022a009

Hiblot J, Gotthard G, Chabriere E, Elias M (2012a) Structural and enzymatic characterization of the lactonase SisLac from Sulfolobus islandicus. PLoS One 7, e47028. doi:10.1371/journal.pone.0047028

Hiblot J, Gotthard G, Chabriere E, Elias M (2012b) Characterisation of the organophosphate hydrolase catalytic activity of SsoPox. Sci Rep. doi:10.1038/srep00779

Hiblot J, Gotthard G, Elias M, Chabriere E (2013) Differential active site loop conformations mediate promiscuous activities in the lactonase SsoPox. PLoS One 8, e75272. doi:10.1371/journal.pone.0075272

Hill CM, Wu F, Cheng T-C et al (2000) Substrate and stereochemical specificity of the organophosphorus acid anhydrolase from Alteromonas sp. JD6.5 toward p-nitrophenyl phosphotriesters. Bioorg Med Chem Lett 10:1285–1288. doi:10.1016/S0960-894X(00)00213-4

Hill CM, Li W-S, Thoden JB et al (2003) Enhanced degradation of chemical warfare agents through molecular engineering of the phosphotriesterase active site. J Am Chem Soc 125:8990–8991. doi:10.1021/ja0358798

Hodgins SM, Kasten SA, Harrison J et al (2013) Assessing protection against OP pesticides and nerve agents provided by wild-type HuPON1 purified from Trichoplusia ni larvae or induced via adenoviral infection. Chem Biol Interact 203:177–180. doi:10.1016/j.cbi.2012.10.015

Horne I, Sutherland TD, Harcourt RL et al (2002) Identification of an opd (organophosphate degradation) gene in an Agrobacterium isolate. Appl Environ Microbiol 68:3371–3376. doi:10.1128/AEM.68.7.3371-3376.2002

Horne I, Qiu X, Russell RJ, Oakeshott JG (2003) The phosphotriesterase gene opdA in Agrobacterium radiobacter P230 is transposable. FEMS Microbiol Lett 222:1–8. doi:10.1016/S0378-1097(03)00211-8

Horne I, Qiu X, Ollis DL et al (2006) Functional effects of amino acid substitutions within the large binding pocket of the phosphotriesterase OpdA from Agrobacterium sp. P230. FEMS Microbiol Lett 259:187–194. doi:10.1111/j.1574-6968.2006.00262.x

Hoskin FCG (1971) Diisopropylphosphorofluoridate and tabun: enzymatic hydrolysis and nerve function. Science 172:1243–1245. doi:10.1126/science.172.3989.1243

Hoskin FC, Roush AH (1982) Hydrolysis of nerve gas by squid-type diisopropyl phosphorofluoridate hydrolyzing enzyme on agarose resin. Science 215:1255–1257. doi:10.1126/science.7058344

Hoskin FC, Steeves DM, Walker JE (1999) Substituted cyclodextrin as a model for a squid enzyme that hydrolyzes the nerve gas soman. Biol Bull 197:284–285

Hossain MS, Fakhruddin ANM, Chowdhury MAZ, Alam MK (2013) Degradation of chlorpyrifos, an organophosphorus insecticide in aqueous solution with gamma irradiation and natural sunlight. J Environ Chem Eng 1:270–274. doi:10.1016/j.jece.2013.05.006

Hu Y, Bai Y, Yu H et al (2013) Degradation of selected organophosphate pesticides in wastewater by dielectric barrier discharge plasma. Bull Environ Contam Toxicol 91:314–319. doi:10.1007/s00128-013-1048-x

Huey R, Morris GM, Olson AJ, Goodsell DS (2007) A semiempirical free energy force field with charge-based desolvation. J Comput Chem 28:1145–1152. doi:10.1002/jcc.20634

Ikehata K, El-Din MG (2006) Aqueous pesticide degradation by hydrogen peroxide/ultraviolet irradiation and Fenton-type advanced oxidation processes: a review. J Environ Eng Sci 5:81–135. doi:10.1139/S05-046

Iyer R, Iken B (2015) Protein engineering of representative hydrolytic enzymes for remediation of organophosphates. Biochem Eng J 94:134–144. doi:10.1016/j.bej.2014.11.010

Jackson C, Kim H-K, Carr PD et al (2005) The structure of an enzyme–product complex reveals the critical role of a terminal hydroxide nucleophile in the bacterial phosphotriesterase mechanism. Biochim Biophys Acta BBA - Proteins Proteomics 1752:56–64. doi:10.1016/j.bbapap.2005.06.008

Jackson CJ, Weir K, Herlt A et al (2009) Structure-based rational design of a phosphotriesterase. Appl Environ Microbiol 75:5153–5156. doi:10.1128/AEM.00629-09

Jaipieam S, Visuthismajarn P, Sutheravut P et al (2009) Organophosphate pesticide residues in drinking water from artesian wells and health risk assessment of agricultural communities, Thailand. Hum Ecol Risk Assess Int J 15:1304–1316. doi:10.1080/10807030903306984

Jeong Y-S, Choi JM, Kyeong H-H et al (2014) Rational design of organophosphorus hydrolase with high catalytic efficiency for detoxifying a V-type nerve agent. Biochem Biophys Res Commun 449:263–267. doi:10.1016/j.bbrc.2014.04.155

Jonidi-Jafari A, Shirzad-Siboni M, Yang J-K et al (2004) Photocatalytic degradation of diazinon with illuminated ZnO–TiO2 composite. J Taiwan Inst Chem Eng. doi:10.1016/j.jtice.2014.12.020

Josse D, Xie W, Masson P, Lockridge O (1999a) Human serum paraoxonase (PON1): identification of essential amino acid residues by group-selective labelling and site-directed mutagenesis. Chem Biol Interact 119–120:71–78. doi:10.1016/S0009-2797(99)00015-0

Josse D, Xie W, Renault F et al (1999b) Identification of residues essential for human paraoxonase (PON1) arylesterase/organophosphatase activities. Biochemistry (Mosc) 38:2816–2825. doi:10.1021/bi982281h

Kalakuntla RK, Wille T, Le Provost R et al (2013) New modified β-cyclodextrin derivatives as detoxifying agents of chemical warfare agents (I). Synthesis and preliminary screening: Evaluation of the detoxification using a half-quantitative enzymatic assay. Toxicol Lett 216:200–205. doi:10.1016/j.toxlet.2012.11.020

Kallnik V, Bunescu A, Sayer C et al (2014) Characterization of a phosphotriesterase-like lactonase from the hyperthermoacidophilic crenarchaeon Vulcanisaeta moutnovskia. J Biotechnol 190:11–17. doi:10.1016/j.jbiotec.2014.04.026

Kamiya M, Kameyama K (2001) Effects of selected metal ions on photodegradation of organophosphorus pesticides sensitized by humic acids. Chemosphere 45:231–235. doi:10.1016/S0045-6535(00)00573-7

Katsemi V, Lücke C, Koepke J et al (2005) Mutational and structural studies of the diisopropylfluorophosphatase from Loligo vulgaris shed new light on the catalytic mechanism of the enzyme†. Biochemistry (Mosc) 44:9022–9033. doi:10.1021/bi0500675

Khan A, Kotta S, Ansari S et al (2013) Recent advances in decontamination of chemical warfare agents. Def Sci J 63:487–496. doi:10.14429/dsj.63.2882

Khersonsky O, Roodveldt C, Tawfik DS (2006) Enzyme promiscuity: evolutionary and mechanistic aspects. Curr Opin Chem Biol 10:498–508. doi:10.1016/j.cbpa.2006.08.011

Khersonsky O, Rosenblat M, Toker L et al (2009) Directed evolution of serum paraoxonase PON3 by family shuffling and ancestor/consensus mutagenesis, and its biochemical characterization. Biochemistry (Mosc) 48:6644–6654. doi:10.1021/bi900583y

Kim S-M, Vogelpohl A (1998) Degradation of organic pollutants by the photo-fenton-process. Chem Eng Technol 187–191

Kim SH, Kim JH, Kang B-K (2007) Decomposition reaction of organophosphorus nerve agents on solid surfaces with atmospheric radio frequency plasma generated gaseous species. Langmuir 23:8074–8078. doi:10.1021/la700692t

Kim K, Tsay OG, Atwood DA, Churchill DG (2011) Destruction and detection of chemical warfare agents. Chem Rev 111:5345–5403. doi:10.1021/cr100193y

Kirby SD, Norris JR, Richard Smith J et al (2013) Human paraoxonase double mutants hydrolyze V and G class organophosphorus nerve agents. Chem Biol Interact 203:181–185. doi:10.1016/j.cbi.2012.10.023

Kondo Y, Ishigami A, Kubo S et al (2004) Senescence marker protein-30 is a unique enzyme that hydrolyzes diisopropyl phosphorofluoridate in the liver. FEBS Lett 570:57–62. doi:10.1016/j.febslet.2004.06.028

Konstantinou IK, Sakellarides TM, Sakkas VA, Albanis TA (2001) Photocatalytic degradation of selected s-Triazine herbicides and organophosphorus insecticides over aqueous TiO2 suspensions. Environ Sci Technol 35:398–405. doi:10.1021/es001271c

Lam MW, Tantuco K, Mabury SA (2003) PhotoFate: a new approach in accounting for the contribution of indirect photolysis of pesticides and pharmaceuticals in surface waters. Environ Sci Technol 37:899–907. doi:10.1021/es025902+

Lee J, Farha OK, Roberts J et al (2009) Metal–organic framework materials as catalysts. Chem Soc Rev 38:1450. doi:10.1039/b807080f

LeJeune KE, Russell AJ (1996) Covalent binding of a nerve agent hydrolyzing enzyme within polyurethane foams. Biotechnol Bioeng 51:450–457. doi:10.1002/(SICI)1097-0290(19960820)51:4<450::AID-BIT8>3.0.CO;2-H

LeJeune KE, Russell AJ (1999) Biocatalytic nerve agent detoxification in fire fighting foams. Biotechnol Bioeng 62:659–665. doi:10.1002/(SICI)1097-0290(19990320)62:6<659::AID-BIT5>3.0.CO;2-N

LeJeune KE, Mesiano AJ, Bower SB et al (1997) Dramatically stabilized phosphotriesterase—polymers for nerve agent degradation. Biotechnol Bioeng 54:105–114. doi:10.1002/(SICI)1097-0290(19970420)54:2<105::AID-BIT2>3.0.CO;2-P

LeJeune KE, Wild JR, Russell AJ (1998) Nerve agents degraded by enzymatic foams. Nature 395:27–28. doi:10.1038/25634

Lessenger JE, Reese BE (1999) Rational use of cholinesterase activity testing in pesticide poisoning. J Am Board Fam Pract 12:307–314. doi:10.3122/jabfm.12.4.307

Letort S, Mathiron D, Grel T et al (2015) The first 2 IB,3 IA-heterodifunctionalized β-cyclodextrin derivatives as artificial enzymes. Chem Commun 51:2601–2604. doi:10.1039/C4CC09189B

Li WF, Furlong CE, Costa LG (1995) Paraoxonase protects against chlorpyrifos toxicity in mice. Toxicol Lett 76:219–226. doi:10.1016/0378-4274(95)80006-Y

Li L, Wu Q, Guo Y, Hu C (2005) Nanosize and bimodal porous polyoxotungstate–anatase TiO2 composites: preparation and photocatalytic degradation of organophosphorus pesticide using visible-light excitation. Microporous Mesoporous Mater 87:1–9. doi:10.1016/j.micromeso.2005.07.035

Liu H, Zhang J-J, Wang S-J et al (2005) Plasmid-borne catabolism of methyl parathion and p-nitrophenol in Pseudomonas sp. strain WBC-3. Biochem Biophys Res Commun 334:1107–1114. doi:10.1016/j.bbrc.2005.07.006

Luo X-J, Kong X-D, Zhao J et al (2014) Switching a newly discovered lactonase into an efficient and thermostable phosphotriesterase by simple double mutations His250Ile/Ile263Trp. Biotechnol Bioeng 111:1920–1930. doi:10.1002/bit.25272

Mackness MI, Arrol S, Durrington PN (1991) Substrate specificity of human serum paraoxonase. Biochem Soc Trans 19:304S

Maher MJ, Ghosh M, Grunden AM et al (2004) Structure of the prolidase from Pyrococcus furiosus. Biochemistry (Mosc) 43:2771–2783. doi:10.1021/bi0356451

Manavathi B, Pakala SB, Gorla P et al (2005) Influence of zinc and cobalt on expression and activity of parathion hydrolase from Flavobacterium sp. ATCC27551. Pestic Biochem Physiol 83:37–45. doi:10.1016/j.pestbp.2005.03.007

Mansee AH, Chen W, Mulchandani A (2005) Detoxification of the organophosphate nerve agent coumaphos using organophosphorus hydrolase immobilized on cellulose materials. J Ind Microbiol Biotechnol 32:554–560. doi:10.1007/s10295-005-0059-y

Masurier N, Estour F, Froment M-T et al (2005) Synthesis of 2-substituted β-cyclodextrin derivatives with a hydrolytic activity against the organophosphorylester paraoxon. Eur J Med Chem 40:615–623. doi:10.1016/j.ejmech.2005.02.008

McDaniel CS, Harper LL, Wild JR (1988) Cloning and sequencing of a plasmid-borne gene (opd) encoding a phosphotriesterase. J Bacteriol 170:2306–2311

Mechrez G, Krepker MA, Harel Y et al (2014) Biocatalytic carbon nanotube paper: a "one-pot" route for fabrication of enzyme-immobilized membranes for organophosphate bioremediation. J Mater Chem B 2:915. doi:10.1039/c3tb21439g

Merone L, Mandrich L, Rossi M, Manco G (2005) A thermostable phosphotriesterase from the archaeon Sulfolobus solfataricus: cloning, overexpression and properties. Extremophiles 9:297–305. doi:10.1007/s00792-005-0445-4

Mohamed KA, Basfar AA, Al-Kahtani HA, Al-Hamad KS (2009) Radiolytic degradation of malathion and lindane in aqueous solutions. Radiat Phys Chem 78:994–1000. doi:10.1016/j.radphyschem.2009.06.003

Mondloch JE, Katz MJ, Isley WC III et al (2015) Destruction of chemical warfare agents using metal–organic frameworks. Nat Mater 14:512–516. doi:10.1038/nmat4238

Morris GM, Goodsell DS, Halliday RS et al (1998) Automated docking using a Lamarckian genetic algorithm and an empirical binding free energy function. J Comput Chem 19:1639–1662. doi:10.1002/(SICI)1096-987X(19981115)19:14<1639::AID-JCC10>3.0.CO;2-B

Mulbry WW, Karns JS, Kearney PC et al (1986) Identification of a plasmid-borne parathion hydrolase gene from Flavobacterium sp. by southern hybridization with opd from Pseudomonas diminuta. Appl Environ Microbiol 51:926–930

Müller S, Koller M, Le Provost R et al (2011) In vitro detoxification of cyclosarin (GF) by modified cyclodextrins. Toxicol Lett 200:53–58. doi:10.1016/j.toxlet.2010.10.014

Muñoz A, Person AL, Calvé SL et al (2011) Studies on atmospheric degradation of diazinon in the EUPHORE simulation chamber. Chemosphere 85:724–730. doi:10.1016/j.chemosphere.2011.06.044

Nakayama K, Ishikawa S, Kawahara K et al (2014) Improvement of organophosphorus hydrolase activity toward nerve agents by amino acid substitutions. Forensic Toxicol. doi:10.1007/s11419-013-0223-4

Naqvi T, Warden AC, French N et al (2014) A 5000-fold increase in the specificity of a bacterial phosphotriesterase for malathion through combinatorial active site mutagenesis. PLoS One 9, e94177. doi:10.1371/journal.pone.0094177

National Research Council US (1994) Recommendations for the disposal of chemical agents and munitions. National Academy Press, Washington, DC

National Research Council US (1996) Review and evaluation of alternative chemical disposal technologies. National Academy Press, Washington, DC

Ningfeng W, Minjie D, Guoyi L et al (2004) Cloning and expression of ophc2, a new organphosphorus hydrolase gene. Chin Sci Bull 49:1245–1249. doi:10.1360/04wc0146

Nowakowska M, Sterzel M, Zapotoczny S, Kot E (2005) Photosensitized degradation of ethyl parathion pesticide in aqueous solution of anthracene modified photoactive dextran. Appl Catal B Environ 57:1–8. doi:10.1016/j.apcatb.2004.10.002

Ohuchi S, Nakamura H, Sligiura H et al (1997) An optical resolution of racemic organophosphorous esters by phosphotriesterase-catalyzing hydrolysis. Appl Biochem Biotechnol 63–65:659–665. doi:10.1007/BF02920464

Organisation for the Prohibition of Chemical Weapons (2005) Convention on the prohibition of the development, production, stockpiling and use of chemical weapons and on their destruction, 3rd edn. The Technical Secretariat of the Organisation for the Prohibition of Chemical Weapons, Hague

Otto TC, Kasten SA, Kovaleva E et al (2010) Purification and characterization of functional human paraoxonase-1 expressed in Trichoplusia ni larvae. Chem Biol Interact 187:388–392. doi:10.1016/j.cbi.2010.02.022

Patel V, Ramasundarahettige C, Vijayakumar L et al (2012) Suicide mortality in India: a nationally representative survey. Lancet 379:2343–2351. doi:10.1016/S0140-6736(12)60606-0

Pearson GS, Magee RS (2002) Critical evaluation of proven chemical weapon destruction technologies (IUPAC Technical Report). Pure Appl Chem 74:187–316

Peterson MW, Fairchild SZ, Otto TC et al (2011) VX Hydrolysis by human serum paraoxonase 1: a comparison of experimental and computational results. PLoS One 6, e20335. doi:10.1371/journal.pone.0020335

Raynes JK, Pearce FG, Meade SJ, Gerrard JA (2011) Immobilization of organophosphate hydrolase on an amyloid fibril nanoscaffold: towards bioremediation and chemical detoxification. Biotechnol Prog 27:360–367. doi:10.1002/btpr.518

Reddy PVL, Kim K-H (2015) A review of photochemical approaches for the treatment of a wide range of pesticides. J Hazard Mater 285:325–335. doi:10.1016/j.jhazmat.2014.11.036

Reddy ST, Wadleigh DJ, Grijalva V et al (2001) Human paraoxonase-3 is an HDL-associated enzyme with biological activity similar to paraoxonase-1 protein but is not regulated by oxidized lipids. Arterioscler, Thromb, Vasc Biol 21:542–547. doi:10.1161/01.ATV.21.4.542

Richins RD, Kaneva I, Mulchandani A, Chen W (1997) Biodegradation of organophosphorus pesticides by surface-expressed organophosphorus hydrolase. Nat Biotechnol 15:984–987. doi:10.1038/nbt1097-984

Richins RD, Mulchandani A, Chen W (2000) Expression, immobilization, and enzymatic characterization of cellulose-binding domain-organophosphorus hydrolase fusion enzymes. Biotechnol Bioeng 69:591–596. doi:10.1002/1097-0290(20000920)69:6<591::AID-BIT2>3.0.CO;2-X

Rochu D, Chabrière E, Masson P (2007) Human paraoxonase: a promising approach for pre-treatment and therapy of organophosphorus poisoning. Toxicology 233:47–59. doi:10.1016/j.tox.2006.08.037

Roodveldt C, Tawfik DS (2005) Directed evolution of phosphotriesterase from Pseudomonas diminuta for heterologous expression in Escherichia coli results in stabilization of the metal-free state. Protein Eng, Des Sel 18:51–58. doi:10.1093/protein/gzi005

Rougier NM, Cruickshank DL, Vico RV et al (2011) Effect of cyclodextrins on the reactivity of fenitrothion. Carbohydr Res 346:322–327. doi:10.1016/j.carres.2010.06.016

Rowland SS, Speedie MK, Pogell BM (1991) Purification and characterization of a secreted recombinant phosphotriesterase (parathion hydrolase) from Streptomyces lividans. Appl Environ Microbiol 57:440–444

Rowland SS, Zulty JJ, Sathyamoorthy M et al (1992) The effect of signal sequences on the efficiency of secretion of a heterologous phosphotriesterase by Streptomyces lividans. Appl Microbiol Biotechnol 38:94–100. doi:10.1007/BF00169426

Sambrook MR, Notman S (2013) Supramolecular chemistry and chemical warfare agents: from fundamentals of recognition to catalysis and sensing. Chem Soc Rev 42:9251. doi:10.1039/c3cs60230c

Scharff EI, Koepke J, Fritzsch G et al (2001a) Crystal structure of diisopropylfluorophosphatase from Loligo vulgaris. Structure 9: 493–502. doi:10.1016/S0969-2126(01)00610-4

Scharff EI, Lücke C, Fritzsch G et al (2001b) Crystallization and preliminary X-ray crystallographic analysis of DFPase from *Loligo vulgaris*. Acta Crystallogr D Biol Crystallogr 57:148–149. doi:10.1107/S0907444900014232

Schofield DA, DiNovo AA (2010) Generation of a mutagenized organophosphorus hydrolase for the biodegradation of the organophosphate pesticides malathion and demeton-S. J Appl Microbiol. doi:10.1111/j.1365-2672.2010.04672.x

Schomburg PDD, Stephan DD (1998) Aryldialkylphosphatase. In: Schomburg PDD, Stephan DD (eds) Enzyme handbook 15. Springer, Berlin, pp 201–206

Scott SH, Bahnson BJ (2011) Senescence marker protein 30: functional and structural insights to its unknown physiological function. Biomol Concepts 2:469–480

Segal-Rosenheimer M, Dubowski Y (2010) Photolysis of methyl-parathion thin films: products, kinetics and quantum yields under different atmospheric conditions. J Photochem Photobiol Chem 209:193–202. doi:10.1016/j.jphotochem.2009.11.014

Seibert CM, Raushel FM (2005) Structural and catalytic diversity within the amidohydrolase superfamily†. Biochemistry (Mosc) 44:6383–6391. doi:10.1021/bi047326v

Serdar CM, Gibson DT, Munnecke DM, Lancaster JH (1982) Plasmid involvement in parathion hydrolysis by Pseudomonas diminuta. Appl Environ Microbiol 44:246–249

Sethunathan N, Yoshida T (1973) A Flavobacterium sp. that degrades diazinon and parathion. Can J Microbiol 19:873–875. doi:10.1139/m73-138

Shen Y, Lu P, Mei H et al (2010) Isolation of a methyl parathion-degrading strain Stenotrophomonas sp. SMSP-1 and cloning of the ophc2 gene. Biodegradation 21:785–792. doi:10.1007/s10532-010-9343-2

Sinderhauf K, Schwack W (2003) Photolysis experiments on phosmet, an organophosphorus insecticide. J Agric Food Chem 51:5990–5995. doi:10.1021/jf034253y

Singh B, Prasad GK, Pandey KS et al (2010) Decontamination of chemical warfare agents (review article). Def Sci J 60:428–441. doi:10.14429/dsj.60.487

Sode K, Nakamura H (1997) Compatibility of phosphotriesterase from Flavobacterium sp. with detergents. Biotechnol Lett 19:1239–1242. doi:10.1023/A:1018402407802

Steiert JG, Pogell BM, Speedie MK, Laredo J (1989) A gene coding for a membrane-bound hydrolase is expressed as a secreted, soluble enzyme in Streptomyces lividans. Nat Biotechnol 7:65–68. doi:10.1038/nbt0189-65

Štěpánková A, Dušková J, Skálová T et al (2013) Organophosphorus acid anhydrolase from Alteromonas macleodii: structural study and functional relationship to prolidases. Acta Crystallograph Sect F Struct Biol Cryst Commun 69:346–354. doi:10.1107/S1744309113002674

Suthiwangcharoen N, Nagarajan R (2014) Enhancing enzyme stability by construction of polymer–enzyme conjugate micelles for decontamination of organophosphate agents. Biomacromolecules 15:1142–1152. doi:10.1021/bm401531d

Szinicz L (2005) History of chemical and biological warfare agents. Toxicology 214:167–181. doi:10.1016/j.tox.2005.06.011

Taysse L, Daulon S, Delamanche S et al (2007) Skin decontamination of mustards and organophosphates: comparative efficiency of RSDL and Fuller's earth in domestic swine. Hum Exp Toxicol 26:135–141

Theriot CM, Grunden AM (2010) Hydrolysis of organophosphorus compounds by microbial enzymes. Appl Microbiol Biotechnol 89:35–43. doi:10.1007/s00253-010-2807-9

Theriot CM, Tove SR, Grunden AM (2009) Characterization of two proline dipeptidases (prolidases) from the hyperthermophilic archaeon Pyrococcus horikoshii. Appl Microbiol Biotechnol 86: 177–188. doi:10.1007/s00253-009-2235-x

Theriot CM, Du X, Tove SR, Grunden AM (2010) Improving the catalytic activity of hyperthermophilic Pyrococcus prolidases for detoxification of organophosphorus nerve agents over a broad range of temperatures. Appl Microbiol Biotechnol 87:1715–1726. doi:10.1007/s00253-010-2614-3

Theriot CM, Semcer RL, Shah SS, Grunden AM (2011) Improving the catalytic activity of hyperthermophilic *Pyrococcus horikoshii* prolidase for detoxification of organophosphorus nerve agents over a broad range of temperatures. Archaea 2011, e565127. doi:10.1155/2011/565127

Tokuriki N, Tawfik DS (2009) Stability effects of mutations and protein evolvability. Curr Opin Struct Biol 19:596–604. doi:10.1016/j.sbi.2009.08.003

Tucker M (2014) Reduced weight decontamination formulation for neutralization of chemical and biological warfare agents. Patent US 8, 741,174 B1.

Tucker M, Comstock R (2004) Decontamination formulation with sorbent additive. Patent US 2004/0022867 A1.

Tucker M, Engler D (2005) Decontamination formulations for disinfection and sterilization. Patent US 2005/0109981 A1.

Tuorinsky SD, Caneva DC, Sidell FR (2009) Triage of chemical casualties. In: Chemical aspects of chemical warfare. Walter Reed Army Medical Center Borden Institute, Washington DC, pp 511–526

Vanhooke JL, Benning MM, Raushel FM, Holden HM (1996) Three-dimensional structure of the zinc-containing phosphotriesterase with the bound substrate analog diethyl 4-methylbenzylphosphonate. Biochemistry (Mosc) 35:6020–6025. doi:10.1021/bi960325l

Vecchio P, Elias M, Merone L et al (2009) Structural determinants of the high thermal stability of SsoPox from the hyperthermophilic archaeon Sulfolobus solfataricus. Extremophiles 13:461–470. doi:10.1007/s00792-009-0231-9

Vyas NK, Nickitenko A, Rastogi VK et al (2010) Structural insights into the dual activities of the nerve agent degrading organophosphate anhydrolase/prolidase. Biochemistry (Mosc) 49:547–559. doi:10.1021/bi9011989

Wales ME, Reeves TE (2012) Organophosphorus hydrolase as an in vivo catalytic nerve agent bioscavenger. Drug Test Anal 4:271–281. doi:10.1002/dta.381

Wan HB, Wong MK, Mok CY (1994) Comparative study on the quantum yields of direct photolysis of organophosphorus pesticides in aqueous solution. J Agric Food Chem 42:2625–2630. doi:10.1021/jf00047a046

Wang S-H, Liu M, Chi M-G et al (2004) Production of human liver prolidase by Saccharomyces cerevisiae as host cells. Acta Pharmacol Sin 25:794–800

Wang SH, Zhi QW, Sun MJ (2006) Dual activities of human prolidase. Toxicol In Vitro 20:71–77. doi:10.1016/j.tiv.2005.06.003

Watkins LM, Mahoney HJ, McCulloch JK, Raushel FM (1997) Augmented hydrolysis of diisopropyl fluorophosphate in engineered mutants of phosphotriesterase. J Biol Chem 272: 25596–25601. doi:10.1074/jbc.272.41.25596

Wille T, Tenberken O, Reiter G et al (2009) Detoxification of nerve agents by a substituted β-cyclodextrin: application of a modified biological assay. Toxicology 265:96–100. doi:10.1016/j.tox.2009.09.018

Wille T, Scott C, Thiermann H, Worek F (2012) Detoxification of G- and V-series nerve agents by the phosphotriesterase OpdA. Biocatal Biotransformation 30:203–208. doi:10.3109/10242422.2012.661724

Wu C, Linden KG (2010) Phototransformation of selected organophosphorus pesticides: roles of hydroxyl and carbonate radicals. Water Res 44:3585–3594. doi:10.1016/j.watres.2010.04.011

Xiang DF, Kolb P, Fedorov AA et al (2009) Functional annotation and three-dimensional structure of Dr0930 from Deinococcus radiodurans, a close relative of phosphotriesterase in the amidohydrolase superfamily†‡. Biochemistry (Mosc) 48:2237–2247. doi:10.1021/bi802274f

Xie J, Zhao Y, Zhang H et al (2014) Improving methyl parathion hydrolase to enhance its chlorpyrifos-hydrolysing efficiency. Lett Appl Microbiol 58:53–59. doi:10.1111/lam.12155

Yang Y-C (1999) Chemical detoxification of nerve agent VX. Acc Chem Res 32:109–115. doi:10.1021/ar970154s

Yang J, Yang C, Jiang H, Qiao C (2008) Overexpression of methyl parathion hydrolase and its application in detoxification of organophosphates. Biodegradation 19:831–839. doi:10.1007/s10532-008-9186-2

Yeung DT, Josse D, Nicholson JD et al (2004) Structure/function analyses of human serum paraoxonase (HuPON1) mutants designed from a DFPase-like homology model. Biochim Biophys Acta BBA - Proteins Proteomics 1702:67–77. doi:10.1016/j.bbapap.2004.08.002

Zhang R, Cui Z, Zhang X et al (2006) Cloning of the organophosphorus pesticide hydrolase gene clusters of seven degradative bacteria isolated from a methyl parathion contaminated site and evidence of their horizontal gene transfer. Biodegradation 17:465–472. doi:10.1007/s10532-005-9018-6

Zhang Y, An J, Ye W et al (2012) Enhancing the promiscuous phosphotriesterase activity of a thermostable lactonase (GkaP) for the efficient degradation of organophosphate pesticides. Appl Environ Microbiol 78:6647–6655. doi:10.1128/AEM.01122-12

Zhongli C, Shunpeng L, Guoping F (2001) Isolation of methyl parathion-degrading strain M6 and cloning of the methyl parathion hydrolase gene. Appl Environ Microbiol 67:4922–4925. doi:10.1128/AEM.67.10.4922-4925.2001

Zuo G-M, Cheng Z-X, Li G-W et al (2007) Study on photolytic and photocatalytic decontamination of air polluted by chemical warfare agents (CWAs). Chem Eng J 128:135–140. doi:10.1016/j.cej.2006.10.006

Zwiener RJ, Ginsburg CM (1988) Organophosphate and carbamate poisoning in infants and children. Pediatrics 81:121–126

I. Synthèse bibliographique

2. Des enzymes pour bloquer la communication bactérienne

2. Des enzymes pour bloquer la communication bactérienne

La communication bactérienne, aussi appelée quorum sensing (QS), permet à une population bactérienne de coordonner un comportement global, et ainsi d'opérer comme une unité multicellulaire[44]. Le QS est lié à la densité bactérienne et est régulé par des autoinducteurs (AIs), qui sont produits lors de la croissance bactérienne et sont excrétés par les bactéries. L'accumulation des AIs dans l'environnement est perçue en continu par les bactéries mais ce n'est que lorsqu'une concentration seuil est atteinte que l'expression de certains gènes est induite entraînant un changement du comportement des bactéries. Par ce système de communication les bactéries peuvent synchroniser leurs comportements à l'échelle de la population bactérienne. Cela induit un changement de phénotypes, avec notamment l'expression de facteurs de virulence, la formation de biofilm, la production de protéases, de sidérophores, de bioluminescence et d'autres paramètres variant selon les espèces[44–46].

Les molécules signal du QS (AIs) sont d'une grande diversité chimique, la plupart sont des petites molécules organiques (moins de 1 000 Da) ou des peptides comportant de 5 à 20 acides aminés **(Figure 4A)**[46]. Les AHLs sont les signaux majoritaires chez les bactéries Gram négatif et ont été retrouvées chez plus de soixante-dix espèces[45,47] **(Table 1)**. D'autres AIs sont utilisés de façon minoritaire chez les bactéries Gram négatif, tels que les PQS (*Pseudomonas* quinolone signal), les DSFs (Diffusible signal factor) ou les AI-3. Certaines molécules signal, comme les AI-2, sont employées chez des bactéries Gram négatif et positif. Les molécules signal AIP (Autoinducer peptide) sont retrouvées chez les bactéries Gram positif **(Table 1** et **Figure 4A)**.

Table 1 : Les différents types d'AIs.

Autoinducteur (AI)	Nature de l'AI	Gram	Bactéries (exemples)	Références
AHL (Acylhomosérine lactone)	Acyl-homosérine lactone	Négatif	*Acinetobacter sp., Aeromonas sp., Erwinia sp.* ou *Vibrio sp.*	45,47
PQS (*Pseudomonas* quinolone signal)	2-heptyl-3-hydroxy-4-quinolone	Négatif	*Pseudomonas aeruginosa*	44,48
DSF (Diffusible signal factor)	Acide méthyl-dodécénoïque	Négatif	*Xanthomonas campestris* ou *Stenotrophomonas maltophilia*	47
AI-3 (Autoinducer-3)	Aromatique	Négatif	*Escherichia coli* ou *Klebsiella pneumoniae*	49,50
AI-2 (Autoinducer-2)	Furanosyl borate diester	Négatif/Positif	*Vibrio harveyi*, *Salmonella enterica* ou *Enterococcus faecalis*	51,52
AIP (Autoinducer Peptide)	Oligopeptide	Positif	*Staphylococcus aureus* ou *Bacillus subtilis*	53,54

Une fois la concentration seuil atteinte l'intégration des AIs se fait de façon intracellulaire pour les AHLs et extracellulaire via des récepteurs pour AI-2 et AIPs **(Figure 4B)**. Cette interaction va déclencher une cascade de signalisation, différente selon la bactérie, entrainant l'expression de multiples gènes impliqués dans le QS[55].

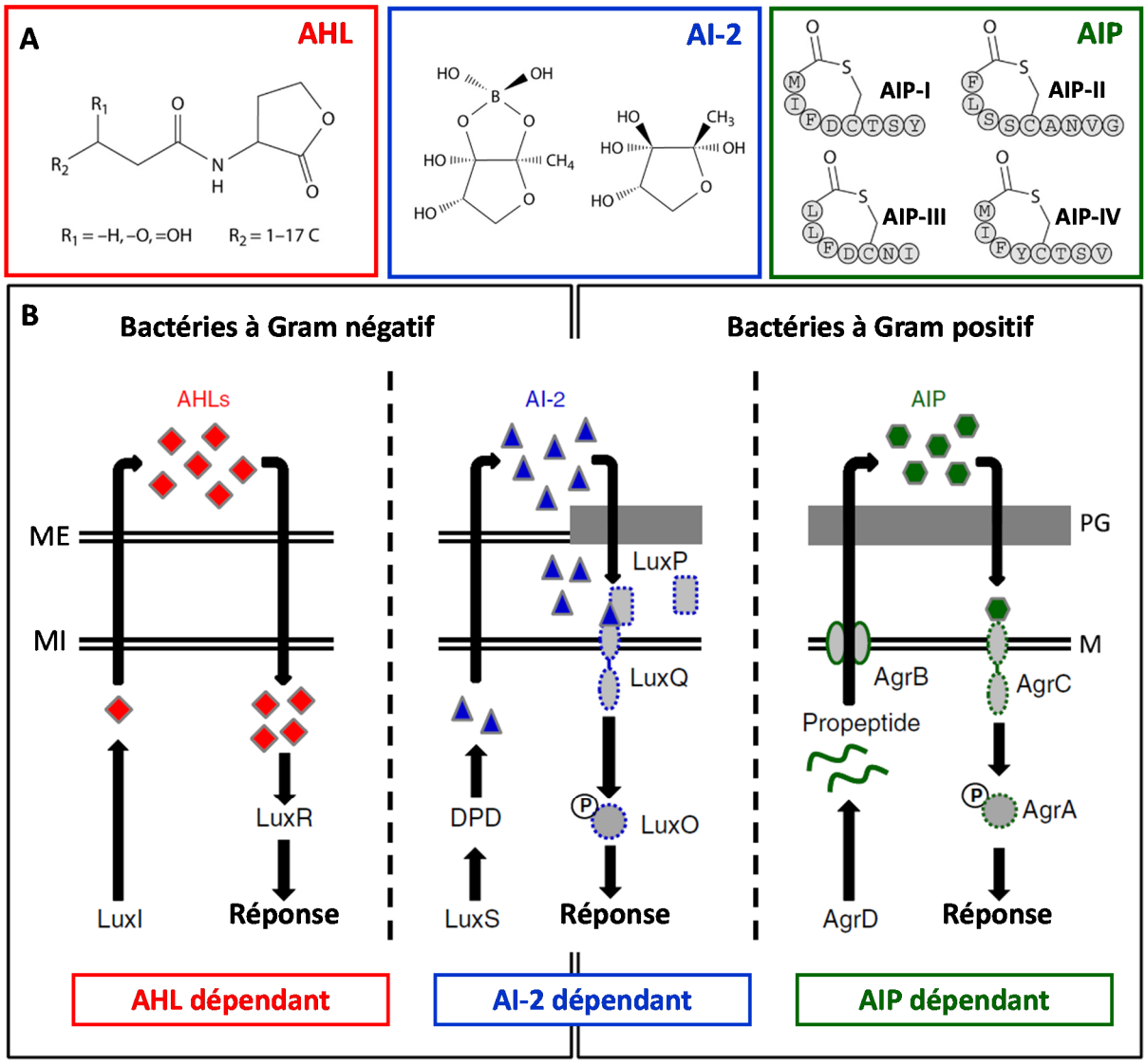


Figure 4 : Autoinducteurs et QS bactériens.
(A) Structures des différents types d'AIs. **(B)** Les trois systèmes principaux de QS chez les bactéries Gram négatif et Gram positif ; QS AHL, AI-2 et AIP dépendant. ME correspond à la membrane externe, MI à la membrane interne, PG au peptidoglycane et M à la membrane. Adapté d'Eberl et al. (2011) et de LaSarre et al. (2013)[50,55].

Plusieurs mécanismes de communication ont donc été mis en évidence. Les bactéries utilisent dans leurs réseaux de signalisation des combinaisons plus ou moins complexes de ces systèmes pouvant être organisés de manière hiérarchique ou parallèle[46]. La bactérie *V. harveyi* utilise par exemple trois AIs distincts intégrés dans une même cascade de régulation. La bactérie *P. aeruginosa* utilise quant à elle deux circuits LuxIR fonctionnant avec deux AHLs en série ainsi que deux autres types d'AIs moins répandus (PQS et IQS, Integrated QS Signal). La bactérie Gram positif *B. subtilis* fonctionne avec deux AIPs en réseau. Quant à *Agrobacterium tumefaciens* son système de QS est activé uniquement à proximité de son hôte[45,56]. Outre de permettre la communication intra-espèces, les AIs sont également impliqués dans la communication inter-espèces, et dans l'interaction avec l'hôte[57–59].

De nombreuses études ont montré le rôle fondamental du QS pour un contrôle global de la physiologie des populations bactériennes. Ainsi, interférer avec le QS permettrait de perturber l'organisation des bactéries et les empêcher de former des biofilms ou d'entrer dans des phases

virulentes. Le QS jouant un rôle important dans l'organisation et la virulence des bactéries, de nombreuses stratégies ont émergé pour renforcer l'arsenal antimicrobien. Ces stratégies sont rassemblées sous le terme quorum quenching (QQ) regroupant l'ensemble des processus capables d'interférer avec le QS. Le QQ pourrait donc être une stratégie potentielle dans des applications industrielles ou thérapeutiques. Le QQ peut être obtenu de différentes façons soit en empêchant la synthèse de l'AI, soit en dégradant l'AI, soit en empêchant la reconnaissance de l'AI par ses récepteurs[60]. Différentes molécules sont utilisées comme inhibiteurs du QS, cela peut être des petites molécules naturelles ou synthétiques (comme les QSI, QS Inhibitor) ou de grosses molécules biologiques (comme des enzymes)[61,62].

Ces recherches ont fait l'objet d'une revue sur l'utilisation d'enzymes pour le QQ et leurs applications ; notamment du potentiel de *Sso*Pox, une enzyme prometteuse pour des applications de QQ. Cette revue regroupe les principales applications pour lesquelles le QQ enzymatique peut apporter une solution innovante. Ces enzymes sont particulièrement intéressantes car elles perturbent le QS de façon catalytique et sans entrer dans la cellule. Elles ne sont pas toxiques pour l'environnement et sont biodégradables. Dans les domaines de l'agriculture et de l'aquaculture, elles représentent une alternative ou un complément aux pesticides pour traiter certains pathogènes des plantes, et de réduire les infections bactériennes dues à certains pathogènes chez les poissons. Les enzymes du QQ peuvent aussi être utilisées pour leur rôle anti-fouling au niveau des membranes de bioréacteurs et des filtres, et également pour lutter contre le biofouling marin. En effet le biofouling est l'accumulation de micro-organismes, de plantes, d'algues ou d'animaux sur les surfaces humides ; cette accumulation débute par la formation d'un biofilm bactérien en partie régulée par le QS[63]. De nombreuses perspectives existent aussi dans le domaine médical avec l'utilisation d'enzymes sur des membranes, des cathéters, en traitements topiques ou par aérosolisation dans le but de réduire les infections nosocomiales (aussi appelées Infections Associées aux Soins, IAS). Le QQ est potentiellement très intéressant car contrairement aux antibiotiques le QQ par voie enzymatique n'a pas d'effet bactéricide diminuant ainsi la pression de sélection et permettant de limiter l'apparition de résistance. Une utilisation complémentaire du QQ et des antibiotiques semble être une solution extrêmement prometteuse, permettant de réduire les doses d'antibiotiques administrées. Il en va de même au niveau de l'anti-fouling, en effet les biocides sont réglementés et pour certains prohibés (directives européennes n°89/677/CEE et n°98/8/CE). Néanmoins, les enzymes, souvent fragiles, ont fréquemment vu leur potentiel applicatif limité car incompatible avec les procédés industrielles. Pour pallier à ces limitations, les enzymes hyperthermostables, telle que *Sso*Pox, ont été considérées. Ces enzymes ont, entre autre, une grande stabilité compatible avec des contraintes industrielles et économiques.

J'ai participé à la réalisation de cette synthèse bibliographique en rédigeant la partie sur l'aquaculture.

Chemico-Biological Interactions xxx (2016) 1–12

Contents lists available at ScienceDirect

Chemico-Biological Interactions

journal homepage: www.elsevier.com/locate/chembioint

Biotechnological applications of quorum quenching enzymes

Janek Bzdrenga [a, 1], David Daudé [b, 1], Benjamin Rémy [a, b], Pauline Jacquet [a], Laure Plener [b], Mikael Elias [c], Eric Chabrière [a, *]

[a] Aix Marseille Université, URMITE, UM63, CNRS 7278, IRD 198, INSERM 1095, Marseille, France
[b] Gene&GreenTK, Faculté de Médecine, 27 boulevard Jean Moulin, 13385 Marseille Cedex 5, France
[c] University of Minnesota, Department of Biochemistry, Molecular Biology and Biophysics & Biotechnology Institute, St. Paul, MN 55108, USA

ARTICLE INFO

Article history:
Received 2 March 2016
Received in revised form
4 May 2016
Accepted 20 May 2016
Available online xxx

Keywords:
Quorum sensing
Quorum quenching
Enzyme
Lactonase
Virulence
Biofilm

ABSTRACT

Numerous bacteria use quorum sensing (QS) to synchronize their behavior and monitor their population density. They use signaling molecules known as autoinducers (AI's) that are synthesized and secreted into their local environment to regulate QS-dependent gene expression. Among QS-regulated pathways, biofilm formation and virulence factor secretion are particularly problematic as they are involved in surface-attachment, antimicrobial agent resistance, toxicity, and pathogenicity. Targeting QS represents a promising strategy to inhibit undesirable bacterial traits. This strategy, referred to as quorum quenching (QQ), includes QS-inhibitors and QQ enzymes. These approaches are appealing because they do not directly challenge bacterial survival, and consequently selection pressure may be low, yielding a lower occurrence of resistance. QQ enzymes are particularly promising because they act extracellularly to degrade AI's and can be used in catalytic quantities. This review draws an overview of QQ enzyme related applications, covering several economically important fields such as agriculture, aquaculture, biofouling and health issues. Finally, the possibility of resistance mechanism occurrence to QQ strategies is discussed.

© 2016 Elsevier Ireland Ltd. All rights reserved.

1. Introduction

Bacterial communication, referred to as quorum sensing (QS), is the molecular mechanism by which bacteria sense their overall population density, allowing them to synchronize their behavior [1]. Bacteria produce small molecules known as autoinducers (AI's) which are secreted in the environment and can be perceived by specific receptors within neighboring cells. This mechanism regulates gene expression patterns [2]. The response of microorganisms to QS is organism-dependent, but some traits are commonly regulated through QS, such as: production of antibiotics, exopolysaccharides, or exoenzymes, expression of secretion systems, swarming motility, and biofilm formation.

This review first summarizes the main aspects of bacterial QS and its implications in virulence and biofilm formation. Consequently, disrupting QS is particularly promising to modify bacterial behavior and moderate their undesirable traits. Different strategies have been considered for this purpose, including the use of QS inhibitors (QSI's) or quorum quenching (QQ) enzymes. Special attention is then dedicated to applications involving QQ enzymes in various fields such as agriculture, animal and human health, and antifouling. The phosphotriesterase-like lactonase (PLL) family is then discussed as many of these enzymes have been found in extreme environments conferring attractive biotechnological capabilities. In addition, the possibility of resistance mechanisms to QQ strategies is discussed. The strengths and the weaknesses of this approach are emphasized in light of recently published research.

2. Quorum sensing

Several autoinducers have been identified as QS molecules. Gram-positive bacteria mainly use autoinducing peptides (AIP's), also referred to as peptide-pheromones, which are specific to species and strains. Gram-negative bacteria use different types of QS systems: (i) acyl homoserine lactones (AHL's), also known as autoinducer-1 (AI-1), are mostly produced by Gram-negative bacteria: it is a molecule composed of a lactone ring and an aliphatic chain whose length and nature may vary (e.g. *Pseudomonas* spp., *Acinetobacter* spp., *Burkholderia* spp.), (ii) autoinducer-2 (AI-2), a

* Corresponding author.
E-mail address: eric.chabriere@univ-amu.fr (E. Chabrière).
[1] Contributed equally to the work.

http://dx.doi.org/10.1016/j.cbi.2016.05.028
0009-2797/© 2016 Elsevier Ireland Ltd. All rights reserved.

Please cite this article in press as: J. Bzdrenga, et al., Biotechnological applications of quorum quenching enzymes, Chemico-Biological Interactions (2016), http://dx.doi.org/10.1016/j.cbi.2016.05.028

furanosyl-borate diester which is found in a wide range of both Gram-negative and Gram-positive bacteria (e.g. *Vibrio* spp., *Pectobacterium* spp.), (iii) AI-3 (epinephrine and norepinephrine) are commonly found in human opportunistic pathogens (e.g. *Enterobacter* spp., *Escherichia* spp., *Klebsiella* spp., *Salmonella* spp.). Other molecules such as (iv) fatty acids (*Xanthomonas* spp.), (v) esters (*Ralstonia* spp.), (vi) α-hydroxy-ketones (*Legionella* spp., *Vibrio* spp.) or (vii) quinolones (*Pseudomonas* spp.) have also been reported [3–9]. Numerous Gram-negative bacteria utilize more than one QS system and may combine these systems either in additive models [10,11], or in hierarchical models when one system induces a second one [12], or with distinct or partially overlapping systems [13]. Considering the variety of signals and complexity of signaling networks, QS is a sophisticated communication system used by bacteria to sense their population density and their surrounding environment [14].

Bacterial pathogens represent increasing concern to human health due to the rapid dissemination of antibiotic-resistant strains. Infections with these pathogens result in increased lethality risks and greater costs for health care systems. In several bacterial pathogens, QS is involved in the switch between commensal, or saprophytic lifestyles, to pathogenic cycles. This is the case for *Pseudomonas aeruginosa* which is naturally present in water and humid environments. Moreover, *P. aeruginosa* is an opportunistic human pathogen that can proliferate in wounds; in such confined environments, QS signals accumulate and QS is triggered leading to the expression of virulence factors and the development of disease [15].

Bacterial pathogens also represent great financial burdens in industries other than health care. For example, bacterial infections of plants result in significant economic losses in agriculture [16]. The most widespread plant bacterial pathogens were recently listed according to their economic or scientific impact (e.g. *Ralstonia solanacearum*, *Xanthomonas* spp., *Pseudomonas syringae* pv., *Erwinia amylovora*) [17,18]. All of the selected bacteria use complex regulation networks where QS plays a central role to induce virulence. Additionally, fish or crustacean bacterial pathogens (e.g. *Vibrio* spp. [19,20]) have economic impacts in aquaculture, causing losses in livestock and contaminations that may be spread to humans.

QS also regulates the formation of biofilms. Biofilms are a specific mode of life where bacteria adhere to a surface and stick together. They build communities embedded in extracellular polymeric substances mainly made of DNA, proteins and polysaccharides that confer protection to environmental stresses (UV, desiccation, antimicrobial compounds). Biofilms are particularly challenging as they can be formed on a wide range of surfaces, biotic or abiotic, and they contribute to the virulence and resistance of bacteria affecting numerous industries, spanning health care (contamination of medical devices), fisheries, and the oil industry [21–25].

Interfering with QS is an attractive strategy to inhibit biofilm formation and limit the pathogenicity of bacteria. This strategy was first described in 2000 through the identification of an enzyme that degrades AHL QS signal molecules [26]. Two QQ strategies can be distinguished: (i) to prevent bacteria from producing or perceiving QS signals and (ii) to degrade QS signals. The first strategy is mainly based on the identification of molecules QSI's by screening natural compounds that will inhibit QS by different means. Halogenated furanones are one of the most common families of QSI's and they were first isolated from a red macroalga, *Delisea pulchra* [27]. Further studies showed that they both target AHL's or AI-2 mediated QS with distinct modes of action: they reduce the stability or binding affinity of the LuxR regulator and they inhibit the synthase, LuxS, by covalent interaction to prevent AI-2 synthesis [28–30]. Many screens have already been performed to identify such molecules. Most results were obtained in laboratory conditions but few direct applications using QQ compounds have been described. Following the example of QSI's, QQ enzymes have also been investigated for their ability to disrupt QS without the need to enter the bacterial cell. Among these, AHL-lactonases, acylases, or oxidoreductases have proved to display QQ activities. The next section is focused on the description of QQ biotechnological applications.

3. Applications

3.1. Plant pathogens

Bacterial plant pathogens rely on sophisticated regulation networks to synchronize the infection process and induce specific virulence factors when in contact with the host plant. Besides the perception of plant signals or nutrient availability, QS plays an essential role in the establishment of the pathogenic cycle. Therefore, QQ strategies are now considered as possible alternatives or complementary strategies to the use of pesticides [17]. Depending on the bacterial pathogens, different QS signaling molecules are produced: AHL's for *Agrobacterium tumefaciens*, *Dickeya* spp., *Erwinia* spp., *Pantoea* spp., *Pectobacterium* spp. and *P. syringae*; AI-2 for *Erwinia* spp., *Pantoea* spp., *Pectobacterium* spp., 3-hydroxypalmitate methyl ester (3-OH-PAME) for *R. solanacearum*, and diffusible signal factors (DSF family) for *Xanthomonas* spp. and *Xylella fastidiosa* [31]. Most of these signals can be degraded by QQ enzymes: an esterase produced by the soil bacterium *Ideonella* sp. 0-0013 degrades 3-OH-PAME from *R. solanacearum*, the enzyme CarAB (a carbamoyl phosphate synthetase) produced by several *Pseudomonas* spp. degrades DSF signals. Lactonases or acylases are produced by many organisms to degrade AHL signals [32,33].

Some soil bacteria such as *A. tumefaciens* or *Bacillus* sp. naturally produce lactonases to degrade AHL's [26,34,35]. For example *Bacillus thuringiensis* was shown to produce a lactonase, called AiiA, which degrades the AHL's produced by *Pectobacterium carotovorum*, thereby reducing its pathogenicity on potato slices [36]. In order to improve the efficiency of the *B. thuringiensis* lactonase AiiA, a fusion with a secretive protein was generated to enhance the dispersion of the lactonase in the environment, resulting in an increased tolerance to *P. carotovorum* on potato [37]. Since the 1960s, *B. thuringiensis* is commonly used as a biological pesticide against insects due to its natural ability to produce endotoxins lethal to moths, butterflies or mosquitoes [38]. Currently, its use against bacterial pathogens in fields has, to our knowledge, not been reported.

Another QQ strategy was also tested against bacterial plant pathogens: some plants were genetically modified using bacterial genes from *Bacillus* spp. or *A. tumefaciens* to produce lactonases. The first transgenic lines were reported in 2001, transforming tobacco and potato lines with the *aiiA* gene from *Bacillus*. The resulting transgenic lines showed an increased tolerance to *P. carotovorum* with symptoms only appearing after inoculation with very high bacterial concentrations [39].

These results showed that QQ has been used as a successful approach to protect plants from bacterial pathogens in laboratory conditions. Nevertheless, this demonstration was only achieved using plant GMO producing lactonases. QQ enzymes that may be used to treat and protect plants from bacterial infections is an attractive alternative to genetically modified plants but is however impaired by the poor stability of enzymes. To circumvent this issue, the development of environmentally stable and chemical-resistant enzymes is crucial.

Another possible drawback in the use of QQ strategies for pest control could be the impact on beneficial or symbiotic bacteria that are naturally found in the environment. The ecological impact of

Please cite this article in press as: J. Bzdrenga, et al., Biotechnological applications of quorum quenching enzymes, Chemico-Biological Interactions (2016), http://dx.doi.org/10.1016/j.cbi.2016.05.028

tobacco lines expressing the lactonase AttM from *A. tumefaciens* was shown to be minimal, as no major difference was recorded between the root microbiota of transgenic and WT tobacco lines [40]. Nevertheless, if the bacterial populations were not impacted, some functions of bacteria using AHL-mediated QS might have been altered. This may prove incompatible with the use of *Pseudomonas* spp. as biocontrol agents. Indeed *Pseudomonas* spp. produce antibiotics and antifungal agents under control of AHL-mediated QS and using QQ strategies may prevent their beneficial effects [41]. To date, all experiments were performed in laboratory conditions with all interacting partners being inoculated simultaneously and at relatively high concentrations. The situation in the field is obviously different and further studies are needed to assess the impact of QQ and balance its drawbacks against its beneficial impact; controlling QQ enzyme specificity might be a way to modify this balance.

3.2. Aquaculture

According to the Food and Agriculture Organization (FAO), aquaculture is the farming of aquatic organisms in both coastal and inland areas involving interventions in the rearing process to enhance production. Economically, world aquaculture production represented about 97 million tonnes in 2013 (live weight) with an estimated value of 157 billion USD and 575 aquatic species registered [43]. Bacterial infections comprise a significant constraint to the development of aquaculture in the world, involving billions of USD in annual losses [44,45]. In the United States in 2012, infectious diseases are a top limiting factor that accounts for approximately 45% of losses in aquaculture [46]. The use of disinfectants and antibiotics has only limited success in treating or preventing aquatic diseases [44,45]. In developed countries, such as in the US, Canada or Norway, antibiotics have been restricted to limit the selection for resistant human pathogens [47]. However, the situation is much more problematic in countries with no or less stringent controls [47]. For example, in Chile, more than 385 tonnes of antibiotics were used in 2007 to produce a yield of 300,000 tonnes of Atlantic salmon [46]. It is estimated that about 1500 tonnes of tetracycline and 478 tonnes of florfenicol were used in salmon aquaculture in Chile between 2000 and 2007, and 950 tonnes of quinolones between 2000 and 2008 for this purpose [48]. More importantly, massive use of antibiotics in aquaculture systems is leading to rapid evolution and spread of multiple antibiotic resistant strains that could potentially threaten human health security in significant ways [49,50]. As a consequence, numerous resistant human pathogens were isolated from aquacultures [51]. Various approaches are used to reduce contamination risks, such as the prevention of pathogen transmission between farms, stress reduction, or increasing hygiene [44]. Biological methods such as the utilization of probiotics [52], bacteriophage therapies, or immunostimulants were also investigated to prevent fish infections [44,53]. Immunostimulants are able to increase non-specific and/or specific immune response. Among these, β-glucans, alginate, or ergosan have been studied for their capacity to stimulate innate immune resistance or to enhance physiological and immunological factors [54,55]. Vaccines are also employed to control the majority of fish pathogens [56]. The methods of administration are immersion, injection, or addition in the food [57]. Injection is preferentially used, but is laborious and not effective for small or young fish [58]. However, none of these methods seem to significantly solve the problems of bacterial infections.

QQ is an appealing strategy that might reduce bacterial infections with a limited possibility that resistances will develop [44]. Numerous Gram-negative bacteria possess a QS system, including major fish pathogens such as *Aeromonas* or *Vibrio* spp. These bacteria use an AHL-LuxR/LuxI QS-like system with LuxR-LuxI homologues and the signal molecules are specific to each bacterium. More precisely, *Aeromonas hydrophila* mainly uses a *N*-butyryl-L-homoserine lactone (C4-HSL) as signal molecule [59], whereas the *Vibrio parahaemolyticus* QS system is regulated by *N*-hexanoyl-L-homoserine lactone (C6-HSL or HHL) [60]. AHL-degrading enzymes were thus investigated for disrupting QS of fish pathogens. Purified lactonases were tested and in particular oral administration of AHL-lactonase from *Bacillus* sp. strain AI96 was shown to decrease *A. hydrophila* infection in zebrafish [59]. Similar results were observed using AHL-lactonase (AiiAB546), from *Bacillus* sp. B546 produced by *Pichia pastoris*, in common carp [61]. Another pathogen, *V. parahaemolyticus*, is responsible for significant infections in shrimp and involves gastroenteritis for people who consume infected shrimp. The pathogen colonization of Indian white shrimp was successfully reduced after injection into the abdominal cavity of AHL-Lactonase from *Bacillus licheniformis* DAHB1 [60].

The use of lactonase-expressing whole cells was investigated as an economically-friendly alternative. For example, *Tenacibaculum* sp. strain 20J was shown to degrade C4-HSL to C14-HSL and was successfully used to decrease *in vitro* concentration of AHL's produced by *Edwardsiella tarda* strain ACC35.1, a bacterium responsible for the Edwardsiella septicemia [62]. In order to select natural AHL's degrading microbial communities, shrimp fed with AHL's were used. One of the generated communities sampled from shrimp intestinal track was shown to protect a euryhaline rotifer from *Vibrio harveyi*. This microbial community proved to be able to degrade the *V. harveyi* HAI-1 autoinducer *in vitro* and *in vivo* [63].

Altogether these results suggest that QQ strategies are particularly attractive for limiting bacterial infections in the aquaculture industry. Moreover, QQ enzymes may be used in combination with prebiotics, probiotics, immunostimulants and vaccines to control and protect fish against a wide spectrum of pathogens.

It should be noted that biofilms in aquaculture pools act as reservoirs for the pathogenic bacteria that are responsible for recurring diseases [64], hence the importance of biofilm and biofouling treatments.

3.3. Antifouling

- Membrane bioreactors and filters

Membrane bioreactors (MBR) are used in many industries or processes to combine a classic bioreactor system with a membrane filtration step. This technology is widely used in wastewater treatment for the bacterial cleaning of soluble pollutants and the retention of microorganisms and solid particles [65]. Fouling is a major concern encountered in such systems due to the accumulation of biological material both onto and into the membrane. In wastewater treatment, the filtration membrane is quickly colonized by organisms, thus reducing the efficiency of the process. To circumvent this drawback, high pressure is often required which represents an important energy consumption [66], as well as increased cleaning frequency, causing additional costs.

In order to counter biofouling, several approaches have been developed, including chemical, physical and biological strategies, for either preventing formation or cleaning [67,68]. In this context, QQ has emerged as a promising technology to inhibit the early stages of biofouling development.

The presence of AHL-producing bacteria in membrane biofouling has been demonstrated, highlighting the presence of species potentially using QS [66]. AHL-degrading enzymes or QS inhibitors are particularly attractive for minimizing the consequences of biofouling. Obviously, this would not avoid using classic cleaning methods, but it could reduce their frequency and decrease

Please cite this article in press as: J. Bzdrenga, et al., Biotechnological applications of quorum quenching enzymes, Chemico-Biological Interactions (2016), http://dx.doi.org/10.1016/j.cbi.2016.05.028

overall maintenance costs.

A study using membrane filters has shown the potential of vanillin to reduce biofilm formation, presumably due to the QQ effect of the molecule [69]. Two more practical studies have described the QQ effect of *Piper Betle* extract to reduce biofouling in MBR [70,71]. Other QS inhibitors could be used to prevent biofouling, but such molecules are usually soluble and would pass through the membrane, causing a secondary contamination.

Another approach is to use QQ enzymes that could disrupt bacterial communication, thus limiting the formation of biofilms and reducing impairment of the filtering system. The efficiency of Porcine kidney acylase I was demonstrated and showed an increasing lifetime of the filter in presence of the enzyme as compared to the control [66]. Most enzymes offer the advantage to be efficient and more stable when immobilized. Former enzymes were thus considered for immobilization strategies onto nanofiltration membrane [72], as well as alginate capsules [73], magnetic ion-exchange resin [74], and magnetic mesoporous silica beads [75]. These all increased stability and efficiency of the enzyme. In order to avoid the immobilization step and to limit the process costs, whole bacterial cells producing QQ enzymes were investigated [76–80]. Indeed, by entrapping the cells in different kinds of systems, be it microvessels or beads, the continuous production of one or more lactonases or acylases was developed. All these studies showed a significant diminution in biofilm formation and an increase of the MBR efficiency at low filtering pressure. In both cases, the QQ did not seem to impact the depolluting efficiency of the wastewater bacteria, confirming the potential of the technology [73,78].

- Marine biofouling

Biofouling is also a major issue for structures in contact with seawater, such as boats, fish nets, or pipelines. Two related phenomenon usually occur on submerged surfaces: microfouling caused by microorganisms such as bacteria or protozoans, and macrofouling linked to algae or barnacles [81]. Biofouling is responsible for friction on boats, inducing excessive fuel consumption, increased maintenance costs, and generates considerable monetary losses annually [81,82]. Since tributyltin (TBT), an efficient antifouling molecule, has been banned due to its high toxicity, current solutions for biofouling prevention include paints and coatings, mainly containing copper as antifouling agent. The use of copper is also considered an environmentally unfriendly method but is still in use [82,83]. Antifouling paints and coatings save an estimated 60 billion USD annually [22].

In the quest for non toxic alternatives, enzymes have been considered for either preventing biofouling formation or destroying biofilms. Several reviews discuss the potential of these different enzymes and even consider actual patents for their incorporation into paints or coatings [81,82,84].

However, mature biofilms remain difficult to degrade and special attention is dedicated to prevent biofouling formation. In this respect, QS disrupting strategies would be of prime interest. First, it could reduce QS-regulated biofilm formation involved in microfouling but may also impact the attraction and fixation of macrobiofouling species. Different studies have demonstrated the influence of bacterial biofilm on the settlement of spores from algae or others [85–87]. A chemical approach would be to use QS inhibitors in the coating to prevent biofouling. In this way, kojic acid has been reported as a non-toxic QS inhibitor and is incorporated into painting, conferring the ability to inhibit both microfouling from bacteria as well as diatom *Amphora coffeaeformis* macrofouling over one month [87]. Even though QQ enzymes have been described in the literature as a solution for MBR fouling, no comparable work has been done yet for marine biofouling. The main constraint would undoubtedly be the lack of stability of enzymes within paints as well as their possible limited activity in seawater. QQ enzymes from extremophile organisms would constitute promising candidates as they usually are highly robust and may be active in non-conventional environments. Furthermore, compared with QS inhibitors, QQ enzymes would constitute an environmentally friendly solution as they may be active while incorporated irreversibly into paints or coatings, their action would be localized to the ship hull. Moreover, in case of releasing, enzymes could be degraded in the environment and would not bio-accumulate. QQ-based approaches, while restrictive as it does not prevent direct settlement of macrofouling species, would be a good complement of available approaches to reduce marine biofouling.

3.4. Medical devices

QS-induced bacterial infections are particularly problematic in medical environments. In the US, *P. aeruginosa* accounts for 7.5% of general healthcare associated infections. Other pathogens, such as *Acinetobacter baumannii*, *Proteus* spp., and *Serratia* spp., are overall responsible for 6.4% of the infections. These pathogens are often found with catheter associated urinary tract infections and ventilator associated pneumonia [88]. As such, healthcare facilities could directly benefit from research on AHL-targeted QQ. Furthermore, QS is responsible for a number of problematic complications such as antibiotic resistance, biofilm formation, competence, and virulence factor expression [89–91]. Hereafter are presented QQ-based devices, mainly based on enzymatic functionalization, to circumvent QS-mediated bacterial infections.

- Quorum quenching membrane

The immobilization of the hyperthermostable Phosphotriesterase-Like Lactonase (PLL) from *Sulfolobus solfataricus*, referred to as *Sso*Pox, onto nanoalumina membranes to quench bacterial communication was investigated [92]. About 95% of the enzyme was successfully immobilized with interactions tight enough to resist high ionic strength washes. The enzymatic activity after immobilization was 25% that of the free enzyme. The addition of membranes containing *Sso*Pox in bacterial cultures of *P. aeruginosa* PAO1 resulted in an overall decrease of pyocyanin expression and elastase activity. For the first time, the authors demonstrated that immobilization of QS-disrupting enzymes may be useful to decrease the virulence of bacterial pathogens and paved the way for the development of innovative medical devices.

- Functionalized catheter

The persistence of pathogens in catheters is quite problematic both in terms of costs and patient health [93]. To address this issue, a central venous catheter coated with the QSI 5-fluorouracil was developed and clinically evaluated [94]. The study was performed with a total of 960 adult patients in 25 US intensive care units and demonstrated that 5-fluorouracil coated catheter is a safe and promising alternative to catheters coated with silver sulfadiazine or chlorhexidine. Catheter functionalization with catalytic quenchers such as enzymes has also been investigated using a silicon catheter coated with multiple layers of an acylase from *Aspergillus melleus* [95]. The adherence of *P. aeruginosa* ATCC 10145 was assessed and showed to be strongly inhibited as compared to the non-treated control. Biofilm quantity was also reduced by about half in the acylase coated catheter, both in static and dynamic models. In itself, the coated catheter proved to be non-toxic against cultured skin fibroblast. Very recently, the development of functionalized urinary

Please cite this article in press as: J. Bzdrenga, et al., Biotechnological applications of quorum quenching enzymes, Chemico-Biological Interactions (2016), http://dx.doi.org/10.1016/j.cbi.2016.05.028

catheters combining both a QQ acylase and a matrix degrading α-amylase was reported. The acylase and amylase limited the biofilm formation of *P. aeruginosa* and *Staphylococcus aureus* respectively. This device was further evaluated in an *in vivo* animal model and was shown to delay biofilm development for up to 7 days [96].

- Topical treatment and dressing perspectives

A burn infection model on mice using *P. aeruginosa* PAO1 was developed to assess the efficiency of a purified lactonase from *Bacillus* sp. ZA12 [97]. Animals were burned to the third degree and infected with a lethal dose of 10^6 bacteria subcutaneously. Topical application with a lactonase-containing gel prevented systemic spread of *P. aeruginosa* through burned skin and reduced animal mortality. When the lactonase was combined with ciprofloxacin no mortality was observed, underlining the synergistic effect of the treatments. This report highlighted the efficiency of quenching enzyme by topical administration alone or in combination with antimicrobial treatments to prevent bacterial infection of wounds. Histological studies demonstrated that fewer damages and inflammatory markers were observable in tissues when the enzyme and antibiotics were used together. This would offer new perspectives for the investigation of enzymatically functionalized dressings and bandages (Fig. 1).

- Aerosolization

The *in vivo* use of an exogenous, engineered hyperthermostable lactonase derived from *Sso*Pox, was reported in a rat pulmonary infection model. The purified enzyme was administered concomitantly to an infection by *P. aeruginosa* PAO1 resulting in a mortality drop, from 75% to 20%, 48 h post infection [99]. The enzyme was also shown to be able to reduce, *in vitro*, the biofilm formation of *P. aeruginosa* PAO1 by up to 65% as compared to the untreated condition. The aerosolized lactonase proved to be efficient to diminish the expression of QS dependent virulence factors and would be particularly relevant for the treatment of cystic fibrosis related infections.

As previously described, many studies have reported the potential of QQ strategies to inhibit bacterial virulence and limit biofilm formation of a wide range of bacterial strains and the corresponding applications are summarized in Table 1. Among these, the use of AHL degrading enzymes was particularly emphasized. Such enzymes may be used in a broad spectrum of applications, from agriculture, bioprocess and anti-fouling, to human and animal healthcare. However, many issues have to be addressed to strengthen their potential. Large-scale production, stability, tolerance to industrial processes, or storage have to be investigated as they represent major constraints to the use of enzymes for biotechnological purposes. In this context, phosphotriesterase-like lactonases appear to be particularly relevant as many of these may be isolated from extreme environments and display both high activity and large substrate specificity. The possible emergence of resistance phenomenon to QQ strategies has also to be considered.

4. Phosphotriesterase-like lactonases (PLL's)

4.1. Highly promiscuous enzymes

PLL's are natural lactonase (EC 3.1.1.25) enzymes with promiscuous catalytic activity against organophosphates (e.g. paraoxon). These enzymes are strongly related to phosphotriesterases (PTE's), constituting their most probable ancestor [100–102]. They belong to the amidohydrolase superfamily and their 3D-structure is formed by a $(\beta/\alpha)_8$-barrel fold, shows an active site containing two metal cations involved in catalysis and coordinated by four histidine residues, as well as a carboxylated lysine and an aspartic acid [103]. The bi-metallic center participates to the catalysis as a Lewis acid involved in the activation of a water molecule into a hydroxide anion that subsequently acts as a nucleophile to attack the substrate. Two subfamilies, PLL-A's and PLL-B's, were identified according to their sequence similarities as well as the length of the

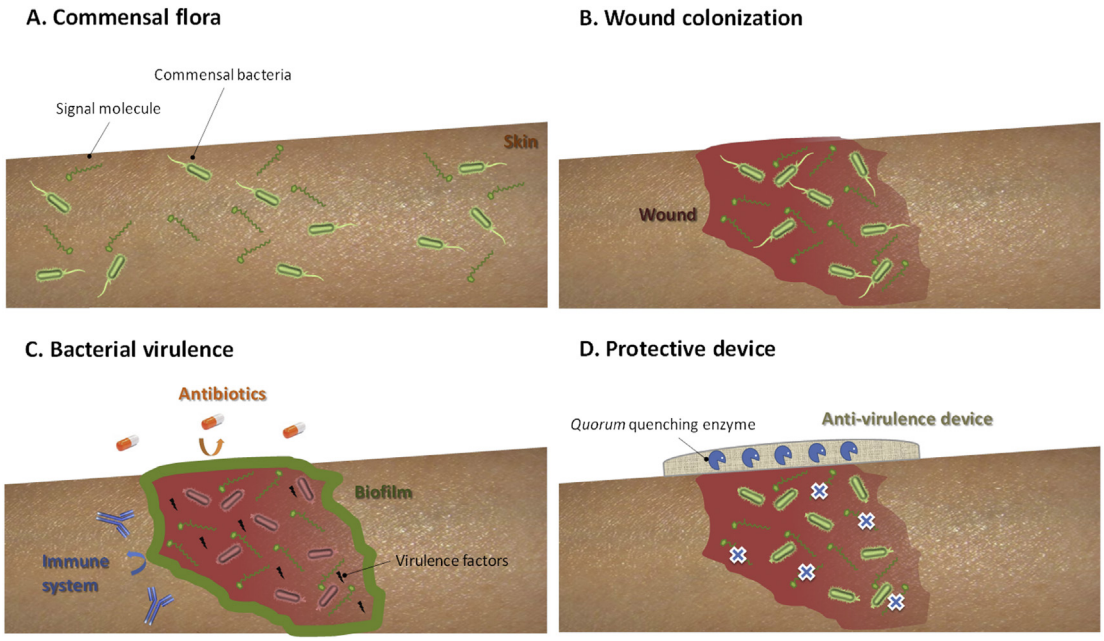


Fig. 1. Enzyme-functionalized anti-virulence device and mechanism of action. **A**) Commensal bacteria are naturally present on healthy skin and use signal molecules to communicate without being virulent. **B**) In case of wound, the bacteria have a favorable medium for their growth and start their colonization step. **C**) When bacterial concentration is over a certain threshold the bacteria adapt their behavior and start being virulent by reducing motility [98], synthesizing a biofilm and secreting virulence factors **D**) Enzyme-containing devices hydrolyze QS signal molecules and prevent infection by decreasing virulence factor secretion, biofilm synthesis and motility.

Please cite this article in press as: J. Bzdrenga, et al., Biotechnological applications of quorum quenching enzymes, Chemico-Biological Interactions (2016), http://dx.doi.org/10.1016/j.cbi.2016.05.028

Table 1
Summary of QQ applications.

Field	Application	Quencher	Reference
Agriculture	Transgenic lines of tobacco and potato	AiiA lactonase from *Bacillus* sp.	[39]
	Transgenic lines of tobacco	AttM lactonase from *A. tumefaciens*	[40]
Aquaculture	Oral administration in zebrafish	AI96 lactonase from *Bacillus* sp.	[59]
	Oral administration in common carp	AiiAB546 lactonase from *Bacillus* sp.	[61]
	Injection in indian white shrimps	Lactonase from *B. licheniformis* DAHB1	[60]
Antifouling			
MBR	Reduce biofouling in MBR	P. betle extract	[70,71]
	Increase filter lifetime	Porcine kidney acylase	[66]
	Nanofiltration membrane	Porcine kidney acylase	[72]
	Alginate capsules	Porcine kidney acylase	[73]
	Magnetic ion-exchange resin	Porcine kidney acylase	[74]
	Magnetic mesoporous silica beads	Porcine kidney acylase	[75]
Marine biofouling	Coating	Kojic acid	[87]
Medical devices	Nanoalumina membrane	PLL *Sso*Pox from *S. solfataricus*	[92]
	Coated catheters	5-fluorouracil	[93,94]
		Acylase from *A.melleus*	[95]
		Acylase from *A. melleus* and α-amylase from *B. amyloliquefaciens*	[96]
	Topical treatment	Lactonase from *Bacillus* sp. ZA12	[97]
	Aerosol	PLL *Sso*Pox from *S. solfataricus*	[99]

two characteristic loops 7 and 8. PLL-A's have been shown to degrade AHL's as well as oxo-lactones, while PLL-B's are specific to oxo-lactones [104]. As such, both PLL-A's and -B's may be considered for QQ strategies and PPL-A's are particularly promising considering their broad substrate promiscuity. Furthermore, PLL's are attractive because this family encompasses numerous representatives from extreme environments. These enzymes exhibit high thermal stability and robustness that is desirable in biotechnological applications. Among these, *Gk*L (isolated from the thermophile *Geobacillus kaustophilus*) [105], *Sac*Pox (isolated from the thermoacidophilic crenarchaeon *Sulfolobus acidocaldarius*) [106], *Sis*Lac (isolated from the hyperthermophilic archaeon *Sulfolobus islandicus*) [107], *Sso*Pox (isolated from the hyperthermophilic archaeon *S. solfataricus*) [103,108–110], or *Vmo*Lac (isolated from the extremophilic crenarchaeon *Vulcanisaeta moutnovskia*) [104,111], have drawn special interest. Regarding their intrinsic stability (e.g. T_m values of 106 °C and 128 °C for *Sso*Pox and *Vmo*Lac, respectively) some of these PLL's have been further considered for directed evolution experiments to improve their potential for QQ purposes [109,112,113].

PLL's have distinct sequences and structures from another family of QQ lactonases (QQL's) belonging to the metallo-β-lactamase superfamily (Fig. 2). This superfamily includes the above-mentioned enzyme AiiA from *B. thuringiensis* [114,115]. Although these proteins share neither sequence nor structural similarity, their active sites show striking similarities [102].

4.2. *SsoPox a promising candidate for QQ applications*

One of the best characterized PLL's so far is *Sso*Pox. This enzyme, isolated from the hyperthermophilic archaeon *S. solfataricus*, was initially investigated for its ability to hydrolyze phosphotriesters (widely used as pesticides and chemical warfare agents) [116]. *Sso*Pox is an extremely stable enzyme [108], active over a wide range of temperatures (10–100 °C) and pH values (5.0–9.0), paving the way for a wide panel of biotechnological applications [116]. Moreover, it is a very proficient lactonase, including at room temperature. The 3D-structure of *Sso*Pox was reported and was found as being a distorted $(\beta/\alpha)_8$ barrel-fold [117]. Conversely to other known phosphotriesterases displaying a similar structural organization, *Sso*Pox differs by the length of two loops. Loop-7 and loop-8 are shorter and longer than other reported PTE's, respectively. These modifications

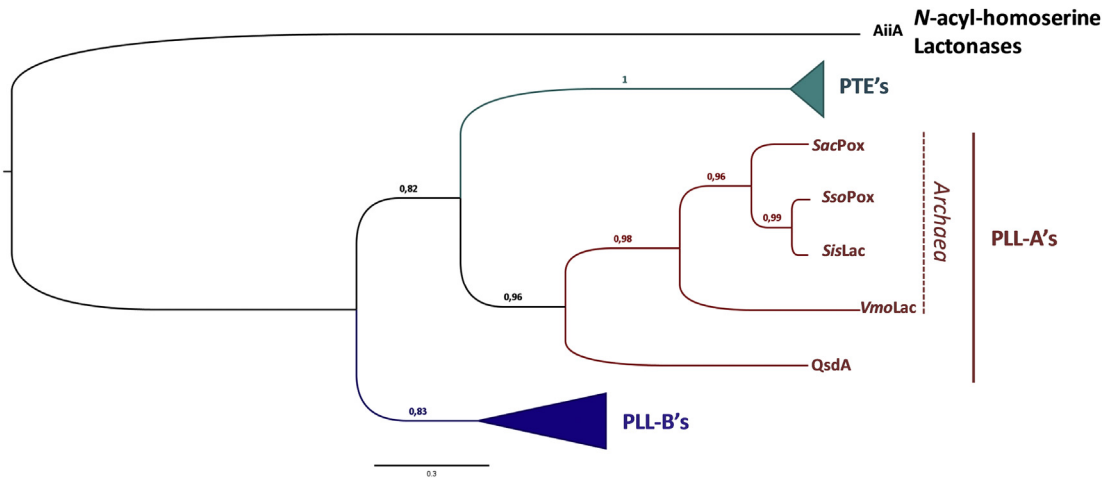


Fig. 2. Phylogenetic tree of PLL's and enzyme-related families. Webtool www.phylogeny.fr/simple_phylogeny.cgi was used for sequence alignment and phylogeny and the tree was obtained with FigTree v1.4.0. Sequence used for the analysis were: AiiA (P0CJ63), PTE's (Q93LD7, P0A434), *Sac*Pox (V9S7Z1), *Sso*Pox (Q97VT7), *Sis*Lac (C4KKZ9), *Vmo*Lac (F0QXN6), QsdA (B1N7B5), PLL's-B (A4IN23, Q5KZU5, Q9RVU2).

Please cite this article in press as: J. Bzdrenga, et al., Biotechnological applications of quorum quenching enzymes, Chemico-Biological Interactions (2016), http://dx.doi.org/10.1016/j.cbi.2016.05.028

are responsible for the creation of a hydrophobic channel that perfectly accommodates the lactone substrate (Fig. 3).

Various lactones were assayed with the wild-type enzyme including AHL's, γ-lactones, or δ-lactones (Fig. 4) [100,109,118]. Catalytic parameters were determined and k_{cat}/K_M values up to $8.0 \times 10^4\ M^{-1}\ s^{-1}$ were reported, suggesting that *Sso*Pox is a natural proficient lactonase. Protein engineering strategies were also considered to further increase its catalytic efficiency towards lactone substrates. Residue W263 was particularly considered as it is located in the active site and is involved in enzyme loop flexibility, mediating its promiscuity [109]. Saturation mutagenesis experiments were performed and led to the identification of extremely efficient variants (e.g. *Sso*Pox-W263I) with k_{cat}/K_M values up to $5.8 \times 10^6\ M^{-1}\ s^{-1}$ at room temperature. About twenty lactones with various chemical structures are known to be hydrolyzed by *Sso*Pox and/or its variants underlining the wide promiscuity of these enzymes (Table 2). Furthermore, *Sso*Pox and its variants exhibit a strong tolerance to proteases, surfactants, and also organic solvents [109,110].

About ten structures, either in *apo* or *holo* form, are now available in the protein database (www.pdb.org). Among these, variant *Sso*Pox-W263I was found to be particularly efficient for lactone hydrolysis and has been co-crystallized with the substrate analogue *N*-decanoyl-L-homocysteinethiolactone (C10HTL) (Fig. 3). This variant is of utmost interest for QQ investigations as it is both highly efficient for lactone hydrolysis and is widely promiscuous towards a large range of substrates. Moreover, *Sso*Pox-W263I retains an impressive thermostability ($T_m = 88\ °C$), albeit lower than the wild-type, and, owing to its properties, might be suitable for a large panel of applications in the various domains afore-mentioned. Altogether, thermostable lactonases are particularly appealing for biotechnological investigations as these enzymes could be more readily compatible with material sciences, such as incorporation into coatings, materials, paints and polymers, and to develop innovative, non-toxic and environmental-friendly alternatives against bacterial infections and biofilms.

5. QQ strategies and resistance

Antibiotics have been widely used over the past decades for treating chronic and acute bacterial infections. Antibiotics induce a strong selection pressure on bacteria by either killing them or inhibiting their growth. However, the intensive use of antimicrobial agents has led to the emergence of adaptive resistance that considerably limits their efficiency and is associated with treatment dose increase [119–121]. QQ has emerged as a promising therapeutic alternative as it can be used to inhibit both the secretion of virulence factors and the formation of biofilm [122], but does not kill bacteria [123–125]. Therefore, QQ strategies are believed to induce a milder selection pressure. However, recent evidence suggests that the effect of QS disruption on bacterial growth was dependent on the culture medium used (*i.e.* nutrient-rich or not) [126], and might thereby introduce a selection pressure, albeit milder than a biocide strategy, and select for resistant bacteria [127,128]. Using QS-disrupted variants, studies have shown that bacterial resistance to QS may arise. Mutations increasing efflux of C-30, an efficient QQ furanone, as well as compensatory mutations were observed as mechanisms to overcome QS disruption [129,130]. Moreover, "Social cheaters", (*i.e.* bacteria that ceased production of quorum regulated factors), were reported [131]. Such QS-insensitive mutants might interfere with QQ efforts [132], but recent experimental studies suggest that QQ resistance would spread slowly, as these mutants were found to be less fit than their counterparts [133].

The emergence of resistance to QQ strategies will certainly depend on the actual used strategy. The use of QQ enzymes is possibly the least resistant-prone of all QQ strategies because enzymes can act remotely and do not need to enter the bacterial cells. Moreover, contrary to QSI's that need to bind to a target protein (the signaling receptor), QQ enzymes act independently. Putative resistance mechanisms to QQ enzymes have been proposed [127,128] and suggest that bacteria may evolve for an increased production of the autoinducer molecule (AHL) to counteract the hydrolysis by QQ enzymes. This could be bypassed by increasing the total enzymatic activity in the environment. Another resistance scenario would consist of modifications to the chemical structure of the autoinducer. This possibility is reduced by the fact that QQ enzymes are naturally broad spectrum enzymes and can be engineered for altered specificity. Another mechanism would consist of the selection of modified LuxR receptors with tremendous affinity for the autoinducer, or with improved response to AHL [134,135], therefore the QQ enzymes would not be active enough at these low concentrations of autoinducers. In this case, enzyme engineering may offer solutions to produce enzymes with higher affinity for AHL's.

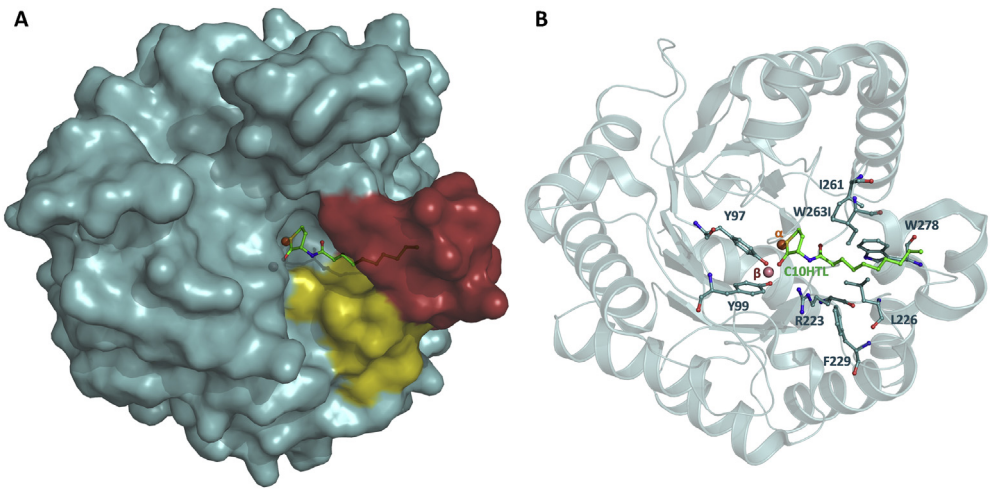


Fig. 3. Representation of *Sso*Pox variant W263I structure (PDB ID: 4KF1) bound with substrate analogue C10HTL. (**A**) Structure is shown as surface and loop-7 and loop-8 are emphasized in yellow and red respectively. (**B**) C10HTL is shown in green stick, surrounding residues are emphasized by blue sticks and divalent cations are drawn as spheres. (For interpretation of the references to colour in this figure legend, the reader is referred to the web version of this article.)

Please cite this article in press as: J. Bzdrenga, et al., Biotechnological applications of quorum quenching enzymes, Chemico-Biological Interactions (2016), http://dx.doi.org/10.1016/j.cbi.2016.05.028

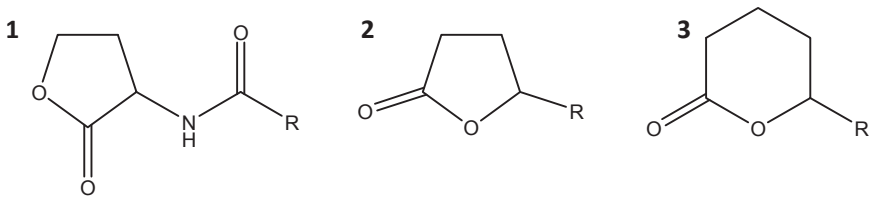


Fig. 4. Chemical structures of *Sso*Pox lactone substrates. (**1**) Acyl-Homoserine Lactones, (**2**) γ-lactones, (**3**) δ-lactones.

6. Conclusion and perspectives

Although it may affect bacterial fitness, QS disruption is a promising strategy to substitute or at least supplement antibiotics. Many studies have shown that biofilm is associated with antibiotic and antimicrobial agent resistance for a wide range of bacteria [21,136–141]. Biofilm formation governs many mechanisms involved in antibiotic resistance, such as limited penetration of the antibiotic, horizontal gene transfer within the bacterial community and changes in gene expression that may influence resistance [142,143]. QS disruption often results in decreased biofilm formation, therefore QQ could be an efficient tool for the restoration of

Table 2
Catalytic parameters of *Sso*Pox wild-type and variants towards lactones with respective reaction conditions. Data were taken from Ref. [100,109,118].

Substrate	Enzyme	Condition	k_{cat} (s^{-1})	K_M (μ M)	k_{cat}/K_M (M^{-1} s^{-1})
3-oxo-C12 AHL (l)	WT	25 °C	1.01	456	2.22×10^3
	W263F	25 °C	0.41	146	2.81×10^3
	W263M	25 °C	ND	ND	ND
	W263L	25 °C	ND	ND	ND
	W263I	25 °C	1.8	17.8	1.01×10^5
	W263V	25 °C	3.0	24.7	1.21×10^5
	W263T	25 °C	6.44	137	4.70×10^4
3-oxo-C10 AHL (l)	WT	25 °C	4.52	143	3.16×10^4
	WT	25 °C + 0.1% SDS	ND	ND	1.96×10^2
	WT	25 °C + 0.01% SDS	0.75	243	3.09×10^3
	W263F	25 °C	3.96	288	1.38×10^4
	W263M	25 °C	ND	ND	ND
	W263L	25 °C	ND	ND	ND
	W263I	25 °C	0.6	1605	3.74×10^2
	W263V	25 °C	0.19	1346	1.41×10^2
	W263T	25 °C	0.11	1000	1.06×10^2
3-oxo-C6 AHL (l)	WT	25 °C	0.08	558	1.49×10^2
3-oxo-C6 AHL (r)	WT	25 °C	0.04	592	6.87×10^1
3-oxo-C8 AHL (l)	WT	25 °C	0.54	123	4.39×10^3
3-oxo-C8 AHL (r)	WT	25 °C	0.42	256	1.63×10^3
Undecanoic-δ-lactone (r)	WT	25 °C	7.38	94	7.86×10^4
	W263F	25 °C	66.5	135.2	4.92×10^5
	W263M	25 °C	71.2	161	4.42×10^5
	W263L	25 °C	56.8	219	2.59×10^5
	W263I	25 °C	58.0	<10	$>5.80 \times 10^6$
	W263V	25 °C	44.8	57	7.92×10^5
	W263T	25 °C	93.3	130	7.17×10^5
Undecanoic-γ-lactone (r)	WT	25 °C	4.95	2099	2.36×10^3
	WT	25 °C + 0.1% SDS	2.23	1250	1.78×10^3
	WT	25 °C + 0.01% SDS	0.46	94	4.89×10^3
	W263F	25 °C	4.63	373	1.24×10^4
	W263M	25 °C	4.25	334	1.27×10^4
	W263L	25 °C	3.92	371.8	1.05×10^4
	W263I	25 °C	1.94	361	5.37×10^3
	W263V	25 °C	5.64	1760	3.20×10^3
	W263T	25 °C	4.55	13	3.49×10^5
γ-butyrolactone	WT	25 °C	ND	ND	1.20×10^3
γ-heptanolide (r)	WT	25 °C	2.92	166	1.76×10^4
Nonanoic-γ-lactone (r)	WT	25 °C	5.54	2943	1.88×10^3
Dodecanoic-γ-lactone (r)	WT	25 °C	2.72	1220	2.23×10^3
δ-valerolactone	WT	25 °C	ND	ND	ND
Nonanoic-δ-lactone (r)	WT	25 °C	15.32	359	4.27×10^4
Dodecanoic-δ-lactone (r)	WT	25 °C	12.65	1678	7.54×10^3
ε-caprolactone	WT	25 °C	4.45	234	1.90×10^4
Dihydrocoumarin	WT	25 °C	7.32	1376	5.32×10^3
5-thiobutyl-γ-butyrolactone	WT	70 °C	29.0	80	3.60×10^5
	R223H	70 °C	0.42	273	1.54×10^3
	Y97W	70 °C	75.7	1540	9.58×10^5
5-thioethyl-γ-butyrolactone	WT	70 °C	9.0	15	7.00×10^5
5-thiohexyl-γ-butyrolactone	WT	70 °C	6.0	70	8.00×10^4

ND corresponds to an undetermined value.

Please cite this article in press as: J. Bzdrenga, et al., Biotechnological applications of quorum quenching enzymes, Chemico-Biological Interactions (2016), http://dx.doi.org/10.1016/j.cbi.2016.05.028

bacterial susceptibility to antibiotics or antimicrobial agents in biofilms [143].

QQ strategies, particularly catalytic quenchers, such as enzymes are appealing to develop new alternatives for QS-disruption and antifouling. Since stability is a major constraint that usually impairs enzyme utilization, intensive efforts have been dedicated to the isolation of robust enzymes from extreme environments. Among these, PLL's (particularly *Sso*Pox) are highly promising as they have already been successfully incorporated into devices while retaining their lactonase activity. Moreover, enzymes are highly attractive as these molecules are usually not toxic and may be integrated into various matrices without being released. The proofs of concept have been widely described and further investigations would obviously permit to develop concrete applications (e.g. medical devices, paintings, coatings …) in order to address the issues of bacterial virulence and biofouling. Furthermore, the applications of QQ enzymes are focused on the disruption of the AI-1-based QS mechanism. The quest for enzymes targeting AI-2, AI-3, or even AIP's is of utmost interest for extending the potential of QQ strategies to a wider panel of Gram-negative and Gram-positive bacteria.

Acknowledgments

P.J. and J.B. are Ph.D students granted by Direction Générale de l'Armement (DGA, France).

B.R. is a Ph.D student granted by the "Emplois Jeunes Doctorants" program of Région Provence-Alpes-Côte d'Azur (PACA, France). We are grateful to Michael Schwab for valuable inputs on the manuscript.

Transparency document

Transparency document related to this article can be found online at http://dx.doi.org/10.1016/j.cbi.2016.05.028.

References

[1] K.H. Nealson, J.W. Hastings, Bacterial bioluminescence: its control and ecological significance, Microbiol. Rev. 43 (1979) 496–518.
[2] M.B. Miller, B.L. Bassler, Quorum sensing in bacteria, Annu. Rev. Microbiol. 55 (2001) 165–199, http://dx.doi.org/10.1146/annurev.micro.55.1.165.
[3] X. Chen, S. Schauder, N. Potier, A. Van Dorsselaer, I. Pelczer, B.L. Bassler, et al., Structural identification of a bacterial quorum-sensing signal containing boron, Nature 415 (2002) 545–549, http://dx.doi.org/10.1038/415545a.
[4] M.E.A. Churchill, L. Chen, Structural basis of acyl-homoserine lactone-dependent signaling, Chem. Rev. 111 (2011) 68–85, http://dx.doi.org/10.1021/cr1000817.
[5] M.M. Kendall, V. Sperandio, Quorum sensing by enteric pathogens, Curr. Opin. Gastroenterol. 23 (2007) 10–15, http://dx.doi.org/10.1097/MOG.0b013e3280118289.
[6] R.P. Ryan, S. An, J.H. Allan, Y. McCarthy, J.M. Dow, The DSF family of cell-cell signals: an expanding class of bacterial virulence regulators, PLoS Pathog. 11 (2015) e1004986, http://dx.doi.org/10.1371/journal.ppat.1004986.
[7] A.B. Flavier, S.J. Clough, M.A. Schell, T.P. Denny, Identification of 3-hydroxypalmitic acid methyl ester as a novel autoregulator controlling virulence in Ralstonia solanacearum, Mol. Microbiol. 26 (1997) 251–259.
[8] S.C. Winans, A new family of quorum sensing pheromones synthesized using S-adenosylmethionine and Acyl-CoAs, Mol. Microbiol. 79 (2011) 1403–1406, http://dx.doi.org/10.1111/j.1365-2958.2011.07551.x.
[9] J. Lee, L. Zhang, The hierarchy quorum sensing network in Pseudomonas aeruginosa, Protein Cell 6 (2015) 26–41, http://dx.doi.org/10.1007/s13238-014-0100-x.
[10] L. Plener, N. Lorenz, M. Reiger, T. Ramalho, U. Gerland, K. Jung, The phosphorylation flow of the vibrio harveyi quorum-sensing cascade determines levels of phenotypic heterogeneity in the population, J. Bacteriol. 197 (2015) 1747–1756, http://dx.doi.org/10.1128/JB.02544-14.
[11] S.A. Jung, C.A. Chapman, W.-L. Ng, Quadruple quorum-sensing inputs control Vibrio cholerae virulence and maintain system robustness, PLoS Pathog. 11 (2015) e1004837, http://dx.doi.org/10.1371/journal.ppat.1004837.
[12] J. Lee, L. Zhang, The hierarchy quorum sensing network in Pseudomonas aeruginosa, Protein Cell 6 (2015) 26–41, http://dx.doi.org/10.1007/s13238-014-0100-x.
[13] N. Schmid, G. Pessi, Y. Deng, C. Aguilar, A.L. Carlier, A. Grunau, et al., The AHL- and BDSF-dependent quorum sensing systems control specific and overlapping sets of genes in Burkholderia cenocepacia H111, PLoS One 7 (2012) e49966, http://dx.doi.org/10.1371/journal.pone.0049966.
[14] S.A. West, K. Winzer, A. Gardner, S.P. Diggle, Quorum sensing and the confusion about diffusion, Trends Microbiol. 20 (2012) 586–594, http://dx.doi.org/10.1016/j.tim.2012.09.004.
[15] K.S. Kaye, J.M. Pogue, Infections caused by resistant gram-negative bacteria: epidemiology and management, Pharmacotherapy 35 (2015) 949–962, http://dx.doi.org/10.1002/phar.1636.
[16] D. Pimentel, Biological Invasions: Economic and Environmental Costs of Alien Plant, Animal, and Microbe Species, CRC Press, 2014.
[17] B.M. Mole, D.A. Baltrus, J.L. Dangl, S.R. Grant, Global virulence regulation networks in phytopathogenic bacteria, Trends Microbiol. 15 (2007) 363–371, http://dx.doi.org/10.1016/j.tim.2007.06.005.
[18] J. Mansfield, S. Genin, S. Magori, V. Citovsky, M. Sriariyanum, P. Ronald, et al., Top 10 plant pathogenic bacteria in molecular plant pathology, Mol. Plant Pathol. 13 (2012) 614–629, http://dx.doi.org/10.1111/j.1364-3703.2012.00804.x.
[19] D.T. Gauthier, Bacterial zoonoses of fishes: a review and appraisal of evidence for linkages between fish and human infections, Vet. J. Lond. Engl. 203 (2015) 27–35, http://dx.doi.org/10.1016/j.tvjl.2014.10.028, 1997.
[20] R.H. Certner, S.V. Vollmer, Evidence for autoinduction and quorum sensing in white band disease-causing microbes on Acropora cervicornis, Sci. Rep. 5 (2015) 11134, http://dx.doi.org/10.1038/srep11134.
[21] J.W. Costerton, P.S. Stewart, E.P. Greenberg, Bacterial biofilms: a common cause of persistent infections, Science 284 (1999) 1318–1322, http://dx.doi.org/10.1126/science.284.5418.1318.
[22] M. Lejars, A. Margaillan, C. Bressy, Fouling release coatings: a nontoxic alternative to biocidal antifouling coatings, Chem. Rev. 112 (2012) 4347–4390, http://dx.doi.org/10.1021/cr200350v.
[23] T. Mattila-Sandholm, G. Wirtanen, Biofilm formation in the industry: a review, Food Rev. Int. 8 (1992) 573–603, http://dx.doi.org/10.1080/87559129209540953.
[24] S.E. Coetser, T.E. Cloete, Biofouling and biocorrosion in industrial water systems, Crit. Rev. Microbiol. 31 (2005) 213–232, http://dx.doi.org/10.1080/10408410500304074.
[25] S. Dürr, D.I. Watson, Biofouling and antifouling in aquaculture, in: S. Dürr, J.C. Thomason (Eds.), Biofouling, Wiley-Blackwell, 2009, pp. 267–287. http://onlinelibrary.wiley.com/doi/10.1002/9781444315462.ch19/summary (accessed 3.12. 15).
[26] Y.H. Dong, J.L. Xu, X.Z. Li, L.H. Zhang, AiiA, an enzyme that inactivates the acylhomoserine lactone quorum-sensing signal and attenuates the virulence of Erwinia carotovora, Proc. Natl. Acad. Sci. U. S. A. 97 (2000) 3526–3531, http://dx.doi.org/10.1073/pnas.060023897.
[27] M. Givskov, R. de Nys, M. Manefield, L. Gram, R. Maximilien, L. Eberl, et al., Eukaryotic interference with homoserine lactone-mediated prokaryotic signalling, J. Bacteriol. 178 (1996) 6618–6622.
[28] M. Manefield, T.B. Rasmussen, M. Henzter, J.B. Andersen, P. Steinberg, S. Kjelleberg, et al., Halogenated furanones inhibit quorum sensing through accelerated LuxR turnover, Microbiol. Read. Engl. 148 (2002) 1119–1127, http://dx.doi.org/10.1099/00221287-148-4-1119.
[29] T. Zang, B.W.K. Lee, L.M. Cannon, K.A. Ritter, S. Dai, D. Ren, et al., A naturally occurring brominated furanone covalently modifies and inactivates LuxS, Bioorg. Med. Chem. Lett. 19 (2009) 6200–6204, http://dx.doi.org/10.1016/j.bmcl.2009.08.095.
[30] T. Defoirdt, C.M. Miyamoto, T.K. Wood, E.A. Meighen, P. Sorgeloos, W. Verstraete, et al., The natural furanone (5Z)-4-bromo-5-(bromomethylene)-3-butyl-2(5H)-furanone disrupts quorum sensing-regulated gene expression in Vibrio harveyi by decreasing the DNA-binding activity of the transcriptional regulator protein luxR, Environ. Microbiol. 9 (2007) 2486–2495, http://dx.doi.org/10.1111/j.1462-2920.2007.01367.x.
[31] Y. Dessaux, E. Chapelle, D. Faure, Quorum sensing and quorum quenching in soil ecosystems, in: G. Witzany (Ed.), Biocommunication Soil Microorg., Springer Berlin Heidelberg, 2011, pp. 339–367. http://link.springer.com/chapter/10.1007/978-3-642-14512-4_13 (accessed 16.11.15).
[32] M. Shinohara, N. Nakajima, Y. Uehara, Purification and characterization of a novel esterase (β-hydroxypalmitate methyl ester hydrolase) and prevention of the expression of virulence by Ralstonia solanacearum, J. Appl. Microbiol. 103 (2007) 152–162, http://dx.doi.org/10.1111/j.1365-2672.2006.03222.x.
[33] K.L. Newman, S. Chatterjee, K.A. Ho, S.E. Lindow, Virulence of plant pathogenic bacteria attenuated by degradation of fatty acid cell-to-cell signaling factors, Mol. Plant-Microbe Interact. MPMI 21 (2008) 326–334, http://dx.doi.org/10.1094/MPMI-21-3-0326.
[34] A. Carlier, S. Uroz, B. Smadja, R. Fray, X. Latour, Y. Dessaux, et al., The Ti plasmid of Agrobacterium tumefaciens harbors an attM-paralogous gene, aiiB, also encoding N-Acyl homoserine lactonase activity, Appl. Environ. Microbiol. 69 (2003) 4989–4993.
[35] H.-B. Zhang, L.-H. Wang, L.-H. Zhang, Genetic control of quorum-sensing signal turnover in Agrobacterium tumefaciens, Proc. Natl. Acad. Sci. U. S. A. 99 (2002) 4638–4643, http://dx.doi.org/10.1073/pnas.022056699.
[36] Y.-H. Dong, X.-F. Zhang, J.-L. Xu, L.-H. Zhang, Insecticidal Bacillus thuringiensis silences Erwinia carotovora virulence by a new form of microbial antagonism, signal interference, Appl. Environ. Microbiol. 70 (2004) 954–960.

[37] L. Zhang, L. Ruan, C. Hu, H. Wu, S. Chen, Z. Yu, et al., Fusion of the genes for AHL-lactonase and S-layer protein in Bacillus thuringiensis increases its ability to inhibit soft rot caused by Erwinia carotovora, Appl. Microbiol. Biotechnol. 74 (2007) 667–675, http://dx.doi.org/10.1007/s00253-006-0696-8.
[38] L. Palma, D. Muñoz, C. Berry, J. Murillo, P. Caballero, Bacillus thuringiensis toxins: an overview of their biocidal activity, Toxins 6 (2014) 3296–3325, http://dx.doi.org/10.3390/toxins6123296.
[39] Y.H. Dong, L.H. Wang, J.L. Xu, H.B. Zhang, X.F. Zhang, L.H. Zhang, Quenching quorum-sensing-dependent bacterial infection by an N-acyl homoserine lactonase, Nature 411 (2001) 813–817, http://dx.doi.org/10.1038/35081101.
[40] C. D'Angelo-Picard, E. Chapelle, P. Ratet, D. Faure, Y. Dessaux, Transgenic plants expressing the quorum quenching lactonase AttM do not significantly alter root-associated bacterial populations, Res. Microbiol. 162 (2011) 951–958, http://dx.doi.org/10.1016/j.resmic.2011.01.009.
[41] L. Molina, F. Constantinescu, L. Michel, C. Reimmann, B. Duffy, G. Défago, Degradation of pathogen quorum-sensing molecules by soil bacteria: a preventive and curative biological control mechanism, FEMS Microbiol. Ecol. 45 (2003) 71–81, http://dx.doi.org/10.1016/S0168-6496(03)00125-9.
[43] FAO, FAO Global Aquaculture Production Database Updated to 2013 – Summary Information, 2015.
[44] T. Defoirdt, N. Boon, P. Bossier, W. Verstraete, Disruption of bacterial quorum sensing: an unexplored strategy to fight infections in aquaculture, Aquaculture 240 (2004) 69–88, http://dx.doi.org/10.1016/j.aquaculture.2004.06.031.
[45] R. Subasinghe, Fish health and quarantine, FAO Fish. Circ. 45 (1997).
[46] A.L. Mortazavi, Poppin' the prophylactics: an analysis of antibiotics in aquaculture, J. Glob. Health. (2014). http://www.ghjournal.org/poppin-the-prophylactics-an-analysis-of-antibiotics-in-aquaculture/.
[47] F.C. Cabello, H.P. Godfrey, A. Tomova, L. Ivanova, H. Dölz, A. Millanao, et al., Antimicrobial use in aquaculture re-examined: its relevance to antimicrobial resistance and to animal and human health, Environ. Microbiol. 15 (2013) 1917–1942, http://dx.doi.org/10.1111/1462-2920.12134.
[48] A.H. Buschmann, A. Tomova, A. López, M.A. Maldonado, L.A. Henríquez, L. Ivanova, et al., Salmon aquaculture and antimicrobial resistance in the marine environment, PLoS One 7 (2012) e42724, http://dx.doi.org/10.1371/journal.pone.0042724.
[49] J. Romero, C. Gloria, P. Navarrete, Antibiotics in aquaculture – use, abuse and alternatives, in: E. Carvalho (Ed.), Health Environ. Aquac., InTech, 2012. http://www.intechopen.com/books/health-and-environment-in-aquaculture/antibiotics-in-aquaculture-use-abuse-and-alternatives (accessed 20.11. 15).
[50] O.E. Heuer, H. Kruse, K. Grave, P. Collignon, I. Karunasagar, F.J. Angulo, Human health consequences of use of antimicrobial agents in aquaculture, Clin. Infect. Dis. Off. Publ. Infect. Dis. Soc. Am. 49 (2009) 1248–1253, http://dx.doi.org/10.1086/605667.
[51] T. Defoirdt, P. Sorgeloos, P. Bossier, Alternatives to antibiotics for the control of bacterial disease in aquaculture, Curr. Opin. Microbiol. 14 (2011) 251–258, http://dx.doi.org/10.1016/j.mib.2011.03.004.
[52] L. Verschuere, G. Rombaut, P. Sorgeloos, W. Verstraete, Probiotic bacteria as biological control agents in aquaculture, Microbiol. Mol. Biol. Rev. MMBR 64 (2000) 655–671.
[53] A. Irianto, B. Austin, Probiotics in aquaculture, J. Fish. Dis. 25 (2002) 633–642.
[54] D.P. Anderson, Immunostimulants, adjuvants, and vaccine carriers in fish: applications to aquaculture, Annu. Rev. Fish. Dis. (1992) 281–307.
[55] E. Ringø, R.E. Olsen, I. Jensen, J. Romero, H.L. Lauzon, Application of vaccines and dietary supplements in aquaculture: possibilities and challenges, Rev. Fish. Biol. Fish. 24 (2014) 1005–1032, http://dx.doi.org/10.1007/s11160-014-9361-y.
[56] A. Adams, K.D. Thompson, Biotechnology offers revolution to fish health management, Trends Biotechnol. 24 (2006) 201–205, http://dx.doi.org/10.1016/j.tibtech.2006.03.004.
[57] B. Magnadottir, Immunological control of fish diseases, Mar. Biotechnol. 12 (2010) 361–379, http://dx.doi.org/10.1007/s10126-010-9279-x.
[58] R. Gudding, W.B. Van Muiswinkel, A history of fish vaccination, Fish. Shellfish Immunol. 35 (2013) 1683–1688, http://dx.doi.org/10.1016/j.fsi.2013.09.031.
[59] Y. Cao, S. He, Z. Zhou, M. Zhang, W. Mao, H. Zhang, et al., Orally administered thermostable N-Acyl homoserine lactonase from bacillus sp. strain ai96 attenuates aeromonas hydrophila infection in zebrafish, Appl. Environ. Microbiol. 78 (2012) 1899–1908, http://dx.doi.org/10.1128/AEM.06139-11.
[60] G. Vinoj, B. Vaseeharan, S. Thomas, A.J. Spiers, S. Shanthi, Quorum-quenching activity of the AHL-Lactonase from Bacillus licheniformis DAHB1 inhibits vibrio biofilm formation in vitro and reduces shrimp intestinal colonisation and mortality, Mar. Biotechnol. 16 (2014) 707–715, http://dx.doi.org/10.1007/s10126-014-9585-9.
[61] R. Chen, Z. Zhou, Y. Cao, Y. Bai, B. Yao, Research High yield expression of an AHL-lactonase from Bacillus sp. B546 in Pichia pastoris and its application to reduce Aeromonas hydrophila mortality in aquaculture, Microb. Cell Factories 9 (2010) 39.
[62] M. Romero, A. Muras, C. Mayer, N. Buján, B. Magariños, A. Otero, In vitro quenching of fish pathogen Edwardsiella tarda AHL production using marine bacterium Tenacibaculum sp. strain 20J cell extracts, Dis. Aquat. Organ 108 (2014) 217–225, http://dx.doi.org/10.3354/dao02697.
[63] N.T.N. Tinh, R.A.Y.S. Asanka Gunasekara, N. Boon, K. Dierckens, P. Sorgeloos, P. Bossier, N-acyl homoserine lactone-degrading microbial enrichment cultures isolated from Penaeus vannamei shrimp gut and their probiotic properties in Brachionus plicatilis cultures: probiotic properties of AHL-degrading enrichment cultures, FEMS Microbiol. Ecol. 62 (2007) 45–53, http://dx.doi.org/10.1111/j.1574-6941.2007.00378.x.
[64] D.G. Bourne, L. Høj, N.S. Webster, J. Swan, M.R. Hall, Biofilm development within a larval rearing tank of the tropical rock lobster, Panulirus ornatus, Aquaculture 260 (2006) 27–38, http://dx.doi.org/10.1016/j.aquaculture.2006.06.023.
[65] A. Drews, Membrane fouling in membrane bioreactors—Characterisation, contradictions, cause and cures, J. Membr. Sci. 363 (2010) 1–28, http://dx.doi.org/10.1016/j.memsci.2010.06.046.
[66] K.-M. Yeon, W.-S. Cheong, H.-S. Oh, W.-N. Lee, B.-K. Hwang, C.-H. Lee, et al., Quorum sensing: a new biofouling control paradigm in a membrane bioreactor for advanced wastewater treatment, Environ. Sci. Technol. 43 (2009) 380–385, http://dx.doi.org/10.1021/es8019275.
[67] Y. Xiong, Y. Liu, Biological control of microbial attachment: a promising alternative for mitigating membrane biofouling, Appl. Microbiol. Biotechnol. 86 (2010) 825–837, http://dx.doi.org/10.1007/s00253-010-2463-0.
[68] Z. Wang, J. Ma, C.Y. Tang, K. Kimura, Q. Wang, X. Han, Membrane cleaning in membrane bioreactors: a review, J. Membr. Sci. 468 (2014) 276–307, http://dx.doi.org/10.1016/j.memsci.2014.05.060.
[69] K. Ponnusamy, S. Kappachery, M. Thekeettle, J.H. Song, J.H. Kweon, Anti-biofouling property of vanillin on Aeromonas hydrophila initial biofilm on various membrane surfaces, World J. Microbiol. Biotechnol. 29 (2013) 1695–1703, http://dx.doi.org/10.1007/s11274-013-1332-2.
[70] M.F. Siddiqui, M. Sakinah, A.F. Ismail, T. Matsuura, A.W. Zularisam, The anti-biofouling effect of Piper betle extract against Pseudomonas aeruginosa and bacterial consortium, Desalination 288 (2012) 24–30, http://dx.doi.org/10.1016/j.desal.2011.11.060.
[71] M.F. Siddiqui, M. Sakinah, L. Singh, A.W. Zularisam, Targeting N-acyl-homoserine-lactones to mitigate membrane biofouling based on quorum sensing using a biofouling reducer, J. Biotechnol. 161 (2012) 190–197, http://dx.doi.org/10.1016/j.jbiotec.2012.06.029.
[72] J.-H. Kim, D.-C. Choi, K.-M. Yeon, S.-R. Kim, C.-H. Lee, Enzyme-immobilized nanofiltration membrane to mitigate biofouling based on quorum quenching, Environ. Sci. Technol. 45 (2011) 1601–1607, http://dx.doi.org/10.1021/es103483j.
[73] W. Jiang, S. Xia, J. Liang, Z. Zhang, S.W. Hermanowicz, Effect of quorum quenching on the reactor performance, biofouling and biomass characteristics in membrane bioreactors, Water Res. 47 (2013) 187–196, http://dx.doi.org/10.1016/j.watres.2012.09.050.
[74] H.-W. Kim, H.-S. Oh, S.-R. Kim, K.-B. Lee, K.-M. Yeon, C.-H. Lee, et al., Microbial population dynamics and proteomics in membrane bioreactors with enzymatic quorum quenching, Appl. Microbiol. Biotechnol. 97 (2012) 4665–4675, http://dx.doi.org/10.1007/s00253-012-4272-0.
[75] B. Lee, K.-M. Yeon, J. Shim, S.-R. Kim, C.-H. Lee, J. Lee, et al., Effective anti-fouling using quorum-quenching acylase stabilized in magnetically-separable mesoporous silica, Biomacromolecules 15 (2014) 1153–1159, http://dx.doi.org/10.1021/bm401595q.
[76] H.-S. Oh, K.-M. Yeon, C.-S. Yang, S.-R. Kim, C.-H. Lee, S.Y. Park, et al., Control of membrane biofouling in MBR for wastewater treatment by quorum quenching bacteria encapsulated in microporous membrane, Environ. Sci. Technol. 46 (2012) 4877–4884, http://dx.doi.org/10.1021/es204312u.
[77] S.-R. Kim, H.-S. Oh, S.-J. Jo, K.-M. Yeon, C.-H. Lee, D.-J. Lim, et al., Biofouling control with bead-entrapped quorum quenching bacteria in membrane bioreactors: physical and biological effects, Environ. Sci. Technol. 47 (2013) 836–842, http://dx.doi.org/10.1021/es303995s.
[78] N.A. Weerasekara, K.-H. Choo, C.-H. Lee, Hybridization of physical cleaning and quorum quenching to minimize membrane biofouling and energy consumption in a membrane bioreactor, Water Res. 67 (2014) 1–10, http://dx.doi.org/10.1016/j.watres.2014.08.049.
[79] T. Maqbool, S.J. Khan, H. Waheed, C.-H. Lee, I. Hashmi, H. Iqbal, Membrane biofouling retardation and improved sludge characteristics using quorum quenching bacteria in submerged membrane bioreactor, J. Membr. Sci. 483 (2015) 75–83, http://dx.doi.org/10.1016/j.memsci.2015.02.011.
[80] S.-R. Kim, K.-B. Lee, J.-E. Kim, Y.-J. Won, K.-M. Yeon, C.-H. Lee, et al., Macroencapsulation of quorum quenching bacteria by polymeric membrane layer and its application to MBR for biofouling control, J. Membr. Sci. 473 (2015) 109–117, http://dx.doi.org/10.1016/j.memsci.2014.09.009.
[81] J.B. Kristensen, R.L. Meyer, B.S. Laursen, S. Shipovskov, F. Besenbacher, C.H. Poulsen, Antifouling enzymes and the biochemistry of marine settlement, Biotechnol. Adv. 26 (2008) 471–481, http://dx.doi.org/10.1016/j.biotechadv.2008.05.005.
[82] A.L. Cordeiro, C. Werner, Enzymes for antifouling strategies, J. Adhes. Sci. Technol. 25 (2011) 2317–2344, http://dx.doi.org/10.1163/016942411X574961.
[83] R. Ciriminna, F.V. Bright, M. Pagliaro, Ecofriendly antifouling marine coatings, ACS Sustain. Chem. Eng. 3 (2015) 559–565, http://dx.doi.org/10.1021/sc500845n.
[84] S.M. Olsen, L.T. Pedersen, M.H. Laursen, S. Kiil, K. Dam-Johansen, Enzyme-based antifouling coatings: a review, Biofouling 23 (2007) 369–383, http://dx.doi.org/10.1080/08927010701566384.
[85] K. Tait, I. Joint, M. Daykin, D.L. Milton, P. Williams, M. Camara, Disruption of quorum sensing in seawater abolishes attraction of zoospores of the green alga Ulva to bacterial biofilms, Environ. Microbiol. 7 (2005) 229–240, http://

Please cite this article in press as: J. Bzdrenga, et al., Biotechnological applications of quorum quenching enzymes, Chemico-Biological Interactions (2016), http://dx.doi.org/10.1016/j.cbi.2016.05.028

dx.doi.org/10.1111/j.1462-2920.2004.00706.x.
[86] S. Dobretsov, H.-U. Dahms, H. YiLi, M. Wahl, P.-Y. Qian, The effect of quorum-sensing blockers on the formation of marine microbial communities and larval attachment: antifouling activity of QS blockers, FEMS Microbiol. Ecol. 60 (2007) 177–188, http://dx.doi.org/10.1111/j.1574-6941.2007.00285.x.
[87] S. Dobretsov, M. Teplitski, M. Bayer, S. Gunasekera, P. Proksch, V.J. Paul, Inhibition of marine biofouling by bacterial quorum sensing inhibitors, Biofouling 27 (2011) 893–905, http://dx.doi.org/10.1080/08927014.2011.609616.
[88] D.M. Sievert, P. Ricks, J.R. Edwards, A. Schneider, J. Patel, A. Srinivasan, et al., National healthcare safety network (NHSN) team and participating NHSN facilities, antimicrobial-resistant pathogens associated with healthcare-associated infections: summary of data reported to the national healthcare safety network at the centers for disease control and prevention, 2009-2010, Infect. Control Hosp. Epidemiol. Off. J. Soc. Hosp. Epidemiol. Am. 34 (2013) 1–14, http://dx.doi.org/10.1086/668770.
[89] W.-L. Ng, B.L. Bassler, Bacterial quorum-sensing network architectures, Annu. Rev. Genet. 43 (2009) 197–222, http://dx.doi.org/10.1146/annurev-genet-102108-134304.
[90] L.C.M. Antunes, R.B.R. Ferreira, M.M.C. Buckner, B.B. Finlay, Quorum sensing in bacterial virulence, Microbiology 156 (2010) 2271–2282, http://dx.doi.org/10.1099/mic.0.038794-0.
[91] E.S. Antonova, B.K. Hammer, Genetics of natural competence in vibrio cholerae and other vibrios, Microbiol. Spectr. 3 (2015), http://dx.doi.org/10.1128/microbiolspec.VE-0010-2014.
[92] F.S.W. Ng, D.M. Wright, S.Y.K. Seah, Characterization of a phosphotriesterase-like lactonase from sulfolobus solfataricus and its immobilization for disruption of quorum sensing, Appl. Environ. Microbiol. 77 (2011) 1181–1186, http://dx.doi.org/10.1128/AEM.01642-10.
[93] S.M. Jacobsen, D.J. Stickler, H.L.T. Mobley, M.E. Shirtliff, Complicated catheter-associated urinary tract infections due to Escherichia coli and Proteus mirabilis, Clin. Microbiol. Rev. 21 (2008) 26–59, http://dx.doi.org/10.1128/CMR.00019-07.
[94] J.M. Walz, R.L. Avelar, K.J. Longtine, K.L. Carter, L.A. Mermel, S.O. Heard, 5-FU Catheter Study Group, Anti-infective external coating of central venous catheters: a randomized, noninferiority trial comparing 5-fluorouracil with chlorhexidine/silver sulfadiazine in preventing catheter colonization, Crit. Care Med. 38 (2010) 2095–2102, http://dx.doi.org/10.1097/CCM.0b013e3181f265ba.
[95] K. Ivanova, M.M. Fernandes, E. Mendoza, T. Tzanov, Enzyme multilayer coatings inhibit Pseudomonas aeruginosa biofilm formation on urinary catheters, Appl. Microbiol. Biotechnol. 99 (2015) 4373–4385, http://dx.doi.org/10.1007/s00253-015-6378-7.
[96] K. Ivanova, M.M. Fernandes, A. Francesko, E. Mendoza, J. Guezguez, M. Burnet, et al., Quorum-quenching and matrix-degrading enzymes in multilayer coatings synergistically prevent bacterial biofilm formation on urinary catheters, ACS Appl. Mater. Interfaces 7 (49) (2015) 27066–27077, http://dx.doi.org/10.1021/acsami.5b09489.
[97] P. Gupta, S. Chhibber, K. Harjai, Efficacy of purified lactonase and ciprofloxacin in preventing systemic spread of Pseudomonas aeruginosa in murine burn wound model, Burns J, Int. Soc. Burn Inj. 41 (1) (February 2015) 153–162, http://dx.doi.org/10.1016/j.burns.2014.06.009.
[98] S.B. Guttenplan, D.B. Kearns, Regulation of flagellar motility during biofilm formation, FEMS Microbiol. Rev. 37 (2013) 849–871, http://dx.doi.org/10.1111/1574-6976.12018.
[99] S. Hraiech, J. Hiblot, J. Lafleur, H. Lepidi, L. Papazian, J.-M. Rolain, et al., Inhaled lactonase reduces pseudomonas aeruginosa quorum sensing and mortality in rat pneumonia, PLoS One 9 (2014) e107125, http://dx.doi.org/10.1371/journal.pone.0107125.
[100] L. Afriat, C. Roodveldt, G. Manco, D.S. Tawfik, The latent promiscuity of newly identified microbial lactonases is linked to a recently diverged phosphotriesterase†, Biochem. (Mosc.) 45 (2006) 13677–13686, http://dx.doi.org/10.1021/bi061268r.
[101] L. Afriat-Jurnou, C.J. Jackson, D.S. Tawfik, Reconstructing a missing link in the evolution of a recently diverged phosphotriesterase by active-site loop remodeling, Biochem. (Mosc.) 51 (2012) 6047–6055, http://dx.doi.org/10.1021/bi300694t.
[102] M. Elias, D.S. Tawfik, Divergence and convergence in enzyme evolution: parallel evolution of paraoxonases from quorum-quenching lactonases, J. Biol. Chem. 287 (2011) 11–20, http://dx.doi.org/10.1074/jbc.R111.257329.
[103] M. Elias, J. Dupuy, L. Merone, L. Mandrich, E. Porzio, S. Moniot, et al., Structural basis for natural lactonase and promiscuous phosphotriesterase activities, J. Mol. Biol. 379 (2008) 1017–1028, http://dx.doi.org/10.1016/j.jmb.2008.04.022.
[104] J. Hiblot, J. Bzdrenga, C. Champion, E. Chabriere, M. Elias, Crystal structure of VmoLac, a tentative quorum quenching lactonase from the extremophilic crenarchaeon Vulcanisaeta moutnovskia, Sci. Rep. 5 (2015) 8372, http://dx.doi.org/10.1038/srep08372.
[105] B. Xue, J.Y. Chow, A. Baldansuren, L.L. Yap, Y.H. Gan, S.A. Dikanov, et al., Structural evidence of a productive active site architecture for an evolved quorum-quenching GKL Lactonase, Biochem. (Mosc.) 52 (2013) 2359–2370, http://dx.doi.org/10.1021/bi4000904.
[106] J. Bzdrenga, J. Hiblot, G. Gotthard, C. Champion, M. Elias, E. Chabriere, SacPox from the thermoacidophilic crenarchaeon Sulfolobus acidocaldarius is a proficient lactonase, BMC Res. Notes 7 (2014) 333, http://dx.doi.org/10.1186/1756-0500-7-333.
[107] J. Hiblot, G. Gotthard, E. Chabriere, M. Elias, Structural and enzymatic characterization of the lactonase SisLac from sulfolobus islandicus, PLoS One 7 (2012) e47028, http://dx.doi.org/10.1371/journal.pone.0047028.
[108] P. Vecchio, M. Elias, L. Merone, G. Graziano, J. Dupuy, L. Mandrich, et al., Structural determinants of the high thermal stability of SsoPox from the hyperthermophilic archaeon Sulfolobus solfataricus, Extremophiles 13 (2009) 461–470, http://dx.doi.org/10.1007/s00792-009-0231-9.
[109] J. Hiblot, G. Gotthard, M. Elias, E. Chabriere, Differential active site loop conformations mediate promiscuous activities in the lactonase SsoPox, PLoS One 8 (2013) e75272, http://dx.doi.org/10.1371/journal.pone.0075272.
[110] J. Hiblot, G. Gotthard, E. Chabriere, M. Elias, Characterisation of the organophosphate hydrolase catalytic activity of SsoPox, Sci. Rep. 2 (2012), http://dx.doi.org/10.1038/srep00779.
[111] J. Hiblot, G. Gotthard, C. Champion, E. Chabriere, M. Elias, Crystallization and preliminary X-ray diffraction analysis of the lactonase VmoLac from Vulcanisaeta moutnovskia, Acta Crystallogr. Sect. F. Struct. Biol. Cryst. Commun. 69 (2013) 1235–1238, http://dx.doi.org/10.1107/S1744309113024846.
[112] J.Y. Chow, L. Wu, W.S. Yew, Directed Evolution of a Quorum-Quenching Lactonase from Mycobacterium avium subsp. paratuberculosis K-10 in the amidohydrolase superfamily, Biochem. (Mosc.) 48 (2009) 4344–4353, http://dx.doi.org/10.1021/bi9004045.
[113] J.Y. Chow, B. Xue, K.H. Lee, A. Tung, L. Wu, R.C. Robinson, et al., Directed evolution of a thermostable quorum-quenching lactonase from the amidohydrolase superfamily, J. Biol. Chem. 285 (2010) 40911–40920, http://dx.doi.org/10.1074/jbc.M110.177139.
[114] Y.-H. Dong, J.-L. Xu, X.-Z. Li, L.-H. Zhang, AiiA, an enzyme that inactivates the acylhomoserine lactone quorum-sensing signal and attenuates the virulence of Erwinia carotovora, Proc. Natl. Acad. Sci. 97 (2000) 3526–3531, http://dx.doi.org/10.1073/pnas.97.7.3526.
[115] D. Liu, P.W. Thomas, J. Momb, Q.Q. Hoang, G.A. Petsko, D. Ringe, et al., Structure and specificity of a quorum-quenching lactonase (AiiB) from Agrobacterium tumefaciens†,‡, Biochem. (Mosc.) 46 (2007) 11789–11799, http://dx.doi.org/10.1021/bi7012849.
[116] L. Merone, L. Mandrich, M. Rossi, G. Manco, A thermostable phosphotriesterase from the archaeon Sulfolobus solfataricus: cloning, overexpression and properties, Extremophiles 9 (2005) 297–305, http://dx.doi.org/10.1007/s00792-005-0445-4.
[117] M. Elias, J. Dupuy, L. Merone, C. Lecomte, M. Rossi, P. Masson, et al., Crystallization and preliminary X-ray diffraction analysis of the hyperthermophilic *Sulfolobus solfataricus* phosphotriesterase, Acta Crystallogr. Sect. F. Struct. Biol. Cryst. Commun. 63 (2007) 553–555, http://dx.doi.org/10.1107/S1744309107023512.
[118] M. Elias, J. Dupuy, L. Merone, L. Mandrich, E. Porzio, S. Moniot, et al., Structural basis for natural lactonase and promiscuous phosphotriesterase activities, J. Mol. Biol. 379 (2008) 1017–1028, http://dx.doi.org/10.1016/j.jmb.2008.04.022.
[119] A.J. Alanis, Resistance to antibiotics: are we in the post-antibiotic era? Arch. Med. Res. 36 (2005) 697–705, http://dx.doi.org/10.1016/j.arcmed.2005.06.009.
[120] G.D. Wright, Bacterial resistance to antibiotics: enzymatic degradation and modification, Adv. Drug Deliv. Rev. 57 (2005) 1451–1470, http://dx.doi.org/10.1016/j.addr.2005.04.002.
[121] A. Kumar, H.P. Schweizer, Bacterial resistance to antibiotics: active efflux and reduced uptake, Adv. Drug Deliv. Rev. 57 (2005) 1486–1513, http://dx.doi.org/10.1016/j.addr.2005.04.004.
[122] M. Hentzer, H. Wu, J.B. Andersen, K. Riedel, T.B. Rasmussen, N. Bagge, et al., Attenuation of Pseudomonas aeruginosa virulence by quorum sensing inhibitors, EMBO J. 22 (2003) 3803–3815, http://dx.doi.org/10.1093/emboj/cdg366.
[123] C.M. Waters, B.L. Bassler, Quorum sensing: cell-to-cell communication in bacteria, Annu. Rev. Cell Dev. Biol. 21 (2005) 319–346, http://dx.doi.org/10.1146/annurev.cellbio.21.012704.131001.
[124] M. Romero, L. Acuna, A. Otero, Patents on quorum quenching: interfering with bacterial communication as a strategy to fight infections, Recent Pat. Biotechnol. 6 (2012) 2–12, http://dx.doi.org/10.2174/187220812799789208.
[125] S. Uroz, Y. Dessaux, P. Oger, Quorum sensing and quorum quenching: the yin and yang of bacterial communication, Chembiochem Eur. J. Chem. Biol. 10 (2009) 205–216, http://dx.doi.org/10.1002/cbic.200800521.
[126] S.P. Diggle, A.S. Griffin, G.S. Campbell, S.A. West, Cooperation and conflict in quorum-sensing bacterial populations, Nature 450 (2007) 411–414, http://dx.doi.org/10.1038/nature06279.
[127] T. Defoirdt, N. Boon, P. Bossier, Can bacteria evolve resistance to quorum sensing disruption? PLoS Pathog. 6 (2010) e1000989, http://dx.doi.org/10.1371/journal.ppat.1000989.
[128] R. García-Contreras, T. Maeda, T.K. Wood, Resistance to quorum-quenching compounds, Appl. Environ. Microbiol. 79 (2013) 6840–6846, http://dx.doi.org/10.1128/AEM.02378-13.
[129] R. García-Contreras, L. Nuñez-López, R. Jasso-Chávez, B.W. Kwan, J.A. Belmont, A. Rangel-Vega, et al., Quorum sensing enhancement of the stress response promotes resistance to quorum quenching and prevents social cheating, ISME J. 9 (2015) 115–125, http://dx.doi.org/10.1038/ismej.2014.98.
[130] T. Maeda, R. García-Contreras, M. Pu, L. Sheng, L.R. Garcia, M. Tomás, et al., Quorum quenching quandary: resistance to antivirulence compounds, ISME

Please cite this article in press as: J. Bzdrenga, et al., Biotechnological applications of quorum quenching enzymes, Chemico-Biological Interactions (2016), http://dx.doi.org/10.1016/j.cbi.2016.05.028

ARTICLE IN PRESS

J. 6 (2012) 493–501, http://dx.doi.org/10.1038/ismej.2011.122.
[131] K.M. Sandoz, S.M. Mitzimberg, M. Schuster, Social cheating in Pseudomonas aeruginosa quorum sensing, Proc. Natl. Acad. Sci. U. S. A. 104 (2007) 15876–15881, http://dx.doi.org/10.1073/pnas.0705653104.
[132] S.B. Tay, W.S. Yew, Development of quorum-based anti-virulence therapeutics targeting Gram-negative bacterial pathogens, Int. J. Mol. Sci. 14 (2013) 16570–16599, http://dx.doi.org/10.3390/ijms140816570.
[133] J.P. Gerdt, H.E. Blackwell, Competition studies confirm two major barriers that can preclude the spread of resistance to quorum-sensing inhibitors in bacteria, ACS Chem. Biol. 9 (2014) 2291–2299, http://dx.doi.org/10.1021/cb5004288.
[134] C.H. Collins, F.H. Arnold, J.R. Leadbetter, Directed evolution of Vibrio fischeri LuxR for increased sensitivity to a broad spectrum of acyl-homoserine lactones, Mol. Microbiol. 55 (2005) 712–723, http://dx.doi.org/10.1111/j.1365-2958.2004.04437.x.
[135] A.C. Hawkins, F.H. Arnold, R. Stuermer, B. Hauer, J.R. Leadbetter, Directed evolution of Vibrio fischeri LuxR for improved response to butanoyl-homoserine lactone, Appl. Environ. Microbiol. 73 (2007) 5775–5781, http://dx.doi.org/10.1128/AEM.00060-07.
[136] T.F. Mah, G.A. O'Toole, Mechanisms of biofilm resistance to antimicrobial agents, Trends Microbiol. 9 (2001) 34–39.
[137] P.S. Stewart, J.W. Costerton, Antibiotic resistance of bacteria in biofilms, Lancet Lond. Engl. 358 (2001) 135–138.
[138] E. Drenkard, F.M. Ausubel, Pseudomonas biofilm formation and antibiotic resistance are linked to phenotypic variation, Nature 416 (2002) 740–743, http://dx.doi.org/10.1038/416740a.
[139] P.S. Stewart, Mechanisms of antibiotic resistance in bacterial biofilms, Int. J. Med. Microbiol. IJMM 292 (2002) 107–113, http://dx.doi.org/10.1078/1438-4221-00196.
[140] T.-F. Mah, B. Pitts, B. Pellock, G.C. Walker, P.S. Stewart, G.A. O'Toole, A genetic basis for Pseudomonas aeruginosa biofilm antibiotic resistance, Nature 426 (2003) 306–310, http://dx.doi.org/10.1038/nature02122.
[141] N. Høiby, T. Bjarnsholt, M. Givskov, S. Molin, O. Ciofu, Antibiotic resistance of bacterial biofilms, Int. J. Antimicrob. Agents 35 (2010) 322–332, http://dx.doi.org/10.1016/j.ijantimicag.2009.12.011.
[142] E.B.M. Breidenstein, C. de la Fuente-Núñez, R.E.W. Hancock, Pseudomonas aeruginosa: all roads lead to resistance, Trends Microbiol. 19 (2011) 419–426, http://dx.doi.org/10.1016/j.tim.2011.04.005.
[143] S. Kiran, P. Sharma, K. Harjai, N. Capalash, Enzymatic quorum quenching increases antibiotic susceptibility of multidrug resistant Pseudomonas aeruginosa, Iran. J. Microbiol. 3 (2011) 1–12.

Please cite this article in press as: J. Bzdrenga, et al., Biotechnological applications of quorum quenching enzymes, Chemico-Biological Interactions (2016), http://dx.doi.org/10.1016/j.cbi.2016.05.028

II. Projet de recherche

Objectifs de la thèse

II. Projet de recherche

Objectifs de la thèse

Ma thèse a consisté à optimiser et mettre en œuvre des variants de l'enzyme hyperthermostable *Sso*Pox pour différentes applications parmi lesquelles la bioremédiation des pesticides, la biodécontamination des agents neurotoxiques de guerre ou encore la lutte contre la virulence bactérienne.

Mes travaux de thèse sont répartis en quatre parties :

Dans une première partie, une stratégie d'évolution dirigée semi-rationnelle a été utilisée afin d'améliorer l'activité de promiscuité phosphotriestérase de la lactonase *Sso*Pox. Cette stratégie qui reposait sur l'homologie de *Sso*Pox avec les phosphotriestérases bactériennes a permis de mettre au point des bioépurateurs à large spectre pour la décontamination des pesticides. Différents variants de *Sso*Pox ont été obtenus permettant de décontaminer la plupart des insecticides commerciaux en seulement quelques minutes. Les structures de ces variants ont été résolues et les relations régissant séquence, structure et fonction de ces enzymes ont été étudiées.

Fort de ces résultats une deuxième partie a consisté en un nouveau tour d'évolution dirigée avec pour objectif d'améliorer de nouveau l'activité phosphotriestérase de *Sso*Pox, sur les pesticides et également sur des analogues d'agents neurotoxiques de guerre. Dans le même temps, une analyse globale de la promiscuité de substrats de l'enzyme et de ses variants a permis de déterminer l'impact de l'augmentation de l'activité phosphotriestérase sur les activités lactonase et arylestérase. L'efficacité de décontamination des meilleurs variants phosphotriestérase a été par la suite étudiée en mesurant leur capacité à protéger l'acétylcholinestérase humaine contre le paraoxon.

Après avoir mis en évidence le fort potentiel des variants de *Sso*Pox pour la décontamination externe des insecticides et analogues d'agents neurotoxiques de guerre. Une troisième partie, a consisté à étudier la capacité de biodécontamination d'un des meilleurs variants pour la dégradation des pesticides, *Sso*Pox-αsD6, dans un modèle animal. La toxicité des OPs et des produits de dégradation enzymatique ont ainsi été étudiés *in vivo* chez la planaire, un ver plat d'eau douce de l'embranchement des plathelminthes. Ce travail a mis en avant la grande efficacité de l'enzyme pour réduire la toxicité des insecticides et leur impact sur le comportement. De plus l'utilisation de l'enzyme a permis de limiter l'effet des insecticides sur le développement et la régénération des planaires.

Enfin, la dernière partie de ma thèse s'est axée sur l'activité lactonase de *Sso*Pox. Un variant ayant une activité améliorée pour la dégradation des 3-oxo-C12-AHL impliquées dans la communication bactérienne de *Pseudomonas aeruginosa* a ainsi été mis en œuvre. L'efficacité du variant pour réduire la virulence de 51 souches bactériennes cliniques issues d'infections du pied diabétique a ainsi été démontrée, l'enzyme se montrant plus efficace que d'autres inhibiteurs du QS et conservant son efficacité après immobilisation.

L'ensemble de mes travaux de thèse s'est donc concentré sur l'amélioration de l'activité enzymatique de *Sso*Pox et des applications utilisant des variants améliorés.

II. Projet de recherche

Partie 1

Ingénierie rationnelle d'une lactonase native hyperthermostable en phosphotriestérase à large spectre

Partie 1 : Ingénierie rationnelle d'une lactonase native hyperthermostable en phosphotriestérase à large spectre

De nombreuses enzymes, telles que les paraoxonases, les organophosphates hydrolases (OPHs) ou les organophosphates acides anhydrolases (OPAAs), sont capables naturellement de dégrader les organophosphorés. Parmi les OPHs, la phosphotriestérase bactérienne de *Brevundimonas diminuta* (*Bd*PTE) est probablement l'enzyme la plus efficace. Cette enzyme est par exemple capable de dégrader l'éthyl-paraoxon avec une efficacité catalytique k_{cat}/K_M de 5.5×10^7 $M^{-1}.s^{-1}$, proche de la limite de diffusion[64]. Ces enzymes mésophiles ont une stabilité thermique modérée[65], pouvant poser problème pour des applications industrielles. D'autres OPHs ont été immobilisées dans des mousses de polyuréthane ou des éponges décontaminantes, cependant des limites sont apparues comme une faible résistance aux solvants ce qui freine fortement leur potentiel industriel[66]. Les enzymes hyperthermostables, comme *Sso*Pox, sont donc particulièrement intéressantes pour pallier ces limitations. En effet ces enzymes ont une grande stabilité qui leur confère une meilleure résistance aux procédés industriels. D'un côté *Bd*PTE est une enzyme modérément stable mais extrêmement efficace et de l'autre *Sso*Pox est passablement efficace mais très stable. Mettant à profit le fait que *Bd*PTE et *Sso*Pox ont des structures similaires avec 31% d'identité de séquence et un RMSD, l'écart quadratique moyen, de l'ensemble des atomes égal à 0.98 Å **(Figure 5)**, l'objectif a été de transférer le site actif hautement performant de *Bd*PTE dans l'architecture extrêmement stable de *Sso*Pox. Ce transfert a été réalisé par évolution dirigée, les positions importantes à muter ont été fixées puis les mutations ont été combinées aléatoirement.

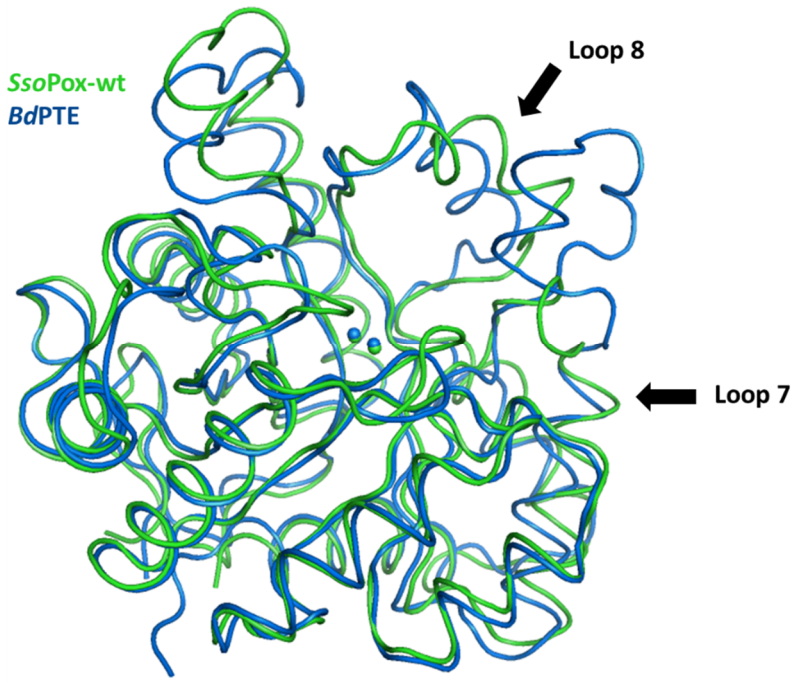


Figure 5 : Superposition de *Sso*Pox-wt (en vert, PDB 2VC5) et *Bd*PTE (en bleu, PDB 1DPM).

Un cycle d'évolution dirigée a été réalisé et les cinq meilleurs variants, parmi les 184 variants isolés, ont été caractérisés et leurs structures résolues. Le variant le plus actif *Sso*Pox-αsD6 montre une forte augmentation de son activité catalytique pour un certain nombre de pesticides comme par

exemple pour le méthyl-parathion pour lequel son activité est 2 210 fois plus importante que celle de l'enzyme sauvage. De plus, l'analyse des structures des cinq variants montre qu'une augmentation de l'activité entraine une déstabilisation de la boucle 8 du site actif impliquée dans la liaison avec le substrat. Ces résultats confortent l'idée que la flexibilité du site actif est essentielle pour l'acquisition d'une spécificité pour un nouveau substrat.

Parmi ces cinq variants seul *Sso*Pox-αsB5 ne contient pas de mutation en W263, résidu préalablement identifié comme jouant un rôle majeur pour l'activité phosphotriestérase de *Sso*Pox[67]. Ainsi une stratégie de mutagénèse à saturation a été utilisée pour tester toutes les 19 substitutions possibles à cette position. Cependant, les variants obtenus n'ont pas une activité améliorée par rapport à *Sso*Pox-αsB5. Il semble que la mutation en W263 et les mutations du variant *Sso*Pox-αsB5 soient incompatibles, probablement à cause de l'effet déstabilisant sur la boucle 8 qui est trop important, ce qui donne lieu à une épistasie négative lorsque ces mutations sont combinées.

Pour mieux cerner le spectre d'action des variants améliorés deux variants obtenus par évolution dirigée, trois variants obtenus par mutagénèse et deux variants avec une unique mutation en W263 ont été caractérisés sur huit pesticides. Ainsi on peut observer une corrélation entre la flexibilité de la boucle 8 et l'élargissement du spectre d'action enzymatique.

Par la suite, le variant *Sso*Pox-αsD6 a été utilisé pour tester l'efficacité de bioremédiation. En effet ce variant possède l'activité phosphotriestérase la plus importante, avec un large spectre d'action allant jusqu'à dix pesticides. Ce variant est donc un excellent candidat pour la bioremédiation des OPs. Ainsi, huit pesticides ont été testés et dégradés à 95% dans des intervalles de temps allant de quelques minutes jusqu'à 40 minutes ; pour la plus forte concentration en enzyme. Ces résultats confirment que ce variant est un très bon candidat pour la bioremédiation externe des pesticides.

Au cours de ces travaux, je suis intervenue sur la mutagénèse dirigée, j'ai produit et purifié huit variants. J'ai déterminé quarante paramètres cinétiques et mesuré sept T_m. J'ai également étudié le potentiel de bioremédiation du variant *Sso*Pox-αsD6. Enfin j'ai participé activement à l'écriture et à la relecture du manuscrit ainsi qu'à la réalisation des figures. Ces travaux ont été publiés dans le journal *Scientific Reports*.

Les figures et tableaux supplémentaires sont en annexe.

1.1. Introduction

Enzymes are extraordinary molecules that can accelerate chemical reactions, including those that spontaneously occur extremely slowly, and can make them happen many times per second[68]. Some of these reactions are of high biotechnological or industrial interest and enzymes are, therefore, the focus of numerous studies[69]. However, enzymes are often not directly compatible with industrial processes for various reasons ranging from their sub-optimality[70,71] or lack of stability under certain conditions[72]. The properties of enzymes can be tuned by molecular engineering to fit these new requirements using high throughput methods such as directed evolution[72–77] and/or low throughput methods, reducing the size of the library by focusing on positions that can be saturated[78–80], or by using phylogenetically-inferred[81,82] or structure-based mutations to create combinatorial[83], reduced libraries[84].

Here, we focus on the molecular engineering of an enzymatic bio-decontaminant of organophosphates compounds (OPs), including nerve agents and insecticides. These compounds are neurotoxic because of their ability to irreversibly inhibit the acetylcholine esterase, a key enzyme in the nervous system[85]. Massively used in agriculture as pesticides[86], they were modified before World War II to increase their toxicity and develop chemical warfare agents[87]. OPs still represent major environmental, health and security concerns, as they cause significant pollution[88,89], and intoxication, and have been used in terrorist attacks[86,87]. However, since current methods for removing them are cost prohibitive and lead to ecological concerns, enzymatic remediation is a promising way of developing efficient bio-decontamination methods[90–92].

Phosphotriesterase-like lactonases (PLLs) are appealing candidates, being natural lactonases endowed with promiscuous phosphotriesterase activity[93]. They have long been related to the bacterial phosphotriesterases (PTEs), enzymes which are capable of hydrolyzing insecticides such as parathion with high catalytic efficiency[94]. PTEs and PLLs belong to the amidohydrolase superfamily[95,96], and share the same $(\alpha/\beta)_8$ barrel topology. Some PLL representatives are extremely thermostable[97–105] and are particularly promising candidates for biotechnological use[16,106] by virtue of their high stability and resistance towards denaturing agents[107]. PLLs, however, exhibit much lower phosphotriesterase activity than PTEs. Engineering experiments with the aim of increasing PLLs' phosphotriesterase activity were performed. In particular, because PTEs and PLLs' active sites mainly differ in their loop length (7 and 8), sequences and conformations[83,93,108], loop grafting experiments were performed and proved to be difficult. This approach resulted in aggregation-prone or inactive enzymes[83,101], but was successful when using a stepwise approach[109]. Recently, more classical engineering techniques were successful in increasing the phosphotriesterase activity of the PLL *Dr*OPH[110].

In this study, we worked on the PLL *Sso*Pox from the hyperthermophilic archaea *Sulfolobus solfataricus*[99,111]. *Sso*Pox exhibits high acyl-homoserine lactones and oxo-lactones hydrolysis abilities[78], and promiscuous, low phosphotriesterase activity[22]. Previous work showed that engineering can successfully improve *Sso*Pox catalytic efficiency against phosphotriesters such as ethyl-paraoxon[78,112]. These previous studies highlighted the role of a key active site loop 8 residue, W263, which modulates the active site loop conformational space[78]. In this study, we aimed to further improve the phosphotriesterase activity of *Sso*Pox, including against phosphothionoesters. *Sso*Pox is a very appealing candidate for the bioremediation of phosphotriesters because of its unique thermal stability, and its ability to resist aging, solvent and protease treatments[113]. On the other hand, *Sso*Pox is a poor phosphothionoesterase, exhibiting a strong preference (100-fold) for methyl-paraoxon over methyl-

parathion, a feature referred to as the thiono-effect[22]. We used a rational strategy: taking advantage of the structural similarity between *Sso*Pox and the bacterial PTE from the mesophilic *Brevundimonas diminuta* (*Bd*PTE)[94], we designed and produced a structure-based combinatorial library, and screened this library for improved phosphotriesterase activity with the aim of obtaining heat stable, highly active variants with broad specificity. We obtained several improved variants, including against methyl-parathion, with a 2,210-fold improvement in activity. All these variants but variant αsB5 contained a mutation at position 263. Interestingly, the addition of the W263 mutation on an αsB5 background revealed an incompatibility of these mutations, instead of the expected increase in phosphotrieseterase activity. Of these improved variants, we obtained a mutant that lost the thiono-effect against methyl-parathion, exhibiting a >2,000-fold (k_{cat}/K_M ~10^4 $M^{-1}.s^{-1}$) as referred to the wild-type enzyme, and a methyl-paraoxon / methyl-parathion activity ratio of ~ 1. The X-ray structures of several improved variants reveal that the selected mutations increase the active site loop conformational flexibility and reshape the active site. The best variants were extensively characterized against eight commercially available insecticides, along with previously reported *Sso*Pox monovariants harboring mutation at residue 263 and their specificity spectrum was determined.

1.2. Results and Discussion

The lactonase *Sso*Pox was engineered for higher phosphotriesterase activity using structure-based combinatorial libraries. By comparing structures of enzymes with similar topology, it has been possible to redesign, using modelling tools, the active site cavity of *Sso*Pox to mimic as closely as possible that of *Bd*PTE **(Figure 6 and Supplementary Table 1)**. This method consisted of two main steps: (i) the identification of mutations corresponding to equivalent positions at the enzyme active sites using structural alignment and (ii) the rational selection of mutations, in a position with no equivalent residue, which mimicked the shape and chemical nature of the target enzyme cavity. A mutation dataset was thus obtained and used to develop a combinatorial library consisting of random combinations of our pre-selected mutations.

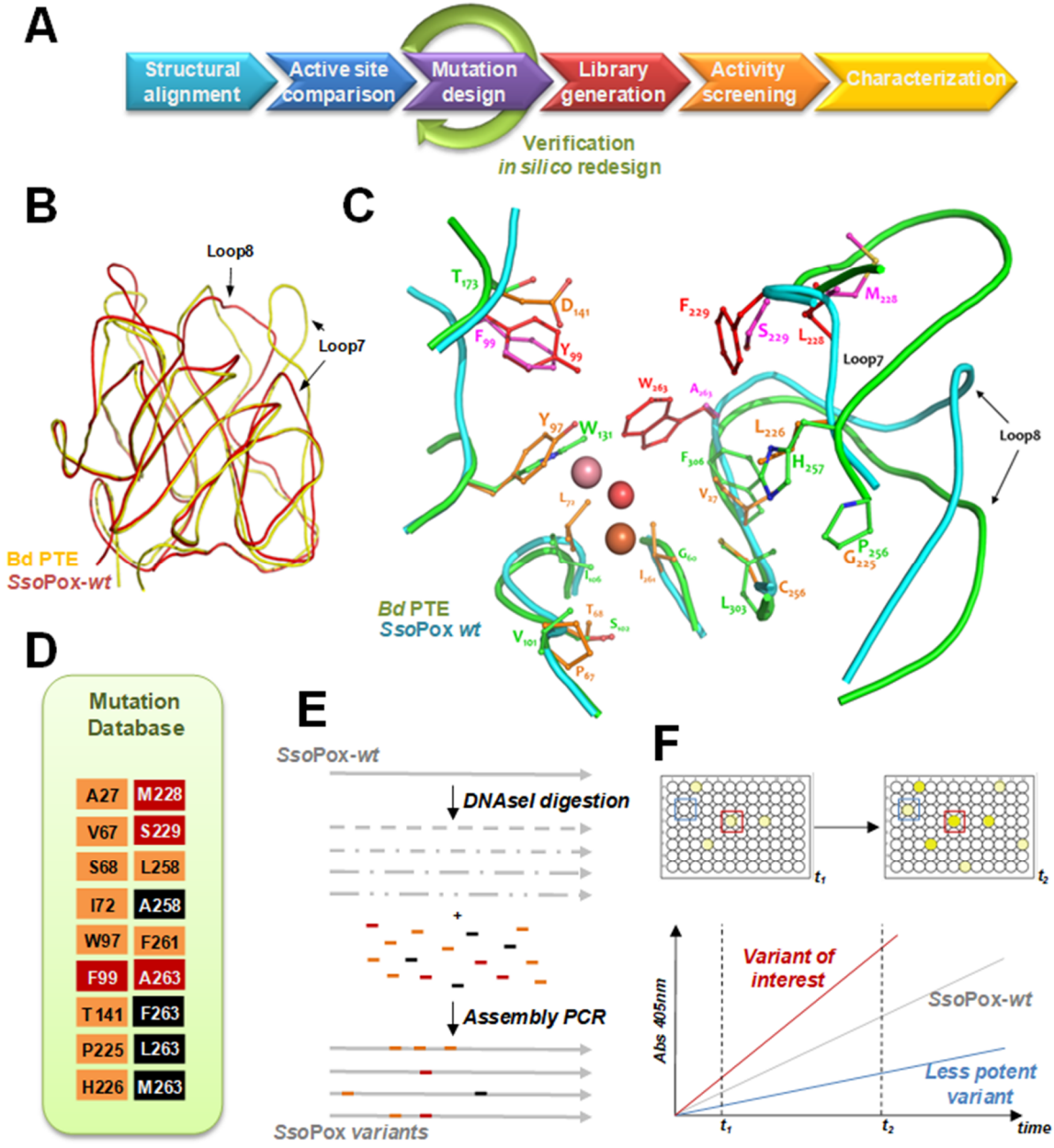


Figure 6 : Structure-based design approach.

(A) Pipeline used for the selection of improved mutants. **(B)** Structural alignments of *Sso*Pox (red) and *Bd*PTE structures (yellow) guided the mutational design. **(C)** Active site superposition of *Bd*PTE (green) and *Sso*Pox (cyan) active sites. Residues with structural equivalent (orange sticks) in both structures were used to design mutations of *Sso*Pox's residues into the *Bd*PTE corresponding residues. Positions with no structural equivalent (red sticks) were designed using modelling tools (purple sticks) to mimic the active site cavity size, shape and chemical properties of the *Bd*PTE crystal structure model **(Supplementary Figure 1)**. **(D)** The mutations data base consists of mutations to the *Bd*PTE sequence when there is a structural equivalence (orange), and of mutations designed when there is no structural equivalence (red). The third set of mutations (black) adds more diversity at two selected positions, 258 and 263. **(E)** Once the library had been validated, primers carrying mutations were used to shuffle them and generate a gene library with random combinations of selected mutations. **(F)** The library was screened for paraoxonase activity to identify enzymes with improved proficiency.

Structure-based design produced mutants with improved phosphotriesterase activity

The structure-based design considerably reshaped the active site cavity of *Sso*Pox, theoretically bringing it closer to that of *Bd*PTE, both in shape and nature **(Supplementary Figure 1)**. A total of 14 key positions within the active site were identified, and were mutated to specific residues, or degenerated into several possible amino acids (see Methods). The paraoxonase activity of 184 randomly selected clones was screened and the 14 best were sequenced. Most of these 14 were found to possess the same mutations (e.g. W263F/L/M/A; 73% of cases) **(Supplementary Figure 2A and Supplementary Table 3)**. Of them, the most active variants, αsA1 (C258L-I261F-W263A), αsA6 (F46L-C258A-W263M-I280T), αsB5 (V27A-I76T-Y97W-Y99F-L130P-L226V), αsC6 (L72I-Y99F-I122L-L228M-F229S-W263L), and αsD6 (V27A-Y97W-L228M-W263M) were subject to kinetic and structural characterization. It should be noted that αsA1 was obtained in a previous engineering effort[112], and that four of the five selected variants contained a substitution of the key residue W263. We previously highlighted the role of this residue in substrate binding and modulation of the active site loop 8 conformation, resulting in an increase in activity against promiscuous substrates[78]. Variant αsB5 does not harbor any substitution at position W263. We therefore decided to test the W263 substitution on an αsB5 background, using saturation mutagenesis strategy.

The five variants (αsA1, αsA6, αsB5, αsC6 & αsD6) were characterized against several phosphotriesters, including ethyl-paraoxon (**I**), ethyl-parathion (**II**), methyl-paraoxon (**III**), methyl-parathion (**IV**) and malathion (**V**) **(Figure 7)**. Overall, all variant exhibits improved catalytic efficiencies against all tested substrates, with the exception of αsA1 with malathion (~ 2-fold decrease) **(Figure 8A and Table 2)**. The best improved variant, αsD6, exhibits a 2,210-fold increase in catalytic efficiency against methyl-parathion **(Table 2)**. The largest improvements were observed for ethyl/methyl-parathion, two bad substrates for wild-type *Sso*Pox. Interestingly, while the wt enzyme shows a clear preference for small substituents[22], most selected variants lost this preference, possibly indicating an enlargement of the active site cavity. These improvements were in the range of what was previously obtained but with higher intensive mutation protocols and for only one OP substrate[114]. Finally, it was noted that two variants (αsA6 & αsC6) presented a substrate inhibition for some thiono-phosphotriesters.

The five selected variants were further evaluated for their lactonase activity **(Table 2)**. Interestingly, variants αsA6 and αsC6 exhibit enhanced lactonase activity against γ- and δ-lactones, while αsA1, αsB5 and αsD6 show reduced lactonase catalytic efficiencies. This emphasizes the fact that the improvement of the phosphotriesterase activity does not necessarily compromise the cognate, lactonase activity of the enzyme. These mutations therefore dramatically increased a new activity (phosphotriesterase) without the complete loss of the native / original function (lactonase)[71]. These mutants are different from those generated on another PLLs, through loop insertion. While the stepwise insertion of residues in loop 7 can significantly increase the ability of PLLs to degrade phosphotriesters, it also drastically decreases their lactonase activity[109]. Insertion in loop 7 has been previously described as a key evolutionary event in the transition from lactonase to phosphotriesterase[115].

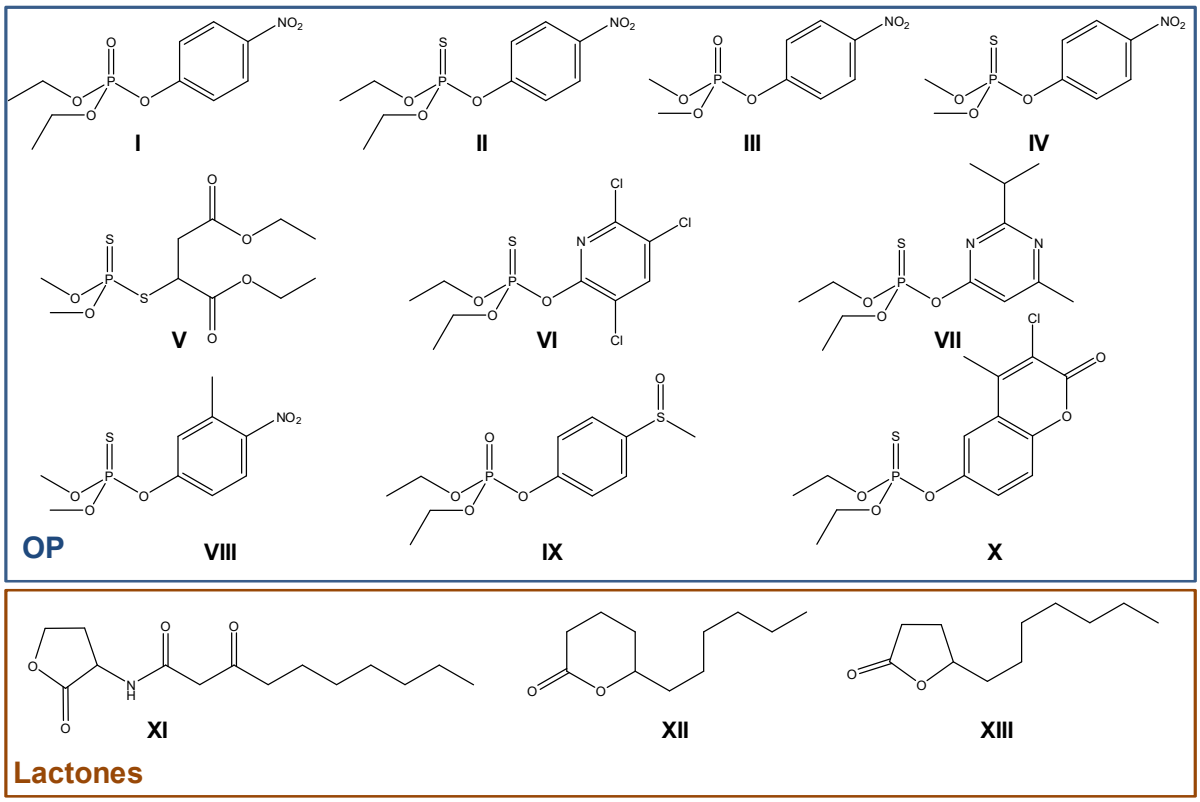


Figure 7 : Chemical structure of substrates used in this study.

The chemical structure of ethyl-paraoxon (**I**), ethyl-parathion (**II**), methyl-paraoxon (**III**), methyl-parathion (**IV**), malathion (**V**), chlorpyrifos (**VI**), diazinon (**VII**), fenitrothion (**VIII**), fensulfothion (**IX**), coumaphos (**X**), 3-oxo-C10 AHL (l) (**XI**), undecanoic-γ-lactone (**XII**) and undecanoic-δ-lactone (X**III**) generated using ChemDraw software.

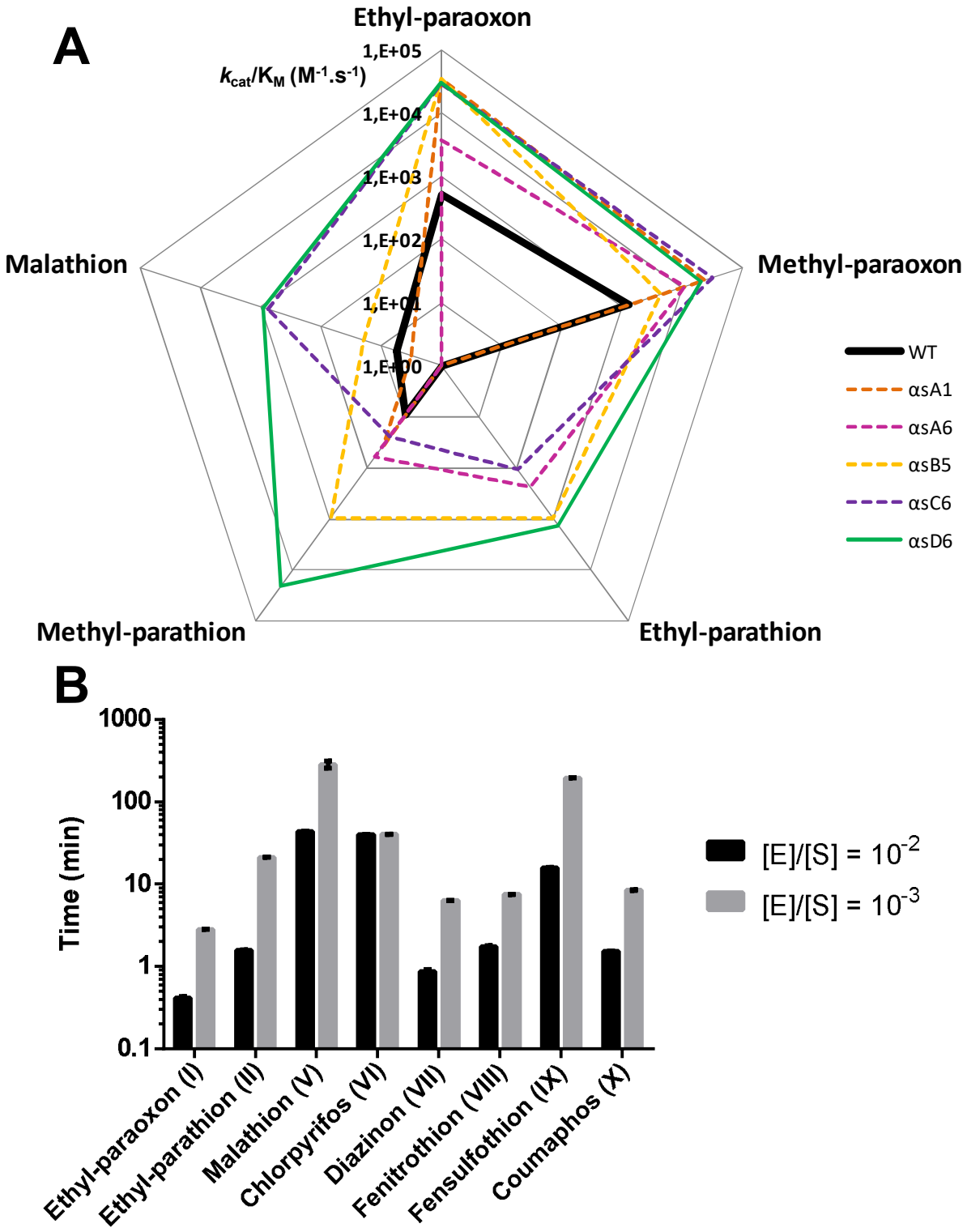


Figure 8 : Activity characterization of the improved variants and bioremediation potential.
(A) Phosphotriesterase catalytic efficiency comparison between wt-*Sso*Pox and the best selected variants. Data for wt-*Sso*Pox are from Hiblot et al. (2012)[22]. **(B)** Determination of the reaction time for hydrolyzing 95 % using the αsD6 variant of a solution of pesticide at 250 µM. Two enzyme-to-substrate ratios ([E]/[S]), 10^{-2} and 10^{-3}, were considered.

Table 2 : Kinetic characterization of *Sso*Pox variants.

* corresponds to undetermined values because enzyme saturation could not be reached.
ND corresponds to undetectable values because substrates were not hydrolyzed or too poorly hydrolyzed to be observable.
° Data taken from Hiblot *et al.* (2012)[22]
+ Date taken from Hiblot *et al.* (2013)[78]

Substrate	*Sso*Pox	k_{cat} (s^{-1})	K_M (µM)	K_I (µM)	k_{cat}/K_M ($M^{-1}.s^{-1}$)	Enhancement/wt
Ethyl-paraoxon (I)	wt°	$1.26 \pm 0.13 \times 10^{1}$	$2.43 \pm 0.37 \times 10^{4}$	-	$5.12 \pm 1.31 \times 10^{2}$	1
	αsA1	$2.70 \pm 0.23 \times 10^{1}$	$8.00 \pm 1.55 \times 10^{2}$	-	$3.37 \pm 0.71 \times 10^{4}$	65
	αsA6	5.87 ± 0.47	$1.63 \pm 0.63 \times 10^{3}$	-	$3.61 \pm 1.43 \times 10^{3}$	7
	αsB5	$2.06 \pm 0.14 \times 10^{1}$	$6.01 \pm 0.96 \times 10^{2}$	-	$3.43 \pm 1.46 \times 10^{4}$	67
	αsC6	$4.27 \pm 0.25 \times 10^{1}$	$1.50 \pm 0.16 \times 10^{3}$	-	$2.86 \pm 0.35 \times 10^{4}$	55
	αsD6	$3.22 \pm 0.18 \times 10^{1}$	$1.09 \pm 0.12 \times 10^{3}$	-	$2.95 \pm 1.55 \times 10^{4}$	58
	αsB5 W263M	*	*	-	$5.62 \pm 0.11 \times 10^{3}$	11
	αsB5 W263L	*	*	-	$8.07 \pm 0.28 \times 10^{3}$	16
	αsB5 W263I	$4.09 \pm 0.89 \times 10^{1}$	$6.64 \pm 1.75 \times 10^{3}$	-	$6.16 \pm 5.07 \times 10^{3}$	12
	W263L+	*	*	-	$2.37 \pm 0.33 \times 10^{3}$	5
	W263M+	6.82 ± 0.57	$9.31 \pm 1.63 \times 10^{2}$	-	$7.33 \pm 1.42 \times 10^{3}$	14
Ethyl-parathion (II)	wt°	ND	ND	ND	ND	ND
	αsA1	ND	ND	ND	ND	ND
	αsA6	$3.20 \pm 0.20 \times 10^{-2}$	$1.34 \pm 0.18 \times 10^{2}$	3 250 ± 1020	$2.39 \pm 0.35 \times 10^{2}$	ND
	αsB5	$2.69 \pm 0.15 \times 10^{-1}$	$2.72 \pm 0.49 \times 10^{2}$	-	$9.86 \pm 3.14 \times 10^{2}$	ND
	αsC6	$8.53 \pm 0.30 \times 10^{-3}$	$7.70 \pm 1.10 \times 10^{1}$	-	$1.10 \pm 0.16 \times 10^{2}$	ND
	αsD6	$7.35 \pm 0.36 \times 10^{-1}$	$5.34 \pm 0.62 \times 10^{2}$	-	$1.38 \pm 0.57 \times 10^{3}$	ND
	αsB5 W263M	$5.24 \pm 0.23 \times 10^{-2}$	$2.02 \pm 0.31 \times 10^{2}$	-	$2.59 \pm 0.74 \times 10^{2}$	ND
	αsB5 W263L	$4.35 \pm 0.16 \times 10^{-2}$	$3.46 \pm 0.37 \times 10^{2}$	-	$1.26 \pm 0.44 \times 10^{2}$	ND
	αsB5 W263I	$4.74 \pm 0.21 \times 10^{-2}$	$2.61 \pm 0.37 \times 10^{2}$	-	$1.82 \pm 0.57 \times 10^{2}$	ND
	W263L	ND	ND	-	ND	ND
	W263M	ND	ND	-	ND	ND
Methyl-paraoxon (III)	wt°	2.71 ± 0.64	$2.14 \pm 0.68 \times 10^{3}$	-	$1.27 \pm 0.70 \times 10^{3}$	1
	αsA1	$4.35 \pm 0.87 \times 10^{1}$	$1.90 \pm 0.52 \times 10^{3}$	-	$2.29 \pm 0.78 \times 10^{4}$	18
	αsA6	5.89 ± 0.55	$5.46 \pm 1.02 \times 10^{2}$	-	$1.08 \pm 0.23 \times 10^{4}$	8
	αsB5	*	*	-	$4.31 \pm 0.14 \times 10^{3}$	3
	αsC6	$2.36 \pm 0.37 \times 10^{1}$	$7.59 \pm 2.04 \times 10^{2}$	-	$3.11 \pm 0.97 \times 10^{4}$	25
	αsD6	$4.25 \pm 0.52 \times 10^{1}$	$2.08 \pm 0.34 \times 10^{3}$	-	$2.04 \pm 0.42 \times 10^{4}$	16
Methyl-parathion (IV)	wt°	$1.10 \pm 0.02 \times 10^{-3}$	$1.21 \pm 0.10 \times 10^{2}$	-	9.09 ± 0.90	1
	αsA1	$1.30 \pm 0.50 \times 10^{-2}$	$3.53 \pm 0.34 \times 10^{2}$	-	$3.68 \pm 1.46 \times 10^{1}$	4
	αsA6	$1.55 \pm 0.15 \times 10^{-2}$	$2.54 \pm 0.39 \times 10^{2}$	1 520 ± 384	$6.10 \pm 1.11 \times 10^{1}$	7
	αsB5	$1.50 \pm 0.04 \times 10^{-1}$	$1.58 \pm 0.15 \times 10^{2}$	-	$9.49 \pm 0.94 \times 10^{2}$	104
	αsC6	$3.00 \pm 0.10 \times 10^{-3}$	$1.21 \pm 0.15 \times 10^{2}$	-	$2.48 \pm 0.32 \times 10^{1}$	3
	αsD6	6.89 ± 0.35	$3.43 \pm 0.44 \times 10^{2}$	-	$2.01 \pm 0.28 \times 10^{4}$	2210
Malathion (V)	wt°	$8.90 \pm 0.40 \times 10^{-4}$	$1.60 \pm 0.29 \times 10^{2}$	-	5.56 ± 1.26	1
	αsA1	$7.10 \pm 0.40 \times 10^{-4}$	$2.22 \pm 0.35 \times 10^{2}$	-	3.20 ± 0.54	0.5
	αsA6	ND	ND	ND	ND	ND
	αsB5	$1.84 \pm 0.16 \times 10^{-2}$	$9.13 \pm 1.61 \times 10^{2}$	-	$2.02 \pm 1.01 \times 10^{1}$	4
	αsC6	$2.47 \pm 0.44 \times 10^{-2}$	$3.20 \pm 1.90 \times 10^{1}$	820 ± 343	$7.72 \pm 4.78 \times 10^{2}$	139
	αsD6	$1.00 \pm 0.02 \times 10^{-1}$	$1.13 \pm 0.10 \times 10^{2}$	-	$9.08 \pm 2.00 \times 10^{2}$	163
	αsB5 W263M	$8.92 \pm 0.67 \times 10^{-3}$	$8.61 \pm 1.32 \times 10^{2}$	-	$1.04 \pm 0.51 \times 10^{1}$	2
	αsB5 W263L	$1.11 \pm 0.08 \times 10^{-2}$	$9.28 \pm 1.32 \times 10^{2}$	-	$1.20 \pm 0.60 \times 10^{1}$	2
	αsB5 W263I	$1.18 \pm 0.08 \times 10^{-2}$	$7.80 \pm 1.08 \times 10^{2}$	-	$1.51 \pm 0.71 \times 10^{1}$	3
	W263L	ND	ND	-	ND	ND
	W263M	ND	ND	-	ND	ND
Chlorpyrifos (VI)	wt	ND	ND	-	ND	ND
	αsD6	*	*	-	$3.12 \pm 0.09 \times 10^{2}$	ND
	αsB5	*	*	-	$2.07 \pm 0.05 \times 10^{2}$	ND
	αsB5 W263M	*	*	-	$1.64 \pm 0.03 \times 10^{2}$	ND

	αsB5 W263L	*	*	-	$1.46 \pm 0.03 \times 10^{2}$	ND
	αsB5 W263I	*	*	-	$1.42 \pm 0.03 \times 10^{2}$	ND
	W263L	ND	ND	-	ND	ND
	W263M	ND	ND	-	ND	ND
Diazinon (VII)	Wt	ND	ND	-	ND	ND
	αsD6	8.93 ± 0.79	$2.30 \pm 0.31 \times 10^{3}$	-	$3.89 \pm 2.56 \times 10^{3}$	ND
	αsB5	1.26 ± 0.06	$4.10 \pm 0.65 \times 10^{2}$	-	$3.03 \pm 0.98 \times 10^{3}$	ND
	αsB5 W263M	$3.89 \pm 0.38 \times 10^{-1}$	$3.91 \pm 1.04 \times 10^{2}$	-	$9.92 \pm 3.65 \times 10^{2}$	ND
	αsB5 W263L	$5.61 \pm 0.23 \times 10^{-1}$	$4.74 \pm 0.53 \times 10^{2}$	-	$1.18 \pm 0.44 \times 10^{3}$	ND
	αsB5 W263I	$4.01 \pm 0.30 \times 10^{-1}$	$3.24 \pm 0.72 \times 10^{2}$	-	$1.24 \pm 0.42 \times 10^{3}$	ND
	W263L	ND	ND	-	ND	ND
	W263M	ND	ND	-	ND	ND
Fenitrothion (VIII)	Wt	ND	ND	-	ND	ND
	αsD6	$7.94 \pm 0.50 \times 10^{-1}$	$5.28 \pm 0.80 \times 10^{2}$	-	$1.50 \pm 0.62 \times 10^{3}$	ND
	αsB5	$1.40 \pm 0.20 \times 10^{-2}$	$3.14 \pm 1.43 \times 10^{2}$	-	$9.11 \pm 1.40 \times 10^{1}$	ND
	αsB5 W263M	$2.22 \pm 0.12 \times 10^{-2}$	$3.31 \pm 0.53 \times 10^{2}$	-	$6.69 \pm 2.31 \times 10^{1}$	ND
	αsB5 W263L	$2.63 \pm 0.13 \times 10^{-2}$	$6.54 \pm 0.75 \times 10^{2}$	-	$4.01 \pm 1.79 \times 10^{1}$	ND
	αsB5 W263I	$2.01 \pm 0.08 \times 10^{-2}$	$3.97 \pm 0.46 \times 10^{2}$	-	$5.05 \pm 1.81\times 10^{1}$	ND
	W263L	$3.66 \pm 0.15 \times 10^{-3}$	$4.15 \pm 0.44 \times 10^{2}$	-	8.82 ± 3.32	ND
	W263M	$9.49 \pm 0.43 \times 10^{-4}$	$1.57 \pm 0.28 \times 10^{2}$	-	6.06 ± 1.55	ND
Fensulfothion (IX)	Wt	ND	ND	-	ND	ND
	αsB5	$4.28 \pm 0.39 \times 10^{-2}$	$9.41 \pm 1.72 \times 10^{2}$	-	$4.55 \pm 2.30 \times 10^{1}$	ND
	αsD6	$4.06 \pm 1.60 \times 10^{-1}$	$8.60 \pm 3.97 \times 10^{3}$	-	$4.72 \pm 4.04 \times 10^{1}$	ND
	αsB5 W263M	*	*	-	$1.12 \pm 0.46 \times 10^{1}$	ND
	αsB5 W263L	$4.94 \pm 1.35 \times 10^{-2}$	$2.57 \pm 1.04 \times 10^{3}$	-	$1.92 \pm 1.30 \times 10^{1}$	ND
	αsB5 W263I	*	*	-	6.50 ± 0.07	ND
	W263L	ND	ND	-	ND	ND
	W263M	ND	ND	-	ND	ND
Coumaphos (X)	Wt	ND	ND	-	ND	ND
	αsD6	*	*	-	$1.64 \pm 0.02 \times 10^{4}$	ND
	αsB5	*	*	-	$7.82 \pm 0.14 \times 10^{3}$	ND
	αsB5 W263M	*	*	-	$1.15 \pm 0.02 \times 10^{3}$	ND
	αsB5 W263L	*	*	-	$1.16 \pm 0.05 \times 10^{3}$	ND
	αsB5 W263I	*	*	-	$1.11 \pm 0.04 \times 10^{3}$	ND
	W263L	*	*	-	6.01 ± 0.18	ND
	W263M	*	*	-	4.80 ± 0.32	ND
3-oxo-C10-AHL (*l*) (XI)	wt°	*	*	-	3.16×10^{4}	1
	αsA1	*	*	-	1.41×10^{2}	0.004
	αsA6	*	*	-	1.78×10^{3}	0.06
	αsB5	ND	ND	-	ND	ND
	αsC6	*	*	-	5.84×10^{2}	0.02
	αsD6	ND	ND	-	ND	ND
Undecanoic-γ-lactone (XII)	wt°	*	*	-	2.36×10^{3}	1
	αsA1	*	*	-	1.63×10^{3}	0.7
	αsA6	*	*	-	4.40×10^{5}	186
	αsB5	*	*	-	9.05×10^{2}	0.4
	αsC6	*	*	-	5.73×10^{5}	243
	αsD6	*	*	-	1.60×10^{4}	7
Undecanoic-δ-lactone (XIII)	wt°	*	*	-	7.86×10^{4}	1
	αsA1	*	*	-	2.55×10^{3}	0.03
	αsA6	*	*	-	9.65×10^{6}	123
	αsB5	*	*	-	5.33×10^{3}	0.08
	αsC6	*	*	-	3.60×10^{5}	5
	αsD6	*	*	-	7.50×10^{4}	0.9

Structural analysis of improved variants reveals increased mobility of the active site loop 8

The crystal structures of variants αsA1, αsA6, αsB5, αsC6 and αsD6 were solved **(Table 3)**. While most structures were solved at high or medium resolutions (1.4-2.55 Å), mutant αsD6 could only be solved at low resolution (2.95 Å). Given this resolution, we limited our interpretations and retained this data for the consistency of the study as it exhibits structural features (loop 8 disorder) that are consistent with all the other mutants. Overall, the mutants' structures are similar to that of wt-*Sso*Pox. However, the active site cavities are larger for the mutants: most selected mutations replace residues with smaller ones: W263 is mutated into M/L/I, V27 into A, I76 into T, L130 into P, Y99 into F. Only two selected substitutions relate to bulkier side chains: Y97W and L228M. This enlargement is difficult to quantify even with the structure of these mutants because of the extremely mobile nature of loop 8 in the variants. Enlarging the active site was a main objective of the active site redesign of *Sso*Pox, to enable the bulkier phosphotriesters to bind within the natural lactonase enzyme. Additionally, the loop 8 conformations differ in mutants, as compared to the wt-enzyme. Because part of loop 8, including position 263, is located at the enzyme dimer interface, altered loop 8 conformations modulate the relative orientation of both monomers. In the case of the mutants characterized in this study, the dimer reorientation yields significant displacement up to 5.2Å (e.g., αsA1, between equivalent carbon α positions), as compared to wt-*Sso*Pox **(Supplementary Figure 5)**. Similar reorientations were previously observed upon substrate binding or mutations of W263[78,108].

Although the active sites of the improved variant structures superpose well onto the wt-structure, all selected mutants display altered loop 8 conformations. Changes are subtle for some of the variants (e.g. αsA1), but are large for others (e.g. αsC6) **(Figure 9)**. Notably, mutant αsA6 was crystallized in two different conformations: one in which loop 8 adopts a wt-like conformation, referred to as closed conformation (CC), and another one where loop 8 is unfolded, referred to as open conformation (OC) **(Supplementary Figure 6)**. In the two other mutants, αsD6 and αsB5, loop 8 could not be modeled due to the lack of electronic density, which was likely to be due to the high level of motion of this enzyme region. Analysis of the normalized thermal motion B-factor supports this hypothesis. It also confirms that loop 8 is highly mobile in all selected mutants, as compared to wt-*Sso*Pox **(Figure 10)**. The higher mobility of loop 8 may also partly explain the improved ability of the variants to hydrolyze phosphotriesters with large substituents.

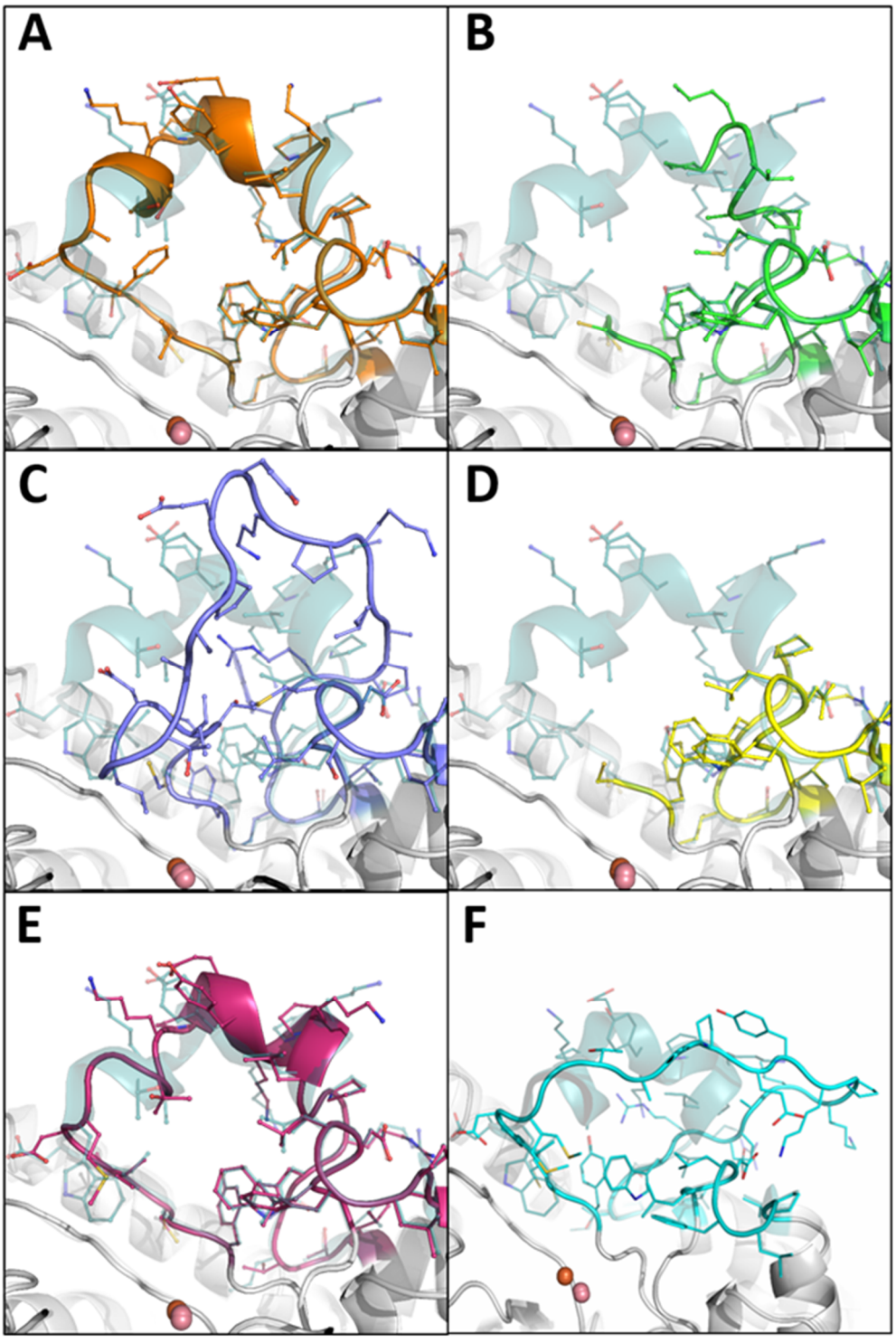


Figure 9 : Loop 8 conformations in improved mutants.
Active site loop 8 region of mutant structures superimposed with the wt-*Sso*Pox structure. The active site location is indicated by the presence of the bi-metallic catalytic center shown as spheres. The wt-*Sso*Pox structure loop 8 conformation is shown as dark green cartoon. **(A)** αsA1's loop 8 is shown in orange cartoon, **(B)** αsD6's loop 8 is shown in green cartoon, and is not entirely visible in the electronic density maps, **(C)** αsC6's loop 8 is shown in blue cartoon, **(D)** αsB5's loop 8 is shown in yellow cartoon, and is not entirely visible in the electronic density maps, **(E)** αsA6-CC's loop 8 is shown in magenta cartoon, **(F)** αsA6-OC's loop 8 is shown in cyan cartoon.

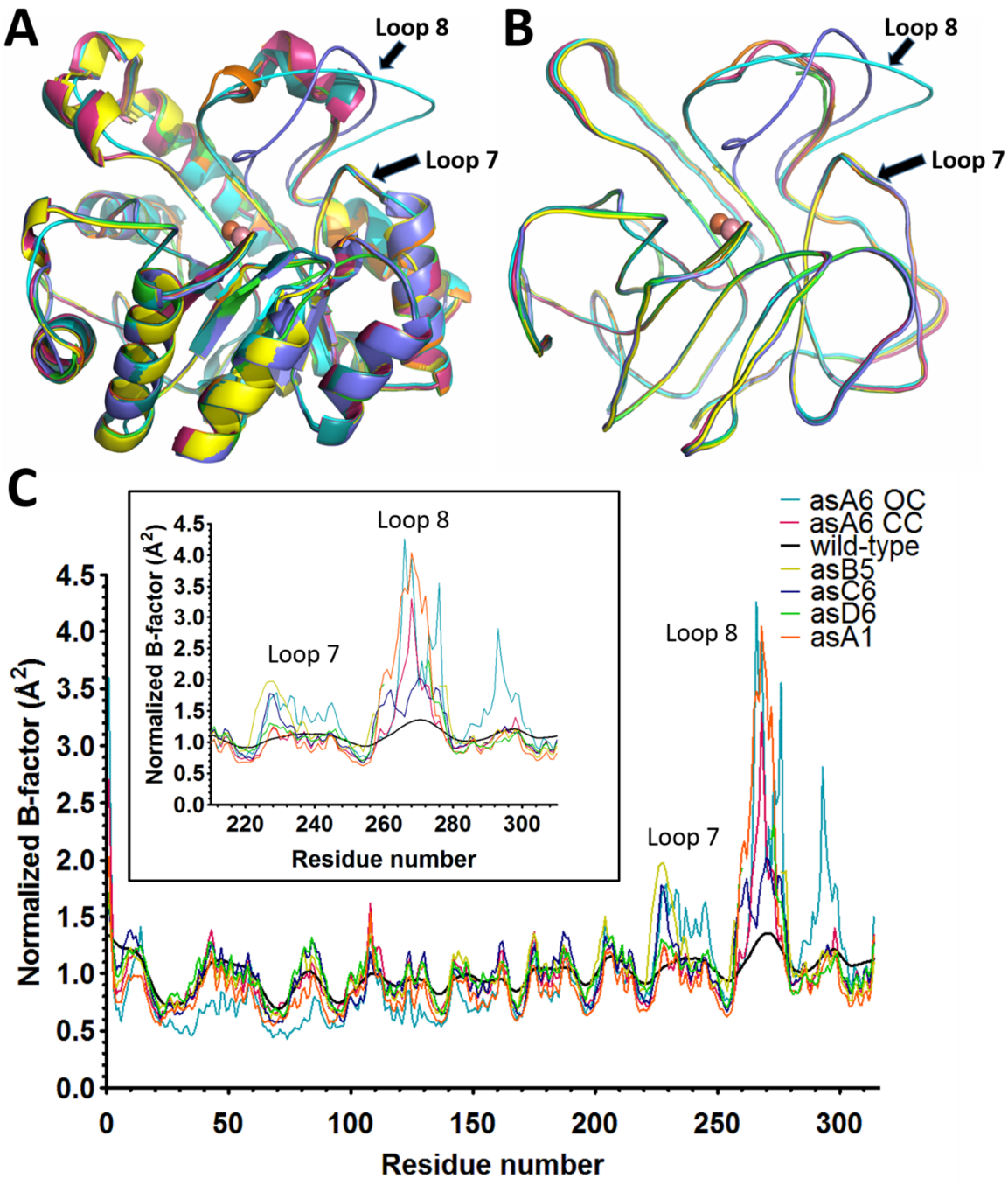


Figure 10 : Mutants' active site loop 8 exhibit higher conformational flexibility.
(A) Cartoon representation of the superposition of the structures (monomers) of wt-*Sso*Pox (dark green), αsA1 (orange), αsB5 (yellow), αsD6 (green), αsC6 (blue), αsA6-CC (magenta) and αsA6-OC (cyan). **(B)** Smoothed ribbon representation of the superposition of the structures (monomers) of of wt-*Sso*Pox (green), αsA1 (orange), αsB5 (yellow), αsD6 (green), αsC6 (blue), αsA6-CC (magenta) and αsA6-OC (cyan). **(C)** Positional distributions of normalized B-factor values (the x-axis represents residue number) for wt-*Sso*Pox (black line), αsA1 (orange), αsB5 (yellow), αsD6 (green), αsC6 (blue), αsA6-OC (blue line) and (magenta line). A zoomed inset highlights the loop 7 and 8 sequence region.

Table 3 : Data collection and refinement statistics of *Sso*Pox variants structures.

Data collections	asA6 open	asA6 closed	asB5	asC6	asD6	asA1
PDB ID	5VRI	5VRK	5W3U	5W3Z	5W3W	5VSA
Wavelength (Å)	0.97934	0.93340	0.97625	1.00882	1.00882	0.99987
Resolution (Å)	1.4	2.15	2.5	2.55	2.95	2.0
Space group	$P2_1$	$P2_12_12_1$	$P2_12_12_1$	$P2_12_12_1$	$P2_12_12_1$	$P2_12_12_1$
Unit cell dimensions						
a (Å)	49.28	87.17	82.93	81.65	82.34	86.6
b (Å)	137.20	103.61	105.95	105.80	105.01	103.100
c (Å)	49.36	152.61	152.83	154.53	153.15	151.8
α (°)	90.0	90.0	90.0	90.0	90.0	90.0
β (°)	98.7	90.0	90.0	90.0	90.0	90.0
γ (°)	90.0	90.0	90.0	90.0	90.0	90.0
No. observed reflections	419571 (75591)	408826 (24712)	206443 (23317)	194083 (10849)	106247 (5379)	703275 (96197)
No. unique reflections	121915 (22376)	74124 (4744)	47092 (5182)	43204 (2416)	28163 (1372)	91103 (12398)
Completeness (%)	96.1 (94.3)	97.8 (95.5)	99.5 (99.8)	97.3 (98.0)	98.3 (99.9)	98.6% (99.7%)
Rmerge (%)	8.2 (33.4)	9.8 (44.6)	6.1 (48.7)	5.55 (42.8)	6.6 (46.0)	9.0% (48.8%)
Rmeasure (%)	9.7 (39.5)	10.8 (49.3)	6.9 (55.4)	6.2 (48.5)	7.7 (52.9)	9.6% (52.6%)
I/σ(I)	9.07 (3.39)	14.31 (3.47)	12.84 (2.50)	15.68 (2.67)	12.89 (2.75)	15.59 (4.23)
Last resolution shell	1.5 - 1.4	2.2 - 2.15	2.6 - 2.5	2.6 - 2.55	3.0 - 2.95	2.1 – 2.0
Redundancy	3.44 (3.38)	5.51 (5.21)	4.38 (4.50)	4.49 (4.49)	3.77 (3.92)	7.72 (7.76)
Refinement statistics						
Resolution range (Å)	48.7128 – 1.40	49.0556 – 2.1500	49.6449 – 2.500	46.313 – 2.55	49.667 – 2.95	48.812 – 2.0
No. Reflections	115818	70416	44736	41042	26754	86547
Rfree /Rwork	16.84 / 13.36	21.35 / 17.23	27.17 / 21.22	24.15 / 19.97	28.31 / 24.68	20.55 / 16.32
No. protein atoms	5368	10122	9310	9657	9683	9987
No. water molecules	634	659	76	154	23	733
Average B factor (Å2)	19.095	24.984	86.6	80.375	95.992	29.885
rmsd from ideal						
Bond lengths (Å)	0.0088	0.0028	0.0050	0.0110	0.0070	0.0211
Bond angles (°)	1.0703	0.7309	0.8490	1.1730	0.9630	0.6950

Improved mutant αsD6 lost the thiono-effect

*Sso*Pox presents a marked preference for oxono-OP substrates as compared to thiono-ones (> 100-fold in catalytic efficiency)[22]. Conversely, PTEs do not exhibit such a drastic preference, paraoxon being a slightly better substrate than parathion for the enzyme[94,116]. Interestingly, some selected variants retained a strong preference for oxono-phosphotriesters (~10-fold), whereas others such as αsD6 lost the thiono-effect **(Supplementary Figure 7)**. The wild-type enzyme exhibits a low K_M value with methyl-parathion (121 µM), but also a very low k_{cat} value ($1.10x10^{-3}$ s^{-1}) **(Table 2)**. This may indicate a stronger interaction between the thiono moiety and the metal cations (low K_M value), which would subsequently impair catalysis (low k_{cat} values)[117]. Interestingly, the improved variants do not exhibit significant difference in K_M values for thiono-phosphotriesters, but show a dramatic increase in k_{cat} values, as compared to wild-type enzymes (e.g. k_{cat} value of 6.89 s^{-1} and $1.10x10^{-3}$ s^{-1}, as compared to

methyl-parathion for the αsD6 variant and wild-type enzymes, respectively). The two selected variants, namely αsB5 and αsD6, which lost the thiono-effect have only two mutations in common: V27A and Y97W. Both residues are located relatively close to the bi-metallic active site, yet do not interact directly with the metals (V27-Fe: 6.7 Å, Y97-Co: 4.3 Å; **Figure 11**). Because other PLLs have been shown to exhibit high charge coupling between the β metal and the conserved tyrosine residue[100,118], Y97 is a likely candidate for the thiono-effect, and will be examined in future studies.

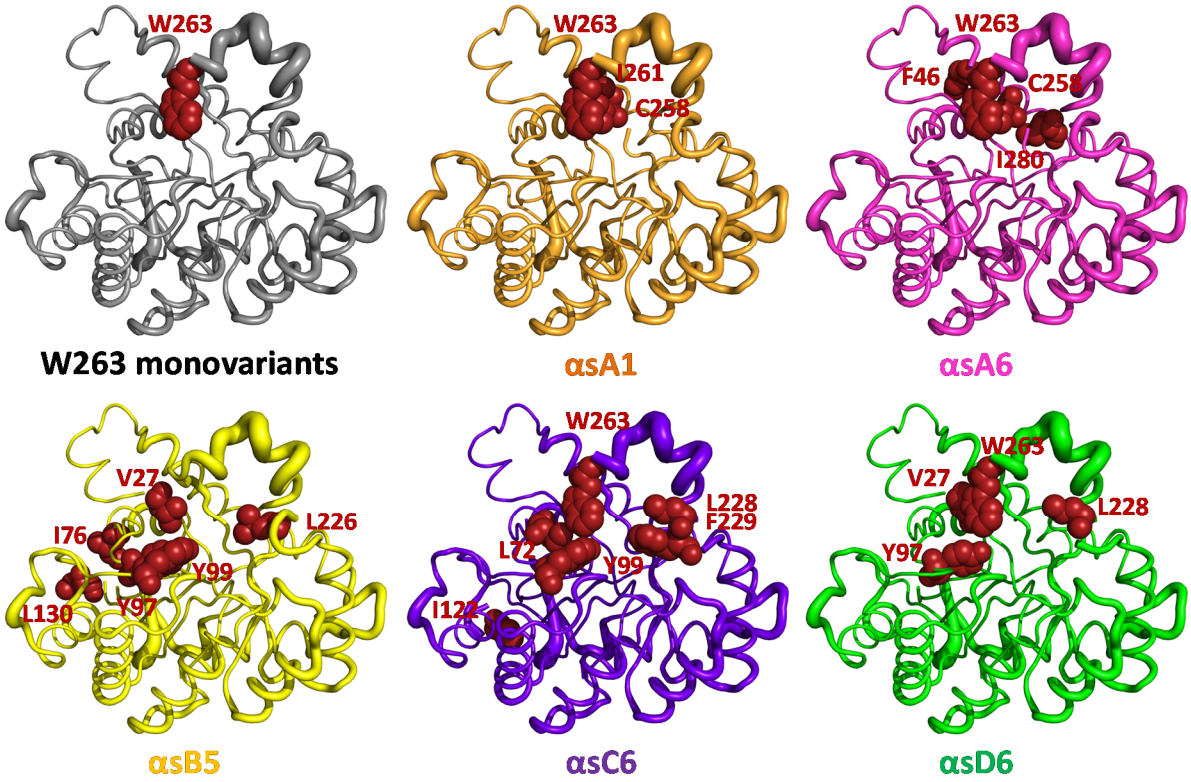


Figure 11 : Localization of mutations harbored by *Sso*Pox monovariants, αsA1, αsA6, αsB5, αsC6 and αsD6. Mutations are highlighted in red spheres using the *Sso*Pox wild-type (PDB 3UF9) as a template.

Mutations of W263 and αsB5 are incompatible

αsB5 (V27A-I76T-Y97W-Y99F-L130P-L226V) is the only selected mutant that does not contain a substitution of position W263. Because W263 substitutions were previously shown to be key for increasing *Sso*Pox's phosphotriesterase activity, we used saturation mutagenesis to introduce W263 mutations to the background of αsB5. The best selected mutants against paraoxon **(Supplementary Figure 2C)** were found to be αsB5-W263I/L/M. Surprisingly, none of these mutants demonstrated an increase in phosphotriesterase activity in comparison with αsB5, but rather a decrease in activity **(Table 2)**. This is intriguing because, taken individually, these mutations have been shown to greatly improve phosphotriesterase activity. For example, with ethyl-paraoxon as a substrate, W263M and αsB5 produce a catalytic efficiency improvement of 14 and 67-fold, respectively, while the combination αsB5-W263M increases activity only 11-fold **(Table 2)**. This example of negative epistasis could be due to the mode of action of these mutations. Structures reveal that αsB5 mutations have a destabilizing effect on loop 8, as illustrated by the B factor analysis. The same was observed for W263M in a previous study[78]. Combining these two destabilizing sets of mutations may have harmed the active site integrity, as previously described with another enzyme as "conformational active site disorder"[119], and in

particular the necessary alignment and pre-organization of the catalytic residues. The destabilizing effect of these mutations can also be observed on the overall enzyme stability, with αsB5, W263M, αsB5-W263M exhibiting T_m values of 70.4°C, 85.3°C and 69.1°C, respectively, as compared to 106°C for the wt enzyme **(Supplementary Table 4)**. Here, the effects of the combined 5 mutations harbored by variant αsB5 together with the previously identified positive substitutions at residue W263 were not additive underlining that single beneficial mutations do not necessarily induce positive epistatic effects. Synergistic effects of mutations are often complex to predict and most engineering strategies usually lead to an optimization plateau difficult to overcome.[120]

Improvement of engineered variants over W263 mutation

In a previous report, we noted that mutation of W263 into all the other 19 residues lead to an increase of the promiscuous paraoxonase activity[78]. Here we note that most of the improved variants (i.e. αsA1, αsA6, αsB5, αsC6 & αsD6) (i) exhibit higher paraoxonase activity than W263L/M, and (ii) foremost are capable of hydrolyzing phosphotriesters that are not substrates for the wild-type enzyme or W263 mutants, such as ethyl-parathion, chlorpyrifos or fensulfothion **(Table 2)**. The activity spectrum of these engineered variants against the tested phosphotriesters is therefore much wider than the wild-type enzyme and W263 mutants.

Relation between active site loop disorder and broad enzymatic specificity

The organophosphorus compound bioremediation potential of several mutants was investigated. In particular, the best variants, αsD6 and αsB5, alongside other improved variants αsB5-W263I/L/M, W263L/M and the *wt*-enzyme, were characterized for their phosphotriesterase activity with ethyl-paraoxon (**I**), ethyl-parathion (**II**), malathion (**V**), chlorpyrifos (**VI**), diazinon (**VII**), fenitrothion (**VIII**), fensulfothion (**IX**) and coumaphos (**X**) **(Figure 7)**. Interestingly, we found that most mutants were able to hydrolyze fensulfothion, previously reported as an inhibitor of the wild-type enzyme[22]. Fensulfothion was indeed previously shown to bind head-to-tail into the wild-type enzyme active side [22], a non-productive binding mode. Changes in the active site loop 8 conformational ensemble of engineered mutants might have allowed for the productive binding of fensulfothion.

All mutants selected and used in this study are destabilized as compared to the wt-enzyme **(Figure 12 and Supplementary Table 4)**. Structures reveal that these mutations, located on loop 8, contribute to increasing the mobility of the loop. Interestingly, the ability of the tested mutants to hydrolyze a wide range of phosphotriesters, including compounds that were inhibitors for the wt-enzyme, correlates with a lower T_m **(Figure 12)**. This correlation suggest that the active site loop 8 degree of disorder may modulate the enzyme's ability to bind and hydrolyze a variety of phosphotriesters, a wider conformational ensemble of loop 8 being correlated with a broader enzyme specificity. This observation is consistent with previous studies highlighting the importance of the destabilization of active site loops to evolve new activities and new substrate specificity[119,121]. Such flexible active site loops involved in enzymatic specificity supports the notion of fold polarity: a portion of the active site (e.g. the loop) is weakly connected to the enzyme scaffold and thereby makes it possible for new functions to evolve with few changes[122].

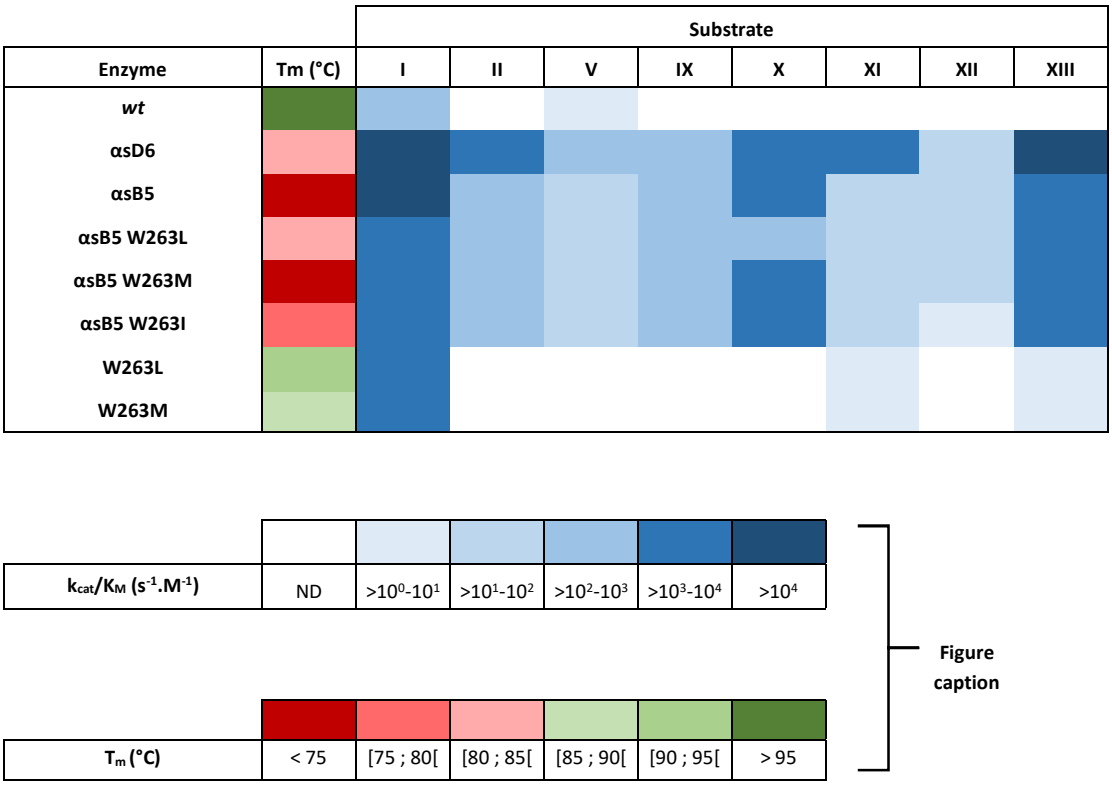


Figure 12 : Overview of *Sso*Pox wild-type and variants properties.
Catalytic efficiencies towards organophosphate-based pesticides are presented using a color code ranging from white to dark blue. Melting temperatures are presented using a color code ranging from red to green.

Mutant αsD6 is an active, broad spectrum phosphotriester biodecontaminant

Mutant αsD6 was further investigated for bioremediation considerations. Organophosphate-based pesticides are usually spread with concentrations in the millimolar range leading to micromolar-ranged contaminations. We thus investigated the potential of αsD6 for decontaminating pesticide solutions at 250 µM to simulate a contamination of groundwater or runoff waters. We investigated two [E]/[S] ratios, 10^{-2} and 10^{-3} respectively, for decontaminating OP solutions and determined the time required to hydrolyze 95 % of pesticide preparations **(Figure 8B and Supplementary Figure 4)**. When considering the [E]/[S] ratio of 10^{-3}, 95% degradation was achieved for four substrates (ethyl-paraoxon, diazinon, fenitrothion and coumaphos) within 10 minutes. Two substrates were decontaminated within an hour (ethyl-parathion and chlorpyrifos) and fensulfothion was degraded in three hours.

When increasing enzyme concentration 10-fold ([E]/[S] ratio of 10^{-2}), five substrates (ethyl-paraoxon, ethyl-parathion, diazinon, fenitrothion and coumaphos) were decontaminated within two minutes, while fensulfothion needed ~ 20 minutes and the two other tested (chlorpyrifos and malathion) required 40 minutes. Given both its catalytic proficiency and high thermal stability (T_m = 82.5 °C), αsD6 is a promising candidate for organophosphorus compound bioremediation and, in particular, the decontamination of water runoffs, soils, food products and materials. Moreover, *Sso*Pox variants were

previously shown to be compatible with immobilization steps including alginate beads and polyurethane-based coatings[113,123], and could be of prime interest for the development of filtration devices for water treatment purposes.

1.3. Materials and Methods

Structure-based identification of mutations. Sharing the same $(\alpha/\beta)_8$ barrel topology, *Sso*Pox and *Bd*PTE structures (Pdb ID 2VC5 and 1DPM, respectively) were superimposed **(Figure 6)** using PyMOL[17], making it possible to identify structurally equivalent residues at their respective active sites. In an effort to reshape the *Sso*Pox active site, side chains that were well superimposed between the two enzymes were mutated using Coot into the residue present in *Bd*PTE[124], with the exception of V27 which was mutated in Ala (and not Gly) to avoid increased entropy **(Figure 6 and Supplementary Table 1)**. However, due to the major differences in loop 8 and 7 between PLLs and PTEs, numerous residues were not superimposable. These active site residues (Y99, L228, F229 and W263) were therefore mutated in an effort to mimic the *Bd*PTE active site cavity in terms of shape and chemical nature, as illustrated by the chimeric reconstruction of *Sso*Pox carrying all these mutations **(Supplementary Figure 1)**. Others mutations were also implemented in the dataset, e.g. C258A and C258L and different substitutions of the key position W263 (F/L/M/A) that have been shown to improve the phosphodiesterase activity[78].

Synthesis of the combinatorial library. The *Sso*Pox coding gene was amplified from the previously described pET22b-*Sso*Pox plasmid[22]. For each of the 14 mutations, a mutagenesis primer of 30-33 bp (~ 10-15 bp from each mutation side) was synthesized **(Supplementary Table 2)**. For close mutations, primers can share several mutations and different primers were synthesized and mixed to keep an equivalent statistical probability for each of the 14 mutations. Typically, 2 pmol of primer mixture and 100 ng of DNaseI (TaKaRa)-generated fragments of the *Sso*Pox gene were assembled as previously described[84], followed by nested PCR with external cloning primers (*Sso*Pox-lib-pET-5'/3') **(Supplementary Table 2)**. The PCR product was then cloned into a customized version of the pET32b(-ΔTrx) plasmid and then electroporated into *E. cloni* cells (Lucigen, USA). After agar-plate growth, plasmid extraction was performed to create the plasmid bank. Variant genes were PCR amplified using T7-prom and pET-RP primers **(Supplementary Table 2)** and sequenced. The combinatorial library shows an average of 5.3 ± 3.3 library mutations by sequencing 10 randomly picked colonies, and 0.43 ± 0.53 random mutations per gene.

Screening of the library. The plasmid library was used to transform the *Escherichia coli* strain BL21(DE_3)-pGro7/GroEL (TaKaRa) to obtain colonies expressing a library of *Sso*Pox variants. Randomly picked clones (184), representing a coverage of 3.8% of the library, were grown on a 96-well plate in 500 µl of ZYP medium as previously described[78]. Production of proteins and chaperones was induced after five hours of culture at 37 °C by reducing the temperature to 25 °C, adding $CoCl_2$ (0.2 mM) and adding arabinose (0.2 %, w/v). After overnight growth, cell lysate was used to perform activity screening with 100 µM of paraoxon substrate **(Supplementary Figure 2B)** after partial purification of the protein with a heating step of 15 minutes incubation at 70 °C[102,114]. The screening was performed in 50 mM HEPES pH 8, 150 mM NaCl, 0.2 mM $CoCl_2$. Kinetics of paraoxon/methyl-parathion were

monitored by following absorbance at 405 nm for 10 minutes using a microplate reader (Synergy HT, BioTek, USA) and the Gen5.1 software.

Saturation library. Saturation mutagenesis directed on residue 263 of the αsB5 variant encoding gene, was performed using NNS degenerated primers (W263NNS direct: 5'-TGCACCATTGATNNSGGCACCGCAAAACCG-3' and W263NNS reverse: 5'-CGGTTTTGCGGTGCCSNNATCAATGGTGCA-3') and pET32b-ΔTrx carrying αsB5 coding gene as template. PCR amplification was performed with 2.5 U of PfuTurbo DNA polymerase (Agilent) according to the manufacturer's recommendations [95 °C, 5 minutes; 20x (95 °C, 30 seconds; 55 °C, one minute; 68 °C, 15 minutes); 68 °C, 25 minutes]. DNA was digested with *Dpn*I to remove the methylated parental template. *E. coli* BL21(DE_3)-pGro7/GroEL (TaKaRa) competent cells were transformed with the plasmid pool and plated on LB-agar supplemented with 100 $\mu g.ml^{-1}$ ampicillin and 34 $\mu g.ml^{-1}$ chloramphenicol. Over a theoretical diversity of 20 sequences, 181 variants were collected in a microplate containing LB (100 $\mu g.ml^{-1}$ ampicillin and 34 $\mu g.ml^{-1}$ chloramphenicol) for characterization. This oversampling by a factor of nearly 10-fold ensure a >99% probability to get the 20 possible substitutions.

Screening was performed as described above **(Supplementary Figure 2C)**. The plasmids corresponding to the most interesting variants were extracted and the *Sso*Pox variant encoding genes were sequenced.

Production-purification of *Sso*Pox wild-type and variants. The genes coding for the *Sso*Pox wild-type and its variant were cloned in a pET32b-Δtrx plasmid. Productions were performed using the *E. coli* BL21(DE_3)-pGro7/GroEL (TaKaRa) chaperone expressing strain. Starter cultures were produced in an auto-inducible ZYP medium (supplemented with 100 $\mu g.ml^{-1}$ ampicillin and 34 $\mu g.ml^{-1}$ chloramphenicol). When OD_{600nm} reached a value of 0.8-1, $CoCl_2$ was added (final concentration 0.2 mM) as well as L-arabinose (final concentration 2 $g.l^{-1}$) to induce the production of chaperones GroEL/ES and the temperature was decreased to 23 °C for 16-20 hours. Cells were harvested by centrifugation (4400 g, 4 °C, 20 minutes) and resuspended in *lysis buffer* (50 mM HEPES pH 8.0, 150 mM NaCl, 0.2 mM $CoCl_2$, 0.25 $mg.ml^{-1}$ lysozyme, 0.1 mM PMSF and 10 $\mu g.ml^{-1}$ DNAseI) and were stored at -80 °C. Cells were thawed and lysed in three steps of 30 seconds of sonication (Qsonica, Q700; Amplitude 45). Cell debris was removed by centrifugation (20000 g, 4 °C, 15 minutes). As *Sso*Pox and its variants are hyperthermostable, a pre-purification step was performed by heating the lysate for 30 minutes at 80 °C. Precipitated host proteins were removed by centrifugation (20000 g, 4 °C, 15 minutes). *Sso*Pox and its variants were collected by ammonium sulfate precipitation (75 %) and resuspended in 8 ml of *activity buffer* (50 mM HEPES pH 8.0, 150 mM NaCl, 0.2 mM $CoCl_2$). The remaining ammonium sulfate was eliminated by injection on a desalting column (HiPrep 26/10 desalting, GE Healthcare; ÄKTA Avant) and concentrated to 2 mL for separation on exclusion size chromatography (HiLoad 16/600 Superdex^{TM} 75pg, GE Healthcare; ÄKTA Avant). Final purity was monitored by SDS-PAGE and protein concentration was measured with a NanoDrop 2000 spectrophotometer (Thermo Scientific).

Kinetic assays.

Generalities. Catalytic parameters were evaluated in triplicate at 25 °C, and recorded using a microplate reader (Synergy HT, BioTek, USA) and the Gen5.1 software, in a 6.2 mm path length cell for 200 µL reaction in 96-well plate, as previously explained[97]. Catalytic parameters were obtained by fitting the data to the Michaelis-Menten (MM) equation using Graph-Pad Prism 6 software. When V_{max}

could not be reached in the experiments, catalytic efficiency was obtained by fitting the linear part of MM plot to a linear regression using Graph-Pad Prism 6 software. For some *Sso*Pox variants, the MM plot was fitted to the substrate inhibition equation using Graph-Pad Prism 6 software enabling us to determine a K_I for several substrates. Consequently, the calculated catalytic efficiencies in these conditions are true only at low substrate concentrations. In some other cases, saturation could not be reached, therefore k_{cat}/K_M values were determined using linear regression. For Coumaphos, data were fitted to one-phase decay non-linear regression.

Phosphotriesterase activity characterization. The kinetic assays were carried out in *activity buffer*. The conditions used for pesticides were as follows: ethyl-paraoxon (**I**), ethyl-parathion (**II**), methyl-paraoxon (**III**) and methyl-parathion (**IV**) hydrolysis was recorded at 405 nm (ε = 17000 $M^{-1}.cm^{-1}$). The concentration interval was between 0.05 and 2 mM from 100 mM stock solution in ethanol[22]. Malathion (**V**) hydrolysis was monitored at 412 nm, (ε = 13400 $M^{-1}.cm^{-1}$)[22]. The concentration interval was between 0.05 and 2 mM from 100 mM stock solution in DMSO. DTNB was added to the activity buffer. Chlorpyrifos (**VI**) hydrolysis was recorded at 310 nm (ε = 5562 $M^{-1}.cm^{-1}$)[51]. The concentration interval was between 0.05 and 2 mM from 100 mM stock solution in 1-propanol. Diazinon (**VII**) hydrolysis was recorded at 228 nm (ε = 3300 $M^{-1}.cm^{-1}$)[94]. The concentration interval was between 0.05 and 2 mM from 200 mM stock solution in ethanol. Fenitrothion (**VIII**) hydrolysis was recorded at 358 nm (ε = 18700 $M^{-1}.cm^{-1}$)[52]. The concentration interval was between 0.05 and 2 mM from 200 mM stock solution in ethanol. Fensulfothion (**IX**) hydrolysis was recorded at 284 nm (ε = 8000 $M^{-1}.cm^{-1}$)[94]. The concentration interval was between 0.05 and 2 mM from 200 mM stock solution in methanol. Coumaphos (**X**) hydrolysis was monitored by fluorescence of released chlorferon (excitation 360/40 and emission 460/40)[51]. A linear correlation between fluorescence and chlorferon was found **(Supplementary Figure 3)**. Measurements were taken at 5 µM from a 200 mM stock solution in DMSO. We assumed that $K_M \gg [S]$, thus enabling us to estimate k_{cat}/K_M.

Lactonase activity characterization. Lactonase kinetics were performed using a previously described protocol[97]. The time course hydrolysis of lactones were performed in *lac buffer* (2.5 mM Bicine pH 8.3, 150 mM NaCl, 0.2 mM $CoCl_2$, 0.25 mM Cresol purple and 0.5 % DMSO) over a concentration range 0-2 mM for 3-oxo-C10 AHLs (**XI**) or 0-5 mM for undecanoic- γ/δ -lactones (**XII, XIII**). Cresol purple (pK_a 8.3 at 25 °C) is a pH indicator used to follow lactone ring hydrolysis by acidification of the medium. Molar coefficient extinction at 577 nm was evaluated recording absorbance of the buffer over an acetic acid range of concentration 0-0.35 mM.

Bioremediation of pesticide solutions at 250 µM. For all OP substrates but malathion, experiments were performed in triplicate at 25°C using a microplate reader (Synergy HT, BioTek, USA). Wavelengths were chosen as described in the kinetic assays section. Degradation of malathion was followed by GC/MS in triplicate. OP concentration was fixed at 250 µM. All the substrates were soluble at this concentration. The best variants of *Sso*Pox for each substrate were used, namely αsD6 for all the OPs. Two enzyme-to-substrate ratios [E]/$[S]$ were used, 10^{-2} and 10^{-3}, corresponding to enzyme concentrations of 90 $\mu g.ml^{-1}$ and 9 $\mu g.ml^{-1}$ respectively. The reactions were monitored until the plateau was reached. Experimental measures were obtained using Gen5.1 software, then analyzed with GraphPad Prism 6 software. Curves were then fitted using One-Phase Decay non-linear regression with the equation: $Y = (Y0 - Plateau) \times e^{(-kt)} + Plateau$

Where $Y0 = 0\%$ and $Plateau = 100\%$. The rate constant *k* was determined and the time required to observe a 95% decontamination was calculated accordingly. The curves and results of the fits are shown in **Supplementary Figure 4**.

Degradation at 95% was confirmed using a final point by GC/MS for all pesticides with a 10^{-3} enzyme-to-substrate ratio. 100 µl of *activity buffer* solution was first extracted with 100 µl chloroform. Organic extracts were analyzed by using a Clarus 500 gas chromatograph equipped with a SQ8S MS detector (Perkin Elmer, Courtaboeuf, France). 1 µl of organic extract was volatilized at 220 °C (split 15 ml.min^{-1}) in a deactivated FocusLiner with quartz wool (SGE, Ringwood, Australia) and compounds separated on an Elite-5MS column (30 m, 0.25 mm i.d., 0.25 mm film thickness) for 12 minutes using a temperature gradient (80-280 °C at 30 °C.min^{-1}, five minutes' hold). Helium flowing at 2 ml.min^{-1} was used as the carrier gas. The MS inlet line was set at 280 °C and the electron ionization source at 280 °C and 70 eV. Full scan monitoring was performed from 40 to 400 *m/z* in order to identify chemicals by spectral database search using MS Search 2.0 operated with the Standard Reference Database 1A (National Institute of Standards and Technology, Gaithersburg, MD, USA). *m/z* is the mass-to-charge ratio of the base peak fragment detected for each molecule. In the case of weak pesticide signals, extracted ion chromatograms were generated with base peak ions to confirm the presence of chemicals (Paraoxon (**I**) and Parathion ethyl (**II**) *m/z* 109; Malathion (**V**) and Fenitrothion (**VIII**) *m/z* 125; Diazinon (**VII**) *m/z* 137; Coumaphos (**X**) *m/z* 97; Fensulfothion (**IX**) *m/z* 293; and Chlorpyrifos (**VI**) *m/z* 197). Selected Ion Recording using base peaks ions was applied in order to specifically monitor pesticides and collect peak areas for kinetics. All samples were analyzed over short periods of time to avoid signal drift. All data were processed using Turbomass 6.1 (Perkin Elmer).

Crystallization. Crystallization assays were performed as previously described[22,108]. Crystallization was performed using the hanging drop vapor diffusion method in 96-well plates (Greiner Microplate, 96 well, PS, F-bottom) on ViewDrop II seals (TPP Labtech). Equal volumes (0.5 µl) of protein and reservoir solutions were mixed, and the resulting drops were equilibrated against a 150 µl reservoir solution containing 20-30 % (w/v) PEG 8000 and 50 mM Tris-HCl buffer (pH 8). Crystals appeared after few days at 4°C.

Data collection and structure refinement. Crystals were first transferred to a cryoprotectant solution consisting of the reservoir solution and 20 % (v/v) glycerol. Crystals were then flash-cooled in liquid nitrogen. X-ray diffraction data were collected at 100 K using synchrotron radiation at the ID23-1 beam line (ESRF, Grenoble, France) and using an ADSC Q315r detector. X-ray diffraction data were integrated and scaled with the *XDS* package **(Table 3)**[125]. The phases were obtained using the native structure of *Sso*Pox (PDB code 2VC5) as a starting model, performing a molecular replacement with MOLREP or PHASER[126,127]. The models were built with *Coot* and refined using REFMAC[124,128]. We note that three structures presented in this work exhibit one disordered monomer (and low corresponding electronic density): αsB5 (monomer D, total of 4 monomers), αsD6 (monomer C, out of a total of 4 monomers) and αsC6 (monomer C, total of 4 monomers). Structure illustrations were performed using PyMOL[17].

Relative B-factor analysis. The occupancies of all residues in all tested structures were set to 1 for this analysis. For residues with alternate conformations, the sums of occupancies were set to 1. Structures were re-refined with REFMAC[124,128]. The relative B-factor values were obtained by normalizing the B-factor values of each residue by the average B-factor of the whole structure as previously described[78,119,122].

Acknowledgements

This work was granted by DGA, France (REI. 2009 34 0045). G.G. and P.J. students granted by DGA. Financial support was also obtained from the MnDrive Initiative (M.E.) to support this work.

Competing financial interest

M.E. and E.C. have a patent WO2014167140 A1 licensed to Gene&GreenTK. D.D. and E.C. report personal fees from Gene&GreenTK during the conduct of the study.

Author contributions statements

P.J, J.H., D.D, C.B., N.A., G.G. performed the experiments, P.J, J.H., D.D, C.B., N.A., G.G., E.C., M.E. analyzed the data, P.J, J.H., D.D, C.B., M.E. wrote the manuscript and prepared the figures, E.C., D.D. and M.E. designed the experiments.

II. Projet de recherche

Partie 2

Transformation d'une lactonase hyperthermostable en une phosphotriestérase hautement active

Partie 2 : Transformation d'une lactonase hyperthermostable en une phosphotriestérase hautement active

A la suite des précédents travaux, un nouveau cycle d'évolution dirigée a été effectué afin d'une part d'améliorer l'activité de *Sso*Pox vis-à-vis des OPs et d'autre part de mieux comprendre l'impact des mutations sur la promiscuité de l'enzyme. Pour cela, la banque de données mutationnelles a été affinée. Les substitutions peu représentées ont été éliminées, comme par exemple les positions P67 et D141, et une diversité plus importante a été générée au niveau des points chauds, comme au niveau des positions Y99 ou L72. Pour finir, d'autres positions observées dans la littérature comme pouvant améliorer l'activité phosphotriestérase ont été ajoutées, telles que les positions R154 et W278. En plus de l'affinement de la banque de données mutationnelle, la méthode de criblage des variants a été améliorée. Ainsi, une étape de criblage sélectif adapté de précédentes études a été mis au point [65,129]. Ce criblage solide permet une première sélection sur éthyl-paraoxon afin de purger les mutations délétères et d'éviter les faux positifs en sélectionnant uniquement les variants actifs.

Environ 4 000 variants ont été étalés, 430 ont été criblés parmi lesquels douze ont été sélectionnés et purifiés. A l'issu du criblage les paramètres cinétiques de ces douze variants ont été déterminés sur cinq substrats. Les résultats obtenus ont ainsi permis d'évaluer l'évolution de la promiscuité chez *Sso*Pox. Pour cela les trois activités de *Sso*Pox ont été étudiées, phosphotriestérase, lactonase et arylestérase. Cette dernière est une seconde activité de promiscuité de *Sso*Pox permettant la dégradation des arylesters, cette activité est également retrouvée chez *Bd*PTE[130]. Les activités phosphotriestérase et arylestérase ont pu être améliorées. Par exemple, l'activité sur éthyl-paraoxon a été augmentée pour les variants *Sso*Pox-IVB10 (V27A/L72C/Y97F/Y99F/W278L) et *Sso*Pox-IIIC1 (L72C/Y97F/Y99F/W263V/I280T) de 530 et 220 fois respectivement par rapport à l'enzyme sauvage. L'activité sur *para*-nitrophénol acétate (*p*NP acétate) a également été augmentée, le variant *Sso*Pox-IG7 (V27G/R154K/I280T) est 5 fois plus actif que l'enzyme sauvage. En revanche, de manière générale les variants sélectionnés sont peu, voire pas efficaces, contre les lactones par rapport à l'enzyme sauvage ou à *Sso*Pox-W263I, le meilleur variant pour la dégradation du 3-oxo-C12-AHL. Par la suite, les douze variants ont été analysés sur cinq analogues d'agents neurotoxiques de guerre (analogues du sarin, cyclosarin, soman, tabun et VX). De façon globale, l'activité des variants est améliorée sur les analogues, par exemple *Sso*Pox-IVE2 (Y97L/R154K/L228M/W263M/I280T) est 1 190 fois plus actif que l'enzyme sauvage sur l'analogue du cyclosarin. Néanmoins ce variant ne montre pas d'amélioration sur l'éthyl-paraoxon, l'éthyl-parathion, le *p*NP acétate ou les lactones, mais est le meilleur variant pour les analogues du sarin, du cyclosarin et du VX. Les variants *Sso*Pox-IVB10 et *Sso*Pox-IG7 ne sont pas efficaces pour la dégradation des analogues contrairement au variant *Sso*Pox-IIIC1 qui est amélioré sur les analogues du sarin, du cyclosarin, du soman et du VX et est le meilleur variant sur l'analogue du tabun. Ainsi, contrairement à ce qui avait été obtenu jusqu'alors, les variants ne sont pas globalement améliorés sur les OPs mais montrent des spécificités différentes sur les pesticides ou sur les analogues des CWAs. Les mutations en L72, Y97 et Y99 semblent être nécessaires pour une haute activité sur éthyl-paraoxon. Pour les analogues, les mutations Y97, W263 et I280 semblent être importantes. Ces mutations permettent d'agrandir le site actif et/ou d'ouvrir la boucle 8. Pour finir les cinq meilleurs variants se sont montrés efficaces pour protéger, en quelques minutes, l'acétylcholinestérase humaine recombinante (rAChE), la cible physiologique des OPs, contre l'éthyl-paraoxon.

Ce travail a permis de mettre en évidence que l'amélioration de l'activité phosphotriestérase se fait au détriment de l'activité lactonase. De plus, nous avons obtenu les variants de *Sso*Pox les plus actifs à l'encontre des OPs jamais obtenus à ce jour. Ces variants se sont montrés particulièrement efficaces pour protéger l'acétylcholinestérase humaine et pourront être considérés pour le développement de solutions de décontamination des OPs.

Au cours de ces travaux, j'ai réalisé les criblages, produit et purifié quatorze variants de *Sso*Pox ainsi que la rAChE. J'ai déterminé soixante paramètres cinétiques et mesuré douze T_m. J'ai également étudié l'efficacité de décontamination de certains variants pour protéger la rAChE de l'éthyl-paraoxon. Enfin j'ai participé activement à l'écriture et à la relecture du manuscrit ainsi qu'à la réalisation des figures. Ces travaux sont en cours de finalisation et je participe à l'affinement des structures tridimensionnelles récemment obtenues.

Cinq structures tridimensionnelles ont été résolues, deux structures sont dans ce manuscrit (*Sso*Pox-IVE2 et -IG7), les trois autres structures sont en cours d'affinement (*Sso*Pox-IVB10, -IIIC1 et -IVA4). Des essais pour l'obtention de complexes sont également en cours.

Les figures et tableaux supplémentaires sont en annexe.

2.1. Introduction

Over the past few years, many attention has been paid to the role of enzyme promiscuity in the emergence of new catalytic functions[131,132]. In contrast to the classical view of enzymes as a one-key lock, it has become an evidence that most enzymes may accept more than one substrate and catalyze more than one specific reaction[133]. Promiscuous activities may moreover confer adaptability and could constitute a selective advantage under selection pressure[134,135]. The transition between phenotypes has been shown to be relatively close in the genotype space, the acquisition of new functions being gradual and smooth in the course of evolution[136,137]. Catalytic promiscuity may therefore be used as a starting point for directed evolution strategies[138].

The wide use of organophosphorus insecticides (OP) since the 1950s for agricultural purpose has led to the emergence of highly efficient OP-degrading enzymes for the mobilization of the poorly-available phosphate[93]. In this way, bacterial phosphotriesterases (PTE), showing great efficacy for the hydrolysis of OP insecticides, have potentially emerged from promiscuous lactonase template belonging to the phosphotriesterase-like lactonase (PLL) family[91,139]. PLL are enzymes naturally able to catalyze the hydrolysis of acyl-homoserine lactones involved in bacterial communication referred to as quorum sensing[16]. Most PLL also show a paraoxonase activity that may be achieved thanks to a reaction intermediate showing a tetrahedral geometry comparable with lactone ring opening[108]. Bacterial PTE, although naturally efficient for the degradation of OP insecticides, have been further engineered *in vitro* for the development of biocatalysts close to catalytic perfection for decontaminating insecticides and chemical warfare agents[140–145]. These variants may found application for bioremediation of agricultural contaminations or for prophylaxis protection against OP poisoning[146,147]. However, most PTE have been isolated from mesophilic microorganisms and show moderate stability limiting their biotechnological and medical potentials[91]. A subfamily of PLL, namely PLL-A, is composed by enzymes isolated from thermostable and hyperthermostable bacteria and archaea. Special attention has thus been paid to PLL-A as robust enzymes may offer numerous biotechnological advantages including resistance to high temperatures, tolerance to solvents and denaturants or long-term storage[92,113]. Moreover thermostable enzymes are relevant for directed evolution strategies as their robustness may buffer deleterious mutations and offer new evolutionary trajectories[148–151]. *Sso*Pox isolated from hyperthermophilic archaeon *Sulfolobus solfataricus* is a natural lactonase with a promiscuous paraoxonase activity that has been particularly considered as regard to its tremendous thermostability (T_m=106 °C)[108,114,152,153]. Considering their strong structural similarity with bacterial PTE, this enzyme has been engineered with both site-directed and combinatorial strategies for generating drastically improved phosphotriesterase variants (part 1)[154,155]. In this article the *Sso*Pox engineering were pursued and allowed to generate the most efficient phosphotriesterase *Sso*Pox variants reported to date **(Figure 13)**. A comparison between the structure of *Sso*Pox and the PTE from *Brevundimonas diminuta* was first realized to allow identify the key residues involved in OP-degrading activity. A combinatorial library was synthesized using degenerated oligonucleotides and a solid screening procedure was used to purge deleterious mutations. A special attention was then paid to the alteration of substrate promiscuity along the variants and 10 substrates were considered including OP insecticides and chemical warfare agent analogues (CWA), lactones and arylester. The most efficient variants were produced and purified, the catalytic parameters and melting temperatures were determined. Tridimensional structures were determined for two variants and discussed as regards to

substrate promiscuity and stability. The potential of enhanced phosphotriesterase variants regarding their capacity to decrease poisoning effects of OP in acetylcholinesterase is also described.

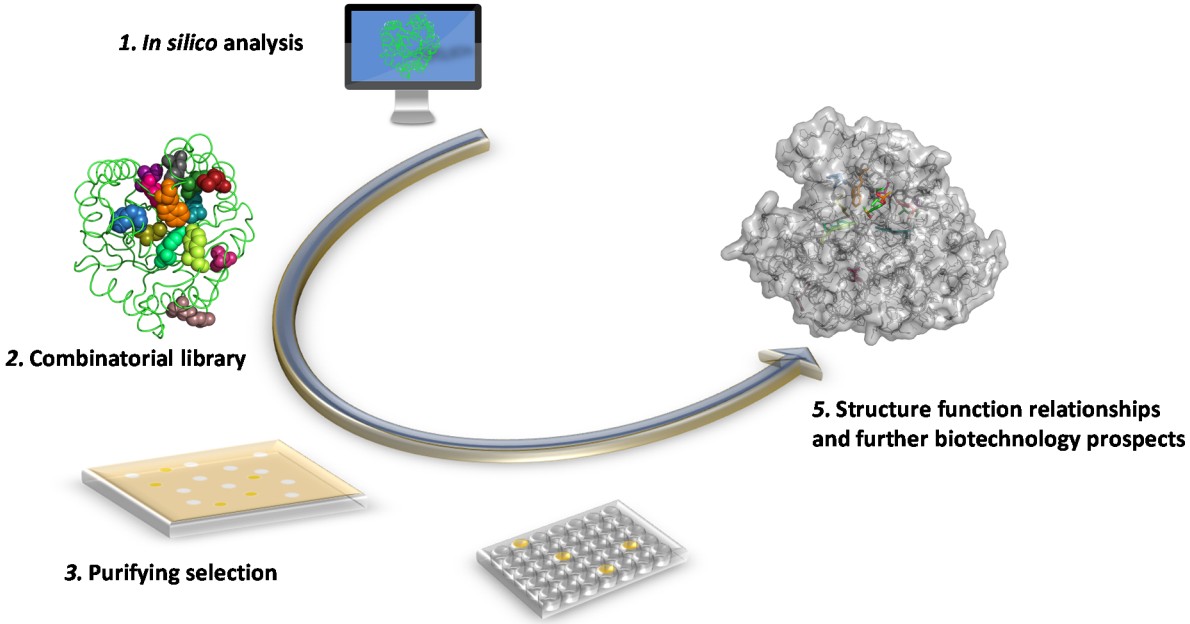


Figure 13 : Schematic representation of the strategy used for modulating substrate promiscuity toward enhanced phosphotriesterase *Sso*Pox variants.

(1) *In silico* analyses were performed to compare *Sso*Pox with bacterial PTE from *Brevundimonas diminuta*. **(2)** 13 residues were targeted for designing a combinatorial library using a degenerated oligonucleotide based strategy. **(3)** A solid-based screening was adapted to identify variants retaining a paraoxonase activity. **(4)** A miniaturized procedure was used to screen a 430-variants library against 9 substrates. **(5)** The most relevant variants were produced purified and characterized.

2.2. Materials and methods

Chemicals. CWA analogues were synthesized by Enamine Ltd. All other chemicals used for kinetic assays were ordered from Sigma-Aldrich.

Synthesis of the combinatorial library. The plasmid library was synthesized by GenScript, using degenerated oligonucleotides procedure to create a randomized and degenerated library. The desired mutations and the corresponding codon are described in **Supplementary Table 5**. Then *Sso*Pox gene was cloned in pET32b-Δtrx vector using *NdeI* and *XhoI* restriction sites.

Screening of the library. The plasmid library was transformed into *Escherichia coli* strain BL21(DE_3)-pGro7/GroEL (TaKaRa). Cells were grown overnight at 37°C on nitrocellulose membranes (Amersham™ Protran™, GE Healthcare) in plates containing ZYP agar medium (supplemented with 100 µg.ml^{-1} ampicillin and 34 µg.ml^{-1} chloramphenicol). For the induction, nitrocellulose membranes were transferred on ZYP agar medium plates (supplemented with 100 µg.ml^{-1} ampicillin and 34 µg.ml^{-1} chloramphenicol) containing L-arabinose 0.2% and $CoCl_2$ 0.2 mM. Plates were incubated at room temperature overnight. Cell lysis was realized by thermal shock, three cycles of 30 seconds at 37°C and -20°C were done. For clones selection, nitrocellulose membrane were transferred on plates containing ethyl-paraoxon 250 µM, agarose 1.5%, *activity buffer* (NaCl 150 mM, HEPES 50 mM, $CoCl_2$ 0.2 mM pH 8). Only active colonies were isolated, 430 variants were obtained.
The selected variants were then express in liquid as previously described (part 1). Shortly, variants were grown on 96-well plates in LB medium (supplemented with 100 µg.ml^{-1} ampicillin and 34 µg.ml^{-1} chloramphenicol) overnight at 37°C. 96-well plates containing 1 ml of ZYP medium in each well were inoculated. After 5 hours of growth at 37°C, L-arabinose 0.2% and $CoCl_2$ 0.2 mM were added for induction and cultures were grown overnight at room temperature. Cells were harvested by centrifugation and lysis realized using *lysis buffer* (50 mM HEPES pH 8.0, 150 mM NaCl, 0.2 mM $CoCl_2$, 0.25 mg.ml^{-1} lysozyme, 0.1 mM PMSF and 10 µg.ml^{-1} DNAseI). Lysates were partially purified by heating at 70°C during 20 min.
Activity tests were realized, on partially purified variants, for nine substrates: paraoxon and *p*-nitrophenol actetate (250 µM, 405 nm), VX, sarin, cyclosarin, tabun and soman analogues (10 µM, fluorescence 360/40, 460/40 nm), 3-oxo-C10 and 3-oxo-C12 AHL (250 µM, 577 nm). In this way, twelve variants were selected, sequenced by GATC Biotech™ and purified.

Production-purification of *Sso*Pox wild-type and variants. *Sso*Pox variants were produced in *E. coli* BL21(DE_3)-pGro7/GroEL (TaKaRa) chaperone expressing strain using a pET32b-Δtrx plasmid[152]. Cultures were performed in auto-inducible ZYP medium (supplemented with 100 µg.ml^{-1} ampicillin and 34 µg.ml^{-1} chloramphenicol), induction took place when OD_{600nm} reached a value of 0.8-1. $CoCl_2$ was added (final concentration 0.2 mM) and L-arabinose (final concentration 2 g.l^{-1}), temperature was also decreased to 23°C for 20 hours. Cultures were stopped and cells harvested by centrifugation (4400 g, 10 °C, 20 minutes), the pellet was resuspended in *lysis buffer* (50 mM HEPES pH 8.0, 150 mM NaCl, 0.2 mM $CoCl_2$, 0.25 mg.ml^{-1} lysozyme, 0.1 mM PMSF and 10 µg.ml^{-1} DNAseI) and stored at -80 °C. Cells were then lysed by sonication (3x30 seconds Qsonica, Q700; Amplitude 45). As a pre-purification step, the lysate was heated for 30 min at 70°C. Cell debris and precipitated host proteins were eliminated by centrifugation (14000 g, 10 °C, 15 minutes). *Sso*Pox and its variants were concentrated by ammonium sulfate precipitation (75 %) and resuspended in 8 ml of *activity buffer* (50 mM HEPES pH 8.0, 150 mM NaCl, 0.2 mM $CoCl_2$). Ammonium sulfate was eliminated by injection on a desalting column (HiPrep

26/10 desalting, GE Healthcare; ÄKTA Avant). The sample was concentrated to 2-3 ml for separation on exclusion size chromatography (HiLoad 16/600 Superdex^{TM} 75pg, GE Healthcare; ÄKTA Avant). At the end, purity was determined by SDS-PAGE and protein concentration was measured with a NanoDrop 2000 spectrophotometer (Thermo Scientific).

Kinetic assays. *Generalities.* Catalytic parameters were measured at 25°C in triplicate in 96-well plates with a reaction volume of 200 µl, recorded by a microplate reader (Synergy HT, BioTek, USA) in a 6.2 mm path length cell and using the Gen5.1 software, as previously explained[152].
Graph-Pad Prism 6 software was used to obtain catalytic parameters by fitting the data to the *Michaelis-Menten (MM)* equation. When V_{max} could not be reached, catalytic efficiency was determined by fitting the linear part of MM plot to a linear regression. For analogues, low concentration of substrates was used (10 µM), k_{cat}/K_M were estimated using *one-phase decay* non-linear regression in Graph-Pad Prism 6 software.
Phosphotriesterase activity characterization. The kinetic assays were done in *activity buffer* (50 mM HEPES pH 8.0, 150 mM NaCl, 0.2 mM $CoCl_2$). The conditions used for pesticides were as follows: ethyl-paraoxon, ethyl-parathion, and *p*-nitophenol actetate hydrolysis took place at 405 nm (ε = 17000 $M^{-1}.cm^{-1}$) within 0.05 and 2 mM as substrate concentration from 100 mM stock solution in ethanol. For CWA analogues[156], measurements were taken at 10 µM from a 100 mM stock solution in DMSO. We assumed that $K_M \gg [S]$, thus enabling us to estimate k_{cat}/K_M. Hydrolysis was followed by fluorescence (360/40, 460/40 nm).
Lactonase activity characterization. Lactonase kinetics were performed as described previously[97]. Kinetic parameters were determined in *lac buffer* (2.5 mM Bicine pH 8.3, 150 mM NaCl, 0.2 mM $CoCl_2$, 0.25 mM Cresol purple and 0.5 % DMSO) over a concentration range of 0-2 mM for 3-oxo-C10 AHLs and 3-oxo-C12 AHLs. Hydrolysis was followed at 577 nm (ε = 2923 $M^{-1}.cm^{-1}$).

Production and partial purification of rAChE. As previously explained[141]. rAChE was produce in *E. coli* Origami B cells transformed with pET32-rAChE-3G4 plasmid. Starter was realized in 2^xYT medium (Trypton 16 $g.l^{-1}$, yeast extract 10 $g.l^{-1}$ and NaCl 5 $g.l^{-1}$) supplemented with ampicillin (100 $\mu g.ml^{-1}$) and grown overnight at 37°C and under stirring. Inoculates were added (1:50 dilution) to 3L of 2^xYT medium with ampicillin and grown at 37 °C until $OD_{600\ nm}$ reach 1. Then IPTG was added (final concentration of 0.2 mM), and temperature was changed to 16°C. Cultures were grown for 24h, cells were harvested by centrifugation (4400 g, 4 °C, 20 minutes), resuspended with 300 mL of *rAChE lysis buffer* (13 mM Tris pH 8.0, 33 mM NaCl, 10 mM EDTA, 10 % glycerol, 0.25 $mg.mL^{-1}$ lysozyme) and stored at -80 °C. Cells were sonicated (3x30 seconds Qsonica, Q700; Amplitude 40). Cell debris were eliminated by centrifugation (14000 g, 10 °C, 15 minutes), and 0.1% of octyl glucoside was added. To eliminate more cell debris and host proteins a first ammonium sulfate precipitation was realized, saturation to 0 at 40% during 2h at 4°C. As previously, a centrifugation was done (14000 g, 10 °C, 15 minutes), and a second ammonium sulfate precipitation was realized saturation 40% to 50% overnight at 4°C to precipitate rAChE. A centrifugation was done (14000 g, 10 °C, 15 minutes) and the pellet was resuspended in *rAChE buffer* (13 mM Tris pH 8.0, 33 mM NaCl, 10 mM EDTA, 10 % glycerol) with 0.1% of octyl glucoside. Ammonium sulfate was removed by injection on a desalting column (HiPrep 26/10 desalting, GE Healthcare; ÄKTA Avant). The sample was concentrated before separation on exclusion size chromatography (HiLoad 16/600 Superdex^{TM} 75pg, GE Healthcare; ÄKTA Avant). At the end, activity of partially purified rAChE was measured using Ellman's reagent (DTNB, 4 mM) and acetylthiocholine (2.5 mM), reaction was followed at 412 nm during 10 min[157]. Fractions with activity were gathered and concentrated to reach around 2-3 $U.ml^{-1}$.

rAChE inhibition assay. Inhibition assays were performed as previously described[141,158]. Briefly, the assay was divided in two steps. First, a reaction mixture containing *Sso*Pox (at 0.1, 1 or 10 µM) and paraoxon (1.5 µM) was started in *activity buffer*, samples were taken every minutes between 0 and 10 min and a final sample at 20 min. The samples were incubated with rAChE for 15 min. The second step consisted in measuring the remaining activity of rAChE using Ellman's reagent (DTNB, 4 mM) and acetylthiocholine (2.5 mM) as described above in *activity buffer* supplemented with DTNB 4 mM. The slopes were used to calculate the remaining percentage of rAChE activity. Curves were fitted with *one-phase decay* equation using GraphPad Prism 6 software.

Melting temperature determination. Melting temperatures (T_m) were obtained using differential scanning fluorimetry (DSF)[159]. Experiments were performed on CFX96 Touch™ Real-Time PCR Detection System (Bio-Rad). *Sso*Pox variants were used at 1 $mg.ml^{-1}$ in *Tris buffer* (50 mM Tris-HCl, pH 7) and with 1X SYPRO® orange (Sigma-Aldrich). Denaturation was followed using FRET channel. Experiments were realized with temperature increase from 35°C up to 95°C (with 0.5°C/15 sec increment). For the most thermostable variants guanidinium chloride or urea was used with a range between 0.5 and 3 M. Data were fitted with *Boltzmann sigmoidal* equation using GraphPad Prism 6 software, and T_m was extrapolated by *linear regression*.

Crystallization. Crystallization assays were performed as previously described[22,108], using the hanging drop vapor diffusion method in 24-well VDX plates with sealant (Hampton research, California, USA). Different protein:precipitant ratios were tried (1:1, 1:2 and 1:3) and the plate was incubate at 292K. Crystals appeared after three days in a solution containing 25% (w/v) PEG 8000 and Tris-HCl buffer (pH 8.5). To obtain quality crystals, micro seeding was performed. Protein crystals were harvested from a drop, placed in 5 µl of mother solution and vortexed during 1 min. Several dilutions of seeds were performed (50, 75 and 100-fold) and 0.1 µl of these solutions were added to drops containing different protein:precipitant ratios.

Data collection and structure refinement. Crystals were transferred to a cryoprotectant solution composed by 20 % (v/v) glycerol and crystallization solution. Crystals were then flash-cooled in liquid nitrogen. X-ray diffraction data were collected at 100 K using synchrotron radiation at the 23-IDD beam line (APS, Argonne, USA) and using a PILATUS detector. X-ray diffraction data were integrated and scaled with the *XDS* package **(Table 7)**[125]. The phases were obtained performing a molecular replacement with MOLREP or PHASER using the structure of *Sso*Pox-wt (PDB code 2VC5) as model[126,127]. The models were built with *Coot* and refined using REFMAC[124,128]. Structure illustrations were obtained using PyMOL[17]. Normalized B-factor were obtained using "high-performance computing at the NIH" website (https://hpcwebapps.cit.nih.gov/structbio/basic.html).

2.3. Results

Design and screening of enzyme library

Three dimensional structures of *Sso*Pox (PDB ID 2VC5) and *Bd*PTE (PDB ID 1DPM) were superimposed with PyMOL[17] based on their $(\alpha/\beta)_8$ topology similarity. Thirteen residues were targeted for the construction of the combinatorial library, V27, L72, Y97, Y99, R154, T177, R223, L226, L228, C258, W263, W278 and I280. A randomized strategy based on degenerated oligonucleotides was applied for creating genetic diversity. The mutations and the corresponding codons are described in **Supplementary Table 5**. A solid screening procedure was adapted from previously reported work to identify clones expressing variants retaining a paraoxonase activity[160]. 430 active variants were selected and screened against organophosphorus compounds (ethyl-paraoxon and previously reported CWA analogues[156,161,162]), acyl-homoserine lactones (3-oxo-C10 AHL and 3-oxo-C12 AHL) and arylester (*para*-nitrophenyl acetate) **(Figure 14)**. Screening results are presented in **Supplementary Figure 8**.

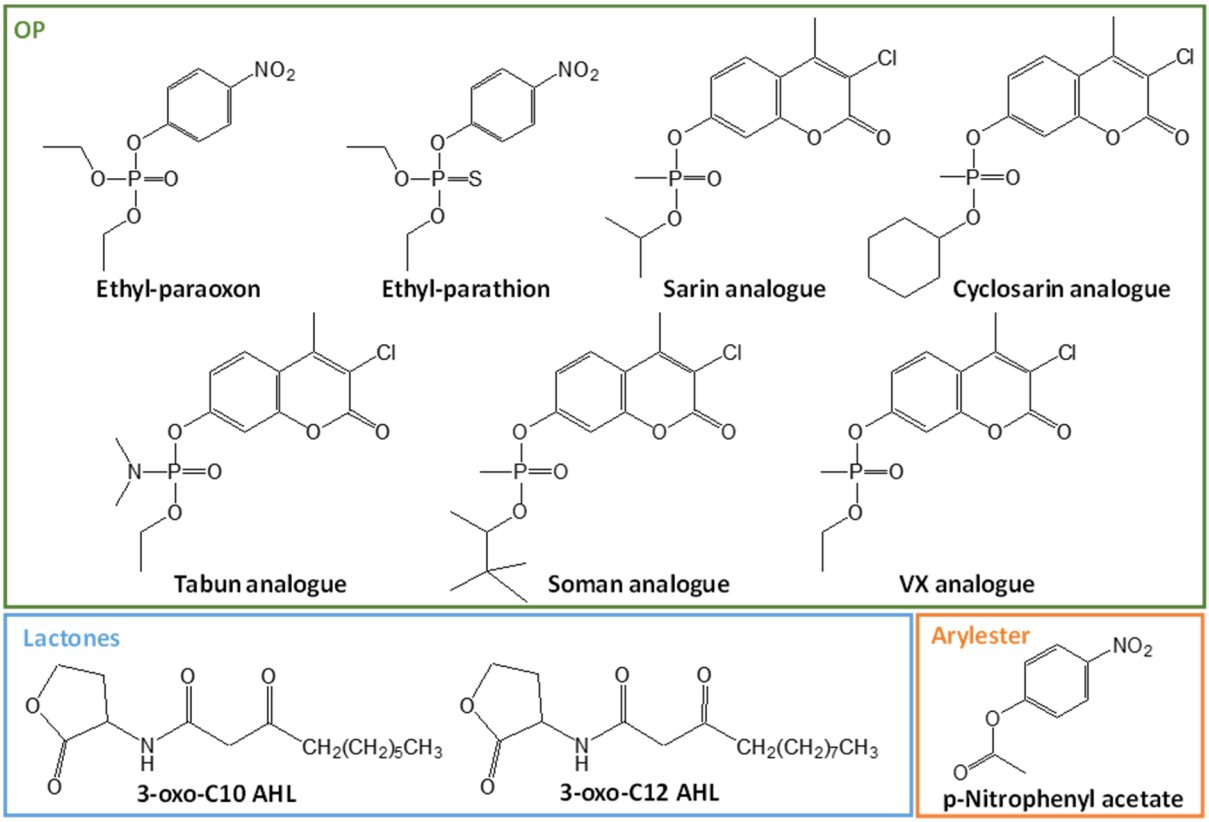


Figure 14 : Compounds selected for this study.
Two organophosphorus insecticides ethyl-paraoxon and ethyl-parathion were targeted as model substrate for probing phosphotriesterase activity and thiono-effect in *Sso*Pox variants. In order to further evaluate the organophosphate degrading activity, five CWA analogues were considered. Two bacterial quorum sensing involved acyl-homoserine lactones were considered for analyzing lactonase activity. Arylesterase activity was investigated with *p*NP acetate.

Probing promiscuity with model substrates

12 variants showing the most promising screening results **(Supplementary Figure 8)** were further considered for catalytic analysis. Variants, harboring from 2 to 6 mutations **(Table 4)**, were produced and purified and their substrate promiscuity was probed with model substrates for phosphotriesterase activity (ethyl-paraoxon and ethyl-parathion), lactonase activity (3-oxo-C10 AHL and 3-oxo-C12 AHL) and arylesterase activity (*p*NP acetate) **(Figure 14)**. The catalytic efficiencies of the 12 variants with the 5 substrates were determined as compared to *Sso*Pox-WT as well as two previously reported variants *Sso*Pox variants W263I and αsD6 with the highest lactonase and phosphotriesterase activity reported so far **(Table 5)** (part 1)[154]. 220- and 530-fold increases for ethyl-paraoxon were obtained for variants IIIC1 and IVB10. This latter was 10 times more active than *Sso*Pox variant αsD6 with the highest paraoxonase activity known so far. Interestingly variants IIIC1 and IVB10 displayed poor parathionase activity underlining that such enzymes were sensitive to thiono-effect. Thiono-effect was highly variable between variants with paraxonase/parathionase ratio values ranging from approximately 9 for variant IVA4 up to 7069 for variant IVB10. Up to 5-fold increased in arylesterase activity was reached for variant IG7. Interestingly for this variant both arylesterase and phosphotriesterase were improved in the same magnitude as compared to wild type value. On the contrary all the variants were drastically altered in their lactonase activity **(Figure 15)**.

Table 4 : Mutations of selected *Sso*Pox variants and corresponding melting temperature values T_m (°C).
* data from Merone *et al.* (2005)[153]

Variant	Mutations	Tm (°C)
IG7	V27G/R154K/I280T	79,1 ± 1,7
IVE2	Y97L/R154K/L228M/W263M/I280T	89,7 ± 0,5
IVG2	V27A/L72C/Y97R/Y99A/I280T	79,2 ± 0,1
IIIC1	L72C/Y97F/Y99F/W263V/I280T	96,3 ± 0,5
IVB10	V27A/L72C/Y97F/Y99F/W278L	85,0 ± 0,2
IVE10	V27A/Y97F/Y99F/R154K/T177D/W263D	81,5 ± 0,1
IIIE11	Y97S/Y99F	84,1 ± 2,7
IH1	Y97Q/Y99F	86,2 ± 0,3
IIIB8	L72I/Y97W/Y99F/W278L/I280T	79,8 ± 0,1
VA7	V27A/Y99D	82,3 ± 0,3
IVA4	V27G/L72C/Y97I/Y99F/R154K	86,7 ± 0,2
IVE5	Y97F/Y99F/R154K/C258L/W263D/I280T	82,3 ± 0,1
αsD6	V27A/Y97W/L228M/W263M	82,5 ± 1,8
W263I	W263I	87,8 ± 1,2
wt*	-	106

Table 5 : Catalytic parameters of selected *Sso*Pox variants as compared to wild-type enzyme (wt) and previously reported enhanced lactonase (W263I) and phosphotriesterase (αsD6) variants.

ND, not detected. *, linear regression or one-phase decay estimation.$^{+}$, data taken from Hiblot *et al.* (2013)[154]. °, date taken from part 1. °°, data taken from Hiblot *et al.* (2012)[97].

Substrate	*Sso* Pox	k_{cat} (s^{-1})	K_M (µM)	k_{cat}/K_M ($M^{-1}.s^{-1}$)	Ratio/wt
Ethyl-paraoxon	wt^{+}	$1,26 \pm 0,13 \times 10^{1}$	$2,42 \pm 0,37 \times 10^{4}$	$5,19 \pm 0,95 \times 10^{2}$	1
	IG7	$1,69 \pm 0,20$	$8,93 \pm 2,12 \times 10^{2}$	$1,89 \pm 0,94 \times 10^{3}$	3,64
	IVE2	$3,30 \pm 0,20 \times 10^{-1}$	$1,19 \pm 0,15 \times 10^{3}$	$2,78 \pm 1,51 \times 10^{2}$	0,54
	IVG2	$2,20 \pm 0,20 \times 10^{-1}$	$1,24 \pm 0,16 \times 10^{3}$	$1,75 \pm 0,96 \times 10^{2}$	0,34
	IIIC1	$6,99 \pm 0,25 \times 10^{1}$	$6,10 \pm 0,50 \times 10^{2}$	$1,14 \pm 0,50 \times 10^{5}$	219,65
	IVB10	$3,06 \pm 0,11 \times 10^{2}$	$1,11 \pm 0,78 \times 10^{3}$	$2,75 \pm 1,46 \times 10^{5}$	529,87
	IVE10	$2,81 \pm 0,09$	$2,04 \pm 0,24 \times 10^{2}$	$1,38 \pm 0,39 \times 10^{4}$	26,59
	IIIE11	$3,00 \pm 0,20 \times 10^{-2}$	$6,01 \pm 0,91 \times 10^{2}$	$4,47 \pm 1,93 \times 10^{1}$	0,09
	IH1	$4,00 \pm 0,30 \times 10^{-2}$	$8,81 \pm 1,41 \times 10^{2}$	$4,38 \pm 2,16 \times 10^{1}$	0,08
	IIIB8	$3,30 \pm 0,20 \times 10^{-1}$	$5,05 \pm 0,68 \times 10^{2}$	$6,47 \pm 2,62 \times 10^{2}$	1,25
	VA7	$2,40 \pm 0,10 \times 10^{-1}$	$2,58 \pm 0,39 \times 10^{2}$	$9,17 \pm 2,86 \times 10^{2}$	1,77
	IVA4	*	*	$1,06 \pm 0,02 \times 10^{4}$	20,42
	IVE5	*	*	$1,69 \pm 0,05 \times 10^{3}$	3,26
	αsD6°	$3,22 \pm 0,18 \times 10^{1}$	$1,09 \pm 0,12 \times 10^{3}$	$2,95 \pm 1,55 \times 10^{4}$	56,84
	W263I^{+}	*	*	$1,21 \pm 0,06 \times 10^{3}$	2,33
Ethyl-parathion	wt^{+}	ND	ND	ND	ND
	IG7	ND	ND	ND	ND
	IVE2	$2,20 \pm 0,10 \times 10^{-3}$	$5,10 \pm 0,84 \times 10^{2}$	$4,44 \pm 1,81$	ND
	IVG2	$2,30 \pm 0,09 \times 10^{-3}$	$3,00 \pm 0,35 \times 10^{2}$	$7,75 \pm 2,57$	ND
	IIIC1	$8,20 \pm 0,40 \times 10^{-2}$	$3,49 \pm 0,49 \times 10^{2}$	$2,35 \pm 0,08 \times 10^{2}$	ND
	IVB10	$2,86 \pm 0,19 \times 10^{-2}$	$7,37 \pm 0,45 \times 10^{2}$	$3,89 \pm 1,81 \times 10^{1}$	ND
	IVE10	$6,71 \pm 0,08 \times 10^{-3}$	$1,45 \pm 0,17 \times 10^{2}$	$4,63 \pm 1,15 \times 10^{1}$	ND
	IIIE11	ND	ND	ND	ND
	IH1	ND	ND	ND	ND
	IIIB8	ND	ND	ND	ND
	VA7	$3,40 \pm 0,08 \times 10^{-3}$	$9,52 \pm 1,04 \times 10^{1}$	$3,63 \pm 0,77 \times 10^{1}$	ND
	IVA4	$4,80 \pm 0,10 \times 10^{-1}$	$3,92 \pm 0,25 \times 10^{2}$	$1,22 \pm 0,45 \times 10^{3}$	ND
	IVE5	ND	ND	ND	ND
	αsD6°	$7,35 \pm 0,36 \times 10^{-1}$	$5,34 \pm 0,62 \times 10^{2}$	$1,38 \pm 0,57 \times 10^{3}$	ND
	W263I	ND	ND	ND	ND
pNP acetate	wt°°	$1,70 \pm 0,07 \times 10^{-1}$	$5,45 \pm 0,35 \times 10^{3}$	$3,12 \pm 0,33 \times 10^{1}$	1
	IG7	$7,08 \pm 0,99 \times 10^{-1}$	$4,65 \pm 0,84 \times 10^{3}$	$1,52 \pm 1,18 \times 10^{2}$	4,87
	IVE2	$2,70 \pm 0,04 \times 10^{-2}$	$8,70 \pm 0,29 \times 10^{2}$	$3,10 \pm 1,52 \times 10^{1}$	0,99
	IVG2	$4,41 \pm 1,13 \times 10^{-3}$	$3,02 \pm 1,10 \times 10^{3}$	$1,46 \pm 1,03$	0,05
	IIIC1	$1,21 \pm 0,29 \times 10^{-2}$	$7,12 \pm 2,03 \times 10^{3}$	$1,71 \pm 1,41$	0,05
	IVB10	$2,75 \pm 0,29 \times 10^{-2}$	$2,11 \pm 0,36 \times 10^{3}$	$1,31 \pm 0,81 \times 10^{1}$	0,42
	IVE10	$2,11 \pm 0,16 \times 10^{-3}$	$1,63 \pm 0,21 \times 10^{3}$	$1,29 \pm 0,77$	0,04
	IIIE11	$2,28 \pm 0,07 \times 10^{-2}$	$2,99 \pm 0,28 \times 10^{2}$	$7,64 \pm 2,53 \times 10^{1}$	2,45
	IH1	$2,13 \pm 0,10 \times 10^{-2}$	$5,80 \pm 0,67 \times 10^{2}$	$3,67 \pm 1,56 \times 10^{1}$	1,18
	IIIB8	$5,92 \pm 0,17 \times 10^{-2}$	$1,86 \pm 0,09 \times 10^{3}$	$3,18 \pm 1,97 \times 10^{1}$	1,02
	VA7	$6,29 \pm 0,16 \times 10^{-2}$	$2,02 \pm 0,08 \times 10^{3}$	$3,11 \pm 1,97 \times 10^{1}$	1,00
	IVA4	ND	ND	ND	ND
	IVE5	ND	ND	ND	ND
	αsD6	*	*	$1,97 \pm 0,27 \times 10^{1}$	0,63
	W263I	$6,71 \pm 0,27 \times 10^{-3}$	$5,79 \pm 0,55 \times 10^{2}$	$1,16 \pm 0,49 \times 10^{1}$	0,37
3-oxo-C10 AHL	wt^{+}	$4,52 \pm 0,10$	$1,43 \pm 0,15 \times 10^{2}$	$3,16 \pm 0,33 \times 10^{4}$	1
	IG7	$2,70 \pm 0,13 \times 10^{-1}$	$2,17 \pm 0,36 \times 10^{2}$	$1,24 \pm 0,54 \times 10^{3}$	0,04
	IVE2	$1,08 \pm 0,03 \times 10^{-2}$	$2,10 \pm 0,26 \times 10^{2}$	$5,14 \pm 1,23 \times 10^{1}$	0,002
	IVG2	ND	ND	ND	ND
	IIIC1	$5,61 \pm 0,29 \times 10^{-1}$	$5,72 \pm 0,81 \times 10^{2}$	$9,80 \pm 3,58 \times 10^{2}$	0,03
	IVB10	$8,88 \pm 0,48 \times 10^{-3}$	$4,19 \pm 0,72 \times 10^{2}$	$2,11 \pm 0,67 \times 10^{1}$	0,001
	IVE10	ND	ND	ND	ND
	IIIE11	$1,68 \pm 0,04 \times 10^{-2}$	$6,43 \pm 1,29 \times 10^{1}$	$2,61 \pm 0,34 \times 10^{2}$	0,01
	IH1	$1,84 \pm 0,03 \times 10^{-2}$	$6,79 \pm 0,91 \times 10^{1}$	$2,71 \pm 0,36 \times 10^{2}$	0,01
	IIIB8	$1,64 \pm 0,06 \times 10^{-2}$	$3,80 \pm 0,47 \times 10^{2}$	$4,33 \pm 1,39 \times 10^{1}$	0,001
	VA7	$2,60 \pm 0,10 \times 10^{-2}$	$1,52 \pm 0,30 \times 10^{2}$	$1,71 \pm 0,35 \times 10^{2}$	0,01
	IVA4	ND	ND	ND	ND
	IVE5	ND	ND	ND	ND
	αsD6°	ND	ND	ND	ND
	W263I^{+}	$6,00 \pm 0,90 \times 10^{-1}$	$1,60 \pm 0,44 \times 10^{3}$	$3,74 \pm 1,17 \times 10^{2}$	0,01
3-oxo-C12 AHL	wt^{+}	$1,01 \pm 0,13$	$4,56 \pm 1,28 \times 10^{2}$	$2,22 \pm 0,68 \times 10^{3}$	1
	IG7	$6,63 \pm 0,51 \times 10^{-2}$	$2,74 \pm 0,58 \times 10^{2}$	$2,42 \pm 0,88 \times 10^{2}$	0,11
	IVE2	$5,93 \pm 0,73 \times 10^{-2}$	$7,50 \pm 1,70 \times 10^{2}$	$7,91 \pm 4,29 \times 10^{1}$	0,04
	IVG2	ND	ND	ND	ND
	IIIC1	$2,31 \pm 0,89$	$2,17 \pm 1,11 \times 10^{3}$	$1,06 \pm 0,80 \times 10^{3}$	0,48
	IVB10	ND	ND	ND	ND
	IVE10	ND	ND	ND	ND
	IIIE11	$7,46 \pm 0,47 \times 10^{-3}$	$1,27 \pm 0,33 \times 10^{2}$	$5,88 \pm 1,44 \times 10^{1}$	0,03
	IH1	$4,22 \pm 0,30 \times 10^{-3}$	$1,79 \pm 0,42 \times 10^{2}$	$2,36 \pm 0,72 \times 10^{1}$	0,01
	IIIB8	ND	ND	ND	ND
	VA7	ND	ND	ND	ND
	IVA4	ND	ND	ND	ND
	IVE5	ND	ND	ND	ND
	αsD6	$1,65 \pm 0,21 \times 10^{-2}$	$7,78 \pm 2,07 \times 10^{2}$	$2,12 \pm 1,04 \times 10^{1}$	0,01
	W263I^{+}	$1,80 \pm 0,05$	$1,78 \pm 0,49 \times 10^{1}$	$1,01 \pm 0,28 \times 10^{5}$	45,50

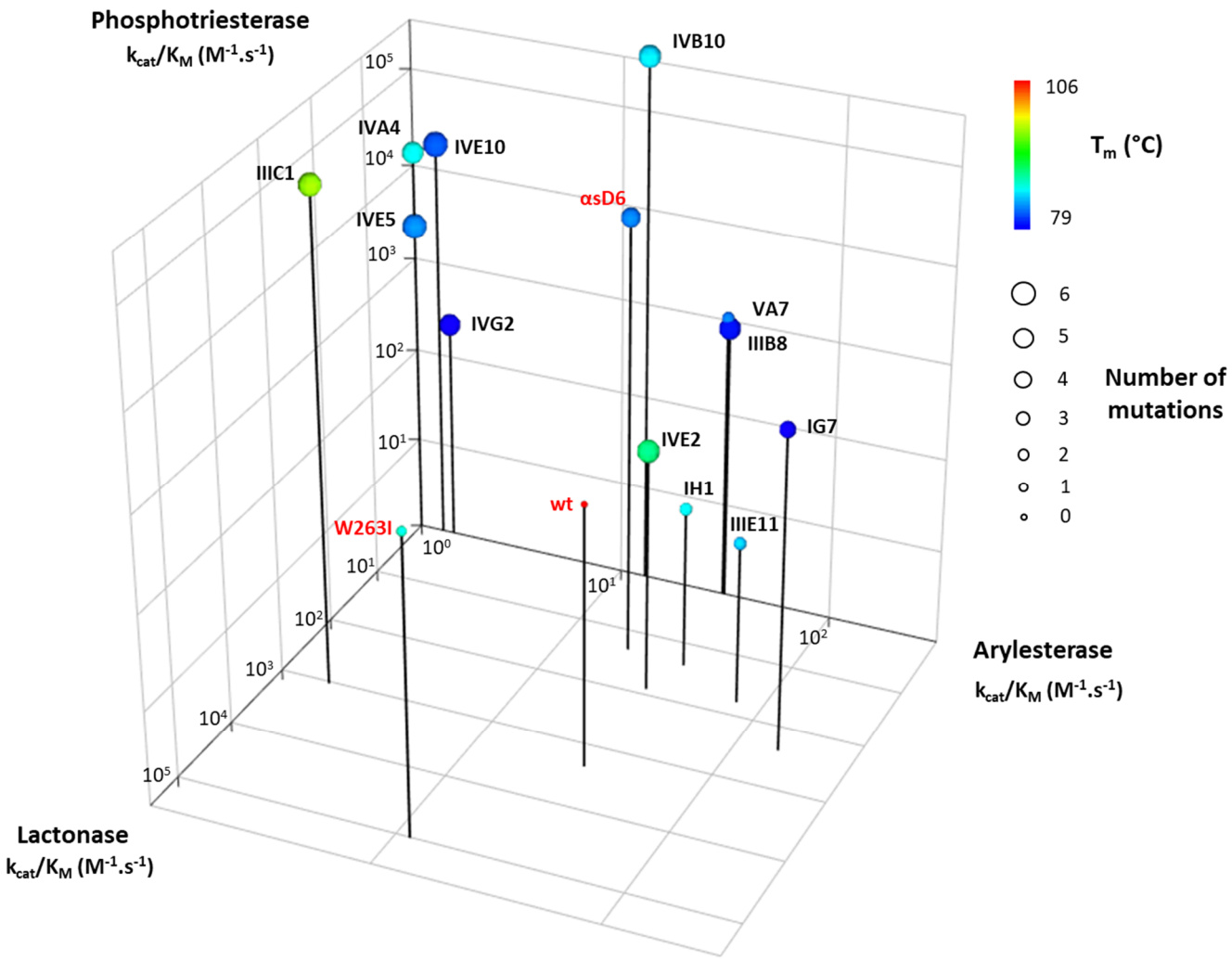


Figure 15 : Promiscuous activities of *Sso*Pox.

3D scatter plot realized with TeraPlot software using kinetic parameters of ethyl-paraoxon for phosphotriesterase activity, 3-oxo-C12-AHL for lactonase activity and *p*NP acetate for arylesterase activity.

Evaluating activity with CWA analogues

In addition to model substrates used to assay the catalytic promiscuity of *Sso*Pox variants, five CWA analogues were targeted to further investigate the phosphotriesterase activity. Previously described coumaric derivatives of sarin, cyclosarin, tabun, soman and VX were considered. *Sso*Pox wild-type showed comparable catalytic efficiency values for VX, sarin and cyclosarin analogues (2.74 x 10^2, 3.00 x 10^2 and 3.93 x 10^2 $M^{-1}.s^{-1}$ respectively). Conversely wild-type enzyme was poorly active for soman analogue (7.63 $M^{-1}.s^{-1}$) and no activity for tabun analogue was observable. Both previously described variants W263I and αsD6 were found to be highly improved for the hydrolysis of the whole substrate spectrum with up to 274.5-fold increase for W263I against VX analogue and 125.4-fold increase against cyclosarin analogue. In addition W263I and αsD6 showed measurable activity for the hydrolysis of tabun analogue, albeit low (8.78 x 10^1 and 1.44 x 10^1 $M^{-1}.s^{-1}$). Variant IVE2 was found to be the most efficient variant with sarin, cyclosarin and VX analogues with k_{cat}/K_M values reaching 4.15 x 10^4, 4.69 x 10^5 and 1.84 x 10^5 $M^{-1}.s^{-1}$. Variant IVE5 showed 561-fold enhancement as compared to wild-type enzyme with soman analogue. Variant IIIC1 activity was improved for the 5 analogues and was the most active variant for the hydrolysis of tabun analogue (5.28 x 10^2 $M^{-1}.s^{-1}$).

Table 6 : Estimation of catalytic parameters of *Sso*Pox variants assayed with CWA analogues as compared to wild-type enzyme (wt) and previously reported enhanced lactonase (W263I) and phosphotriesterase variants (αsD6). ND, not detected.

Substrate	*Sso* Pox	k_{cat}/K_M ($M^{-1}.s^{-1}$)	Ratio/wt
Sarin analogue	wt	$3,00 \pm 0,08 \times 10^{2}$	1
	IG7	$2,47 \pm 0,02 \times 10^{2}$	0,82
	IVE2	$4,15 \pm 0,02 \times 10^{4}$	138,33
	IVG2	$1,18 \pm 0,004 \times 10^{2}$	0,39
	IIIC1	$5,62 \pm 0,14 \times 10^{3}$	18,73
	IVB10	$7,99 \pm 0,12 \times 10^{1}$	0,27
	IVE10	$1,05 \pm 0,003 \times 10^{3}$	3,50
	IIIE11	$1,89 \pm 0,08 \times 10^{4}$	63,00
	IH1	$2,29 \pm 0,03 \times 10^{3}$	7,63
	IIIB8	$9,81 \pm 0,05 \times 10^{1}$	0,33
	VA7	$5,59 \pm 0,01 \times 10^{1}$	0,19
	IVA4	$4,60 \pm 0,02 \times 10^{2}$	1,53
	IVE5	$4,46 \pm 0,13 \times 10^{3}$	14,87
	αsD6	$9,01 \pm 0,02 \times 10^{3}$	30,03
	W263I	$1,99 \pm 0,08 \times 10^{4}$	66,33
Cyclosarin analogue	wt	$3,93 \pm 0,20 \times 10^{2}$	1
	IG7	$2,12 \pm 0,09 \times 10^{3}$	5,39
	IVE2	$4,69 \pm 0,11 \times 10^{5}$	1193,38
	IVG2	$8,98 \pm 0,12 \times 10^{2}$	2,28
	IIIC1	$3,90 \pm 0,08 \times 10^{3}$	9,92
	IVB10	$1,74 \pm 0,04 \times 10^{2}$	0,44
	IVE10	$8,79 \pm 0,15 \times 10^{3}$	22,37
	IIIE11	$4,46 \pm 0,09 \times 10^{3}$	11,35
	IH1	$1,31 \pm 0,02 \times 10^{3}$	3,33
	IIIB8	$1,97 \pm 0,01 \times 10^{2}$	0,50
	VA7	$1,29 \pm 0,004 \times 10^{2}$	0,33
	IVA4	$3,98 \pm 0,04 \times 10^{2}$	1,01
	IVE5	$2,07 \pm 0,09 \times 10^{4}$	52,67
	αsD6	$4,93 \pm 0,01 \times 10^{4}$	125,45
	W263I	$1,59 \pm 0,05 \times 10^{4}$	40,46
Soman analogue	wt	$7,63 \pm 0,52$	1
	IG7	ND	ND
	IVE2	$8,16 \pm 0,26 \times 10^{2}$	106,95
	IVG2	ND	ND
	IIIC1	$1,32 \pm 0,01 \times 10^{2}$	17,30
	IVB10	ND	ND
	IVE10	$1,75 \pm 0,19 \times 10^{3}$	229,36
	IIIE11	$1,05 \pm 0,01 \times 10^{2}$	13,76
	IH1	$6,91 \pm 0,06 \times 10^{1}$	9,06
	IIIB8	ND	ND
	VA7	ND	ND
	IVA4	$3,77 \pm 0,03 \times 10^{1}$	4,94
	IVE5	$4,28 \pm 0,35 \times 10^{3}$	560,94
	αsD6	$2,87 \pm 0,02 \times 10^{2}$	37,61
	W263I	$1,97 \pm 0,01 \times 10^{2}$	25,82
Tabun analogue	wt	ND	ND
	IG7	ND	ND
	IVE2	$7,62 \pm 0,04$	ND
	IVG2	ND	ND
	IIIC1	$5,28 \pm 0,11 \times 10^{2}$	ND
	IVB10	ND	ND
	IVE10	ND	ND
	IIIE11	$5,09 \pm 0,04$	ND
	IH1	ND	ND
	IIIB8	ND	ND
	VA7	ND	ND
	IVA4	$5,37 \pm 0,05$	ND
	IVE5	ND	ND
	αsD6	$1,44 \pm 0,01 \times 10^{1}$	ND
	W263I	$8,78 \pm 0,06 \times 10^{1}$	ND
VX analogue	wt	$2,74 \pm 0,02 \times 10^{2}$	1
	IG7	$3,55 \pm 0,02 \times 10^{2}$	1,30
	IVE2	$1,84 \pm 0,10 \times 10^{5}$	671,53
	IVG2	$3,11 \pm 0,03 \times 10^{2}$	1,14
	IIIC1	$3,03 \pm 0,33 \times 10^{4}$	110,58
	IVB10	$7,12 \pm 0,08 \times 10^{2}$	2,60
	IVE10	$6,29 \pm 0,95 \times 10^{3}$	22,96
	IIIE11	$8,86 \pm 0,20 \times 10^{3}$	32,34
	IH1	$4,52 \pm 0,08 \times 10^{3}$	16,50
	IIIB8	$1,51 \pm 0,02 \times 10^{2}$	0,55
	VA7	$8,62 \pm 0,02 \times 10^{1}$	0,31
	IVA4	$3,16 \pm 0,03 \times 10^{2}$	1,15
	IVE5	$6,50 \pm 0,13 \times 10^{3}$	23,72
	αsD6	$3,91 \pm 0,08 \times 10^{3}$	14,27
	W263I	$7,52 \pm 0,72 \times 10^{4}$	274,45

Enzymes for the protection against organophosphorus poisoning

Enhanced phosphotriesterase variants (IIIC1, IVB10, IG7, IVE10 and IVA4) were identified in this study. To further investigate the potential of these enzymes for OP degradation. We adapted a procedure based on the inhibition of Human AChE to evaluate the capacity of the variants to protect the real physiological target of OP chemicals[141,158]. Ethyl-paraoxon poisoning of a previously reported stabilized recombinant variant of Human AChE (rAChE) was considered to assay *Sso*Pox variants as compared to wild-type enzyme. rAChE activity was measured for different time periods to determine the rate of detoxification with *Sso*Pox variants. IIIC1 and IVB10 were shown to be particularly efficient for the protection of rAChE within 3 minutes with an enzyme concentration of 0.1 µM **(Figure 16)**. Conversely *Sso*Pox wild-type required more than ten minutes while involving a 100-fold higher enzyme concentration. These results were in accordance with the high k_{cat}/K_M values observed for IIIC1 and IVB10.

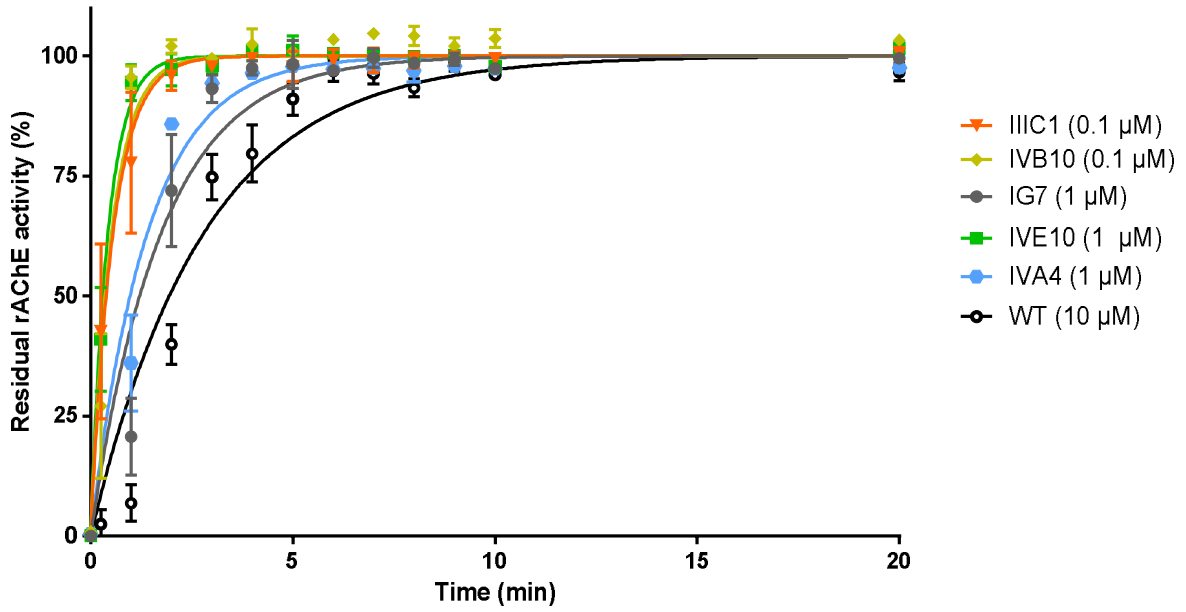


Figure 16 : Protection of recombinant human AChE with enhanced phosphotriesterase *Sso*Pox variants.
AChE activity was evaluated after incubation of paraoxon with *Sso*Pox wild type and variants (IIIC1, IVB10, IG7, IVE10, IVA4) for different times. The resulting curves were fitted with one-phase decay equation using GraphPad Prism 6 software.

Sequence/Structure/Function relationships

The relationships between sequence, structure and function were evaluated, first by compiling a heat map of the overall activities and also by clustering the substrates and the variants **(Figure 17)**. The heat map highlight that phosphotriesterase activity was improved as compared to wild-type enzyme conversely to lactonase activity that was drastically decreased for all new variants. The best variants such as *Sso*Pox-IVE2, -IIIC1 and -IVB10 have five mutations and *Sso*Pox-IG7 three mutations. These mutations do not destabilized much their structures indeed these variants remains highly stable with T_m of 89.7, 96.3, 85.0 and 79.1°C respectively. The 3D structures of most interesting variants were solved **(Table 7)**. Structure of *Sso*Pox-IVE2 has an open loop 8 compared to *Sso*Pox-wt and a widening of the active site due to Y97L and W263M mutations. Structure of *Sso*Pox-IG7 also an open loop 8 yet the active site remain the same as wt enzyme. I280T mutation seems to impact in the opening of loop 8 **(Figure 18A)**. Loop 7 and 8 flexibility is more important in both *Sso*Pox variants as illustrated by the B-factors **(Figure 18B)**. Otherwise these structures are very similar, with a RMSD of 0.29 Å between *Sso*Pox-wt and *Sso*Pox-IVE2 and of 0.30 Å between *Sso*Pox-wt and *Sso*Pox-IG7 (on all atoms, determined with PyMOL).

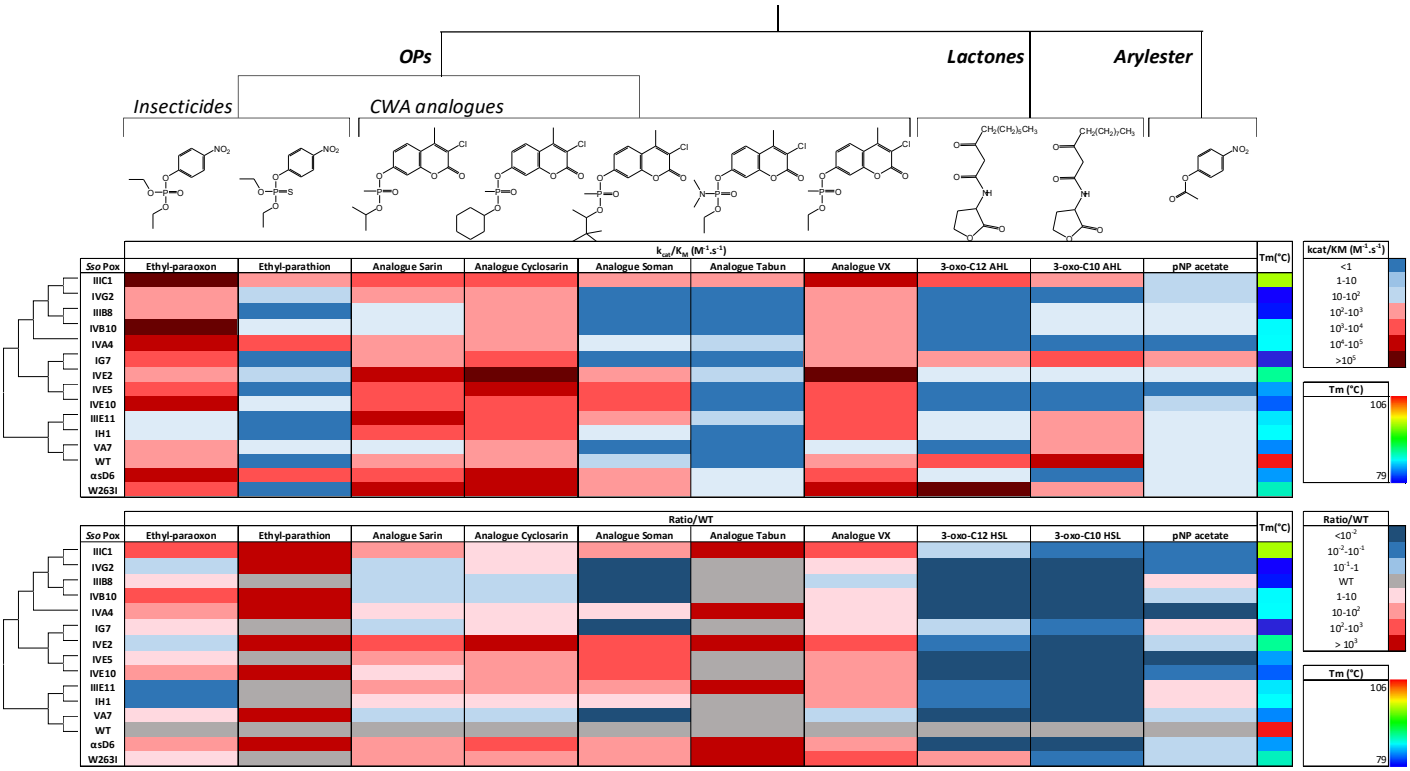


Figure 17 : Activities on the ten substrates and T_m values of selected *Sso*Pox variants.
The heat maps show the catalytic efficiencies and fold change of selected variants. Each raw represents the data for a different *Sso*Pox variant while each column shows the results on a different substrate. The last columns reports the melting temperatures values. Substrates are clustered according to the related enzymatic activity (phosphotriesterase, lactonase and arylesterase). Variants are clustered according to phylogeny analysis performed with MEGA7.

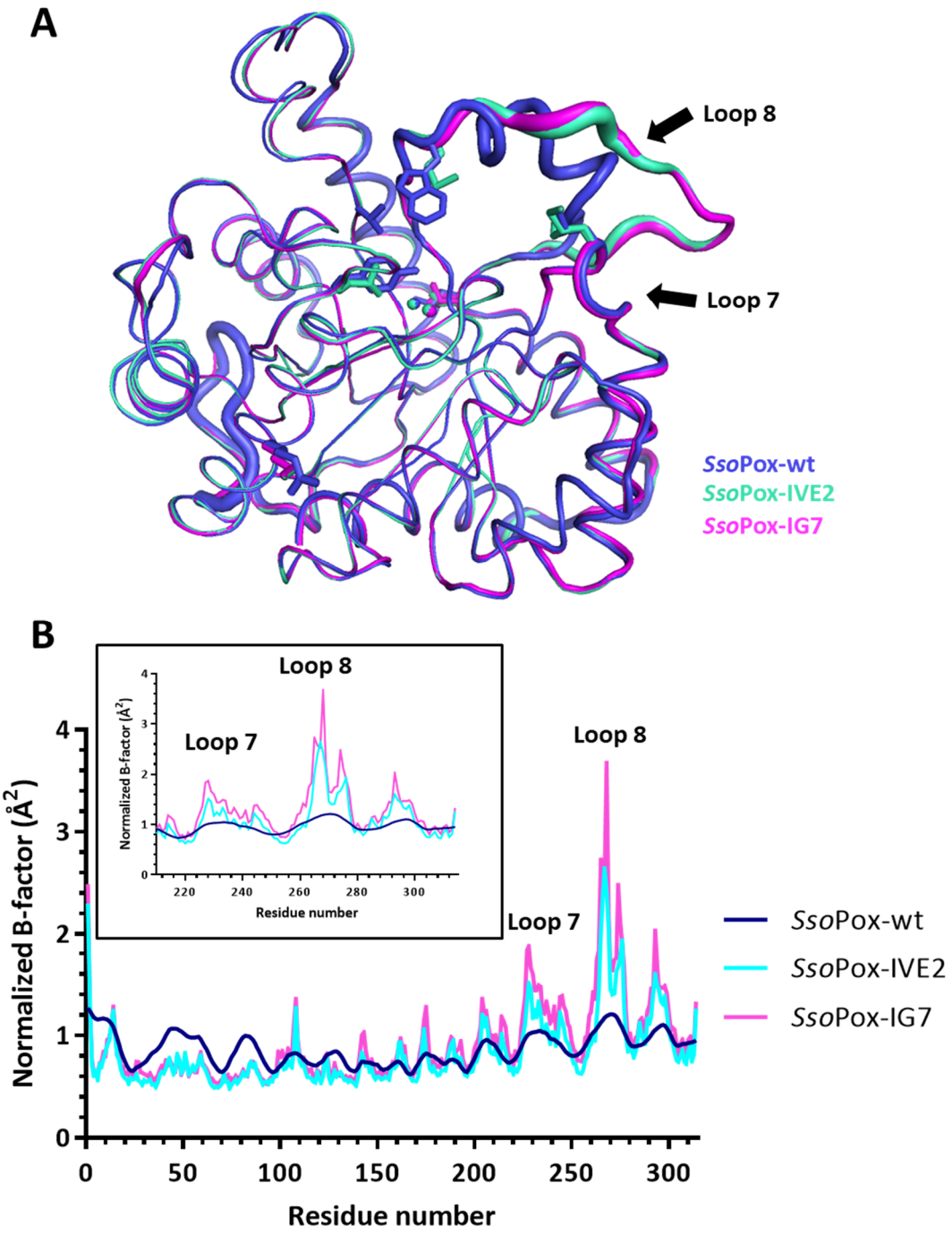


Figure 18 : Structural analysis of *Sso*Pox variants.
(A) Structural alignment of *Sso*Pox-wt (2VC5, cyan), *Sso*Pox-IVE2 (dark blue) and *Sso*Pox-IG7 (magenta). Positions with mutations are show as sticks both in wt and variants. Representations are in cartoon putty realized with PyMOL. **(B)** Representation of normalized B-factors alongside the polypeptide chain. Highlight of loop 7 and 8 region.

Table 7 : Data collection and structure refinement statistics.

Data collections	IVE2	IG7
PDB ID		
Wavelength (Å)	0.96802	0.96802
Resolution (Å)	1.4	1.4
Space group	$C222_1$	C222
Unit cell dimensions		
a (Å)	66.06	65.43
b (Å)	74.67	74.66
c (Å)	137.40	137.47
α (°)	90	90
β (°)	90	90
γ (°)	90	90
No. observed reflections (last bin)	477153 (85133)	370589 (67218)
No. unique reflections (last bin)	67061 (12397)	66114 (12236)
Completeness (%) (last bin)	100 (99.9)	99.3 (99.1)
Rmeasure (%) (last bin)	6.3 (63.3)	4.4 (64.3)
I/σ(I) (last bin)	19.91 (3.26)	20.00 (2.87)
Last resolution shell	1.5 – 1.4	1.5 – 1.4
Redundancy (last bin)	4.34 (5.61)	5.60 (5.49)
Refinement statistics		
Resolution range (Å)	49.48 – 1.4	49.21 – 1.4
No. Reflections	63707	62776
Rfree /Rwork	15.30 / 17.33	14.76 / 20.38
No. protein atoms	3044	2869
No. water molecules	407	380
Average B factor (Å2)	18.542	26.200
rmsd from ideal		
Bond lengths (Å)	0.0273	0.0301
Bond angles (°)	2.5746	2.5436

2.4. Discussion

*Sso*Pox promiscuous activities were evaluated on phosphotriester, lactone and arylester substrates. Improved variants were obtained for phosphotriester and arylester substrates, such as *Sso*Pox-IVB10 (V27A/L72C/Y97F/Y99F/W278L) which is the best variant on ethyl-paraoxon along with *Sso*Pox-IIIC1 variant (L72C/Y97F/Y99F/W263V/I280T), also *Sso*Pox-IG7 (V27G/R154K/I280T) enhanced on *p*NP acetate. Conversely, all the variants were decreased against lactones substrates as compared to wt enzyme. A decrease of lactonase activity was expected, actually other works show that when enzyme activity is shifted from one activity to specialized in another, the native activity is generally greatly diminished[5]. Interestingly, the latent arylesterase activity was enhanced for some variants but remained lower by orders of magnitude than phosphotriesterase activity **(Figure 15)**.

As *Sso*Pox-αsD6, the variant *Sso*Pox-IVA4 (V27G/L72C/Y97I/Y99F/R154K) lost the thiono-effect. These variants degrade with nearly the same efficiency oxono-OP (ethyl-paraoxon) and thiono-OP (ethyl-parathion) conversely to *Sso*Pox-wt which was shown to only hydrolyzed ethyl-paraoxon[152]. Here were shown that positions V27 and Y97 are crucial in thiono-effect as previously reported.

Thereafter, to assess the potential of *Sso*Pox variants for CWA degradation, analogues were used[156]. In general the variants are improvement on CWA analogues. For example, *Sso*Pox-IVE2 variant (Y97L/R154K/L228M/W263M/I280T) is greatly enhanced on CWA analogues, but paraoxonase, lactonase and arylesterase activities are low compared to wt enzyme. *Sso*Pox-IIIC1 variant is very interesting with a great activity against OP such as ethyl-paraoxon, ethyl-parathion and also CWA analogues, however no arylesterase activity and lactonase activity near *Sso*Pox-wt. Other variants with no or little ($k_{cat}/K_M < 2\ M^{-1}.s^{-1}$) arylesterase activity such as *Sso*Pox-IVA4,-IVE5,-IVG2 and -IVE10 have no lactonase activity neither on 3-oxo-C10- or 3-oxo-C12-AHL **(Figure 15)**. Specific variants for the hydrolysis of pesticides (*Sso*Pox-IVB10) or CWA analogues (*Sso*Pox-IVE2) as well as broad spectrum variant on OP (*Sso*Pox-IIIC1) were obtained, yet at the cost of lactonase activity.

The variants contains two up to six mutations and a thermal stability (T_m) between 79.1 to 96.3°C, lower than wt enzyme (106°C) nevertheless thermal stability remains high for an enzyme. For example, the most stable variant, *Sso*Pox-IIIC1, has a T_m of 96.3°C and contains five mutations. Even the less stable variant, *Sso*Pox-IG7, show a T_m of 79.1°C and contains three mutations. The gain of new activity and/or specificity is usually associated with a decrease in overall stability to increase enzyme flexibility. Here the tremendous robustness of *Sso*Pox allow to buffer destabilizing mutations and to enhance evolvability[163]. We were able to maintain the balance between them to obtain enhanced variants on OP and arylester. This equilibrium is also observed in 3D structure of *Sso*Pox-IVE2 where the near catalytic site stay the same, except for Y97 and W263 positions which allow a widening of the active site and as for the loop 8 is opened. These rearrangements confer *Sso*Pox-IVE2 the ability to efficiently degrade some CWA analogues. For *Sso*Pox-IG7 structure, the loop 8 opening allows an enhanced arylesterase activity while maintaining the activity against ethyl-paraoxon.

To go further, we evaluated the potential of *Sso*Pox variants to protect rAChE from OP poisoning[141]. Within a few minutes *Sso*Pox variants were able to degrade ethyl-paraoxon which lead to the protection of rAChE. As expected the fastest variant for protected rAChE was *Sso*Pox-IVB10. rAChE being the physiological target of OP, this test shows the interest of *Sso*Pox for potential prophylaxis application.

To conclude, laboratory driven evolution is a powerful method to improve enzyme activity. The switch in activities in enzyme is allowed by a subtle equilibrium between rigidity, flexibility and stability allowing catalytic plasticity while maintaining well folded structure. All these improved variants pave the way for numerous applications such as bioremediation of pesticides for external decontamination and also for prophylaxis application as more remote prospects.

II. Projet de recherche

Partie 3

La dégradation enzymatique des insecticides organophosphorés diminue la toxicité et améliore la régénération chez les planaires

Partie 3 : La dégradation enzymatique des insecticides organophosphorés diminue la toxicité et améliore la régénération chez les planaires

Les OPs, en plus d'être neurotoxiques, sont suspectés d'engendrer des perturbations du développement[164]. La recherche de nouvelles stratégies efficaces est donc cruciale pour remédier à leur impact sur l'environnement et la santé humaine. L'utilisation d'enzymes pour la décontamination externe, et plus particulièrement de *Sso*Pox, est une alternative très intéressante pour la bioremédiation. Cependant, si la toxicité des insecticides organophosphorés est avérée, celle des produits de dégradation enzymatique est encore mal connue et a été peu étudiée jusqu'alors. Ainsi, un modèle *in vivo* utilisant la planaire, un ver plat de l'embranchement des plathelminthes a été développé. Cet organisme, *Schmidtea mediterranea*, est un modèle d'étude particulièrement intéressant puisque, outre l'étude de la toxicité, il est doté d'une capacité de régénération permettant également d'étudier le développement. La planaire a donc été retenue pour étudier l'impact des OPs et des produits de dégradation sur la neurotoxicité ainsi que sur la perturbation du développement de ce ver.

Pour cette étude quatre pesticides ont été utilisés : l'éthyl-paraoxon, l'éthyl-parathion, le diazinon et le fenitrothion. La décontamination enzymatique a été réalisée avec le variant *Sso*Pox-αsD6 obtenu précédemment. Ce variant possède l'activité phosphotriestérase la plus importante sur la plupart des substrats et le spectre d'action le plus étendu. Le site de clivage et les produits de dégradation enzymatique ont tout d'abord été identifiés par GC/MS. Les OPs étant des inhibiteurs de l'AChE, une phylogénie a été réalisée pour évaluer la trajectoire putative d'évolution de la AChE de planaire, *Smed*-AChE, par rapport à la AChE humaine : elles partagent 35% d'identité de séquence et semblent avoir divergé à partir d'un ancêtre commun. L'activité AChE a également été confirmée dans un broyat de planaire et la susceptibilité de *Smed*-AChE à l'exposition aux OPs et aux produits de dégradation a été vérifiée. L'activité AChE du broyat de planaires est sensible aux pesticides et plus particulièrement à l'éthyl-paraoxon. Les produits de dégradation, quant à eux, ont un faible impact sur l'activité AChE confirmant leur faible neurotoxicité.

Par la suite, les planaires ont été exposées à différentes concentrations en OPs et leurs produits de dégradation ; la mortalité et la régénération (de la tête et de la queue après coupure) ont été observées. La dégradation enzymatique permet de fortement diminuer la mortalité due aux insecticides, on peut le voir grâce à la NOEC, « No Observed Effect Concentration », qui correspond à la plus forte concentration testée pour laquelle aucun effet sur l'organisme vivant n'a été observé. Par exemple, pour l'éthyl-parathion la NOEC passe de 100 µM à 800 µM après dégradation enzymatique. La mobilité est également impactée par les OPs mais est restaurée après dégradation. Les mêmes observations sont constatées pour la régénération, elle est plus rapide après action de l'enzyme. Les OPs ont un effet perturbateur du développement qui est largement diminué après dégradation. Pour l'éthyl-parathion, par exemple, la NOEC passe de 10 µM à 300 µM. L'ensemble de ces résultats montrent que la décontamination enzymatique est une alternative prometteuse pour la bioremédiation externe des OPs.

Dans le cadre de ce projet, j'ai produit et purifié les lots d'enzymes utilisés pour la décontamination des insecticides. J'ai réalisé la majorité des tests de dégradation des OPs et j'ai participé aux analyses de GC/MS pour l'identification des sites de coupure et des produits de

dégradation. Pour le reste j'ai participé à l'écriture, à la réalisation des figures et à la relecture du manuscrit. Ces travaux ont été publiés dans le journal *Scientific Reports*.

Les figures et tableaux supplémentaires sont en annexe.

3.1. Introduction

Organophosphorus pesticides (OPs) are highly toxic chemicals that have been widely developed for agricultural purposes since the 1950s[87]. Their widespread use has led to serious contamination worldwide and constitutes a major health and environmental issue[165]. The acute toxicity of OPs is due to their capacity to inhibit acetylcholinesterase, a key enzyme involved in the overall regulation of the central and peripheral nervous system. OPs disrupt nervous signals by deactivating AChE through phosphorylation and irreversible binding to the catalytic serine causing acetylcholine accumulation and cholinergic overstimulation[166]. Exposure to high doses of OPs is associated with many symptoms including salivation, diaphoresis, emesis, miosis, and tremors that may cause paralysis and death[167,168]. Furthermore, low dose chronic exposure to OPs may have deleterious effects including impaired neurobehavioral performance and may negatively affect human fetal and childhood health[169,170]. Some reports have also pointed out the possible link between low level chronic exposure to OPs and health problems[171,172].

Considering the high toxicity of OPs and their intensive use, finding efficient methods of decontamination is a major concern. Numerous approaches, including chemical, physical and biological methods, have been considered for developing decontamination strategies against OPs. However, these methods usually involve harsh conditions, are not compatible with the decontamination of people, and cannot be considered for large-scale environmental remediation[91]. Recently, enzymes have emerged as a promising alternative to smoothly and quickly decontaminate OPs. Of these, the phosphotriesterase-like lactonase *Sso*Pox from the archaea *Sulfolobus solfataricus* is an appealing candidate for remediation. This enzyme has been engineered and proven to be highly efficient for degrading a broad panel of OPs[78,108,173,174]. This enzyme displays a phosphotriesterase activity that enable to degrade OPs through an hydrolysis reaction leading to two degradation products, a phosphodiester and an alcohol. Due to its extremophilic origin, *Sso*Pox is also tremendously robust, including resistance to solvents and detergents[99] and long-term storage or activity over a wide range of temperatures[113]. The enzyme is, moreover, highly convenient for immobilization and could be used in filtration devices to treat effluents soiled with OPs[113,123,175]. Recently, *Sso*Pox was engineered and variants with drastically enhanced phosphotriesterase activity were generated (part 1). Of these, variant *Sso*Pox-αsD6 was of utmost interest and it is this which we considered in this study.

Although enzyme decontamination would decrease the neurotoxicity of OPs, little is known about the toxicity of the generated degradation products and little research effort has been dedicated to their fate. This may require further consideration, as these molecules may affect the environment and non-targeted organisms[176]. The lack of a convenient and easy-to-handle *in vivo* model that could be used to assess both neurotoxicity and developmental perturbation may explain the low levels of attention that have been given this topic. Freshwater planarians, a Platyhelminthes have a large proportion of stem cells that give them an unconventional capacity for regeneration and are, subsequently, highly interesting for developmental studies[177,178]. Indeed, planarians appear to be particularly relevant for investigating developmental disruption in addition to classic toxicological investigations. Recently, planarians have emerged as an alternative animal model for toxicology and neurotoxicology[179,180]. *Dugesia japonica*[181], *D. gonocephala*[182], *D. dorotocephala*[183], and *D. tigrina*[184] have been shown to be negatively affected by OP exposure. Cholinesterase activity was demonstrated in planarians and their sensitivity to OPs has been highlighted albeit lower than *Homo sapiens* AChE (*Hs*-AChE)[181]. Moreover,

evolutionary considerations have suggested that AChE from Platyhelminthes, including planarian and *Schistosoma*, are probably early cholinesterase related to other lower vertebrates such as the medaka *Oryzias latipes* and the hagfish *Myxine glutinosa*[185–187]. Such evolutionary trajectory may explain the difference in sensitivity to OP exposure with higher vertebrates for which a gene duplication event lead to a divergence between AChE and butyrylcholinesterase[188].

Here, we investigated the toxicity of four widely used insecticides, paraoxon-ethyl, parathion-ethyl, diazinon and fenitrothion, which have been widely used in agriculture, as well as their respective degradation products generated by enzymatic hydrolysis with *Sso*Pox-αsD6. Mortality, behavior and regeneration were assessed in *Schmidtea mediterranea*. OPs were shown to be toxic to planarians and to affect both mobility and regeneration capacity while the use of a decontaminating enzyme drastically decreased the deleterious effects of OPs. The global toxicity of both pesticides and their corresponding degradation products were thus assessed and the results underlined the strong potential of *Sso*Pox for bioremediation.

3.2. Results

GC/MS analysis of enzymatically-generated degradation products

*Sso*Pox has been previously reported to efficiently degrade a broad spectrum of organophosphorus insecticides. Here, the cleavage site for each substrate was unambiguously assigned. The leaving groups generated through enzyme hydrolysis were characterized by GC/MS and were consistent with the phosphotriesterase mechanism of *Sso*Pox. Paraoxon-ethyl and parathion-ethyl hydrolysis led to 4-nitrophenol while diazinon and fenitrothion led to 6-methyl-2-propan-2-yl-1H-pyrimidin-4-one and 3-methyl-4-nitrophenol respectively **(Figure 19)**.

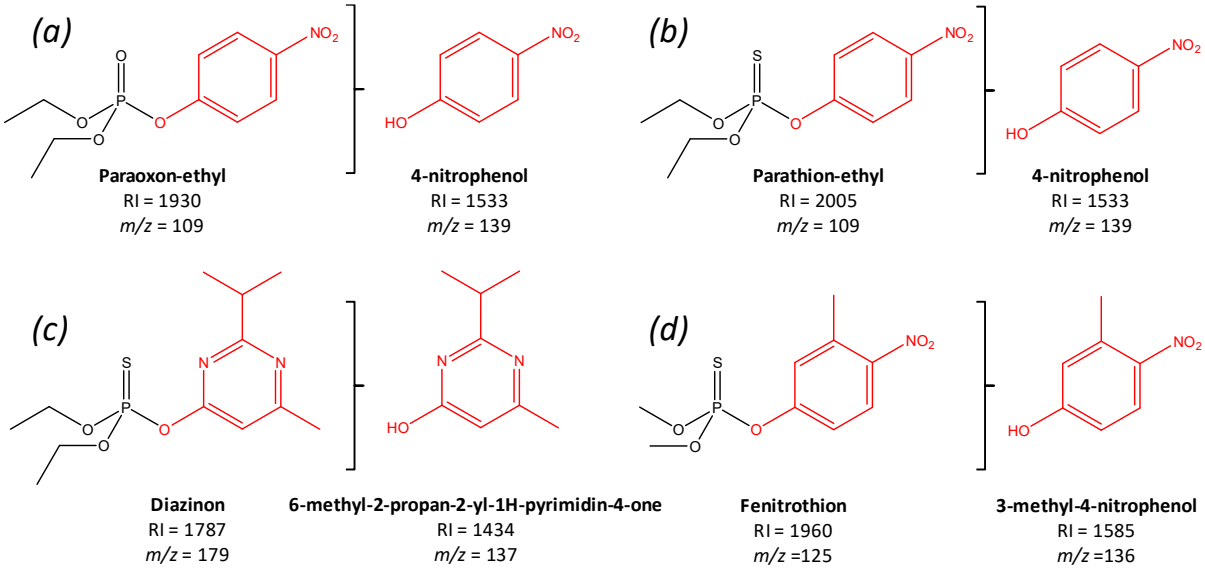


Figure 19 : **GC/MS characterization of the enzymatically-generated degradation products.**
RI is the experimental Kovats retention index of the molecule and *m/z* is the mass-to-charge ratio of the base peak fragment detected for each molecule. The leaving group and the corresponding degradation product are emphasized in red. ***(a)*** Paraoxon-ethyl (CAS 311-45-5) led to 4-nitrophenol (CAS 100-02-7); ***(b)*** Parathion-ethyl (CAS 56-38-2) led to 4-nitrophenol (CAS 100-02-7); (***c***) Diazinon (CAS 333-41-5) led to 6-methyl-2-propan-2-yl-1H-pyrimidin-4-one (CAS 2814-20-2); (***d***) Fenitrothion (CAS 122-14-5) led to 3-methyl-4-nitrophenol (CAS 58864-63-4).

Phylogeny

Phylogenetic analysis was performed to evaluate the evolutionary trajectory of putative planarian AChE as compared to characterized AChE from other phyla **(Figure 20)**. AChE sequences from *Schmidtea mediterranea*, *S. polychroa*, *Dendroceleum lacteum*, *Planaria torva* and *Polycelis tenuis* were predicted and found to be closely related to other classes belonging to Platyhelminthes. These AChE are referred to here as *Smed*-AChE, *Spol*-AChE, *Dlac*-AChE, *Ptor*-AChE, *Pten*-AChE following the gene nomenclature guidelines previously described[189]. *Smed*-AChE, *Spol*-AChE, *Dlac*-AChE and *Pten*-AChE shared more than 60% identity at the amino acid level, while *Ptor*-AChE shared only 35%. AChE from planarians also appear to share a common ancestor with Chordata and shared on average 35% identity at the amino acid level with *Hs*-AChE, suggesting that planarians may constitute a potential alternative for the study of OP poisoning.

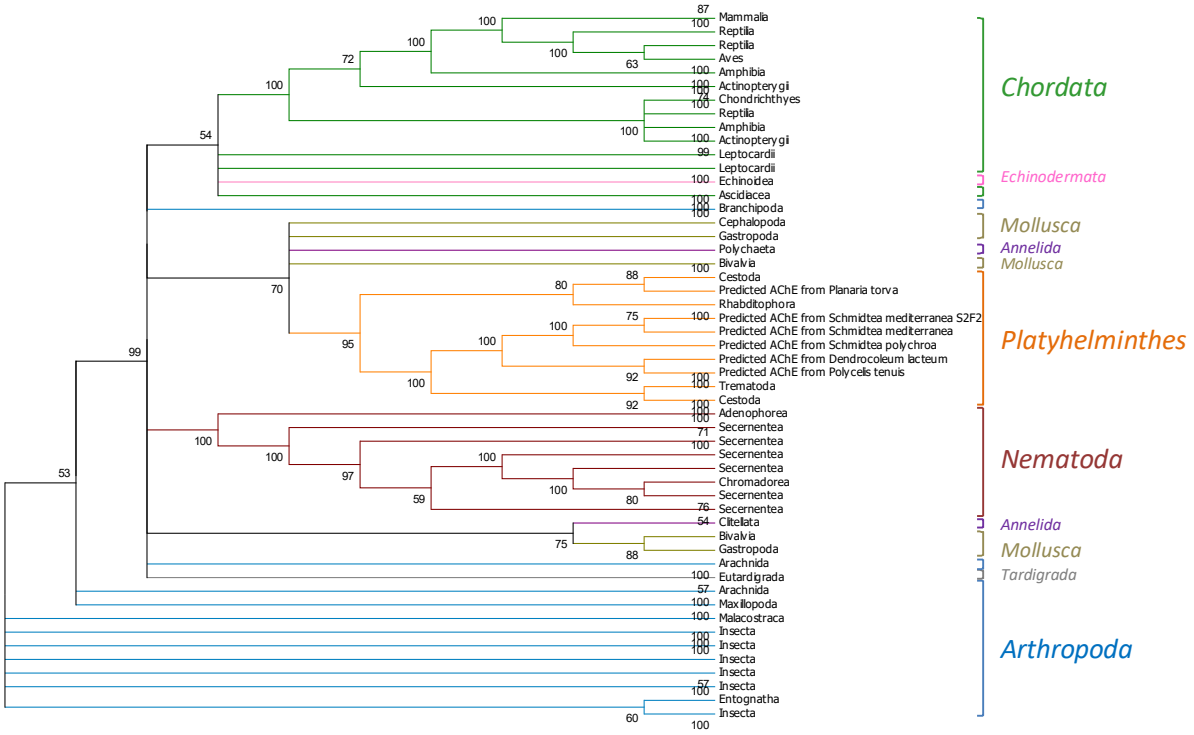


Figure 20 : Phylogenetic tree of AChE.

AChE from planarians were predicted using PlanMine (http://planmine.mpi-cbg.de)[190] and used as template for BLAST in UNIPROT (http://www.uniprot.org/blast/). Sequence alignment and Phylogeny were performed with MEGA[191,192]. Predicted AChE from planarians were found to be closely related to other species from Platyhelminthes.

Acetylcholinesterase activity in *Schmidtea mediterranea* (*Smed*-AChE)

Acetylcholinesterase activity was determined in *S. mediterranea* using acetylthiocholine as a substrate and Ellman's assay[193]. Significant activity was measured in planarian homogenates, suggesting the presence of AChE in *S. mediterranea* **(Figure 21)**. As organophosphorus insecticides are spread in the millimolar range, a panel of concentrations from the micromolar up to the millimolar scale was considered. Acetylcholinesterase activity was reduced when incubated with insecticides. *Smed*-AChE activity was almost zero when paraoxon-ethyl concentration reached 400 µM, while 40 to 60% of activity was retained with 1 mM of parathion-ethyl and diazinon or fenitrothion respectively. Paraoxon-ethyl had a greater impact on *Smed*-AChE activity than parathion-ethyl and other assayed insecticides, suggesting that the oxo form is more toxic than thiono-derivatives. In contrast to insecticides, AChE activity was only slightly affected after enzymatic degradation of the molecules, suggesting that degradation products are poor inhibitors of *Smed*-AChE. Nevertheless, paraoxon-ethyl degradation products were found to decrease *Smed*-AChE activity to 50% at high concentrations.

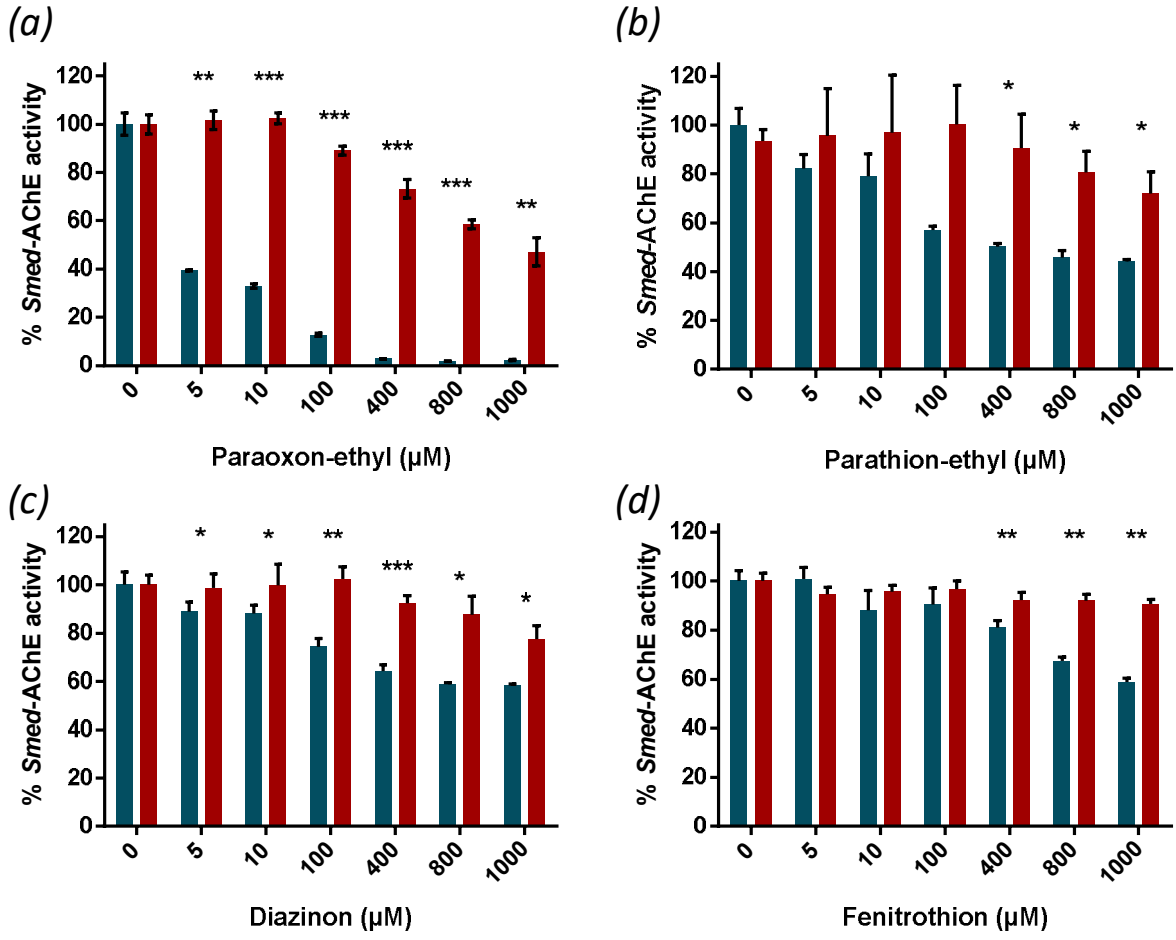


Figure 21 : Characterization of *Smed*-AChE activity in planarian homogenates.
Evaluation of *Smed*-AChE inhibition by insecticides and the associated enzymatically-generated degradation products in planarian homogenates. Blue and red bars represent the inhibition of *Smed*-AChE by insecticides and their degradation products respectively for paraoxon-ethyl (***a***), parathion-ethyl (***b***), diazinon (***c***) and fenitrothion (***d***). The values represent the mean ±SD (standard deviation) of three replicates. Black stars (*) indicate a significant difference between insecticide and degradation product for a given concentration (one star to indicate $p < 0.05$; two stars to indicate $p < 0.005$; three stars to indicate $p < 0.0005$ according to Student's *t*-test).

Toxicity of OPs in *S. mediterranea*

The toxicity of four widespread insecticides (paraoxon-ethyl, parathion-ethyl, diazinon, fenitrothion) was evaluated. Dose-responses were assessed by following the survival rate of planarians exposed to increasing concentrations of chemicals **(Figure 22a,c,e,g)**. Paraoxon-ethyl was entirely fatal down to 50 µM, while no mortality was observed for 10 µM (NOEC for "No Observed Effect Concentration" regarding mortality results) after 12 days. Parathion-ethyl, the thiono-analogue of paraoxon-ethyl was much less toxic than its oxono counterpart, being completely lethal down to 400 µM and with a NOEC value of 100 µM. Diazinon and fenitrothion induced complete mortality at 200 µM and 400 µM and showed NOEC values of 100 µM after 12 days of exposure.

Enzymatic degradation of OPs drastically decreased the deleterious effects in planarians **(Figure 22b,d,f,h, Supplementary Figure 9)**. After complete hydrolysis, diazinon did not induce any mortality for the tested concentrations. NOEC values for parathion-ethyl and fenitrothion were increased up to 800 µM and 400 µM respectively. The degradation products of parathion-ethyl did not induce complete mortality even for the highest assayed concentration (1 mM). After paraoxon-ethyl degradation, significant toxicity was observed for the enzymatically generated products, albeit at lower levels than for the initial insecticide. NOEC was increased to 50 µM but concentrations from 200 µM up to 400 µM were still fatal to planarians. After enzymatic degradation of OPs, NOEC values were increased by four and five-fold for fenitrothion and paraoxon-ethyl respectively and by up to eight-fold for both parathion-ethyl and diazinon **(Supplementary Table 6)**.

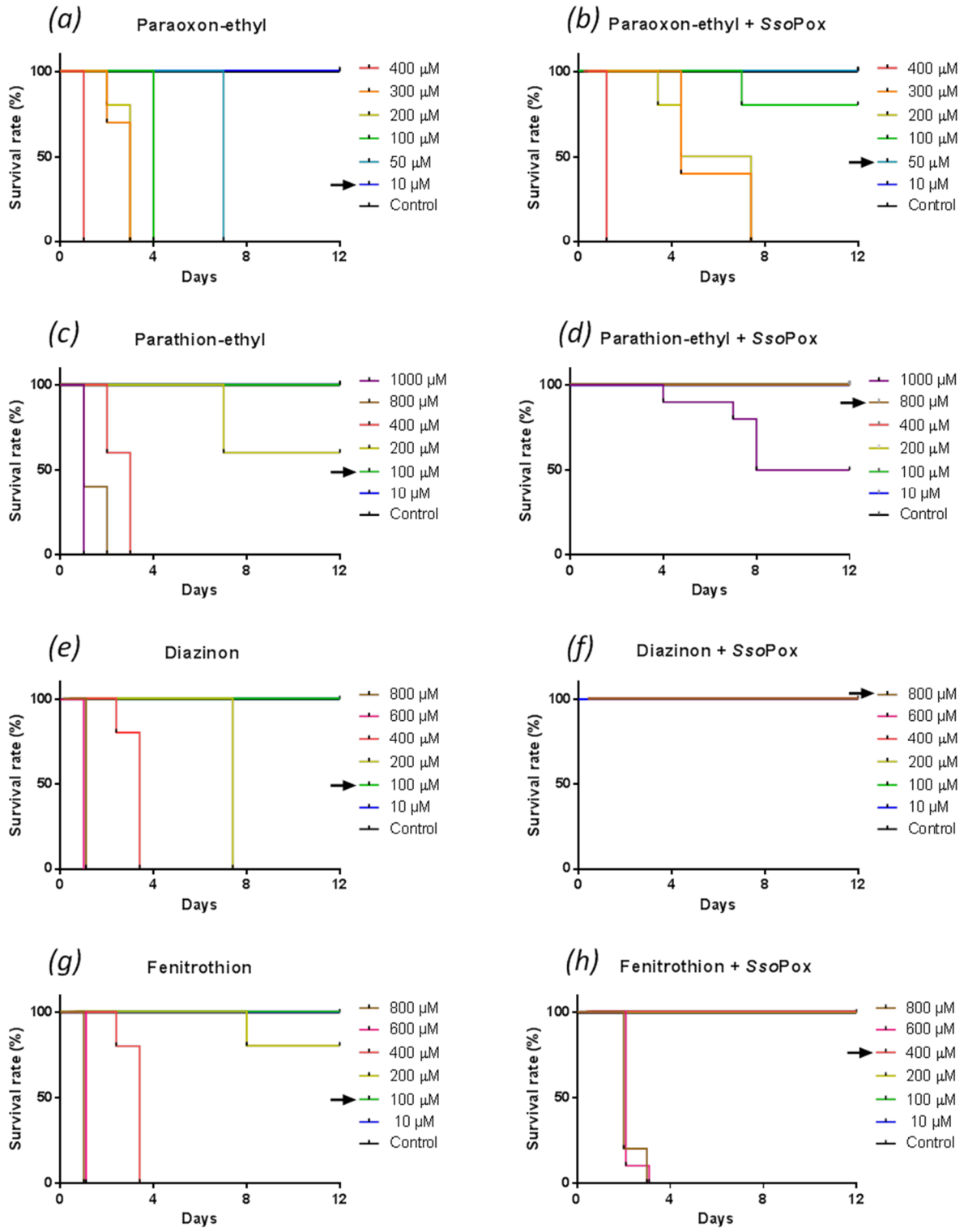


Figure 22 : Enzymatic degradation of insecticides increases survival rate in planarians.
The toxicity of paraoxon-ethyl, parathion-ethyl, diazinon and fenitrothion before and after degradation by *Sso*Pox was evaluated for concentrations ranging from 10 µM up to 1000 µM. The curves represent the survival rates for 10 planarians exposed to pesticides and the enzymatically generated degradation products paraoxon-ethyl (***a, b***), parathion-ethyl (***c, d***), diazinon (***e, f***), fenitrothion (***g, h***). Arrows indicate NOEC values.

Effect of OPs on mobility

The impact of insecticides and their associated degradation products on planarian behavior was evaluated **(Figure 23a-e)**. Planarians were incubated in aqueous solutions containing lethal or sub-lethal concentrations of insecticides. For all insecticides, disruption of mobility was observed. The modifications of mobility were classified into three types: “mobile at normal speed” when planarians moved normally; “immobile” when planarians were prostrate and “non-normally mobile” when planarians were neither normally mobile nor immobile **(Supplementary Figure 10)**. Direct visual evaluation of mobility was performed by several observers blinded to the treatment. These observations were reproducible and did not affect the results. The highest concentrations of insecticides led to complete immobility of planarians, followed by death. Low concentrations altered mobility by significantly slowing down the planarian and no or low modification was observed for the lowest 10 µM concentration. After enzymatic degradation of insecticides, planarian mobility was drastically enhanced. Planarians recovered normal behavior for concentrations up to 50 µM, 100 µM and 200 µM for paraoxon-ethyl, diazinon and fenitrothion respectively. For the highest concentrations, enzymatic degradation improved both mobility and survival rate although no complete remission was observed. Mortality was still observed after degradation by the enzyme at concentrations of 200 µM and 600 µM of paraoxon-ethyl and fenitrothion respectively. Ten worms were used for each concentration and the phenotype presented in **Figure 23** was reproducible and was shared by a minimum of 80% of the population. As pesticides were initially prepared in ethanol before dilution in water to reach final concentration, control solutions with the final ethanol concentrations for each condition were performed. We found no effect of ethanol up to the maximum concentration assayed of 0.4%.

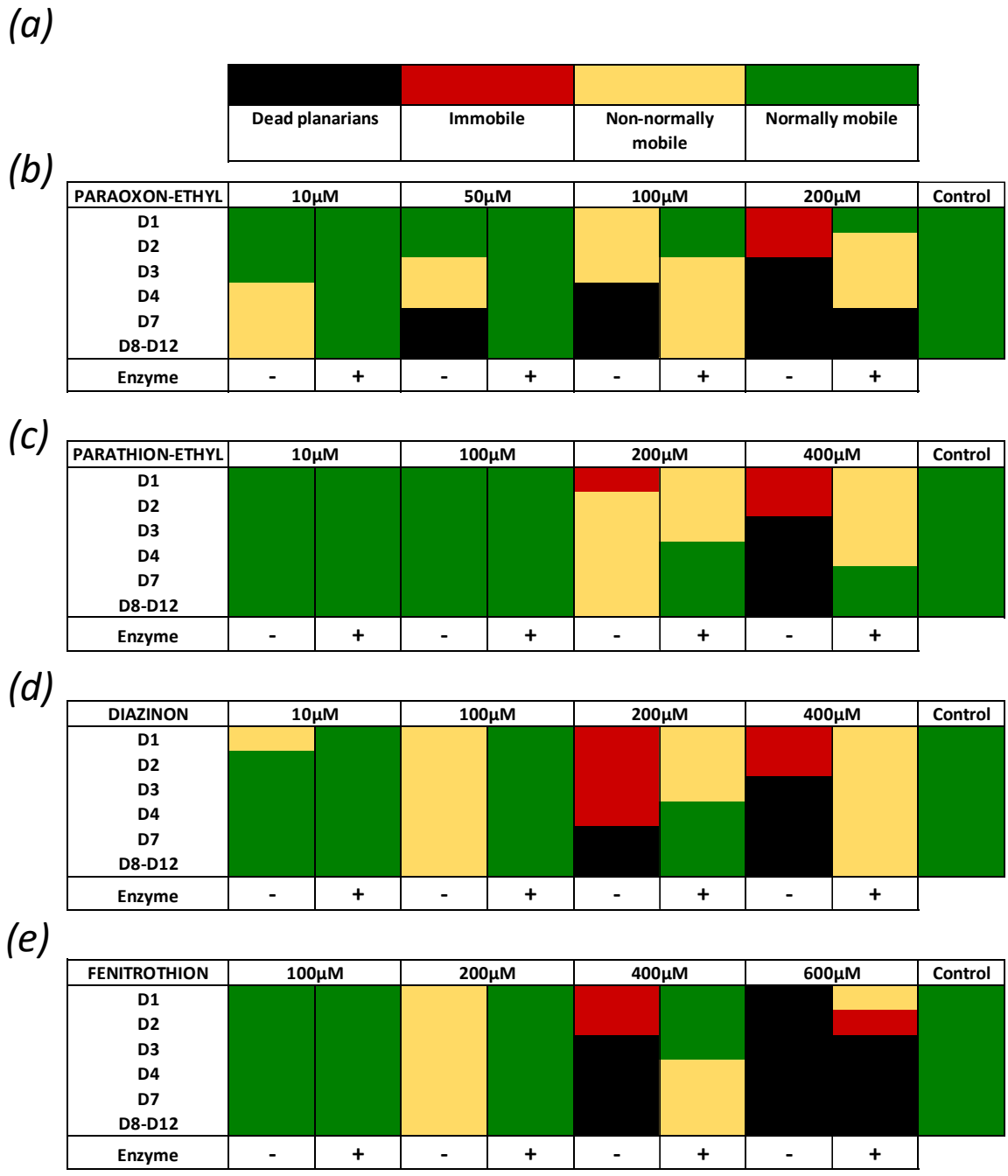


Figure 23 : 12 days' incubation of planarians in insecticides and related degradation product solutions and evaluation of the impact on mobility.

The average mobility of ten planarians for 12 days (D1 to D12) is presented using a color code describing normal mobility (green), non-normal mobility (yellow), immobility (red) and death (black) (***a***). (+) and (-) describe the solution with and without enzymatic degradation. Paraoxon-ethyl (***b***), parathion-ethyl (***c***), diazinon (***d***), fenitrothion (***e***) and the related degradation products were evaluated. As pesticides were initially solubilized in ethanol before dilution in water to reach final concentration, the control solutions represent the maximum final ethanol concentration for each insecticide.

Effect on planarian regeneration

Planarians have the capacity to regenerate an entire worm from a tissue fragment. Under normal conditions, regeneration is complete 14-15 days after amputation. The effect of sub-lethal or partially lethal concentration exposure to insecticides and their degradation products, on planarian regeneration was monitored over 15 days **(Figure 24a-f)**. Head and tail regeneration were followed from tail and head fragments respectively. A visual categorization was used for representing regeneration stages. These criteria were used to characterize the regeneration process and were sufficiently clear to be not dependent on the observer, three different experimentors obtaining the same results.

Insecticides were found to drastically alter head regeneration. Lethal concentrations were decreased down to 100 µM for diazinon and down to 50 µM for parathion-ethyl and fenitrothion as compared to whole planarians. NOEC values were decreased for parathion-ethyl, diazinon and fenitrothion down to 10 µM, 75 µM and 10 µM respectively **(Supplementary Table 6)**. For diazinon and fenitrothion, regeneration progressively improved when the concentration was decreased, while a binary behavior was observed for paraoxon-ethyl and parathion-ethyl at threshold concentration of 50 µM. Impressively, no alteration of the regeneration was observed after the enzymatic decontamination of insecticides. Interestingly, no ectopic growth was observed after one regeneration cycle. Five worms were used for each concentration and the phenotype presented in **Figure 24** was reproducible and was shared by a minimum of 80% of the population. As for mobility and toxicity analyses, no effect of ethanol was observed in the range of the tested concentrations. Very similar results were obtained when studying tail regeneration **(Supplementary Figure 11a-f)**.

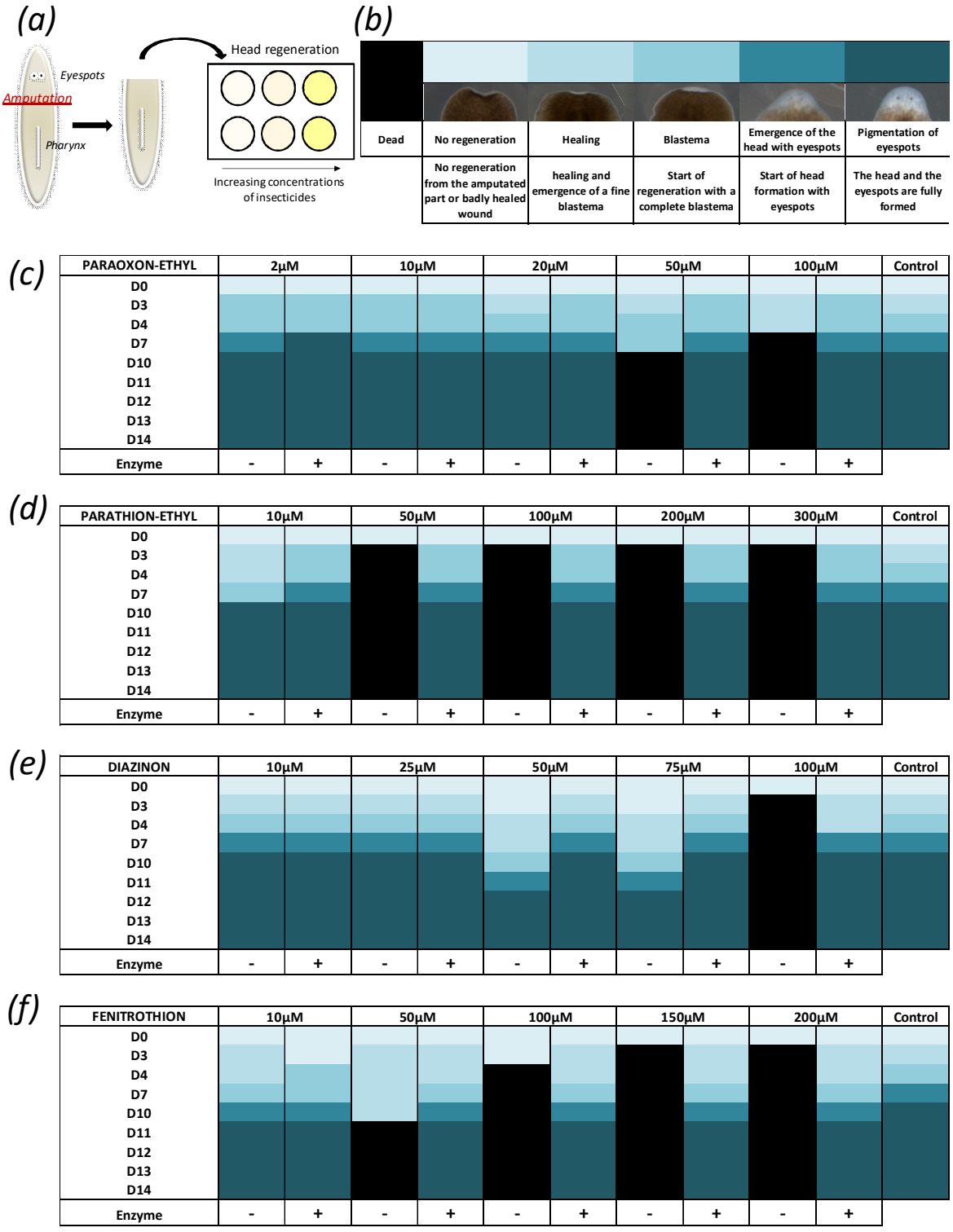


Figure 24 : Evaluating the impact of insecticides and their enzymatically-generated degradation products on planarian head regeneration.

Five planarians were cut above the pharynx and incubated in insecticide solutions (***a***). Head regeneration of planarians over 15 days (D0 to D14) is presented using a color code from light to dark blue describing initial to final regeneration stages as presented in figure caption (***b***). Paraoxon-ethyl (***c***), parathion-ethyl (***d***), diazinon (***e***), fenitrothion (***f***) and the related degradation products were evaluated. Dead planarians are colored black. (**+**) and (-) describe the solution with and without enzymatic degradation. As pesticides were initially solubilized in ethanol before dilution in water to reach final concentration, the control solutions represent the maximum final ethanol concentration for each insecticide.

3.3. Discussion

The toxicity of four widespread insecticides (paraoxon-ethyl, parathion-ethyl, diazinon, fenitrothion) and their corresponding degradation products generated through enzyme hydrolysis was addressed. The cleavage sites for each substrate were unambiguously confirmed by GC/MS analysis and were found to be in accordance with previously reported catalytic mechanisms[108]. OPs are inhibitors of acetylcholinesterase, but little is known about their toxicity after degradation. To tackle this issue, the planarian, an original flatworm from Platyhelminthes was considered, as this model can be used to evaluate both toxicity and regeneration disruption.

Acetylcholinesterase activity of *S. mediterranea* homogenates was confirmed and this activity was further shown to be susceptible to OP exposure. All four insecticides decreased *Smed*-AChE activity after incubation, although paraoxon-ethyl was the most detrimental substrate. Paraoxon-ethyl had a greater impact on *Smed*-AChE activity than parathion-ethyl, suggesting that, like *Hs*-AChE, *Smed*-AChE is significantly affected by OP in the oxon form. Indeed, many studies have demonstrated that oxon insecticides are drastically more toxic than phosphorothionates which are first activated *in vivo* during metabolization by cytochrome P450 monooxygenase[194–196]. Phylogenetic analysis also showed that predicted AChE from planarians are clustered in a same branch of Platyhelminthes connected to the Chordata phylum, thus confirming that planarians may share an ancient common ancestor with mammalians, as pointed out in a previous study[181].

Degradation products had a lower impact on *Smed*-AChE activity than insecticides. Degradation of parathion-ethyl, diazinon and fenitrothion led to very low *Smed*-AChE inhibition, underlining their moderate neurotoxicity. Only paraoxon-ethyl degradation products had a significant impact on *Smed*-AChE activity at concentration greater than 400 µM. Because paraoxon-ethyl and parathion-ethyl share one of their two degradation products, namely 4-nitrophenol, it can be safely assumed that the toxic effect observed after paraoxon-ethyl degradation is due to the phosphodiester released, while the phosphorothionate diester analogue, generated through parathion-ethyl degradation, is less toxic. It should be noted that measurements of *Smed*-AChE activity were performed with crude planarian homogenates containing other proteins and metabolites that may also interact with the compounds. Nevertheless, similar inhibitions of AChE were observed when exposing whole planarians in insecticides.

The deleterious effect of OP exposure in whole planarians was further evaluated after incubation in diluted insecticide solution. Insecticide concentrations from 10 µM up to 1 mM were assayed and were in accordance with previous studies. Concentrations up to 800 µM paraoxon-ethyl were used for incubating planarians[182], while concentrations ranging from 13 µM up to 57 µM were reported for diazinon, fenitrothion, parathion, chlorpyrifos and malathion[183,184]. The viability of *D. japonica* for concentrations up to 500 µM was also described and the authors showed that dichlorvos was 100 times more toxic than chlorpyrifos suggesting that toxicity is strongly dependent on the insecticide[179]. This difference was supposed to be related with the oxon form of dichlorvos which is probably more toxic than thiono insecticides. The toxicity of oxon insecticides was further highlighted in *Djap*-AChE and diazinon oxon was shown to have the highest effect[181]. In this study we found that paraoxon-ethyl was highly toxic in *S. mediterranea,* causing complete mortality at concentrations down to 50 µM. Thiono insecticides were found to be less toxic, causing complete mortality at concentrations down to 200 µM for diazinon and 400 µM for both parathion-ethyl and fenitrothion. After enzymatic

degradation of insecticides, the survival of planarians was drastically enhanced. Diazinon and parathion-ethyl have two distinct leaving groups but generate the same phosphorothionate diester. The differences observed in the toxicity of these compounds after decontamination may thus be strongly ascribable to their variable leaving group. Moreover, because only low impacts of the degradation products on *Smed*-AChE activity were observed, their neurotoxicity appears lower as compared to insecticides.

The effect of insecticides on planarian mobility was also evaluated. At sub-lethal concentrations, paraoxon-ethyl and diazinon induced mobility disruption down to 10 µM, while the observable effects of parathion-ethyl and fenitrothion occurred only at 200 µM. At low but lethal concentrations, the mobility of planarians was strongly altered in the early days of exposure and was followed by death. Enzymatic decontamination of insecticides before exposure of planarians enhanced mobility. For most assayed concentrations, a non-exposed type behavior was recovered and enzyme degradation enhanced the survival rate. However, for the highest concentrations of paraoxon-ethyl and fenitrothion, death still occurred but was delayed in comparison to insecticide-treated samples. These results highlight that the enzyme improved planarian mobility, although for highest assayed concentrations, degradation products may also cause disruption, while only a low impact on *Smed*-AChE activity was observed. Although degradation products induced deleterious effects on mobility from 200 µM for 4-nitrophenol and 6-methyl-2-propan-2-yl-1H-pyrimidin-4-one or 400 µM for 3-methyl-4-nitrophenol their impact on planarian behavior was reduced as compared to insecticides.

To further investigate the toxicity of insecticides and their degradation products, their impact on planarian regeneration was observed. Planarians have the capacity to regenerate an entire flatworm from a tissue fragment thanks to abundant stem cells. Alteration of this capacity by low-level OP exposure was followed by a 15 day long full regeneration cycle. The worms were cut into two, allowing both head and tail regeneration from tail and head fragments respectively. Surprisingly, both fragments appeared to be more sensitive to OP exposure than full worms and were characterized by lower NOEC values, as previously discussed. The lowest concentrations did not induce any delay in regeneration, but increasing insecticide concentration either delayed regeneration or caused mortality. In a few cases, planarians died after one week, although the regeneration process had started. Impressively, for all the conditions that were assayed, enzymatic decontamination improved survival and/or regeneration of planarian fragments. No disruption was observed after paraoxon-ethyl, parathion-ethyl and diazinon degradation and only a slight delay was observed for fenitrothion degradation products. Taken together, these results suggest that insecticides may have a stronger impact on planarian development than their degradation products. However, the degradation products were only found to slightly alter *Smed*-AChE activity in contrast to insecticides, underlining a lower neurotoxicity[197].

Enzymatic remediation of insecticides appears to be a promising approach to decreasing the deleterious effects induced by OP exposure. *Sso*Pox, which is active towards a broad range of OPs and which is highly stable may thus be further considered for decontamination purposes. Previous reports have shown that the enzyme can be produced at a large scale and retain its catalytic activity after immobilization into alginate beads or polyurethanes which may be considered in particular for incorporation into filtration devices[113,123]. Although degradation products may not be completely innocuous, these compounds were found to be much less toxic than insecticides and reduced poisoning effects by increasing NOEC values by up to eight-fold. Enzymatic decontamination also

drastically limited the detrimental consequences to planarian mobility and enabled recovery of a non-exposed like regeneration process.

3.4. Materials and Methods

Production-purification of *Sso*Pox-αsD6. *Sso*Pox-αsD6 was cloned in a pET32b-Δtrx plasmid and produced using an *E. coli* BL21(DE_3)-pGro7/GroEL (TaKaRa) chaperone expressing strain as previously described[78,173]. In short, auto-inducible ZYP medium (supplemented with 100 µg.ml^{-1} ampicillin and 34 µg.ml^{-1} chloramphenicol) was used for growth. When OD_{600nm} reached a value of 0.8-1, $CoCl_2$ and L-arabinose was added (final concentrations respectively 0.2 mM and 2 g.l^{-1}) to induce chaperones GroEL/ES expression, the temperature was decreased to 23 °C for 16-20 hours. Cells were harvested by centrifugation (4,400 g, 4 °C, 20 minutes) and the pellet was resuspended in *lysis buffer* (50 mM HEPES pH 8.0, 150 mM NaCl, $CoCl_2$ 0.2 mM, lysozyme 0.25 mg.ml^{-1}, PMSF 0.1 mM and DNAseI 10 µg.ml^{-1}) and stored at -80 °C. The lysate was thawed and lysed by three 30-second steps of sonication (Qsonica, Q700; Amplitude 45). Cell debris were removed by centrifugation (14,000 g, 4 °C, 15 minutes). As *Sso*Pox-αsD6 is hyperthermostable a pre-purification step was conducted by heating the lysate for 30 minutes at 70 °C. Precipitated *E. coli* proteins were removed by centrifugation (14,000 g, 4 °C, 15 minutes). *Sso*Pox-αsD6 was concentrated by ammonium sulfate precipitation (75%) and resuspended in 8 ml of *activity buffer* (50 mM HEPES pH 8.0, 150 mM NaCl, $CoCl_2$ 0.2 mM). The remaining ammonium sulfate was eliminated by desalting column (HiPrep 26/10 desalting, GE Healthcare; ÄKTA Avant), concentrated to 2 ml and injected on size exclusion chromatography (HiLoad 16/600 Superdex^{TM} 75pg, GE Healthcare; ÄKTA Avant). Final purity was verified by 10% SDS-PAGE and protein concentration was determined with a NanoDrop 2000 spectrophotometer (Thermo Scientific).

Planarian. Freshwater planarians belonging to the *Schmidtea mediterranea* species (asexual clonal line ClW4) were used for all experiments. The planarians were maintained in autoclaved water at 19 °C in the dark and fed twice per week with calf liver. The animals were starved for at least one week prior to the experiments. The water was changed every two days and did not contains antibiotics.

Acetylcholinesterase activity assays. Acetylcholinesterase activity was measured using Ellman's assay[193]. Worms were manually selected to fall within a certain range of sizes, around 0.8-1 cm in length. Thirty animals were processed in a Fastprep 24 5g (three cycles of 10 seconds, 6,0m/s) in 600 µL of activity buffer (20 mM 2-amino-2-(hydroxymethyl)propane-1,3-diol, 100 mM NaCl, pH 8.0). Experiments were conducted in the same buffer complemented with 4 mM 5,5'-Dithiobis (2-nitrobenzoic acid). 10 µL of the planarian supernatant was added to 140 µL of activity buffer in a 96-well plate. 50 µL of 0.01 M acetylthiocholine iodide in the activity buffer was added to each well to start the reaction and the OD_{412nm} was followed with a microplate reader (Synergy HT, BioTek, USA) for 10 minutes. This activity was normalized to 100%. As negative controls, experiments without planarian supernatant and without acetylthiocholine iodide were carried out. The reproducibility of the crude homogenate preparation was demonstrated with three independent replicates **(Supplementary Figure 12)**.

Experiments with pesticides (paraoxon-ethyl, parathion-ethyl, diazinon and fenitrothion) were conducted as previously described after incubation of the supernatant from the planarian with the

pesticide for 45 minutes to ensure reaching inhibition plateau **(Supplementary Figure 13)**. An additional control was carried out using only pesticide in the activity buffer.

Experiments with degradation products of pesticides were carried out as previously described after a degradation by *Sso*Pox-αsD6 variant at a final concentration of 0.25 µM. The reaction was monitored by measuring the absorbance of the product released until complete degradation. The planarians were then incubated for 45 minutes in the decontaminated solution **(Supplementary Figure 9)**. Supplementary controls were conducted using only the degradation products in the activity buffer.

The activity results after incubation with pesticides or degradation products were normalized as compared to the activity value without inhibition set to 100%.

Toxicity assays and perturbation of behavior. Worms were manually selected to fall within a certain range of sizes, around 0.8-1 cm in length. The animals were starved for at least one week prior to the experiments. Observations were carried out using a Leica M165 FC lens connected to the IC Capture 2.4 software. Four pesticides (Sigma Aldrich) were used for these experiments at different concentrations (paraoxon-ethyl, parathion-ethyl, diazinon and fenitrothion).

4 mL of solution was prepared for each organophosphorus compound at different concentrations (paraoxon-ethyl: 10 µM-400 µM, parathion-ethyl: 10 µM-1000 µM, diazinon: 10 µM-800 µM and fenitrothion: 10 µM-800 µM) without and with degradation by *Sso*Pox-αsD6 variant at a final concentration of 0.25 µM into a 12-well plate. Five planarians were used in each well and experiments were conducted in duplicate. In the same well, mortality and mobility were analyzed over 12 days. As a negative control, the same experiments were carried out without pesticides, with enzyme, and with the pesticide solvent alone (ethanol) at the higher concentration of pesticides.

Perturbation of development. To study regenerating animals, specimens were cut into two, the head and the tail, using a scalpel just above the pharynx. 4 ml of solution was prepared in a 12-well plate for each organophosphorus compound at different sub-lethal concentrations determined from toxicity assays (paraoxon-ethyl: 2 µM-100 µM, parathion-ethyl: 10 µM-300 µM, diazinon: 10 µM-100 µM and fenitrothion: 10 µM-200 µM) without and with degradation by *Sso*Pox-αsD6 variant at a final concentration of 0.25 µM. After amputation of five planarians, the heads and tails were regrouped respectively in a well and regeneration was monitored over 14 days. As a negative control, the same experiments were conducted without pesticides, with enzyme, and with the pesticide solvent alone (ethanol).

GC/MS analysis of degradation products. In order to identify the degradation products, 100 µl of the pesticide solution degraded by *Sso*Pox-αsD6 variant was first extracted with 100 µl of chloroform. Organic extracts were analyzed using a Clarus 500 gas chromatograph equipped with a SQ8S MS detector (Perkin Elmer, Courtaboeuf, France). 1 µl of organic extract was volatilized at 220 °C (split 15 $ml.min^{-1}$) in a deactivated FocusLiner with quartz wool (SGE, Ringwood, Australia) and compounds were separated on an Elite-5MS column (30 m, 0.25 mm i.d., 0.25 mm film thickness) for 12 minutes using a temperature gradient (80-280 °C at 30 $°C.min^{-1}$, five minutes' hold). Helium flowing at 2 $ml.min^{-1}$ was used as carrier gas. The MS inlet line was set at 280 °C and electron ionization source at 280 °C and 70 eV. Full scan monitoring was performed from 40 to 400 *m/z* to identify chemicals by spectral database search using MS Search 2.0 operated with the Standard Reference Database 1A (National Institute of Standards and Technology, Gaithersburg, MD, USA). Identification was confirmed with reverse and forward scores above 800. Product identities were then validated with the Kovats

Retention Index from the injection of an alkane standard (Sigma Aldrich, France). In the case of weak degradation product signals (4-nitrophenol *m/z* 139, 6-methyl-2-propan-2-yl-1H-pyrimidin-4-one *m/z* 137, 3-methyl-4-nitrophenol *m/z* 136), extracted ion chromatograms were generated with base peak ions to confirm the absence of chemicals (Paraoxon-ethyl and parathion-ethyl *m/z* 109; Fenitrothion *m/z* 125; Diazinon *m/z* 179). All data were processed using Turbomass 6.1 (Perkin Elmer).

Phylogeny. To identify a planarian homolog of *Homo sapiens* AChE (*Hs*-AChE) isoform E4-E5 precursor (NP_056646.1), we examined, via TBLASTN, the planarian transcriptome database PlanMine (http://planmine.mpi-cbg.de/planmine/begin.do)[190] particularly the following flatworm species: *S. mediterranea, P. torva, P. tenuis, D. lactum* and *S. polychroa*. We identified sequences producing a significant alignment with the genes of interest. The top BLAST hit was used to predict *Smed*-AChE, *Pto*-AChE, *Pte*-AChE, *Dl*-AChE and *Sp*-AChE via FGENESH+ (http://www.softberry.com/). Homology at the protein level between predicted *Smed*-AChE and *Hs*-AChE was analyzed using BLAST.

The previous predicted sequences were used as template for BLAST in UNIPROT (http://www.uniprot.org/blast/) and 250 sequences were collected. Sequence alignment, including planarian predicted sequences and Phylogeny, were performed with MEGA[191,192]. A maximum likelihood tree was constructed and tested using the bootstrap method with a 100 replications.

Statistical analysis. For *Smed*-AChE activity **(Figure 21)** the values represent the mean ±SD (standard deviation) of the percentage of three technical replicates. Black stars (*) indicate a significant difference between insecticide and degradation product for a given concentration. According to Student's t-test, one star indicates $p < 0.05$, two stars indicate $p < 0.005$ and three stars indicate $p < 0.0005$.

Acknowledgements

L.P. and P.J. are PhD students funded by the Direction Générale de l'Armement (DGA). C.T. is a fellow of the French Ministry for Research and Technology and the "Fondation pour la Recherche Médicale" (FRM FDT20160435255). This work was supported by "Investissements d'avenir" program (Méditerranée Infection 10-IAHU-03) of the French Agence Nationale de la Recherche (ANR). The funding sources had no role in study design, data collection and analysis, decision to publish, or manuscript preparation. The authors are grateful to Mélissa Guibet for technical assistance.

Competing financial interests: E.C. has a patent WO2014167140 A1 licensed to Gene&GreenTK. D.D. and E.C. report personal fees from Gene&GreenTK during the course of the study.

Author contributions

L.P., L.B., P.J., C.L., N.A., D.D., performed the experiments; L.P., L.B., P.J., C.L., N.A., C.T., D.D., E.C., E.G. analyzed the data; D.D., E.C. and E.G. conceived and designed the experiments; and L.P., P.J., D.D., E.C., E.G. wrote the manuscript.

II. Projet de recherche

Partie 4

Evaluation de l'efficacité du quorum quenching par une lactonase sur des isolats cliniques de *Pseudomonas aeruginosa* et comparaison avec des inhibiteurs du quorum sensing

Partie 4 : Evaluation de l'efficacité du quorum quenching par une lactonase sur des isolats cliniques de *Pseudomonas aeruginosa* et comparaison avec des inhibiteurs du quorum sensing

*Sso*Pox est une lactonase naturelle capable de dégrader les AHLs impliquées dans la communication de certaines bactéries. De ce fait, elle est capable de perturber le QS ce qui lui confère un fort potentiel thérapeutique. Le variant *Sso*Pox-W263I auparavant amélioré par mutagénèse sur les substrats de type lactones a été employé pour perturber le QS[23]. Ces travaux ont été menés sur *P. aeruginosa*, une bactérie Gram négatif pathogène de l'homme qui est impliquée dans de nombreuses infections telles que les pneumonies ou encore les ulcères du pied diabétique. Cette bactérie utilise le QS pour adopter un comportement collectif en synchronisant l'expression de certains gènes nécessaires à la virulence bactérienne. *Sso*Pox est capable de perturber cette communication bactérienne grâce à sa capacité à hydrolyser les molécules de communication (AHLs) ; de fait sans AHLs les bactéries ne sont plus capables de synchroniser leur comportement et leur virulence. A l'instar de *Sso*Pox, d'autres molécules sont capables d'interférer avec le QS. C'est le cas des inhibiteurs chimiques du QS (QSI). Ces composés miment la structure des molécules de communication et vont inhiber spécifiquement le QS en empêchant la bactérie de détecter les autoinducteurs endogènes.

Dans ces travaux, des souches cliniques de *P. aeruginosa* ainsi que les souches modèles PAO1 et PA14 ont été testées en présence de *Sso*Pox. Trois facteurs de virulence caractéristiques des *P. aeruginosa* que sont la production de pyocyanine, la sécrétion de protéases et la formation du biofilm ont été mesurés. Des phénotypes très distincts sont observés parmi les 51 souches testées, 16 souches produisent les trois facteurs de virulence dans les conditions testées, la plupart des souches en produisant seulement un ou deux. Bien que les souches cliniques montrent une large diversité, l'enzyme *Sso*Pox-W263I s'est montrée capable de diminuer la virulence sur l'ensemble des isolats. Par la suite, les effets de *Sso*Pox ont été comparés aux deux QSIs les plus efficaces connus, le 5-fluorouracil et le C-30[198,199]. Les 16 souches de *P. aeruginosa* produisant les trois facteurs de virulence ont été utilisées. L'enzyme *Sso*Pox se montre l'agent le plus efficace dans les conditions des tests, les QSI n'ayant que des effets très modérés. Pour finir, dans l'optique de prouver l'efficacité de l'enzyme pour une utilisation dans des dispositifs médicaux, l'enzyme a été immobilisée dans du polyuréthane et son efficacité a été évaluée sur la souche modèle PAO1. L'enzyme immobilisée s'est montrée tout aussi efficace que l'enzyme libre pour inhiber *in vitro* la virulence de PAO1. Ces résultats couplés à la grande stabilité de l'enzyme montrent le fort potentiel de *Sso*Pox pour des applications médicales comme une incorporation dans les dispositifs médicaux tels que des pansements ou des cathéters.

Dans le cadre de ces travaux, j'ai produit et purifié plusieurs grammes d'enzyme nécessaires pour les tests microbiologiques. J'ai également participé à l'écriture et à la relecture du manuscrit. Ces travaux ont été publiés dans le journal *Frontiers in Microbiology*.

Les figures et tableaux supplémentaires sont en annexe.

4.1. Introduction

Pseudomonas aeruginosa is a human opportunistic pathogen involved in many infection types and which causes serious health complications[200,201]. In 2006/2007, this Gram negative bacterium alone was responsible for 8 % of general healthcare associated infections in the USA[202]. *P. aeruginosa* is involved in both community-acquired and hospital-acquired infections including otitis, keratitis, wound and burn infections, pneumonia and urinary tract infections[201]. Furthermore, *P. aeruginosa* is, along with *Staphylococcus aureus*, the most common pathogen isolated from diabetic foot infections notably in South East Asia, and is also highly involved in infections when an alteration of the skin occurs[201].

Many bacteria, including *P. aeruginosa*, use a molecular communication system, referred to as quorum sensing (QS), to synchronize the expression of certain genes and adopt a group behaviour. Among QS-regulated traits, virulence factors production such as pyocyanin and proteases[203], motility[204] and biofilm formation[205] are involved in the development of infections.

QS in *P. aeruginosa* depends on four different hierarchically organised systems: Las, Iqs, Rhl and Pqs. The first system to be activated is the Las system which depends on the production and perception of an acyl-homoserine lactone (AHL): *N*-(3-oxododecanoyl)-homoserine lactone (OdDHL or 3-oxo-C_{12} AHL)[206,207]. Induction of the Las system triggers the expression of the Las protease and elastase and activates the other QS systems. Despite its dominant role in the QS circuitry, eliminating LasR activation only results in a delayed activation of the *Pseudomonas* quinolone signal (PQS) system but does not completely eliminate QS[208]. In addition, the QS system of *P. aeruginosa* is interconnected with other regulatory networks involved in environmental cues such as phosphate, iron and oxygen sensing[209].

Regarding the importance of bacterial communication in the development of virulence, strategies for QS disruption, known as quorum quenching (QQ), have emerged to maintain bacteria in a commensal lifestyle. To this end, quorum sensing inhibitors (QSI) and QQ enzymes have been particularly considered[210–214]. QSI, such as brominated furanones, aim to prevent bacteria from perceiving endogenous QS molecules. Pyrimidine analogue has also been reported as a QS disruptor[199]. QQ enzymes such as acylases or lactonases degrade AHL signals[16,106]. Among these, the enzyme *Sso*Pox, isolated from the archaea *Sulfolobus solfataricus,* has been considered based on both its lactonase activity and tremendous stability due to its extremophile origin[113].

Many QQ examples have been reported and describe the reduction of virulence factor secretion (e.g. siderophores, proteases, rhamnolipids, etc.)[215,216] and/or biofilm formation, especially using QSI molecules[203]. However a large proportion of these reports is dedicated to investigating model strains *P. aeruginosa* PAO1 and PA14, and only a few reports have described the response of clinical isolates to QS disruption, whereas natural isolates frequently harbour mutations in QS genes[217].

In this article, we investigated the effectiveness of the QQ enzyme *Sso*Pox-W263I, a variant of *Sso*Pox with increased catalytic effectiveness against 3-oxo-C_{12} AHL[78,113], previously reported as being efficient to drastically reduce the mortality in a rat pneumonia model[218], to modulate virulence factors in 51 clinical *P. aeruginosa* isolates collected from diabetic foot ulcers. We also compared its QQ potential to the most common QSI, the brominated furanone C-30 and the pyrimidine analogue 5-fluorouracil (5-FU), by quantifying three virulence factors: pyocyanin production, protease secretion and biofilm

formation[198,199]. Finally the lactonase was immobilised to assess its ability to functionalise medical devices and was proved to maintain sufficient activity for QQ.

4.2. Materials and Methods

Bacterial strains and growth conditions. Experiments were performed with *P. aeruginosa* strains from samples held by the Department of Microbiology of the Nîmes University Hospital. The strains were isolated from diabetic patients with a suspected newly presenting episode of diabetic foot infection for a period of one year (2014). All the patients received an oral information, were anonymized and gave a non opposition statement to bacterial storage. This study was approved by the local ethics committee (South Mediterranean III) and was carried out in accordance with the Declaration of Helsinki as revised in 2008. The samples were frozen at -80 °C. Bacterial strains were cultivated on Luria Bertani (LB) agar plates at 37 °C.

The model strains *P. aeruginosa* PAO1 and PA14 (Taxonomy ID: 208964 and 652611) and the clinical isolates were inoculated from a single colony and pre-cultivated in LB (10 $g.l^{-1}$ NaCl, 10 $g.l^{-1}$ tryptone, 5 $g.l^{-1}$ yeast extract) for 6 h at 37 °C with shaking at 650 rpm. Subsequently, 3 ml of LB supplemented with 2 % sheep blood (Biomérieux, France) was inoculated with 3 µl pre-culture and incubated at 37 °C with shaking at 650 rpm. Pyocyanin production and protease activity were measured 24 h post-inoculation. Biofilm weight was determined 48 h post-inoculation.
The enzyme *Sso*Pox was added at 0.5 $mg.ml^{-1}$ and the QSI 5-FU and C-30 (Sigma) were used at 60 and 30 µM respectively as determined by a dose response experiment **(Supplementary Figure 14 - Supplementary Figure 16)**.

Bacterial identification. All strains were checked using Matrix-assisted laser desorption ionization–time of flight (MALDI-TOF) as previously described[219]. In brief, isolates were grown overnight on blood agar at 37 °C under aerobic conditions. Single colonies were applied as a thin film to a 96-spot steel plate (BrukerDaltonics) and allowed to visibly dry at room temperature. Subsequently, 2 µl of MALDI matrix (saturated solution of alpha-cyano-4-hydroxy-cinnamic acid, 500 µl HPLC-grade acetonitrile, 475 µl HPLC-grade water, 25 µl trifluoacetic acid) was applied on the spots and dried at room temperature. Isolates were tested in duplicate by MALDI-TOF mass spectrometry. The MALDI target plate was introduced into a microflex LT MALDI-TOF mass spectrometer for automated measurement and controlled by the FlexControl 3.3 (Bruker®) program. The spectra were collected in a mass range between 2,000-20,000 m/z then analyzed using the Bruker Biotyper 3.0 software package and compared to reference spectra for identification.

Protein production and purification. Enzyme production was performed using *E. coli* BL21(DE3)-pGro7/GroEL strain (TaKaRa) carrying plasmid pET22b-*Sso*Pox-W263I as previously described[220,221]. In brief, cells were grown in ZYP medium supplemented with 100 $µg.ml^{-1}$ ampicillin and 34 $µg.ml^{-1}$ chloramphenicol at 37 °C until OD_{600nm} reached 0.8-1. L-arabinose was added to a final concentration of 0.2 % (w/v) in order to induce chaperones expression. Subsequently, 0.2 mM $CoCl_2$ was added and the temperature was reduced to 23 °C for an additional 20 h. Cells were harvested by centrifugation (4,400 g, 4 °C, 20 min), the supernatant was discarded and the pellet was resuspended in lysis buffer (50 mM HEPES pH 8.0, 150 mM NaCl, 0.2 mM $CoCl_2$, 0.25 $mg.ml^{-1}$ lysozyme, 0.1 mM Phenylmethylsulfonyl fluoride (PMSF) and 10 $µg.ml^{-1}$ DNaseI) and stored at -80 °C overnight. Frozen

cells were thawed at 37 °C for 15 min and disrupted by three 30 seconds sonication steps (QSonica sonicator Q700; amplitude at 45). Cell debris were removed by centrifugation (21,000 g, 4 °C, 15 min). Crude extract was incubated for 30 min at 80 °C and was further centrifuged to precipitate *E. coli* proteins (21,000 g, 4 °C, 30 min). *Sso*Pox-W263I was concentrated by overnight ammonium sulfate precipitation (75 % saturation), and resuspended in activity buffer (50 mM HEPES pH 8.0, 150 mM NaCl, 0.2 mM $CoCl_2$). Remaining ammonium sulfate was eliminated via desalting (HiPrep 26/10 desalting, GE Healthcare; ÄKTA Avant). The obtained protein sample was concentrated to 2 ml and subsequently loaded onto a size-exclusion chromatography column and purified to homogeneity (HiLoad 16/600 Superdex^{TM} 75pg, GE Healthcare; ÄKTA Avant). The purity of the protein was checked by 10 % SDS-PAGE **(Supplementary Figure 17)** separation and protein concentration was measured using a NanoDrop 2000 spectrophotometer (Thermo Scientific).

Proteolytic activity. Cell-free culture supernatants were prepared by centrifugation for 5 min at 12,000 g. Protease activity was determined using azocasein (Sigma, St. Louis, USA) as a substrate[222]. The reaction was performed in Phosphate-buffered saline (PBS) solution pH 7.0 with 50 µl of azocasein (30 mg ml^{-1} in water) and with 25 µl of culture supernatant for a final volume of 750 µl. The reaction was incubated at 37 °C for 1 h and stopped by adding 125 µl of 20 % (w/v) trichloroacetic acid. The blank assay was realised using 25 µl of culture medium with and without 0.5 $mg.ml^{-1}$ of *Sso*Pox. After centrifugation at 12,000 g for 5 min, the absorbance of the supernatant was measured at OD_{366nm} using a plate reader (Synergy HT, BioTek, USA).

Pyocyanin production. Pyocyanin was extracted from 500 µl of cell-free supernatant using 250 µl of chloroform. The mix was vortexed for 20 sec, and centrifuged at 12,000 g for 5 min. The absorbance of the lower organic phase was measured at OD_{690nm} using a plate reader (Synergy HT, BioTek, USA)[223].

Biofilm weight measurement. After 48 h, each culture was sieved through a 100 µm pore-size cell strainer (Corning, New York, USA) to separate biofilm from planktonic cells. The biofilm was washed with 2 ml PBS and centrifuged at 600 g for 5 min. Biofilms were weighed directly in the cell strainers using a precision scale **(Supplementary Figure 18)**.

Immobilisation. In a 25 cm^2 culture flask (Corning, New York, USA), 1 ml of 5 % Impranil® DLU polyurethane (Covestro, Leverkusen, Germany) mixed with 20 $mg.ml^{-1}$ of *Sso*Pox-W263I and 0.5 % Glutaraldehyde (Sigma) in purified water was dried over 12 h at 37 °C. As a control, the same volume of activity buffer was added instead of *Sso*Pox-W263I. Before being used for culture, the flask was rinsed with 3 ml of purified water and then 3 ml of LB.

Enzymatic activity measurement. Enzymatic activities were measured after 24 h based on the paraoxonase activity of *Sso*Pox using ethyl paraoxon as a substrate and the apparition of para-nitrophenol, paraoxon degradation product, was followed at OD_{405nm}.

Released enzyme was measured after 24 h from culture supernatants. 5 µl of cell-free culture supernatant was transferred into a 96 well plate containing 95 µl of activity buffer (50 mM HEPES, 150 mM NaCl, pH 8). Then 100 µl of 2 mM ethyl paraoxon (Sigma) in activity buffer was added and OD_{405nm} was monitored during 10 min with a plate reader (Synergy HT, BioTek, USA) and the slope corresponding to paraoxon degradation kinetics was calculated.

Fixed enzyme was determined by adding 3 ml of a 1 mM ethyl paraoxon solution. After 3 min of incubation with shaking (300 rpm), 200 µl of paraoxon solution was transferred into a 96-well plate

and OD_{405nm} was measured. The slope ($OD.min^{-1}$) was calculated and compared to a standard with a known enzyme concentration to calculate the amount of enzyme immobilised in the PU coating.

4.3. Results

Dose-response determination

P. aeruginosa model strains PAO1 and PA14 were used to determine the optimal concentrations of the QQ enzyme *Sso*Pox and the QSI 5-FU and C-30 to decrease virulence factor production. Time points for sampling were determined by performing dose response experiments at different concentrations **(Supplementary Figure 14 - Supplementary Figure 16)**. Under our conditions and in the absence of quenchers, protease and pyocyanin levels were similar for both strains (data not shown). The use of *Sso*Pox did not induce any delay in growth and maximal quenching was obtained for a concentration of 0.5 $mg.ml^{-1}$ of enzyme corresponding to 14.5 µM after 16 h of cultivation **(Supplementary Figure 14)**. At this time point, pyocyanin production was almost completely abolished for both strains and protease production was reduced to 10 % as compared to the control (untreated sample) for PAO1 and 43 % for PA14. Biofilm formation was measured after 48 h to allow complete biofilm formation and direct weighing of cell aggregates **(Supplementary Figure 18)**. The addition of *Sso*Pox (0.5 $mg.ml^{-1}$) reduced biofilm formation by 90 % for PAO1 and 60 % for PA14, and increasing *Sso*Pox concentration did not enhance quenching. The QSI molecule 5-FU only weakly impacted production of pyocyanin and protease in PAO1 but had a greater influence on PA14, with pyocyanin and protease productions reduced to 10 and 50 % respectively compared to the untreated culture. Biofilm formation was reduced in both strains when concentrations of 5-FU of 60 µM or higher were used. According to these results, quorum quenching of the clinical isolates was tested using 0.5 $mg.ml^{-1}$ *Sso*Pox or 60 µM 5-FU and 30 µM C-30. The same values were also reported in previous studies[224,225]. Pyocyanin and protease productions were determined after 24 h and biofilm formation 48 h post-inoculation.
Importantly, the addition of 5-FU to the culture led to a delay in growth, but this delay was recovered after 24 h for PAO1 **(Supplementary Figure 19)**. The second QSI molecule, C-30, had much less impact in our experiment set-up as protease level remained up to 90 % of the control for both PAO1 and PA14, and pyocyanin production was not reduced.

Quenching of virulence factors by *Sso*Pox

In the experimental conditions used here, the two model strains PAO1 and PA14 both produced the three virulence factors tested. Among the 51 clinical isolates of *P. aeruginosa*, 16 strains produced the three virulence factors studied, 13 produced two virulence factors and 22 produced only one virulence factor **(Figure 25)**. Proteolytic activities ranged from 0.47 to 1.37 with a median value at 1.08 **(Figure 26A)**. Median pyocyanin production, among the 26 strains producing pyocyanin, was measured at 0.17 and this virulence factor showed the highest variations ranging from 0.01 to 1.00 **(Figure 26B)**. Finally, the most common feature between the clinical isolates was biofilm formation as 42 strains out of 51 produced biofilm. Among these strains, the median value for wet biofilm was 73 mg with values ranging from 15 mg to 289 mg **(Figure 26C)**. *Sso*Pox was used at a concentration of 0.5 $mg.ml^{-1}$ and pyocyanin and protease quantities were determined after 24 h. In these conditions, *Sso*Pox reduced protease activity of 26 out of 28 strains, with 20 of them being reduced by more than 50 % and complete quenching was achieved for 16 of them. No clinical isolate harboured a higher value upon

treatment with *Sso*Pox than without **(Figure 27A)**. Pyocyanin production was reduced in 25 strains out of 26 and 20 of them were reduced by more than half the control level. Furthermore, pyocyanin production was completely eliminated in six strains. As noticed for protease production, no strain had increased pyocyanin production when the QQ enzyme *Sso*Pox was added **(Figure 27B)**. Biofilm was reduced in 37 strains out of 42, 36 of them were reduced by more than half and 20 of them completely lost their ability to grow in biofilms. Unlike pyocyanin and protease production, one clinical isolate, A12, had a slightly thicker biofilm upon treatment with *Sso*Pox than without but this difference was not statistically significant **(Figure 27C)**.

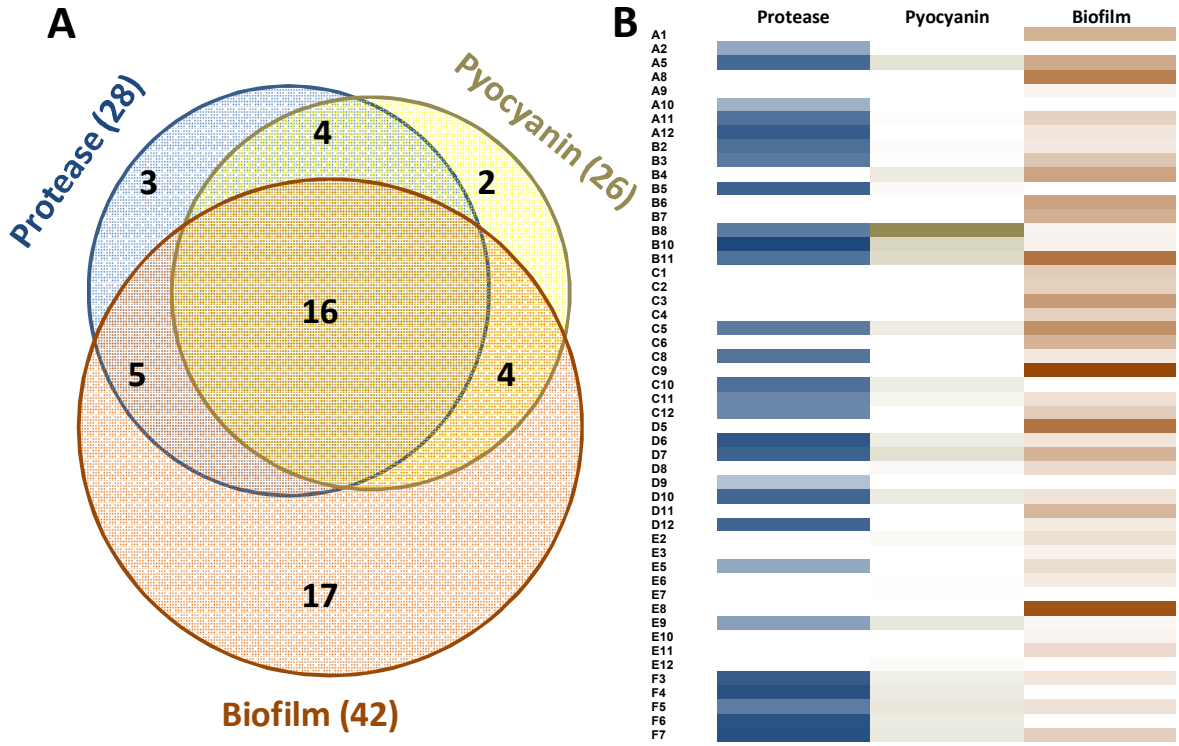


Figure 25 : Measurable virulence factor expression among the 51 clinical isolates of *P. aeruginosa*.
(A) Venn diagram describing the distribution of the 51 strains according to their production of virulence factors. **(B)** Proteolytic activities are presented according to OD_{366nm} value ranging from 0 to 1.37. Pyocyanin values represent the OD_{690nm} and range from 0 to 1. Biofilm values correspond to the weight of biofilm formed after 48 h for 3 ml of culture and range from 0 to 289 mg.

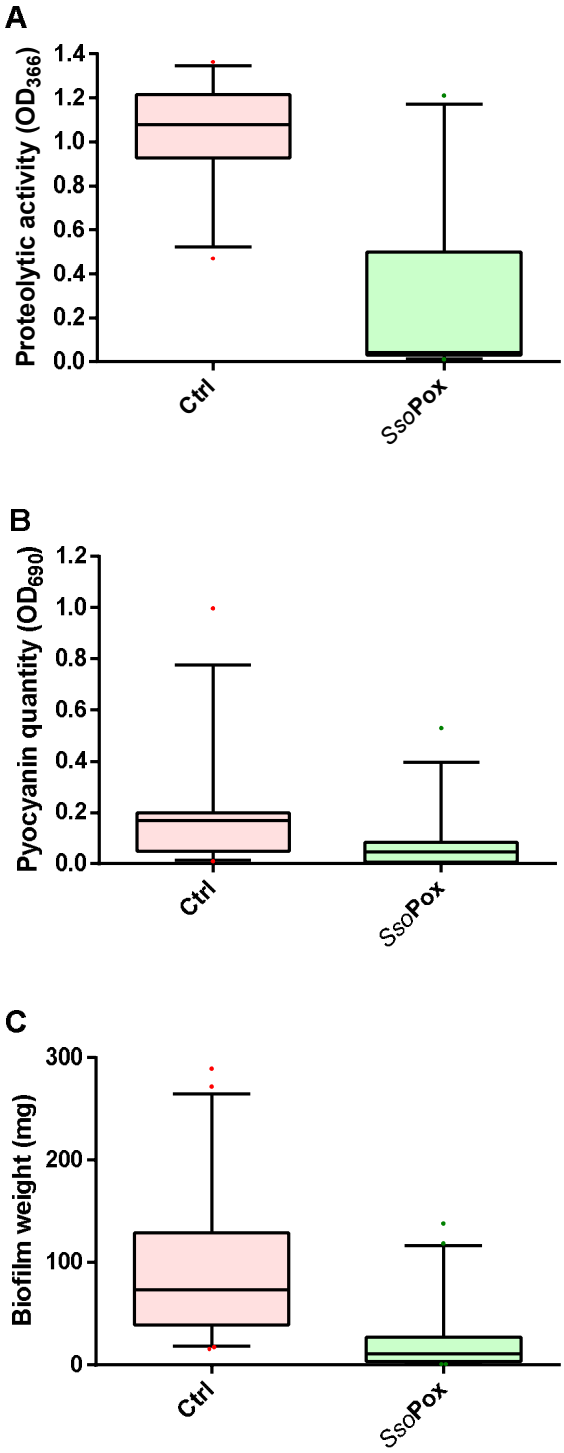


Figure 26 : Distribution plots of virulence factor values with and without quenching treatment of the 51 clinical isolates.

Values of proteolytic activity **(A)**, pyocyanin quantity **(B)** and biofilm formation **(C)** are shown as whiskers plots down to the 5th percentile and up to the 95th. Control samples (without enzyme) are shown in red while *Sso*Pox treated samples are in green. *Sso*Pox was added to cell cultures at a concentration of 0.5 mg.ml^{-1}. Points below and above the whiskers represent outlier values.

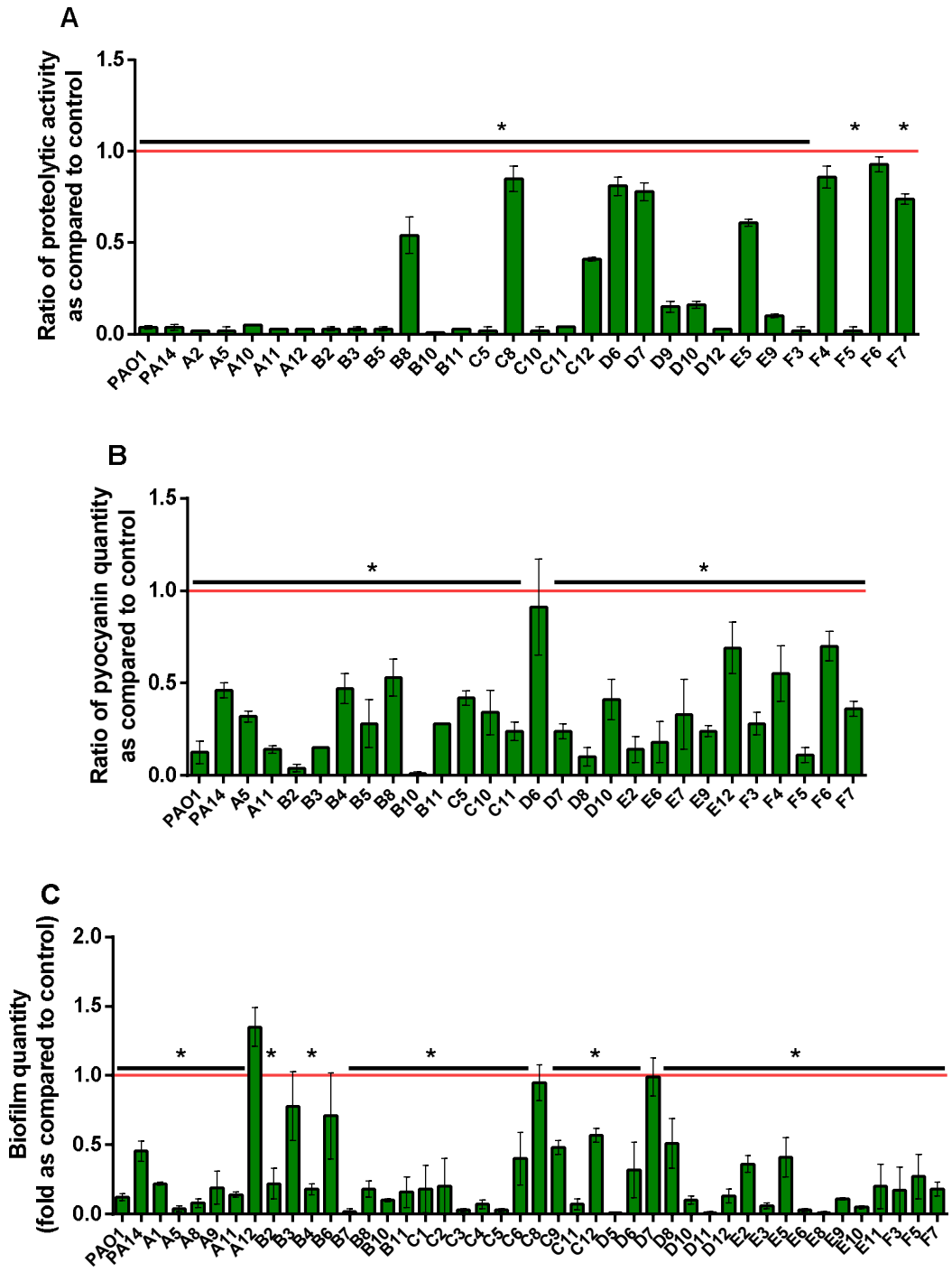


Figure 27 : Quenching of virulence factors using *Sso*Pox.

For each strain, bars represent the mean ratios of protease **(A)**, pyocyanin **(B)** and biofilm **(C)** levels between the treated culture with 0.5 mg.ml^{-1} *Sso*Pox versus the untreated culture of three experiments. Error bars represent the standard deviations of three replicated experiments. Stars indicate p-values<0.05 according to Student's t-test.

Comparison between *Sso*Pox and the QSI 5-FU and C-30

To compare quorum quenching potentials between *Sso*Pox and QSI molecules, the 16 clinical strains producing the three virulence factors were tested with 0.5 $mg.ml^{-1}$ *Sso*Pox, 30 µM C-30, 60 µM 5-FU and both QSI. Under our conditions, C-30 showed very little quorum quenching potential either with the model strains PAO1 and PA14 or with the clinical isolates **(Figure 28 and Supplementary Figure 16)**. Only five strains showed a slight decrease in protease production, the maximum decrease measured was 20 % for strain B2. Pyocyanin production was only reduced for two strains, B10 and B11, with ratios of 0.57 and 0.39 respectively. Concerning biofilm formation only one strain showed a statistically significant decrease with a ratio of 0.4 as compared to the control. More importantly, many strains showed significantly higher virulence factor production after treatment with C-30.

The results obtained using 5-FU indicated more quorum quenching activity than C-30 in these experimental conditions. Indeed, 7 strains out of 16 presented decreased proteolytic activity, two strains had decreased pyocyanin production and 10 strains formed less biofilm upon treatment with 5-FU. The combination of both QSI molecules did not lead to an increase in quenching potential as compared to the use of 5-FU alone. *Sso*Pox was the most active quorum quenching agent, reducing proteolytic activities in every strain tested, reducing pyocyanin production in all but one strain and reducing biofilm formation in 12 strains out of 16.

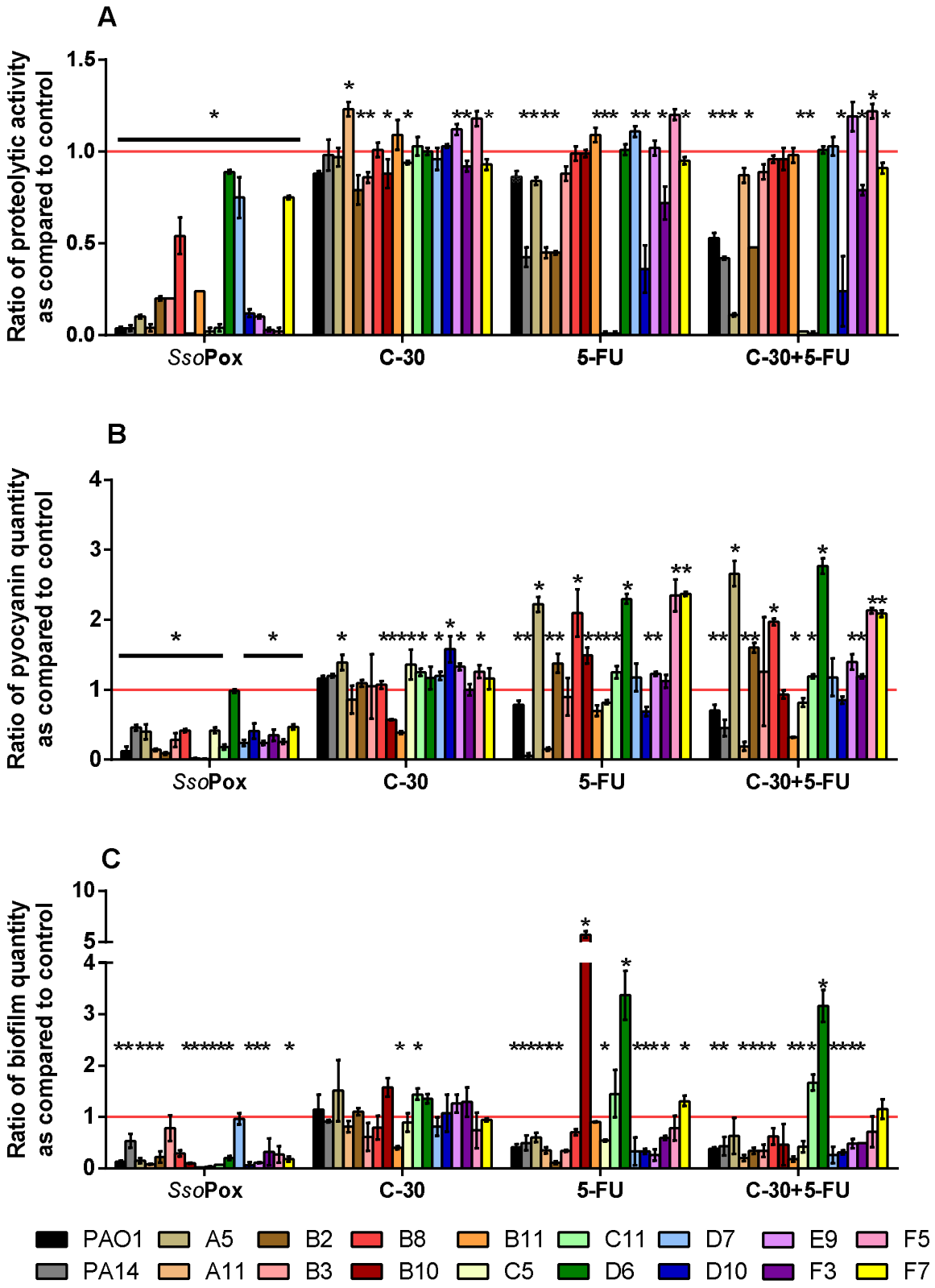


Figure 28 : Comparison of quenching by *Sso*Pox and QSI C-30 and 5-FU.

For each strain, bars represent the mean ratios of protease **(A)**, pyocyanin **(B)** and biofilm **(C)** levels between the treated culture with optimal concentrations of quorum quenching agents (0.5 mg.ml^{-1} *Sso*Pox, or 30 µM C-30 and/or 60 µM 5-FU) versus the untreated culture of three experiments. Error bars represent the standard deviations of three replicated experiments. Stars indicate p-values<0.05 according to Student's t-test.

Immobilisation

To prove the effectiveness of *Sso*Pox-W263I in medical device-like conditions, the enzyme was immobilised in a waterborne polyurethane coating with the cross-linking agent glutaraldehyde. The influence of the PU coating without enzyme on growth and virulence factor production of PAO1 model strain was assessed to ensure that PU did not have a major impact on bacterial metabolism **(Figure 29)**. Neither growth nor protease production differed. Pyocyanin and biofilm productions were slightly impacted with a decrease of pyocyanin production and an increase in biofilm formation. Despite these differences inherent to PU coating the impact of enzyme could be measured and quenching was successfully achieved. Indeed, in the same culture conditions as free enzymes, the immobilised *Sso*Pox was able to decrease pyocyanin production by 2.1, protease activity by 24 and biofilm quantity by 6.5 as compared to the control with polyurethane coating. Enzyme release was determined by measuring enzymatic activity of culture supernatants after 24 h of growth. No enzyme activity was detected in culture supernatants indicating that the immobilisation is effective and no enzyme is released after fixation. About 200 µg of active enzyme were detected in 25 cm² flask corresponding to a final concentration of 8-10 µg.cm^{-2}. In these conditions, the *Sso*Pox coating was effective in reducing significantly the production of all tested virulence factors.

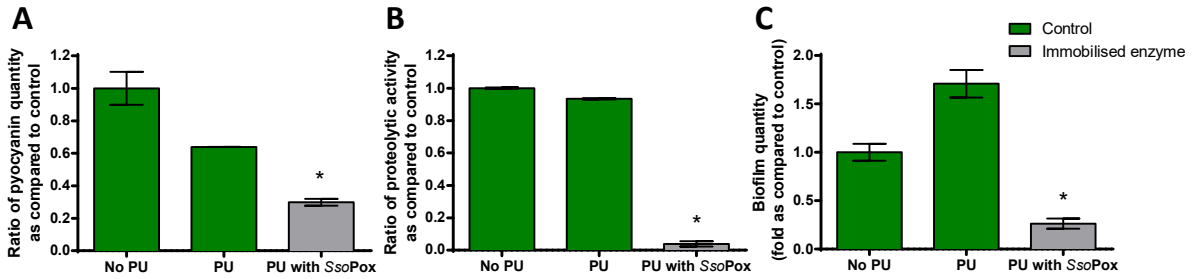


Figure 29 : Quenching P. aeruginosa PAO1 with enzyme immobilised in polyurethane (PU).
Bars represent the mean ratios of pyocyanin **(A)**, protease **(B)** and biofilm **(C)** levels between the treated culture with immobilised *Sso*Pox (PU with *Sso*Pox) versus the untreated culture containing a polyurethane coating (PU) or without coating (No PU). Error bars represent the standard deviations of two replicate experiments. Stars indicate p-values<0.05 according to Student's t-test using control with PU as reference.

4.4. Discussion

Foot ulcers are common in diabetic patients mainly due to arteriopathy and neuropathy. The risk of lower-extremity amputation for patients suffering from diabetes is up to 155 times higher than for non-diabetic people[226,227]. Diabetic foot ulcers are often polymicrobial, bacteria from various types can maintain a chronic infection on their own, or act synergistically in a pathogenic biofilm to cause infection. *P. aeruginosa* is one of the most frequent pathogens isolated in diabetic foot ulcers, particularly in warmer countries (Asia and Africa) where Gram-negative bacilli are more prevalent[228]. This bacterium has developed many strategies to counteract antimicrobial treatments such as antibiotics[229]. Biofilm formation[205], β-lactamases[230] and increased efflux rates[231] are part of the molecular arsenal that *P. aeruginosa* deploys to resist antibacterial agents, resulting in severe economic and health outcomes[232]. The quest for new therapeutic strategies to fight *P. aeruginosa* infections is highly challenging.

Remarkably, among the 51 strains assayed in this study, the clinical isolates of *P. aeruginosa* harboured distinct phenotypes with only 16 strains producing the three virulence factors as the model strains PAO1 and PA14. Most strains produced only one or two of the studied virulence factors in the conditions tested. In addition, the levels of each virulence factor were highly variable from one isolate to another. Such phenotypic variations have already been reported and underline the necessity to test potential therapeutic molecules on clinical isolates[233].

In this study, the ability of the lactonase variant *Sso*Pox-W263I to decrease virulence in clinical isolates of *P. aeruginosa* was evaluated. This variant was selected for an increased catalytic efficiency towards 3-oxo-C_{12} AHL (45-fold increase as compared to the wild-type enzyme) while maintaining a high thermostability (T_m=88°C). Three virulence factors were assayed: pyocyanin production, protease secretion and biofilm formation. *Sso*Pox-W263I was shown to drastically affect the synthesis of both virulence factors and biofilm while the QSI C-30 and 5-FU only showed moderate abilities, at their optimum dose, in the same conditions. These results were obtained *in vitro* using a rich medium in which bacterial growth is fast and without pre-treatment of the cultures with the QSI which could explain their poor activity. Notably, the use of 5-FU on PAO1 cultures led to a reduced growth rate of bacteria, possibly indicating some level of toxicity.

Even though *Sso*Pox targets, in principle, only one QS system used by *P. aeruginosa* its QQ potential was very effective. Proteolytic activity was decreased by at least half in 67 % of the strains, pyocyanin production in 68 % and biofilm in 82 %. The use of lactonases as biocontrol agents in bacterial infection therefore seems very promising. Moreover, upon lactonase treatment, no increase in proteolytic activity or pyocyanin production was noticed, only biofilm formation of one strain was slightly enhanced upon treatment with *Sso*Pox but was not statistically relevant. Conversely, the increase of virulence factor production after treatment with QSI molecules has already been reported, when clinical strains of *P. aeruginosa* isolated from cystic fibrosis patients were treated with C-30 and 5-FU and when isolates from diverse origins (urinary tract, wound infection, blood and respiratory tract) were exposed to natural inhibitors such as catechin, caffeine, curcumin and salicylic acid[224,225,234]. Similar observations are made in this study with several tested isolates after treatment with C-30 or 5-FU but never after treatment with *Sso*Pox, showing that *Sso*Pox does not induce any deleterious effect *in vitro* as compared to the QSI under the conditions used here.

Resistance of *P. aeruginosa* clinical isolates to QSI has previously been described[224,225,235]. The reported resistance mechanisms involved increased activity of antibiotic efflux pumps to move C-30 more efficiently out of the bacterial cell. Such mutations were obtained *in vitro* by evolving a model strain in the presence of C-30. They were also identified in natural isolates that had never been challenged with C-30. Other reported mutations induce a reduced uptake of C-30[236]. Nevertheless such mutant strains would not show any resistance to *Sso*Pox quenching potential as the enzyme neither enters the bacteria nor binds to a cellular receptor. Even though no growth delay was observed using *Sso*Pox, suggesting no or very low selection pressure, other resistance mechanisms could appear. Bacteria could increase AHL production, produce an enzyme inhibitor, or modify the AHL molecule to prevent its recognition by the enzyme. However AHL overproduction would represent a significant metabolic cost that would decrease the bacterial fitness in non selective environments. Modifying the AHL molecules would involve several mutations, first at the level of the synthase then at the level of the receptor. Furthermore, such resistance mechanisms could be easily circumvented by increasing the amount of enzyme or by broadening its spectrum to target more diverse AHL molecules.

Lastly, *Sso*Pox was successfully immobilised in the cultivation flasks using polyurethane and glutaraldehyde. Under these conditions the enzyme was still active and quorum quenching was achieved with a reduction of each virulence factor tested. In addition, no release of the enzyme was measured. Other enzymes have already been described and successfully used to quench *P. aeruginosa*. For example acylases from *Pectobacterium atrosepticum* and *Agrobacterium tumefaciens* have been used to degrade AHL from *P. aeruginosa*[237]. Even though the acylases efficiently decreased PAO1 virulence factor production, the stability of these enzymes at high temperatures (above 60°C) was really poor offering a limited industrial potential. The acylase from *Aspergillus meleus* was immobilized in coatings and decreased *P. aeruginosa* biofilm formation[238,239]. Nevertheless these reports do not mention the industrial potential of such enzymes regarding their stability and tolerance to solvents, temperature and bacterial secretions. Regarding the use of lactonases as QQ agents, MomL, a lactonase produced by the marine bacterium *Muricauda olearia* was showed to degrade AHL *in vitro* and to decrease virulence of *P. aeruginosa* PAO1[240]. To our knowledge, unlike QSI no QQ enzyme was tested on a wide range of clinical isolates but only on model strains which behaviours differ from natural isolates. The biochemical characteristics of *Sso*Pox-W263I have already been assessed and reported[113,220]. The data presented here, together with the high resistance of *Sso*Pox and its potential to meet industrial constraints, open the way to incorporating *Sso*Pox in medical devices such as functionalised catheters and anti-virulence dressings. To fully assess the quenching potential of *Sso*Pox and its effect on virulence, infection models should be used.

Acknowledgements

This work is granted by a project RAPID (LACTO-TEX) from Direction Générale de l'Armement (DGA, France). B. Rémy is a Ph.D student granted by the "Emplois Jeunes Doctorants" program of Région Provence-Alpes-Côte d'Azur (PACA, France). J. Bzdrenga and P. Jacquet are Ph.D students granted by Direction Générale de l'Armement (DGA).

Conflict of Interest Statement

M. Elias and E. Chabrière have a patent WO2014167140 A1 licensed to Gene&GreenTK.
L. Plener, D. Daudé, M. Elias and E. Chabrière report personal fees from Gene&GreenTK during the conduct of the study.

III. Conclusions et perspectives

III. Conclusions et perspectives

Au cours de ces travaux, la compréhension et l'amélioration d'une enzyme possédant plusieurs activités catalytiques ont permis de mettre au point des biocatalyseurs performants et d'en évaluer le potentiel *in vitro* et *in vivo*.

Conclusions

Les enzymes peuvent être améliorées suivant différents procédés tels que l'évolution rationnelle, semi-rationnelle ou dirigée[241,242]. Il s'agit le plus souvent de réaliser un compromis entre connaissance des relations séquence/structure/fonction et capacité de criblage. Ici, des "small but smart libraries"[243] ont été générées et ont permis d'obtenir des améliorations très significatives en criblant un nombre limité de variants. Deux tours d'évolution ont donné lieu à la synthèse d'une vingtaine de variants, ayant des profils d'action différents améliorés sur les pesticides, les analogues d'agents neurotoxiques de guerre, les arylesters et/ou les lactones. Ces variants ont conservé une stabilité thermique importante, bien que diminuée de 10°C pour le variant le plus stable (*Sso*Pox-IIIC1) à 37°C pour le variant le moins stable (*Sso*Pox-αsB5-W263M) par rapport à l'enzyme sauvage. Ceci montre une nouvelle fois que les enzymes hyperthermostables sont de très bons candidats pour l'évolution car leur grande robustesse leur permet de tolérer un nombre important de mutations potentiellement déstabilisantes.

Le premier tour d'évolution a permis d'obtenir des variants comme *Sso*Pox-αsD6 ou *Sso*Pox-αsB5, qui ont des spectres d'action larges sur les pesticides. En effet ces deux variants sont efficaces sur dix pesticides, contre quatre pour l'enzyme sauvage, avec des efficacités catalytiques allant de 10^1 à 10^4 $M^{-1}.s^{-1}$. De plus, on observe une grande diversité dans la structure des substrats reconnus certains possédant des liaisons P-S ou P-O (malathion et chlorpyrifos) ou encore des formes oxono ou thiono-OP (paraoxon et parathion). Ces variants tolèrent une grande diversité au niveau des groupes partants des substrats et sont capables d'accommoder des structures aussi diverses que des groupements phényles fonctionnalisés, pyridines ou coumariques. Certains variants comme *Sso*Pox-αsA6 et *Sso*Pox-αsC6 sont, quant à eux, améliorés sur les lactones undécanoïques montrant que les mutations incorporées jouent un rôle crucial dans la modulation des activités de promiscuité. En parallèle, l'association des mutations du variant *Sso*Pox-αsB5 avec une dégénération sur la position W263, préalablement identifiée comme jouant un rôle primordial dans l'activité de l'enzyme, a été réalisée. Cependant ces combinaisons ont donné lieu à une épistasie négative, avec des variants ayant des capacités d'hydrolyses inférieures à *Sso*Pox-αsB5. Pour l'ensemble des variants au niveau structural, leurs sites actifs sont élargis et la mobilité de la boucle 8 est augmentée ce qui a pour conséquence une réorientation du dimère. Ces modifications structurales peuvent expliquer l'élargissement du spectre d'action des variants. A l'issue de ce tour d'évolution, les différents variants obtenus ont une activité phosphotriestérase globalement améliorée et avec des effets modérés sur l'activité lactonase.

Un second tour d'évolution a par la suite été réalisé afin d'améliorer l'activité phosphotriestérase de l'enzyme et de mieux comprendre l'impact des mutations sur sa promiscuité catalytique. Un affinement du design a été réalisé et les mutations délétères pour l'activité

phosphotriestérase ont été purgées grâce à un criblage solide d'activité. Douze variants présentant des propriétés améliorées ont été plus amplement étudiés. Ainsi le meilleur variant de *Sso*Pox sur éthyl-paraoxon obtenu à ce jour, *Sso*Pox-IVB10, a été caractérisé et montre une activité catalytique de 2.75×10^5 $M^{-1}.s^{-1}$. L'impact de ces modifications sur l'activité de promiscuité a été évalué sur des substrats lactone et arylester. L'activité lactonase s'est montré globalement diminuée par rapport à l'enzyme sauvage avec peu voire pas d'activité sur les oxo-lactones (par exemple pour les variants *Sso*Pox-IVB10 et *Sso*Pox-IIIC1). Des améliorations dans l'activité arylesterase ont néanmoins pu être mises en évidence, par exemple pour le variant *Sso*Pox-IG7 qui conserve une activité phosphotriestérase similaire à l'enzyme sauvage mais une amélioration d'un facteur 5 sur *p*NP acétate. Il semble donc que l'amélioration de l'activité phosphotriestérase se fasse au détriment de l'activité lactonase et que l'augmentation de l'activité arylester n'affecte pas nécessairement l'activité phosphotriestérase. De plus, lors du second tour, l'efficacité des variants sur des analogues d'agents neurotoxiques de guerre a été déterminée. Certains sont très prometteurs comme *Sso*Pox-IVE2 et *Sso*Pox-IIIC1, et montrent des profils d'activité différents. En effet, *Sso*Pox-IVE2 est peu actif sur les insecticides éthyl-paraoxon et éthyl-parathion mais est particulièrement efficace sur les analogues des CWAs (tels que le sarin, cyclosarin et VX) alors que *Sso*Pox-IIIC1 se distingue seulement sur certains analogues des CWAs (comme le tabun) et l'éthyl-paraoxon. Pour finir, les meilleurs variants du second tour ont un effet protecteur de la rAChE contre l'éthyl-paraoxon, en effet l'activité acétylcholinestérase est protégée après seulement quelques minutes d'action. Lors de ce second tour, l'affinement des paramètres expérimentaux a permis d'obtenir des variants spécialisés pour l'activité phosphotriestérase, pour les pesticides ou les analogues des CWAs, ces améliorations se faisant au détriment de l'activité native lactonase. En parallèle, l'ensemble des variants obtenus au cours des deux tours d'évolution ont été testés sur les agents réels dans le cadre d'un projet DANUBE financé par la DGA certains se montrant très efficace pour la dégradation du tabun.

Dans le but de mettre en évidence le potentiel de *Sso*Pox pour la décontamination des pesticides, la capacité de biodécontamination du meilleur variant phosphotriestérase (*Sso*Pox-αsD6) a été évaluée *in vivo* chez la planaire pour quatre pesticides. La planaire est un ver d'eau douce qui permet, à l'instar des autres modèles animaux, d'évaluer la toxicité d'une substance mais il permet également d'observer son impact sur le développement. En effet, la planaire, constituée à 20-30% de cellules souches pluripotentes, possède la propriété de se régénérer à partir d'un fragment de tissu et constitue un excellent modèle de développement[244]. Ainsi, outre le suivi de mortalité, nous avons pu étudier l'impact des pesticides sur la régénération de ce ver. Cette étude a permis de confirmer que les pesticides sont toxiques pour *S. mediterranea* et plus particulièrement l'éthyl-paraoxon qui est hautement toxique pour la planaire. Après décontamination par l'enzyme, la mortalité des planaires s'est révélée largement diminuée. Il en va de même pour la régénération des planaires qui, est largement améliorée après dégradation des insecticides. Les produits d'hydrolyse générés par action de l'enzyme sont donc moins toxiques que les pesticides dont ils sont issus ce qui souligne le fort potentiel des enzymes pour la bioremédiation des insecticides.

Enfin, des travaux préalablement réalisés au laboratoire ont permis d'obtenir un variant (*Sso*Pox-W263I) particulièrement efficace pour la dégradation des lactones. Ce dernier a donc été considéré pour lutter contre la virulence bactérienne en inhibant le QS chez *Pseudomonas aeruginosa*. L'effet anti-QS de l'enzyme a été confirmé sur 51 souches cliniques de *P. aeruginosa* isolées du pied diabétique. *Sso*Pox est efficace pour réduire la production de pyocyanine, des protéases et la formation du biofilm. De plus, les effets anti-QS de *Sso*Pox, dans les conditions étudiées sont biens

meilleurs que deux autres inhibiteurs du QS largement décrits dans la littérature, C-30 et 5-FU. Dans l'optique d'utiliser l'enzyme pour des applications médicales, les effets QQ de l'enzyme immobilisée dans du polyuréthane ont été évalués. Ainsi, l'enzyme immobilisée ne perd pas son activité lactonase, ni ses effets anti-QS sur PAO1. Ces résultats sont une base pour aller plus loin avec l'utilisation de *Sso*Pox comme agent anti-virulence, par exemple pour des applications médicales.

Pour conclure, *Sso*Pox est un candidat de choix pour l'évolution dirigée ainsi que pour une utilisation industrielle, de par sa stabilité thermique et sa résistance à de nombreux détergents et solvants cette enzyme peut être considérée pour une large gamme d'applications biotechnologiques. Cette thèse m'a permis de participer à un projet de recherche global, depuis l'ingénierie protéique de l'enzyme jusqu'aux applications possibles des meilleurs variants obtenus grâce au travail en collaboration avec la société Gene&GreenTK.

Perspectives

Ces travaux ouvrent la voie à un large panel de possibilités pour la dégradation des OPs en utilisant *Sso*Pox. Une possibilité serait de poursuivre les travaux sur l'évolution dirigée semi-rationnelle de *Sso*Pox, en continuant d'affiner la banque mutationnelle. Néanmoins, cette technique a quelques limitations, les meilleures améliorations ont lieu au niveau des premiers tours au bout d'un certain nombre de tours d'évolution un plateau est atteint pour l'amélioration[245]. Par exemple sur l'évolution dirigée d'une PTE transformée en arylesterase réalisée en 18 tours d'évolution les variants à partir du tour six sont beaucoup moins améliorés[246]. Donc il est possible de faire encore quelques tours pour améliorer l'activité phosphotriestérase sur les pesticides mais il ne semble pas utile d'aller aussi loin que 18 tours d'évolution. En revanche pour la dégradation des CWAs, il reste une énorme marge de possibilité, *Sso*Pox étant uniquement actif pour la dégradation du tabun. Cependant l'évolution dirigée de *Sso*Pox pour dégrader les CWAs nécessitera des efforts conséquents puisque la création d'activité est généralement plus délicate que l'amélioration d'une activité préexistante.

Une autre approche pour la dégradation des OPs, et notamment des CWAs, serait d'utiliser la phosphotriestérase bactérienne, *Bd*PTE, moins stable que *Sso*Pox mais déjà optimisée pour hydrolyser les OPs, dont le VX, sarin, soman ou encore le cyclosarin[247]. Un processus inverse à celui employé pour *Sso*Pox pourrait être utilisé pour cette fois stabiliser *Bd*PTE. Encore une fois plusieurs possibilités sont envisageables, une stratégie d'évolution dirigée couplée à un criblage phénotypique pourrait être considérée pour sélectionner des mutations stabilisatrices[248]. La reconstruction des protéines ancestrales (ancestral protein reconstruction, APR) est également souvent utilisée pour améliorer la stabilité des enzymes[249,250]. Cette méthode permet de déterminer des séquences protéiques ancestrales en utilisant des méthodes statistiques de phylogénie se basant sur les séquences actuelles des protéines à améliorer[251]. Cette technique est souvent plus rapide que l'évolution dirigée et a un fort potentiel pour améliorer des protéines, comme augmenter l'activité d'une enzyme, sa stabilité thermique ou encore sa solubilité. La reconstruction ancestrale a ainsi permis la résurrection de β-lactamases précambriennes, enzymes hydrolysant les antibiotiques ayant un cycle β-lactame, possédant des propriétés largement améliorées. L'enzyme moderne a un T_m de 55°C et un k_{cat}/K_M de 2.6×10^3 $M^{-1}.s^{-1}$ pour le céfotaxime, alors qu'un ancêtre obtenu par APR a un T_m de 90°C et un k_{cat}/K_M de 1.2×10^6 $M^{-1}.s^{-1}$ pour le même substrat[252]. De plus, cette technique permet également d'améliorer

la solubilité d'une protéine, comme par exemple avec la production de la HPBP (human phosphate-binding protein) ancestrale bien plus soluble que l'enzyme moderne, 12 mg d'enzyme ancestrale purifiée ont été obtenus alors que l'enzyme moderne n'a pu être purifiée à cause de la formation d'agrégats[253]. Ainsi cette technique a été mise en œuvre pour améliorer la stabilité de *Bd*PTE. Les résultats suivant ont été obtenus récemment et font l'objet d'un dépôt de brevet. L'ancêtre de *Bd*PTE obtenu est plus stable et plus actif que l'enzyme moderne. En outre, la formulation de cet ancêtre a été optimisée pour améliorer sa stabilité de stockage, en ajoutant un détergent et en utilisant la lyophilisation. Des résultats prometteurs ont été obtenus avec une stabilité de stockage de l'enzyme lyophilisée d'au moins 3 mois. Cette technique a également été appliquée sur *Sso*Pox dans l'optique d'améliorer son activité sur les CWAs. Des ancêtres de *Sso*Pox ont été réalisés, ils sont en cours de caractérisation. Cependant cette méthode a aussi ses limitations par exemple l'activité enzymatique n'est pas toujours augmentée[252]. C'est pourquoi, une combinaison d'évolution dirigée et de reconstruction de protéines ancestrales peut aussi être envisageable pour maximiser les probabilités d'obtenir des enzymes thermostables et des activités améliorées[254]. Par ailleurs, l'évolution dirigée et/ou la reconstruction des protéines ancestrales pourrait être mises en œuvre pour améliorer l'activité lactonase de *Sso*Pox pour obtenir des variants à large spectre sur les lactones.

Concernant les applications possibles pour la décontamination externe des OPs, de nombreuses perspectives sont envisageables allant de l'incorporation de l'enzyme dans des tissus décontaminants, dans des mousses de décontaminations ou une utilisation pour la bioremédiation en champ. De plus une perspective plus lointaine serait de passer de la décontamination externe vers la prophylaxie pour protéger les personnes d'intoxication aux OPs. Par exemple en encapsulant l'enzyme dans des liposomes ou en utilisant la pegylation pour éviter une réaction immunitaire en cas d'injection de l'enzyme[255,256]. Ces enzymes pourraient également trouver des applications pour la détection des OPs, en ajoutant les enzymes dans des capteurs ou bio-senseurs permettant de détecter les intoxications aux OPs et de déterminer l'agent incriminé. Une collaboration a récemment été démarrée avec l'université de Rome pour l'élaboration de tels capteurs.

Pour finir, les perspectives concernant la partie lactonase sont également vastes. L'évaluation du spectre d'action sur d'autres souches que *P. aeruginosa* comme *Acinetobacter baumannii* ou *Burkholderia* sp. pourrait permettre de déterminer le potentiel anti-virulent de l'enzyme. L'effet anti-virulence ou anti-biofilm de l'enzyme avec des inocula multi-bactériens, issus de l'environnement ou de prélèvements cliniques pourrait également être étudié. Des essais sur des modèles *in vivo* d'infections sont aussi à étudier et pourraient constituer une première phase préclinique. L'évaluation de l'action combinée de l'enzyme avec des antibiotiques pour lutter contre les infections bactériennes pourra également être considérée.

La possibilité d'intégrer l'enzyme dans des dispositifs médicaux, tels que des pansements, des cathéters ou des systèmes de filtration est également prometteuse. Enfin l'incorporation de l'enzyme dans des peintures anti-fouling pour limiter l'agrégation de matériel biologique sur les coques de bateaux constitue un champ d'application prometteur compte tenu du fort impact économique de ce phénomène à l'échelle mondiale. Là encore la forte résistance de l'enzyme à de nombreux solvants, à la température et sa grande durée de vie constitueront un atout pour le développement.

*Sso*Pox par sa promiscuité catalytique et sa haute stabilité apparait comme un candidat de choix pour de nombreuses applications biotechnologiques dans des domaines variés allant de la défense à l'anti-fouling en passant par la bioremédiation et les dispositifs médicaux.

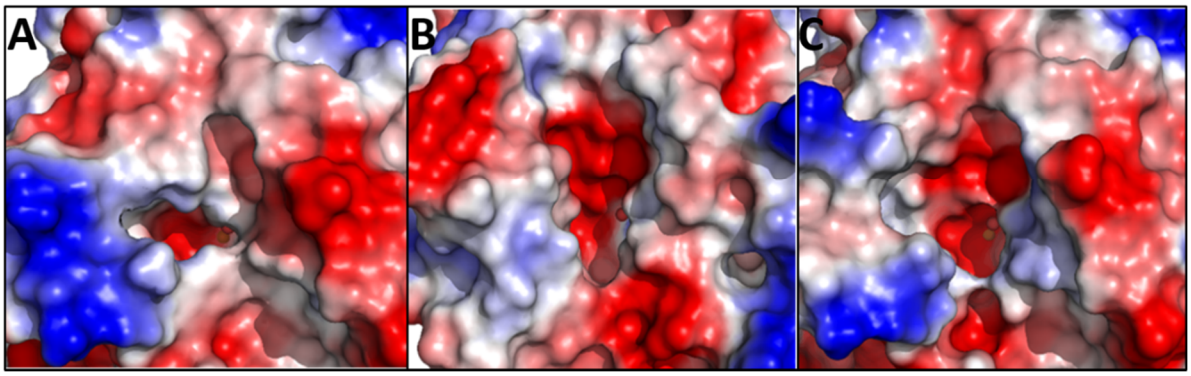
IV. Annexes

1. Données supplémentaires du projet de recherche

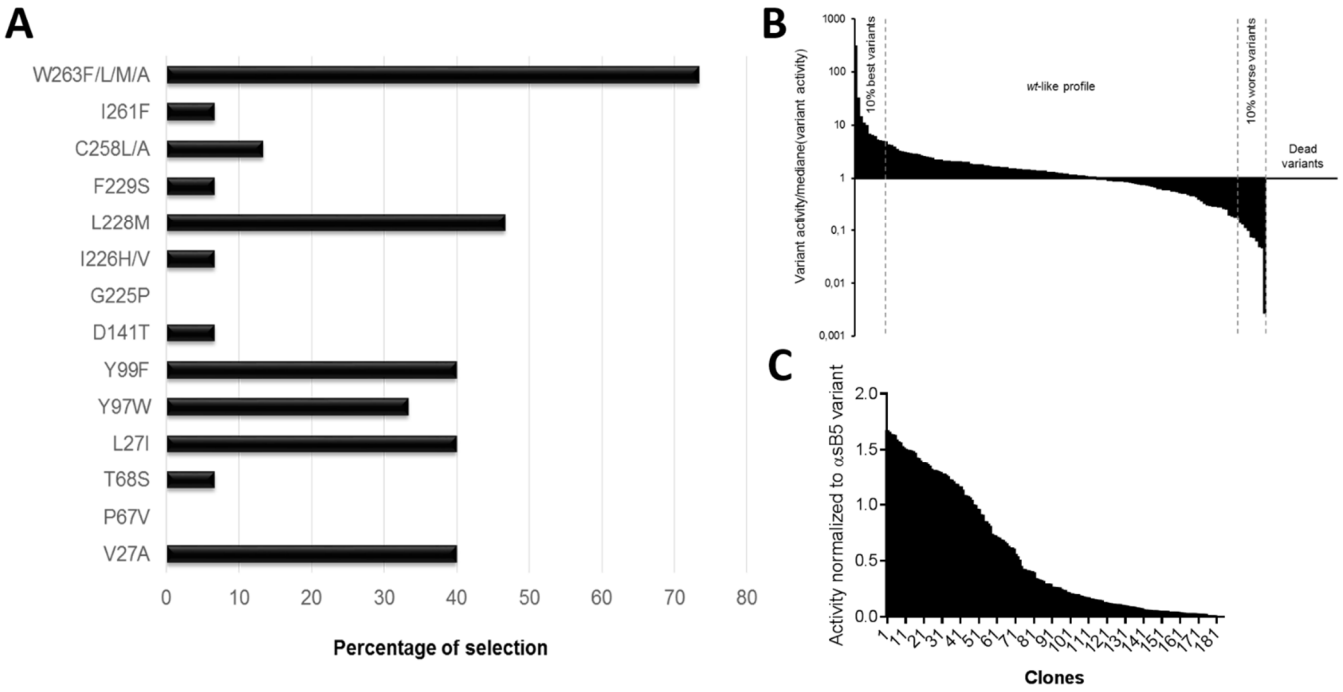
IV. Annexes

1. Données supplémentaires du projet de recherche

1.1. Partie 1 : Ingénierie rationnelle d'une lactonase native hyperthermostable en phosphotriestérase à large spectre

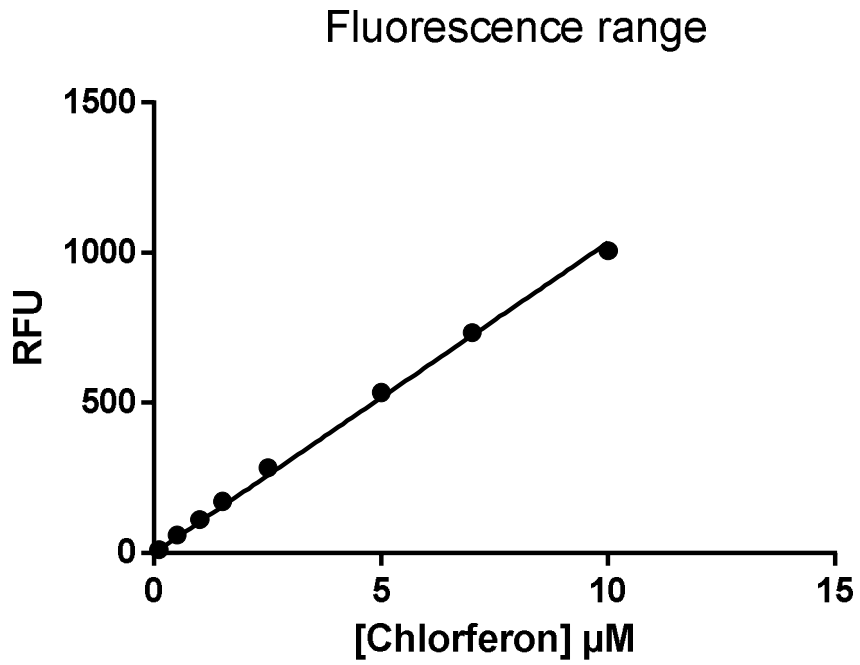


Supplementary Figure 1 : Structure-based active site cavity redesign.
Active site cavity view of **(A)** wt *Sso*Pox, **(B)** *Bd*PTE and **(C)** *Sso*Pox modelled with all 14 designed mutations **(Supplementary Table 1)**. The mutations modelled were constructed *in silico* and energy was minimized using *Swiss PDB viewer*[257]. Electrostatic potentials were calculated using PyMOL[17] and are shown on the molecular surface. Electrostatic potentials are represented at the enzyme's surfaces. Blue, red and white indicates positively-, negatively-, and neutrally-charged areas, respectively.



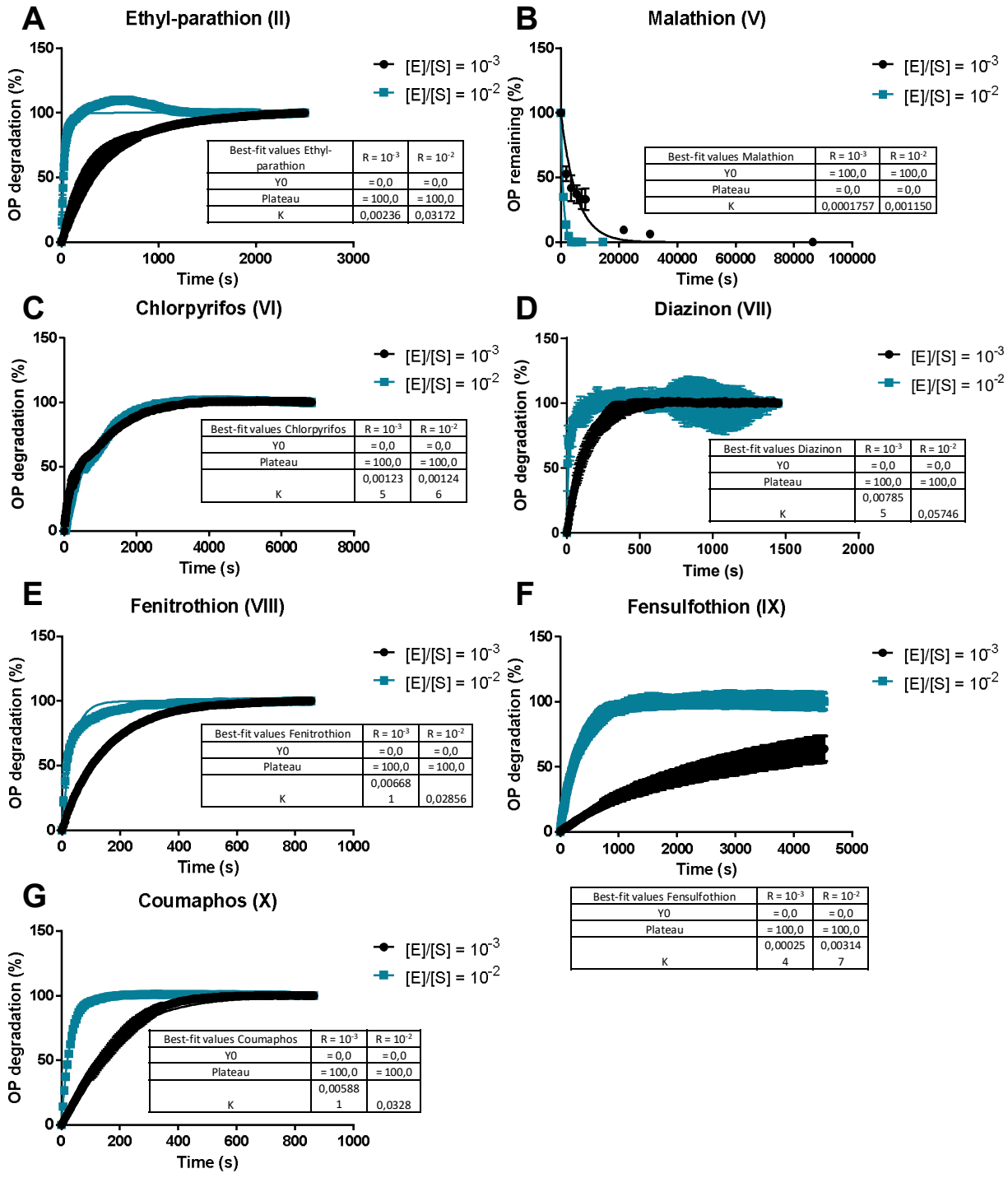
Supplementary Figure 2 : Library screening data.

(A) Occurrence of mutations in the 14 best sequenced clones. **(B)** Screening profile of the combinatorial mutation library (184 clones) with paraoxon as a substrate. Activities ($mOD_{405nm}.min^{-1}$) were normalized to the median value. **(C)** Screening of the position 263 saturation library (αsB5 background) with paraoxon as the substrate. Activity was normalized to αsB5 paraoxonase activity.

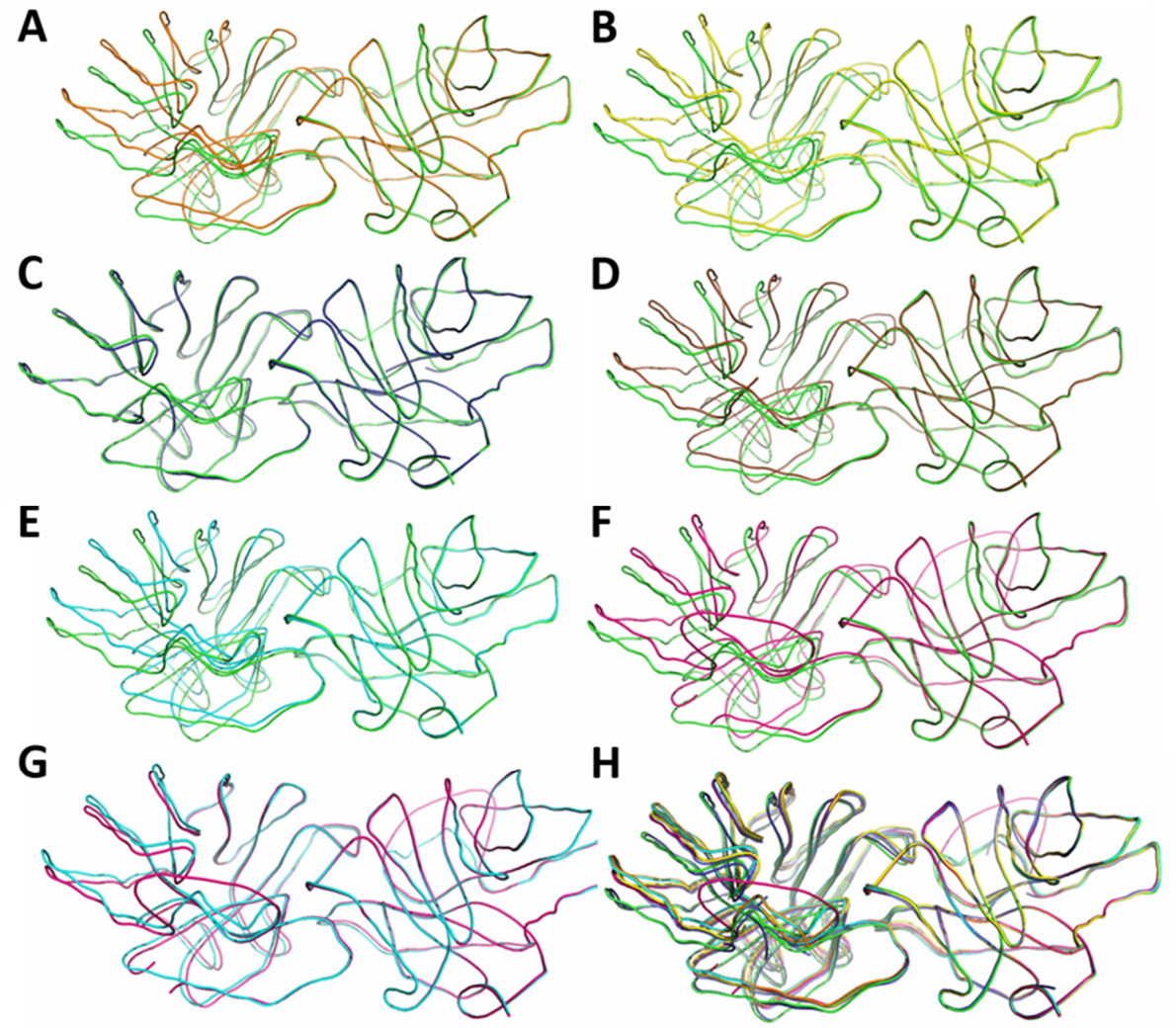


Best-fit values	
Slope	103,3 ± 0,6551
Equation	Y = 103,3*X - 0,0
R^2	0.9975

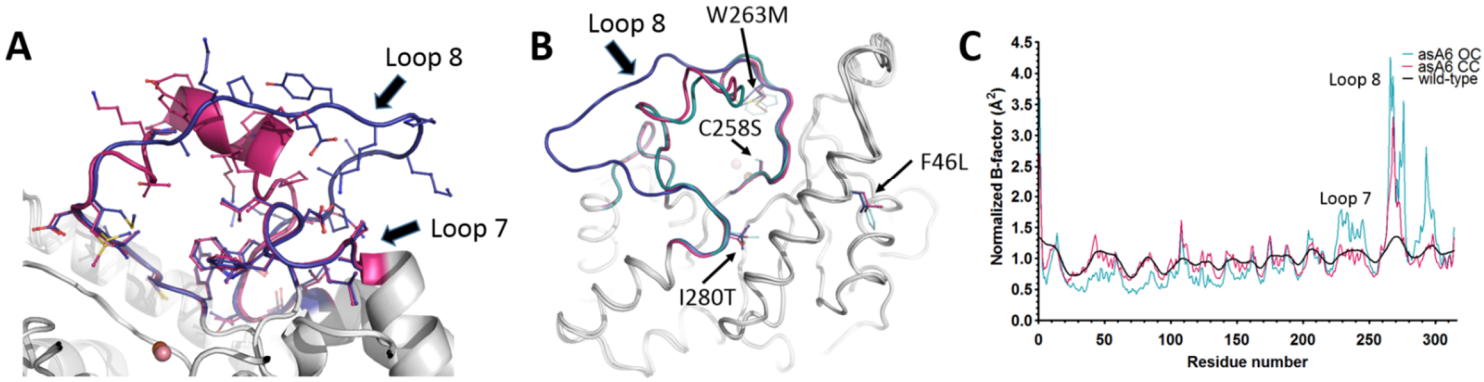
Supplementary Figure 3 : Chlorferon vs Fluorescence (360 (40) / 460 (40)) range of linearity.



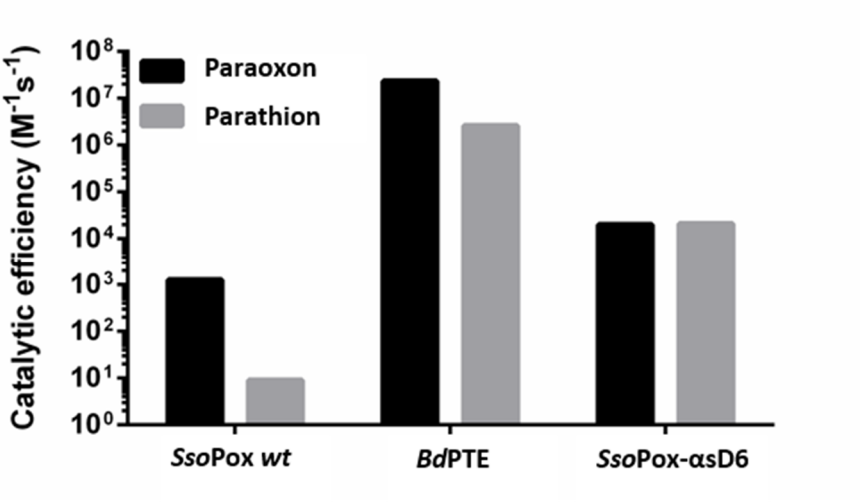
Supplementary Figure 4 : Bioremediation of organophosphorus insecticides (250 µM).



Supplementary Figure 5 : Structural superposition of wt-*Sso*Pox and mutants dimers.
The monomers on the right were superimposed, and the difference with the left monomers indicates the relative reorientation of dimerized monomers. **(A)** Superposition of wt-*Sso*Pox (green) and αsA1 (orange). **(B)** Superposition of wt-*Sso*Pox (green) and αsB5 (yellow). **(C)** Superposition of wt-*Sso*Pox (green) and αsC6 (blue). **(D)** Superposition of wt-*Sso*Pox (green) and αsD6 (brown). **(E)** Superposition of wt-*Sso*Pox (green) and αsA6-CC (cyan). **(F)** Superposition of wt-*Sso*Pox (green) and αsA6-OC (magenta). **(G)** Superposition of αsA6-OC (magenta) and αsA6-CC (cyan). **(H)** Superposition of wt-*Sso*Pox (green), αsA1 (orange), αsB5 (yellow), αsD6 (brown), αsC6 (blue), αsA6-OC (magenta) and αsA6-CC (cyan).



Supplementary Figure 6 : Mutant αsA6 loop-8 conformational flexibility.
(A) Superposition of the open conformation (OC, blue) and the closed conformation (CC, magenta), of loop 8 in two distinct mutant αsA6 crystal structures. **(B)** Location of the four mutations of mutant αsA6 in the structure. The wt-*Sso*Pox, the CC, and the OC loop 8 conformations are shown in green, magenta and blue, respectively. We note that I280T and C258S are located at the very beginning and end of loop 8. **(C)** Positional distributions of normalized B-factor values (the x-axis represents residue number) for wt-*Sso*Pox (black line), αsA6-OC (blue line) and (magenta line).



Supplementary Figure 7 : Thiono-effect in *Sso*Pox.
Catalytic efficiencies of enzymes, *Sso*Pox, *Bd*PTE and *Sso*Pox-αsD6 with methyl-paraoxon (black) and methyl-parathion (gray) as substrates are shown.

Supplementary Table 1 : Mutation database.

	*Sso*Pox position	Corresponding position in *Bd*PTE	Redesign	Additional mutations	Mutations in database
First set of mutations	V27	G60	-	-	V27A
	P67	V101	-	-	P67V
	T68	S102	-	-	T68S
	L72	I106	-	-	L72I
	Y97	W131	-	-	Y97W
	D141	T173	-	-	D141T
	G225	P256	-	-	G225P
	L226	H257	-	-	L226H
	C258	L303	-	A	C258/A-L
	I261	F306	-	-	I261F
Second set of mutations	Y99	-	F	-	Y99F
	L228	-	M	-	L228M
	F229	-	S	-	F229S
	W263	-	A	Saturation	W263/All

Supplementary Table 2 : Oligonucleotide sequences used in this study.

	Primer name		Primer sequence
Clonage	T7-prom		TAA TAC GAC TCA CTA TAG GG
	pET-RP		GCT AGT TAT TGC TCA GCG G
	*Sso*Pox-lib-pET-5'		CAT GCC ATG GCG CGC ATT CCG CTG GTT GGT AAA G
	*Sso*Pox-lib-pET-3'		AAG GAA AAA AGC GGC CGC TTA TTA GCT AAA GAA TTT TTT CGG ATT TTC
Primer name		**Encoding variation**	**Primer sequence**
Primers used in ISOR protocol	SP1	V27A	GAA CAT CTG CGT **GCA** TTT AGC GAA GCA GTT
	SP2	P67V-T68S	AAA ACC ATT GTT GAT **GTG AGT** GTT ATG GGT
	SP3	P67V	AAA ACC ATT GTT GAT **GTG** ACC GTT ATG GGT
	SP4	T68S	AAA ACC ATT GTT GAT CCG **AGT** GTT ATG GGT
	SP5	L72I	GTT ATG GGT **ATT** GGT CGT GAT ATT CGT TTT
	SP6	Y97W-Y99F	GGC ACC GGT ATT **TGG** ATT **TTT** ATC GAT CTG CCG
	SP7	Y97W	GGC ACC GGT ATT **TGG** ATT TAT ATC GAT CTG CCG
	SP8	Y99F	GGC ACC GGT ATT TAT ATT **TTT** ATC GAT CTG CCG
	SP9	D141T	AAA ATT GCA GCC **ACC** GAA CCG GGT ATT ACC
	SP10	L226H-228L/M-229F/S	GAT CGT TAT GGT **CAC** GAC **MTG TYT** CTG CCG GTT
	SP11	L226V-228L/M-229F/S	GAT CGT TAT GGT **GTG** GAC **MTG TYT** CTG CCG GTT
	SP12	G225P-228L/M-229F/S	GAT CGT TAT **CCG** CTG GAC **MTG TYT** CTG CCG GTT
	SP13	G225P-L226H-228L/M-229F/S	GAT CGT TAT **CCG CAC** GAC **MTG TYT** CTG CCG GTT
	SP14	G225P-L226V-228L/M-229F/S	GAT CGT TAT **CCG GTG** GAC **MTG TYT** CTG CCG GTT
	SP15	228L/M-229F/S	GAT CGT TAT GGT CTG GAC **MTG TYT** CTG CCG GTT
	SP16	C258L	ATT AGC CAT GAT TAT **CTG** TGC ACC ATT GAT
	SP17	C258A	ATT AGC CAT GAT TAT **GCC** TGC ACC ATT GAT
	SP18	I261F	GAT TAT TGC TGC ACC **TTT** GAT TGG GGC ACC
	SP19	W263F	TGC ACC ATT GAT **TTT** GGC ACC GCA AAA CCG
	SP20	W263M	TGC ACC ATT GAT **ATG** GGC ACC GCA AAA CCG
	SP21	W263L	TGC ACC ATT GAT **CTG** GGC ACC GCA AAA CCG
	SP22	W263A	TGC ACC ATT GAT **GCG** GGC ACC GCA AAA CCG

Supplementary Table 3 : Selected positions for phosphotriesterase activity improvement.

Position	27	67	68	72	97	99	141	225	226	228	229	258	261	263	Additional	Total variations
wt	V	P	T	L	Y	Y	D	G	I	L	F	C	I	W		
B3	A			I	W					M						V27A/L72I/Y97W/L228M
F2										M				L		L228M/W263L
F8				I										M	K54I	K54I/L72I/W263M
B2	A			I		F	T			M				M	G7S/V28A	G7S/V27A/V83A/L72I/Y99F/D141T/L228M/ W263M
H8			S		W	F				M						T68S/Y97W/Y99F/L228M/
E3	A			I										M	V83A/E173T	V27A/L72I/V83A/E173T/W263M
A4						F				M				M	G193S	Y99F/G193S/L228M/W263M
A1												L	F	A		C258L/I261F/W263A
A6												A		M	F46L/I280T	F46L/C258A/W263M/I280T
B5	A				W	F			V						I76T/L130P	V27A/I76T/Y97W/Y99F/L130P/L226V
C6				I		F				M	S			L	I122L	L72I/Y99F/I122L/L228M/F229S/W263L
D6	A				W					M				M		V27A/Y97W/L228M/W263M
D1					W											Y97W
D5				I										F		L72I/W263F
A5	A					F								L		V27A/L72I/Y99F/W263L
Incorporation	6	0	1	6	5	6	1	0	1	7	1	2	1	11		
Ratio	0.4	0	0.07	0.4	0.33	0.4	0.07	0	0.07	0.47	0.07	0.13	0.07	0.73		

Supplementary Table 4 : T_m values of *Sso*Pox variants.

Enzyme	Mutations	T_m (°C)
wt	*	106
αsD6	V27A/Y97W/L228M/W263M	82.5 ± 1,8
αsB5	V27A/I76T/Y97W/Y99F/L130P/L226V	70.4 ± 3,1
αsB5 W263M	V27A/I76T/Y97W/Y99F/L130P/L226V/W263M	69.1 ± 2,3
αsB5 W263L	V27A/I76T/Y97W/Y99F/L130P/L226V/W263L	80.2 ± 4,0
αsB5 W263I	V27A/I76T/Y97W/Y99F/L130P/L226V/W263I	77.9 ± 1,3
W263M	W263M	85.3 ± 0,9
W263L	W263L	92.0 ± 2,1

Melting temperature determination. Circular Dichroism (CD) spectra were obtained using a Jasco J-815 CD spectrometer with a Pelletier-type temperature control system (Jasco MPTC-490S) in a 1 mm thick quartz Starna® cell and using Spectra Manager software. Experiments were carried out in 10 mM phosphate buffer at pH 8.0. Proteins concentrations were within 0.2–0.4 $mg.ml^{-1}$, denaturation was followed at 222 nm with temperature increased from 25 to 85°C (with 5°C.min^{-1} increment). A range of between 0.5 and 3 M of guanidinium chloride in 10 mM phosphate buffer at pH 8.0 was applied. Data were analyzed with GraphPad Prism 6 using Boltzmann sigmoidal equation, and T_m at 0 M of guanidinium chloride was then extrapolated by linear regression.

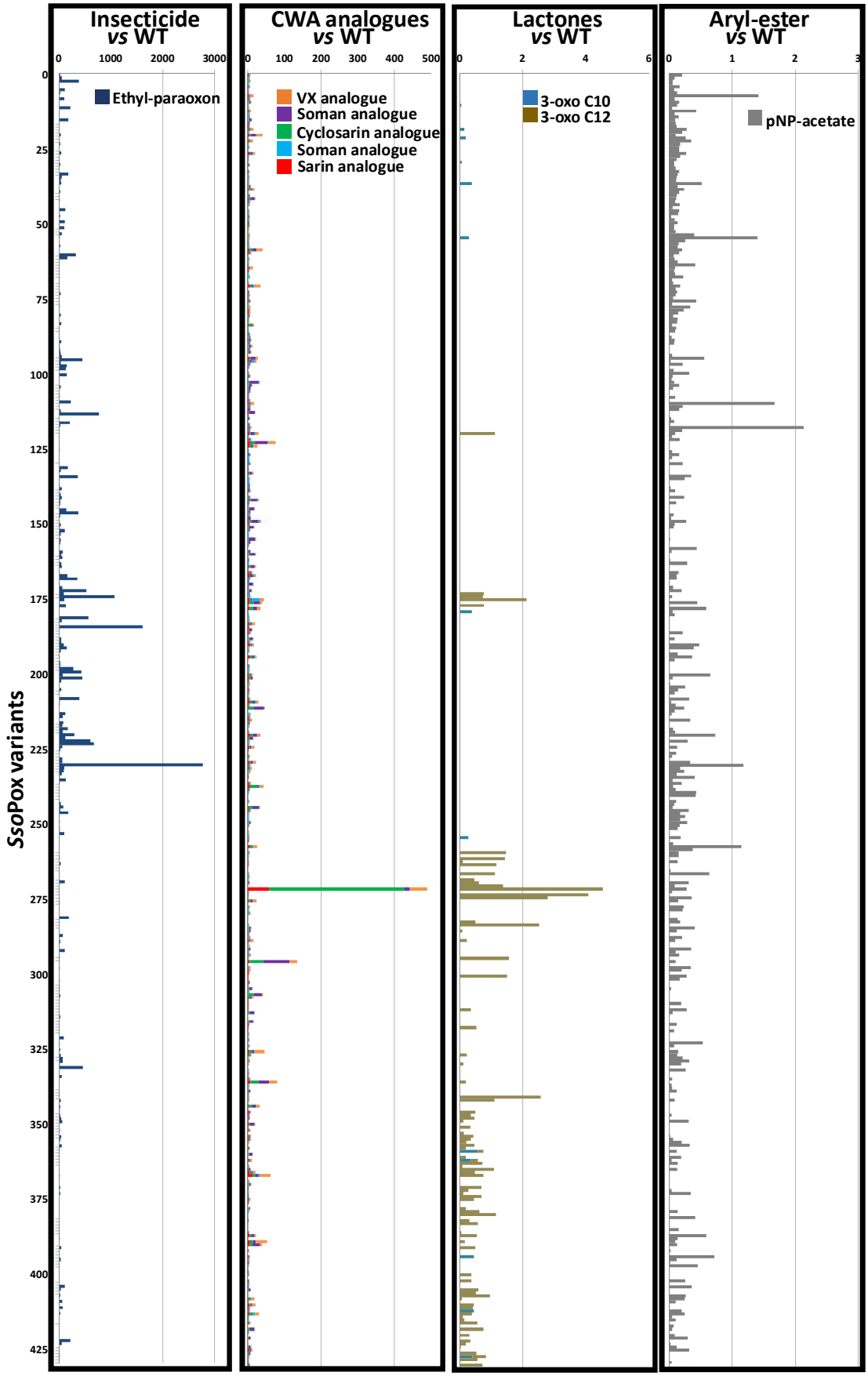
Thermal stability of the engineered variants

We measured the melting temperature of variants αsD6, αsB5, αsB5-W263L, αsB5-W263M and αsB5-W263I in this study while the T_m values of wt, W263M and W263L were previously reported **(Supplementary Table 4)**[78]. All variants showed decreased T_m values as compared to the wild-type enzyme. These values ranged from 69 °C to 92 °C for αsB5-W263M and W263L, respectively. As previously reported, the role of residue 263 is crucial for overall enzyme stability. The stability of mono-substituted variants was globally less affected than the αsD6 and αsB5 scaffolds. The latter's T_m value decreased by 36 °C as compared to *Sso*Pox-wt, while the addition of a mutation at position W263 to its background was not destabilizing, suggesting that their contribution to stability may be different. While the T_m values for the best variants have decreased, they remain very stable (e.g. αsD6 has a T_m of 82.5°C), as compared with their mesophilic counterparts ($T_{m,BdPTE}$=67°C)[65]. Additionally, the expression level of the *Sso*Pox and its mutants were ≈100-150 $mg.l^{-1}_{culture,}$ a higher level than the *Bd*PTE (≈3 $mg.l^{-1}_{culture}$) and ≈50 $mg.l^{-1}_{culture}$ for the improved *Bd*PTE-S5 variant[65].
Interestingly, the range of recognized substrate was broadened when thermostability decreased which is consistent with previous reports suggesting that mutations often increase activity at the cost of stability **(Figure 12)**[148,149].

1.2. Partie 2 : Transformation d'une lactonase hyperthermostable en une phosphotriestérase hautement active

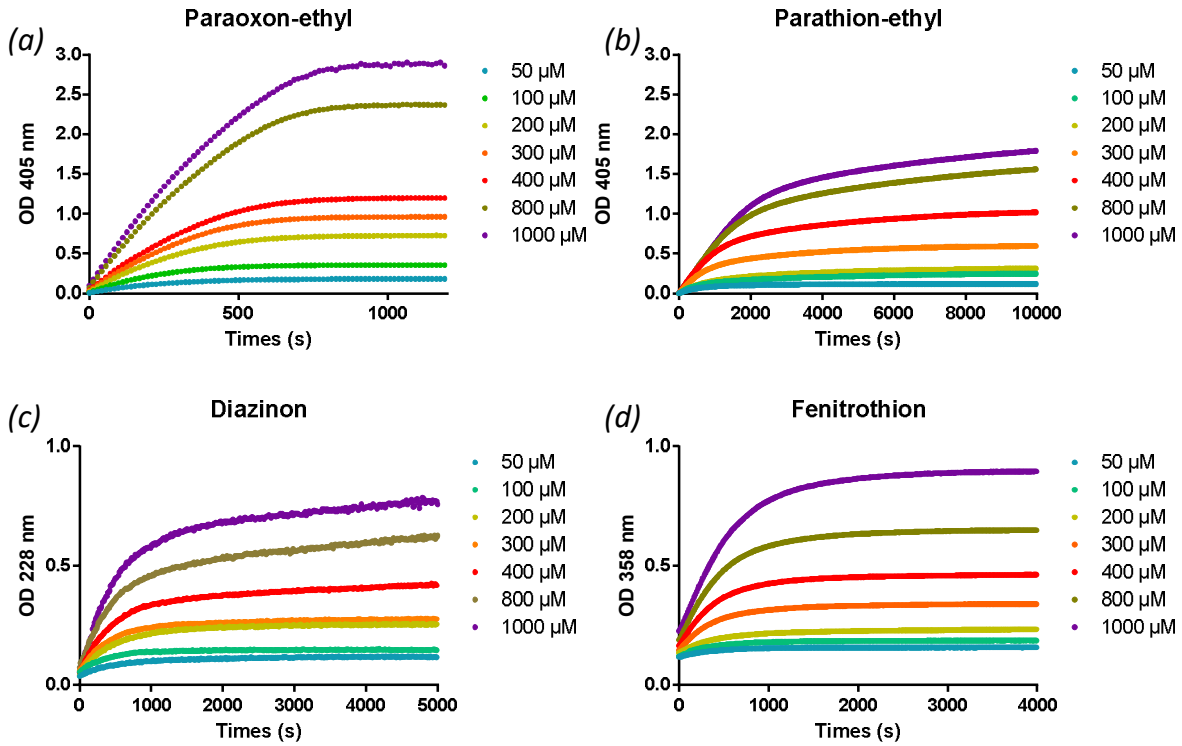
Supplementary Table 5 : Desired mutations and corresponding codons used to synthesize the variants library.

Residue position	Residue	Codon	Potential mutation	Potential codon	Codon used in oligonucleotides
27	V	GTT	V/A/G	GTT/GCA/GGC	GBT
72	L	CTG	L/C/I	CTG/TGT/ATT	TGT/MTT
97	Y	TAT	all	all	NNS
99	Y	TAT	Y/A/D/E/F	TAT/GCA/GAT/GAG/TTT	KAT/GMA/TTT
154	R	CGT	R/K	CGT/AAA	ARG
177	T	ACC	T/D	ACC/GAC	ACC/GAC
223	R	CGT	all	all	NNS
226	L	CTG	L/Q/F	CTG/CAG/TTT	TTT/CWG
228	L	CTG	L/M	CTG/ATG	MTG
258	C	TGC	C/G/L	TGC/GGC/CTG	KGC/CTG
263	W	TGG	all	all	NNS
278	W	TGG	W/L	TGG/CTG	TKG
280	I	ATT	I/T	ATT/ACT	AYT

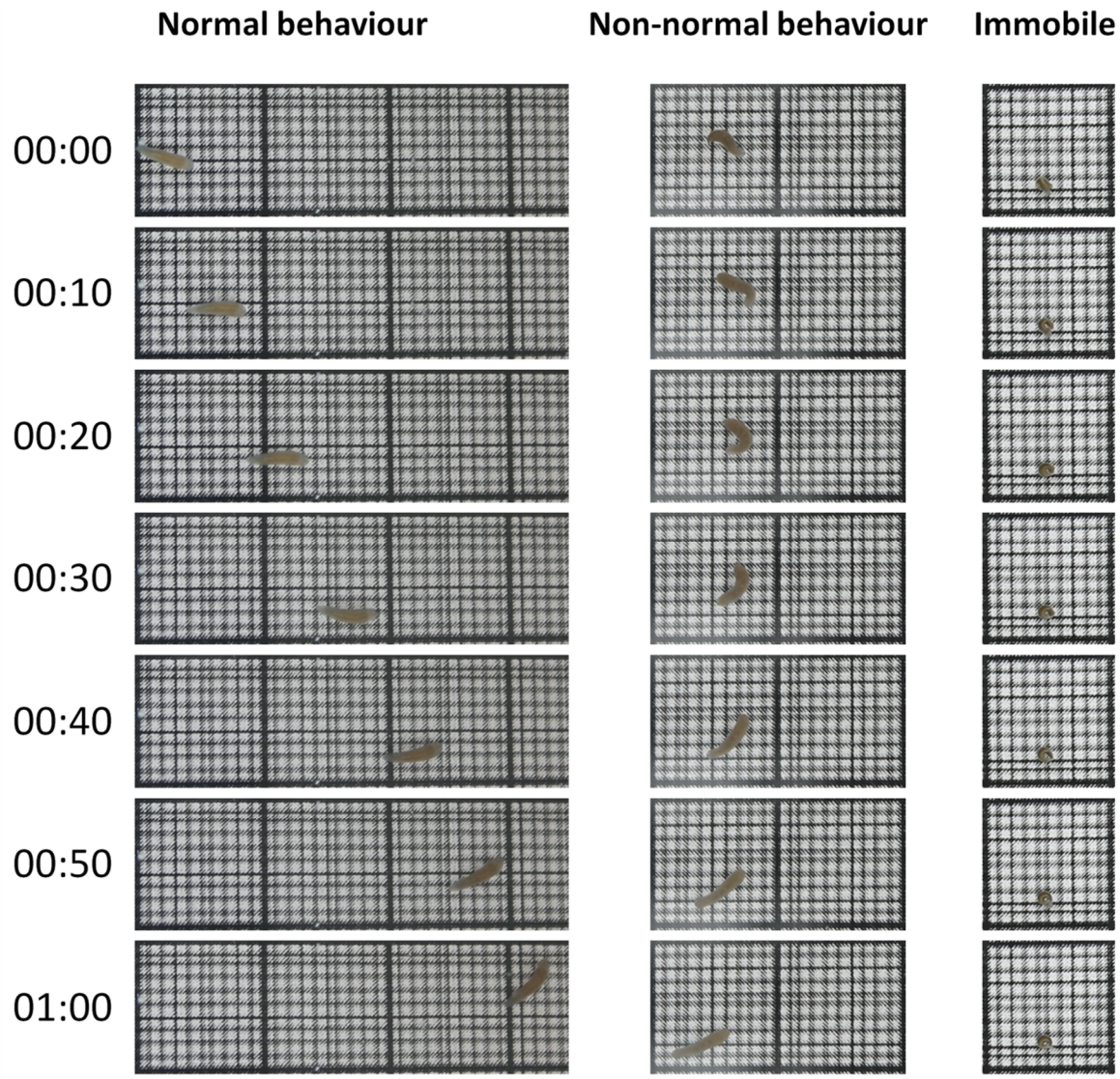


Supplementary Figure 8 : Screening results of the 430 *Sso*Pox variants assayed with 9 substrates as compared to wild-type enzyme.

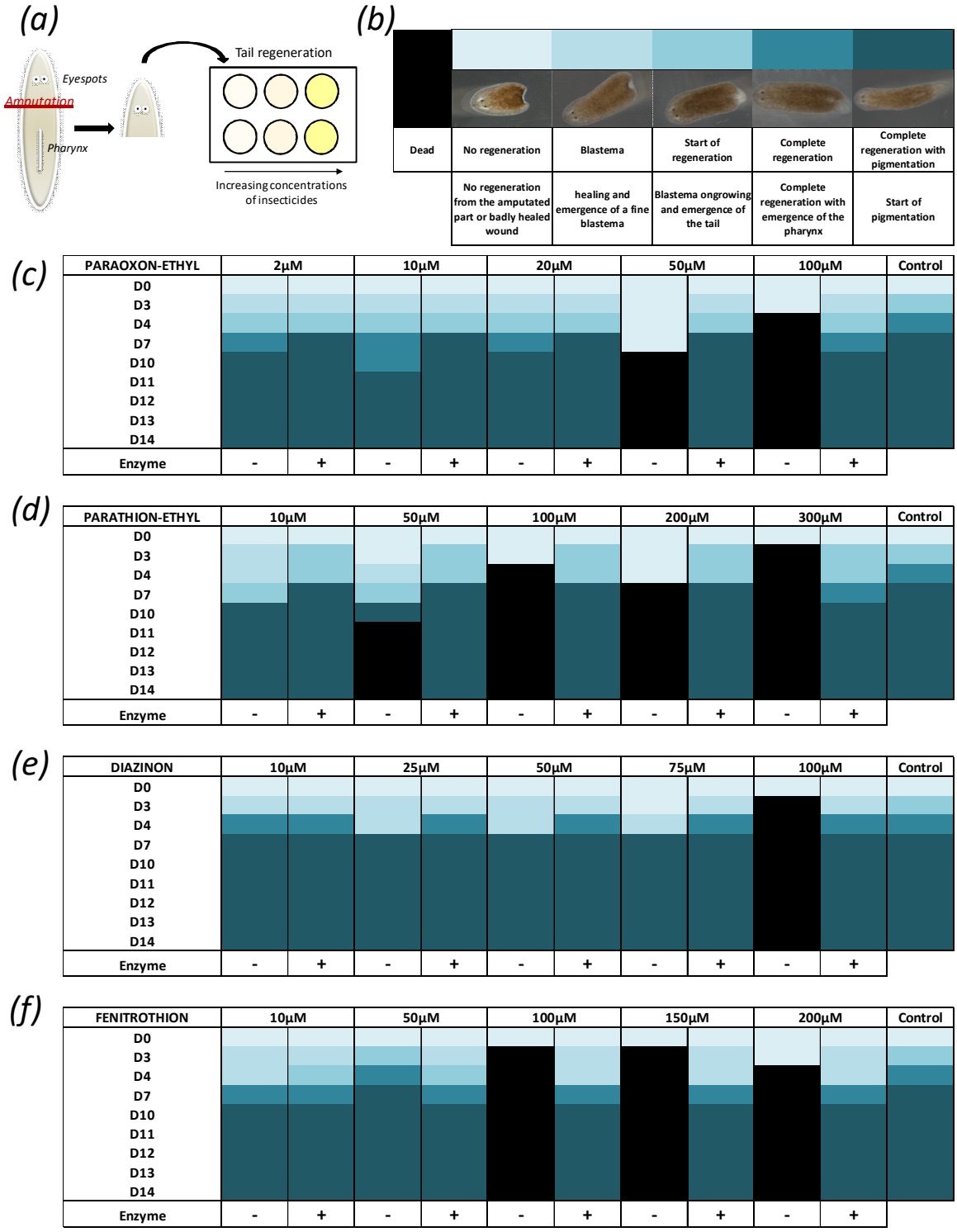
1.3. Partie 3 : La dégradation enzymatique des insecticides organophosphorés diminue la toxicité et améliore la régénération chez les planaires



Supplementary Figure 9 : Enzymatic degradation of insecticides.
Insecticide hydrolysis was followed by measuring absorbance of the product released at 405 nm for paraoxon-ethyl (***a***) and parathion-ethyl (***b***), 228 nm for diazinon (***c***) and 358 nm for fenitrothion (***d***). Curves represent the mean of three replicates.

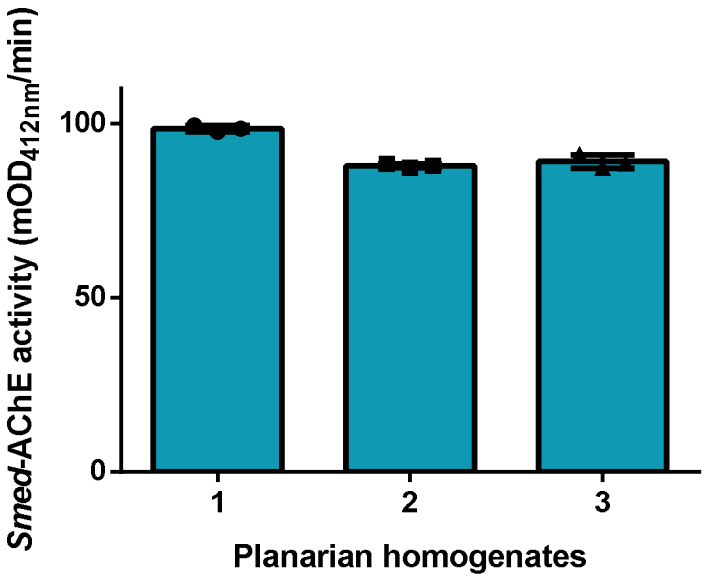


Supplementary Figure 10 : Defining mobility criteria.
The modifications of planarian mobility by insecticides or their degradation products were observed and classified in three categories.

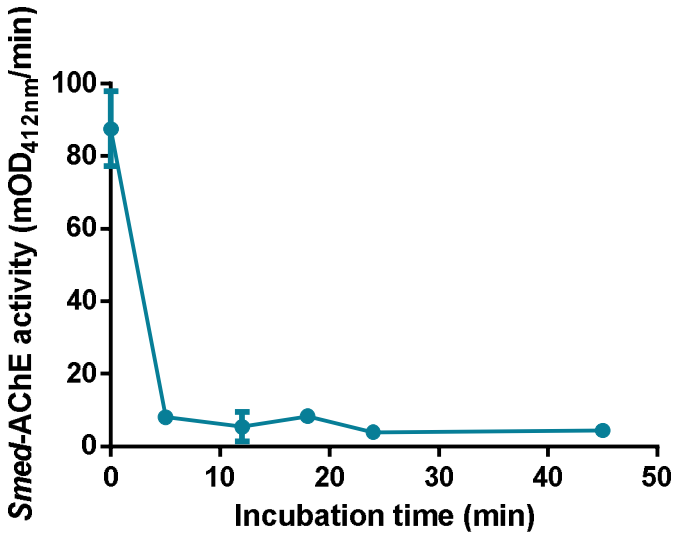


Supplementary Figure 11 : Evaluating the impact of insecticides and their enzymatically-generated degradation products on planarian tail regeneration.

Five planarians were cut above the pharynx and incubated in insecticide solutions (***a***).The tail regeneration of planarians is presented using a color code from light to dark blue describing initial to final regeneration stages as presented in figure caption (***b***). Paraoxon-ethyl (***c***), parathion-ethyl (***d***), diazinon (***e***), fenitrothion (***f***) and the related degradation products were evaluated. Dead planarians are colored black. (+) and (-) describe the solution with and without enzymatic degradation. As pesticides were initially solubilized in ethanol before dilution in water to reach final concentration, the control solutions represent the maximum final ethanol concentration for each insecticide.



Supplementary Figure 12 : Evaluating the reproducibility of planarian homogenate preparation.
The overall AChE activity of planarians homogenates was consistent for three independent preparations.

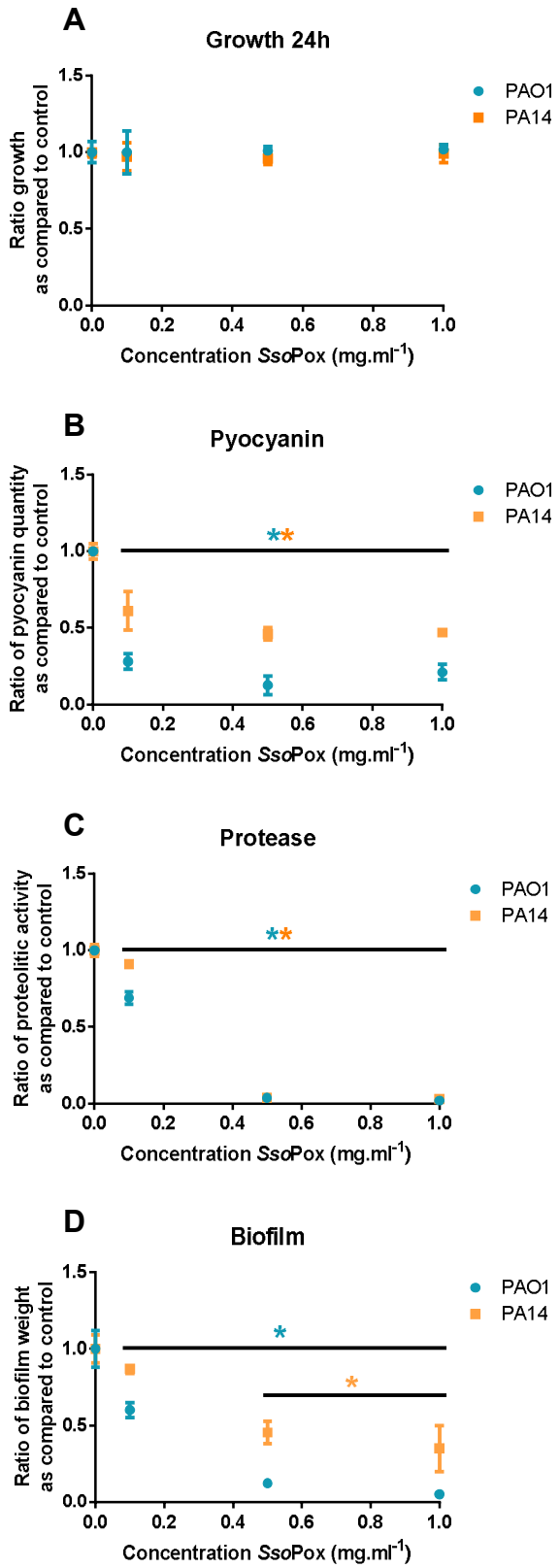


Supplementary Figure 13 : Influence of incubation time on acetylcholinesterase inhibition with 800 µM paraoxon-ethyl.

Supplementary Table 6 : **Summary of NOEC values for full and amputated worms incubated in insecticides or degradation products**.

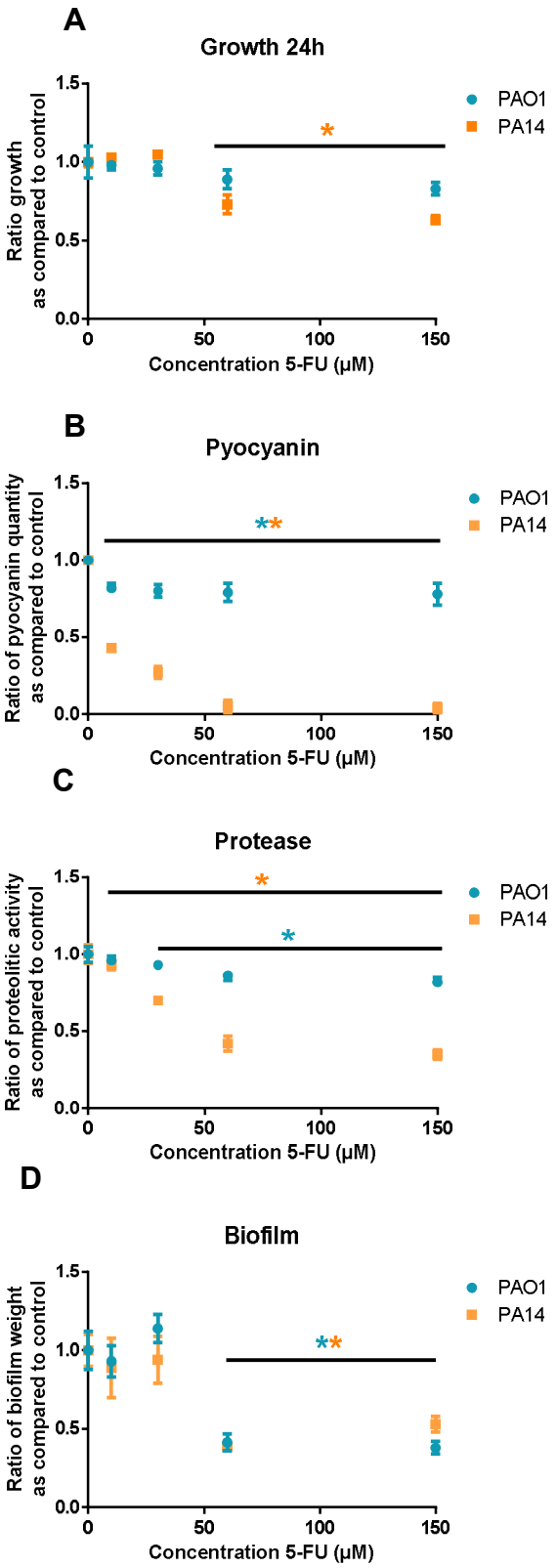
NOEC	Full worm		Amputated worm			
	Pesticide	Degradation product	Head		Tail	
			Pesticide	Degradation product	Pesticide	Degradation product
Paraoxon-ethyl	10µM	50µM	20µM	≥100µM	20µM	≥100µM
Parathion-ethyl	100µM	800µM	10µM	≥300µM	10µM	≥300µM
Diazinon	100µM	800µM	75µM	≥100µM	75µM	≥100µM
Fenitrothion	100µM	400µM	10µM	≥200µM	50µM	≥200µM

1.4. Partie 4 : Evaluation de l'efficacité du quorum quenching par une lactonase sur des isolats cliniques de *Pseudomonas aeruginosa* et comparaison avec des inhibiteurs du quorum sensing

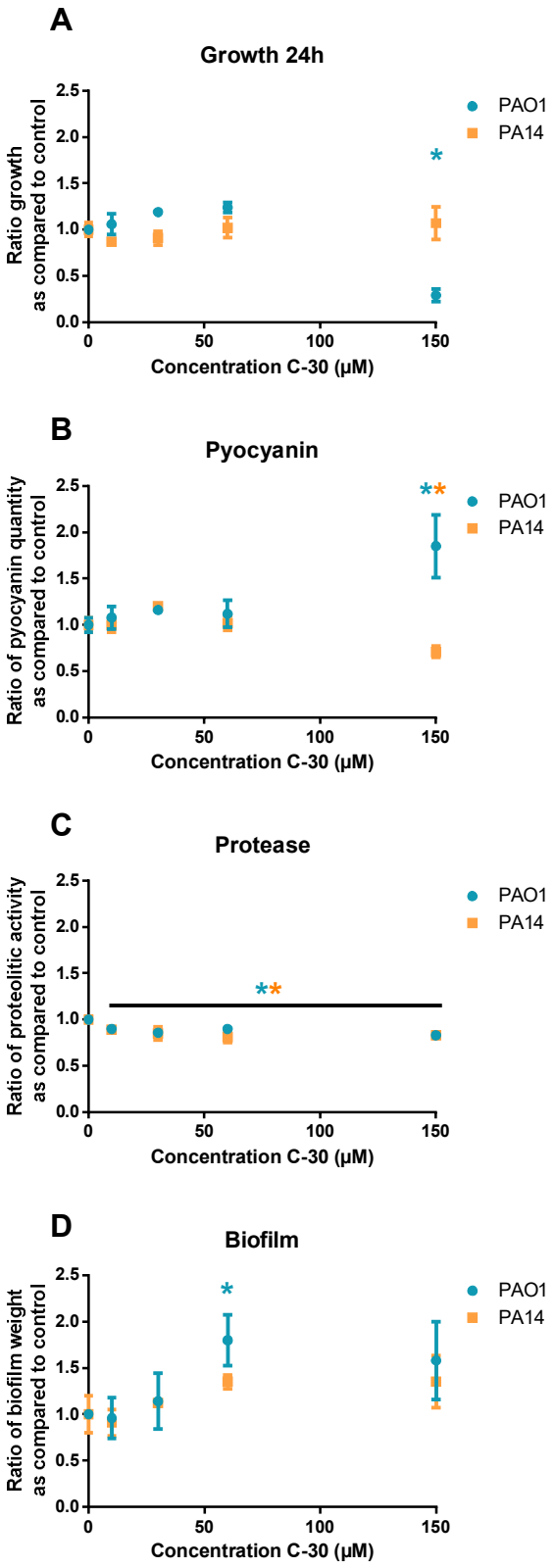


Supplementary Figure 14 : Dose response of *Sso*Pox with the model strains PAO1 and PA14.

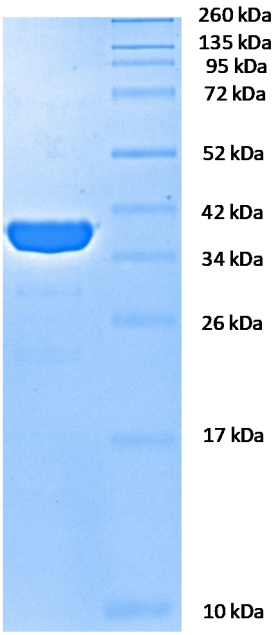
Three *Sso*Pox concentrations (0.1 mg.ml^{-1}, 0.5 mg.ml^{-1}, 1.0 mg.ml^{-1}) were used. Values represent the mean ratios between treated and untreated samples of three experiments. The effect of the QQ enzyme on growth, pyocyanin secretion, protease activity and biofilm formation was evaluated. Stars indicate a p-value<0.05 according to Student's t-test.



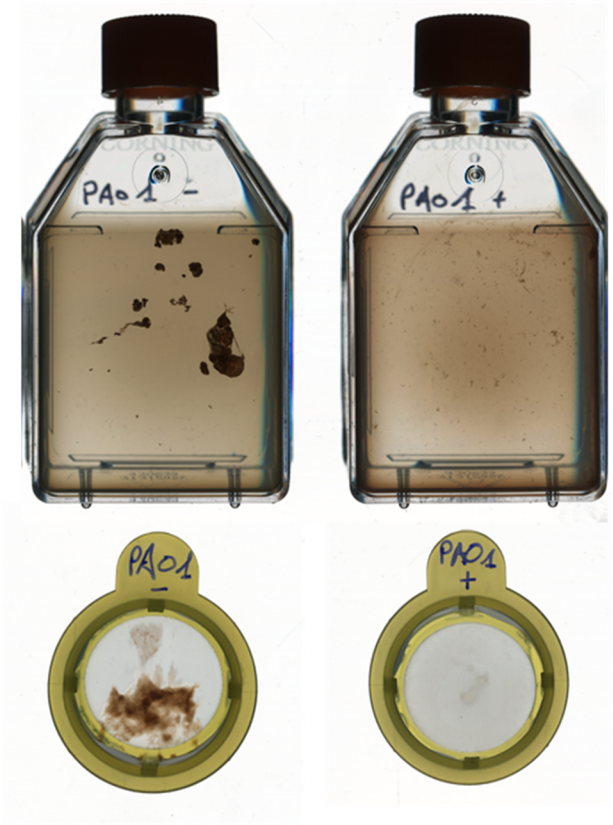
Supplementary Figure 15 : Dose response of 5-FU with the model strains PAO1 and PA14.
Four 5-FU concentrations (10 µM, 30 µM, 60 µM, 150 µM) were used. Values represent the mean ratios between treated and untreated samples of three experiments. The effect of QSI on growth, pyocyanin secretion, protease activity and biofilm formation was evaluated. Stars indicate a p-value<0.05 according to Student's t-test.



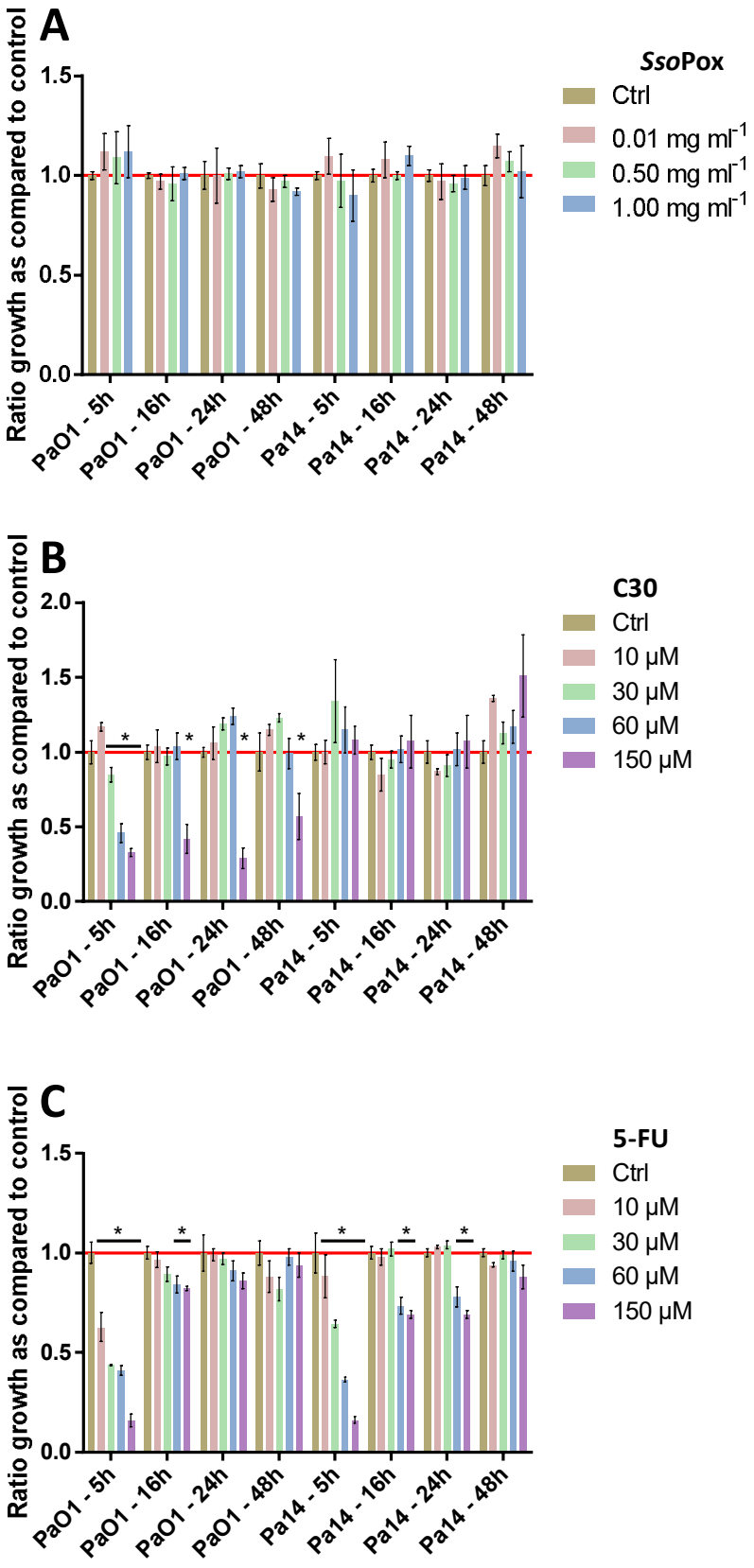
Supplementary Figure 16 : Dose response of C-30 with the model strains PAO1 and PA14.
Four C-30 concentrations (10 µM, 30 µM, 60 µM, 150 µM) were used. Values represent the mean ratios between treated and untreated samples of three experiments. The effect of QSI on growth, pyocyanin secretion, protease activity and biofilm formation was evaluated. Stars indicate a p-value<0.05 according to Student's t-test.



Supplementary Figure 17 : SDS-PAGE of *Sso*Pox-W263I obtained after gel filtration purification.



Supplementary Figure 18 : Direct measurement of biofilm by direct weighing of cell aggregates.
After 48 h of growth, cells were filtered through a 100 µm cell strainer to separate planktonic cells from biofilms. Biofilms were directly weighed in the cell strainers. Left picture represents a culture without *Sso*Pox while right picture represents a culture treated with the enzyme.



Supplementary Figure 19 : Impact of QQ enzyme and QSI on bacterial growth.
The impact of *Sso*Pox (A), C30 (B) and 5-FU (C) on bacterial growth of PAO1 and PA14 for different concentrations.

IV. Annexes

2. Publication annexe

2. Publication annexe

Poirier, L., Jacquet, P., Elias, M., Daudé, D. & Chabrière, E. La décontamination des organophosphorés : vers de nouvelles alternatives. *Annales Pharmaceutiques Françaises* (2017). doi:10.1016/j.pharma.2017.01.004

Annales Pharmaceutiques Françaises (2017) xxx, xxx—xxx

Disponible en ligne sur ScienceDirect www.sciencedirect.com

Elsevier Masson France EM|consulte www.em-consulte.com

REVUE GÉNÉRALE

La décontamination des organophosphorés : vers de nouvelles alternatives

Decontamination of organophosphorus compounds: Towards new alternatives

L. Poirier[a,1], P. Jacquet[a,1], M. Elias[b], D. Daudé[c,*], E. Chabrière[a,c,*]

[a] *Inserm, CNRS, IRD, URMITE, Aix Marseille université, Marseille, France*
[b] *Department of Biochemistry, Molecular Biology and Biophysics & Biotechnology Institute, University of Minnesota, St. Paul, MN 55108, États-Unis*
[c] *Gene&GreenTK, faculté de médecine, 27, boulevard Jean-Moulin, 13385 Marseille cedex 5, France*

Reçu le 16 septembre 2016 ; accepté le 24 janvier 2017

MOTS CLÉS
Bioremédiation ;
Phosphotriestérase ;
Organophosphorés ;
Insecticides ;
Agents chimiques de guerre ;
*Sso*Pox ;
Enzyme ;
Décontamination

Résumé Les organophosphorés (OP) sont des composés hautement toxiques principalement utilisés en tant qu'insecticides. Certains d'entre eux sont des agents de guerre neurotoxiques dont l'utilisation est proscrite. Ces composés sont des inhibiteurs de l'acétylcholinestérase, une enzyme clé pour la régulation des systèmes nerveux central et périphérique. De nombreuses approches chimiques, physiques et biologiques, ont été considérées pour développer des méthodes de décontamination contre les OP. Cette revue dresse un bilan des stratégies actuelles et émergentes pour la décontamination externe des OP avec une attention particulière portée aux techniques enzymatiques. Ces dernières années, de nombreuses études ont permis le développement de biocatalyseurs efficaces pour la dégradation des OP. Parmi ces derniers, de récents résultats ont mis en lumière un biocatalyseur prometteur, *Sso*Pox, isolé de l'archée *Sulfolobus solfataricus*. Cette enzyme hyper-thermostable s'avère particulièrement intéressante pour des applications de décontamination externe de par ses propriétés catalytiques et son impressionnante stabilité.
© 2017 Académie Nationale de Pharmacie. Publié par Elsevier Masson SAS. Tous droits réservés.

* Auteurs correspondants.
Adresses e-mail : david.daude@gene-greentk.com (D. Daudé), eric.chabriere@univ-amu.fr (E. Chabrière).
[1] Contribution équivalente au travail.

http://dx.doi.org/10.1016/j.pharma.2017.01.004
0003-4509/© 2017 Académie Nationale de Pharmacie. Publié par Elsevier Masson SAS. Tous droits réservés.

Pour citer cet article : Poirier L, et al. La décontamination des organophosphorés : vers de nouvelles alternatives. Ann Pharm Fr (2017), http://dx.doi.org/10.1016/j.pharma.2017.01.004

KEYWORDS
Bioremediation;
Phosphotriesterase;
Organophosphorus coumpounds;
Insecticides;
Chemical warfare agents;
*Sso*Pox;
Enzymes;
Decontamination

Summary Organophosphorus coumpounds (OP) are toxic chemicals mainly used for agricultural purpose such as insecticides and were also developed and used as warfare nerve agents. OP are inhibitors of acetylcholinesterase, a key enzyme involved in the regulation of the central nervous system. Chemical, physical and biological approaches have been considered to decontaminate OP. This review summarizes the current and emerging strategies that are investigated to tackle this issue with a special emphasis on enzymatic remediation methods. During the last decade, many studies have been dedicated to the development of biocatalysts for OP removal. Among these, recent reports have pointed out the promising enzyme *Sso*Pox isolated from the archaea *Sulfolobus solfataricus*. Considering both its intrinsic stability and activity, this hyperthermostable enzyme is highly appealing for the decontamination of OP.
© 2017 Académie Nationale de Pharmacie. Published by Elsevier Masson SAS. All rights reserved.

Introduction

Les organophosphorés (OP) sont des composés hautement toxiques initialement développés à des fins militaires en tant qu'agents neurotoxiques (CWNAs pour « chemical warfare nerve agents ») dans le but de blesser, tuer ou encore incapaciter les opposants. La première production massive des OP a été réalisée par des scientifiques allemands avant et pendant la Seconde Guerre mondiale, avec différentes molécules appelées Agents G (pour « Germany ») telles que le tabun (1936), le sarin (1937) et le soman (1944) [1]. Après la Seconde Guerre mondiale, d'autres molécules toxiques appelées Agents V (pour « victory », « venomous » ou « viscuous ») ont été développées par divers pays telles que le VX (États-Unis), le RVX (Russie) ou encore le CVX (Chine) (Fig. 1). D'importants stocks de ces composés ont été accumulés durant la guerre Froide [2]. En 1993, une convention internationale visant, d'une part, à arrêter le développement de ces armes chimiques, et d'autre part, à amorcer un processus de destruction des stocks existants avant 2007, a été signée par deux cents pays environ [2,3]. Cependant, d'importants stocks existent encore, en partie lié au manque de solutions à bas prix, rapide, sans danger pour l'environnement et l'homme pour détruire ces composées chimiques. De plus, certains agents neurotoxiques, comme le sarin, ont été détournés à des fins terroristes comme en témoignent les attaques à Matsumoto et dans le métro de Tokyo (Japon) en 1994 et 1995.

Les OP et plus particulièrement les dérivés des Agents V, ont aussi été commercialisés en tant qu'insecticides dans les années 1950 sous le nom Amiton. Ils ont progressivement remplacé l'insecticide Dichlorodiphenyltrichloroéthane (DDT), un organochloré proscrit dans les années 1970. Étant moins persistants dans l'environnement que le DDT, l'utilisation des OP a été néanmoins restreinte en Europe et aux États-Unis. Cependant, ils restent massivement utilisés dans certains pays pour l'agriculture intensive. Les insecticides OP les plus utilisés sont le malathion, l'éthyl- ou méthylparathion et le chlorpyrifos (Fig. 1). Les OP font partie des principaux polluants environnementaux (sols, eaux et des aliments) [4] et leur utilisation serait responsable de 3 millions d'intoxications, et 300 000 décès dans le monde par an. La plupart de ces décès sont associés à des suicides après ingestion délibérée de pesticides [5,6]. Par ailleurs, les insecticides organophosphorés présentent également une sérieuse menace sécuritaire puisqu'ils sont à la fois fortement toxiques et largement répandus et pourraient alors être utilisés à des fins terroristes ou dans le cadre des conflits asymétriques.

La toxicité extrême des OP provient de leur capacité à inhiber de manière irréversible l'acétylcholinestérase (AChE), une enzyme clef du système nerveux. En effet, l'AChE termine la dégradation du neurotransmetteur acétylcholine au niveau de la fente synaptique et des jonctions neuromusculaires. Lorsque l'AChE est inhibée, l'acétylcholine s'accumule et sature les récepteurs cholinergiques. Une intoxication aiguë par les OP mène à l'apparition de divers symptômes parmi lesquels convulsion, salivation, larmoiement, miction, diaphorèse, troubles gastro-intestinaux, myosis et vomissements [7,8]. Le mécanisme d'inhibition est composé d'une première étape durant laquelle les OP réagissent avec la serine catalytique (Ser200) de l'AChE humaine, via phosphylation, formant alors une phosphoenzyme covalente [9]. Cet intermédiaire OP-AChE peut ensuite subir, selon la nature de l'OP, un processus de vieillissement (une désalkylation sur le produit d'addition). Ce processus empêche la réactivation de la phosphoenzyme. La cinétique de vieillissement est un paramètre très important à prendre en compte lors d'un traitement contre l'empoisonnement aux OP.

En raison de la menace présentée par les OP à la fois au niveau sécuritaire, sanitaire et écologique, une attention particulière a été consacrée à l'élaboration de stratégies de décontamination. Idéalement, une solution de décontamination devrait offrir une grande efficacité, un large spectre d'action, une utilisation douce compatible avec la peau, les muqueuses ou le matériel sensible, sans impact environnemental, aucune contamination secondaire et un faible coût. Ci-après est présenté un aperçu des méthodes de décontamination actuelles et émergentes qu'elles soient physiques, chimiques ou biologiques. Leurs caractéristiques respectives sont résumées et de nouveaux développements ainsi que les perspectives d'avenir sont discutés.

Méthodes actuelles de décontamination des OP

Les méthodes actuelles de décontamination des insecticides et des CWNA peuvent être séparées en trois catégories :

- décontamination physique : cela comprend toutes les méthodes passives visant à éliminer l'agent contaminant

Pour citer cet article : Poirier L, et al. La décontamination des organophosphorés : vers de nouvelles alternatives. Ann Pharm Fr (2017), http://dx.doi.org/10.1016/j.pharma.2017.01.004

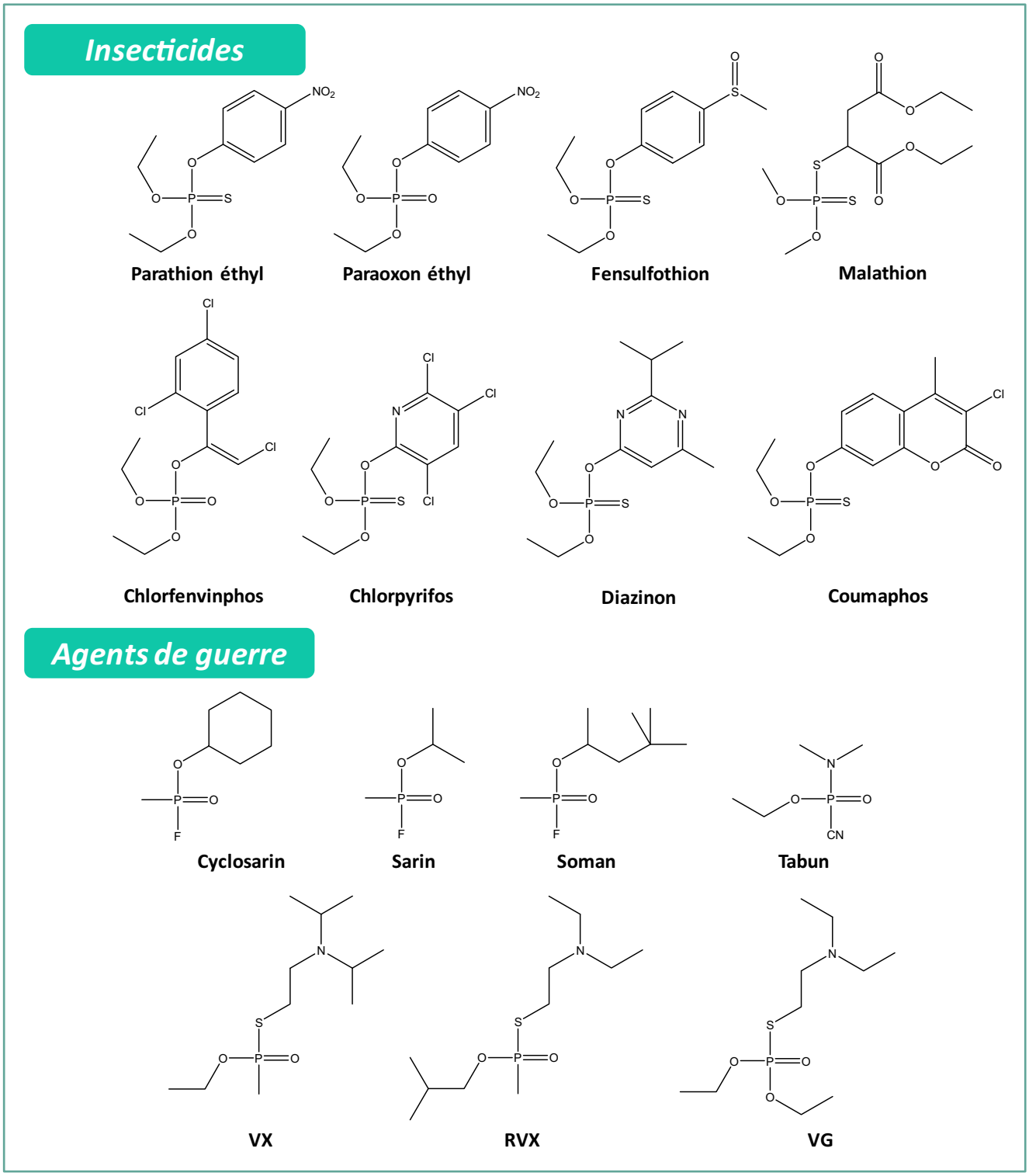


Figure 1. Structures chimiques des principaux insecticides et agents neurotoxiques de guerre organophosphorés.
Chemical structures of organophosphorus insecticides and warfare nerve agents.

d'une surface donnée, biotique ou abiotique. Elle repose sur une action mécanique permettant de dégrader l'agent ou le plus souvent de le piéger sans le détruire ;

- décontamination chimique : cela correspond à toutes les méthodes permettant de neutraliser l'agent par des réactions chimiques telles que l'hydrolyse, l'oxydation ou la réduction ;
- décontamination enzymatique : cette méthode se rapporte à l'utilisation d'enzymes capables d'hydrolyser les insecticides ou les CWNA.

Pour citer cet article : Poirier L, et al. La décontamination des organophosphorés : vers de nouvelles alternatives. Ann Pharm Fr (2017), http://dx.doi.org/10.1016/j.pharma.2017.01.004

Un dispositif de décontamination pourrait combiner plusieurs méthodes appartenant aux catégories présentées ci-dessus, permettant un nettoyage de surface combinée avec une neutralisation rapide et efficace et/ou la destruction de l'agent contaminant, maximisant ainsi les effets et réduisant les risques pour la santé et l'environnement.

Décontamination à grande échelle

La décontamination à grande échelle concerne principalement les surfaces après une exposition massive aux OP. L'objectif consiste à la fois à éliminer la contamination in situ ainsi que de réduire le potentiel de contamination croisée, par exemple entre la victime et le personnel traitant. Les méthodes actuelles sont bien adaptées pour la décontamination de matériel, cependant elles sont souvent agressives et ne peuvent pas être utilisées pour traiter les victimes. Les solutions présentées ici sont un panel non exhaustif des solutions disponibles.

Hypochlorite

La décontamination par une solution d'hypochlorite de sodium peut être utilisée à une concentration de 0,5 % pour le personnel et de 5 % pour les équipements [10]. Cette solution se révèle utile à la fois pour éliminer l'agent neurotoxique de la surface et pour le dégrader par oxydation. Cette méthode reste cependant très agressive pour les yeux, la peau et les plaies en raison de son fort potentiel corrosif.

Hydroxyde de sodium

L'hydroxyde de sodium est utilisé pour réaliser une hydrolyse alcaline des OP par attaque nucléophile de l'ion hydroxyde sur l'atome de phosphore. Cela permet la dégradation de grandes quantités d'agents neurotoxiques en leur acide phosphorique correspondant non toxique.

La combinaison des deux produits présentés précédemment, appelée eau de javel super tropicale avec 93 % d'hypochlorite de calcium et d'hydroxyde de sodium à 7 %, est utilisée pour la décontamination du matériel avec une grande efficacité [11]. Cependant, cette méthode est très corrosive et ne peut être utilisée ni pour la décontamination de matériel sensible, ni pour celle du personnel.

BX-24 et BX-29

Ces solutions de décontamination, utilisées par les forces de l'OTAN, agissent par oxydation et hydrolyse. Le BX-29 est une solution de décontamination pour le personnel alors que le BX-24 est plus particulièrement utilisé pour décontaminer le matériel. Ces solutions contiennent des composés amphotères, des amides et un tensioactif et sont annoncées comme sûres. En cas d'urgence, une solution diluée de BX-24 peut être utilisée pour la décontamination du personnel, cependant la température de la solution ne doit pas dépasser 34 °C pour limiter la pénétration transcutanée des agents chimiques.

Décontamination du personnel

La cinétique de pénétration de l'agent neurotoxique dans le corps est si rapide que la décontamination et le traitement doivent être réalisés le plus tôt possible lors de la prise en charge des individus. En effet, le temps de transport vers des installations médicales appropriées, sans traitement topique au préalable, réduirait considérablement les chances de survie du patient et menacerait le personnel médical par une exposition à des contaminations secondaires. Actuellement les méthodes utilisées pour faire face à une exposition aux agents neurotoxiques reposent sur une décontamination externe suivie d'un traitement médical des personnes exposées. Des kits pour la décontamination individuelle sont utilisés par les armées du monde entier. Ils doivent se conformer aux exigences opérationnelles et donc constituer le meilleur compromis en termes de taille, de poids, de facilité d'utilisation et bien sûr d'efficacité.

M291 « skin decontamination kit » (SDK)

Adopté par l'armée américaine en 1989, le M291 SDK est une compresse en fibres non tissées remplie d'un absorbant et d'une résine. L'absorbant est un composé carboné de surface de contact élevée afin d'éliminer l'agent de la peau. La résine est elle-même composée de deux résines échangeuses d'ions, l'une anionique et l'autre cationique, capable de neutraliser les contaminants par hydrolyse [12]. Cette technologie a été utilisée par l'armée américaine jusqu'à son remplacement progressif, autour de 2007, par la « reactive skin decontamination lotion » (RSDL). Son efficacité est très faible sur le VX et limitée contre le soman par rapport à d'autres méthodes de décontamination, comme l'eau savonneuse 1 % et l'eau de javel 0,5 % [13,14]. Cette méthode ne convient pas pour une décontamination des yeux et des plaies.

« Reactive skin decontamination lotion » (RSDL)

Le RSDL est la solution actuelle fournie aux soldats ainsi qu'au personnel de sécurité civile afin de faire face à une exposition locale aux OP. Cette technique se compose d'une éponge, emballée individuellement, imprégnée d'une solution contenant du diacétylmonoxime et du Dekon 139 — un mélange breveté — dissous dans de polyéthylène glycol monométhyl éther [15]. Cette formulation permet une désorption de l'agent neurotoxique de la peau et sa dégradation chimique par une réaction nucléophile. Le temps nécessaire pour achever la décontamination est inférieur à trois minutes pour les Agents V et G [16]. Son efficacité surpasse celle du M291 envers les agents tels que le VX et le soman [13,14]. Le rapport de protection (défini comme le rapport entre la DL_{50} du groupe traité par rapport au non traité) de la RSDL sur des cochons d'Inde est environ 60 fois plus élevé que celui du M291 contre le VX (66,4 et 1,1 respectivement) [13]. Pour le soman, le rapport de protection de la RSDL est 5 fois meilleur que celui du M291 (14 et 2,7 respectivement) [14]. La RSDL est efficace pour décontaminer la peau lorsqu'elle est appliquée quelques minutes après l'exposition. Comme pour le M291, la RSDL n'est pas compatible pour la décontamination des yeux et des plaies.

Terre à foulon

Utilisée par plusieurs pays de l'OTAN, cette méthode repose uniquement sur une adsorbance physique et passive de l'OP. La terre à foulon est principalement composée de poudre

Pour citer cet article : Poirier L, et al. La décontamination des organophosphorés : vers de nouvelles alternatives. Ann Pharm Fr (2017), http://dx.doi.org/10.1016/j.pharma.2017.01.004

fine de silicate d'aluminium avec une grande surface, ce qui permet une bonne adsorption locale des contaminants [17]. Le principal inconvénient d'une telle méthode est lié à la production de poussières contaminées présentant alors un risque d'inhalation.

Actuellement, il existe un manque de solutions non corrosives, compatibles à la fois pour la décontamination du matériel sensible et du personnel. La majorité des techniques disponibles peuvent éliminer la menace liée aux CWNA mais laisseront par la suite une contamination chimique désastreuse. De plus, il est important de noter que la décontamination du personnel par l'utilisation de tensioactifs (eau savonneuse) représente un risque de propagation de l'agent neurotoxique sur une surface plus large de la peau. Même si les tensioactifs contribuent à solubiliser les produits chimiques, ils peuvent affecter négativement l'objet même de la décontamination. Il est donc de la plus haute importance d'opter pour des méthodes permettant la séquestration et/ou la destruction rapide des agents neurotoxiques.

Alternatives chimiques et physiques pour la décontamination des OP

Cyclodextrines (CD)

Les CD sont des oligosaccharides cycliques composés de 6 à 8 unités de α-D-glucopyranoside. Elles forment une cavité hydrophobe capable de recevoir des molécules hydrophobes et apolaires [18]. Cette capacité de catalyse biomimétique permet aux CD de piéger les OP.

Les CD naturelles (α-CD, β-CD et γ-CD) ont dans un premier temps été utilisées pour inactiver les CWNA et parmi ces dernières, la β-CD s'avère la plus efficace (Fig. 2) [19,20]. Les CD sont en effet capables d'accélérer les réactions d'hydrolyse de certains organophosphorés via une attaque nucléophile de l'oligosaccharide sur le substrat complexé. L'efficacité de l'hydrolyse dépend alors de plusieurs paramètres tels que le positionnement du substrat et de son hydrophobie [21]. En partant de la β-CD comme précurseur, des CD substituées telles que l'iodosobenzoate-β-CD (IBA-β-CD) ont été développées pour accélérer l'inactivation des OP [22]. Le potentiel nucléophile de l'IBA a ainsi permis de catalyser l'hydrolyse du soman et du dimebu (un isomère du soman possédant un seul centre chiral) [188,189]. L'importance de la présence d'un nucléophile en α tel que l'IBA a alors été soulignée. D'autres dérivés ont été synthétisés comme l'*O*-benzyl-β-CD, des dérivés complètement méthylés de la β et l'α-CD (TRIMEB et TRIMEA respectivement) et un dérivé partiellement méthylé de la β-CD (DIMEB) présentent une meilleure solubilité dans les solvants organiques et dans l'eau. Les CD sont des composés prometteurs qui pourraient être utilisés pour la peau, les muqueuses et les plaies [23]. En dépit de ces avantages, certaines limitations doivent être soulignées pour l'utilisation de CD, comme leur poids moléculaire élevé (1134 g/mol^{-1} pour la β-CD) et un faible turn-over. De plus, les CD actuelles ne sont capables de dégrader le VX et les OP contenant une liaison P-S du fait de la grande stabilité de cette liaison [24,25]. En outre, le *p*-nitrophénol (produit de dégradation du paraoxon) inhibe l'efficacité du processus de dégradation du paraoxon par la β-CD [26,27]. On peut supposer que d'autres produits

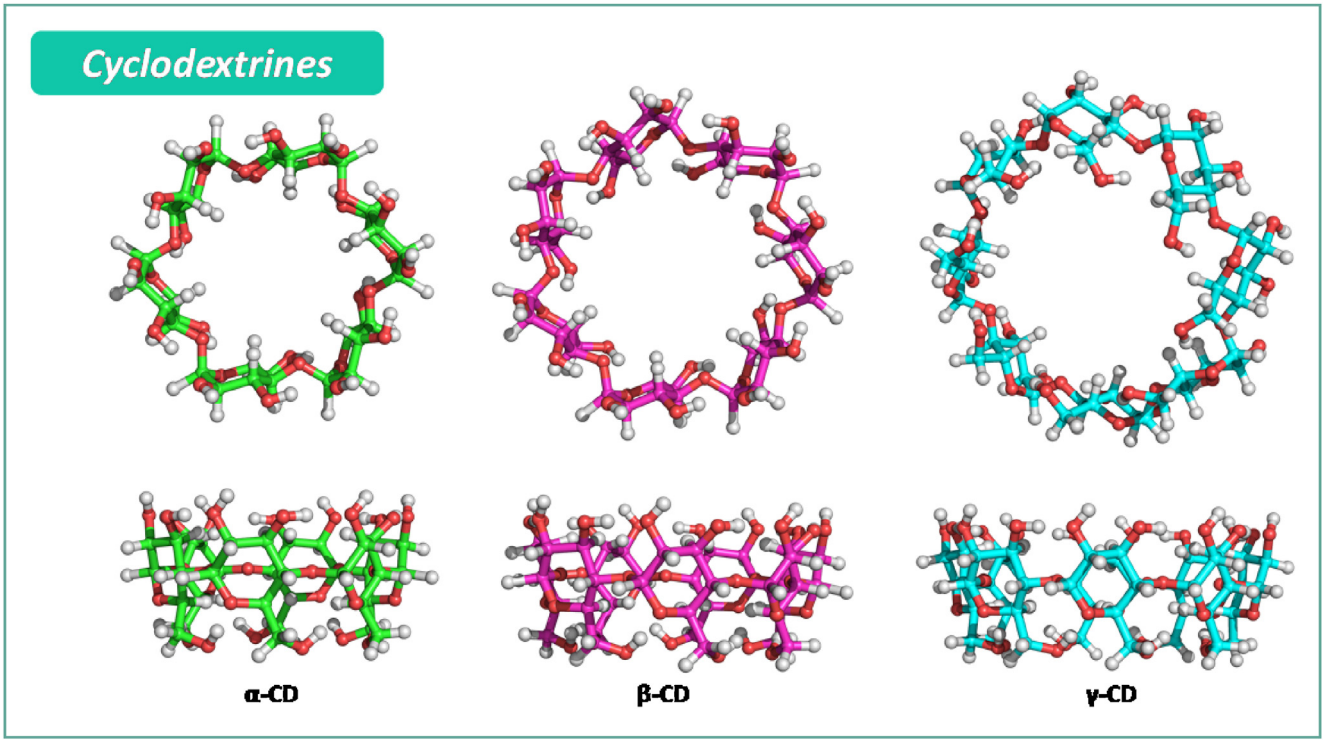


Figure 2. Structure des cyclodextrines α, β et γ comportant respectivement 6, 7 et 8 unités α-D-glucopyranoside.
Structures of α, β and γ cyclodextrins.

Pour citer cet article : Poirier L, et al. La décontamination des organophosphorés : vers de nouvelles alternatives. Ann Pharm Fr (2017), http://dx.doi.org/10.1016/j.pharma.2017.01.004

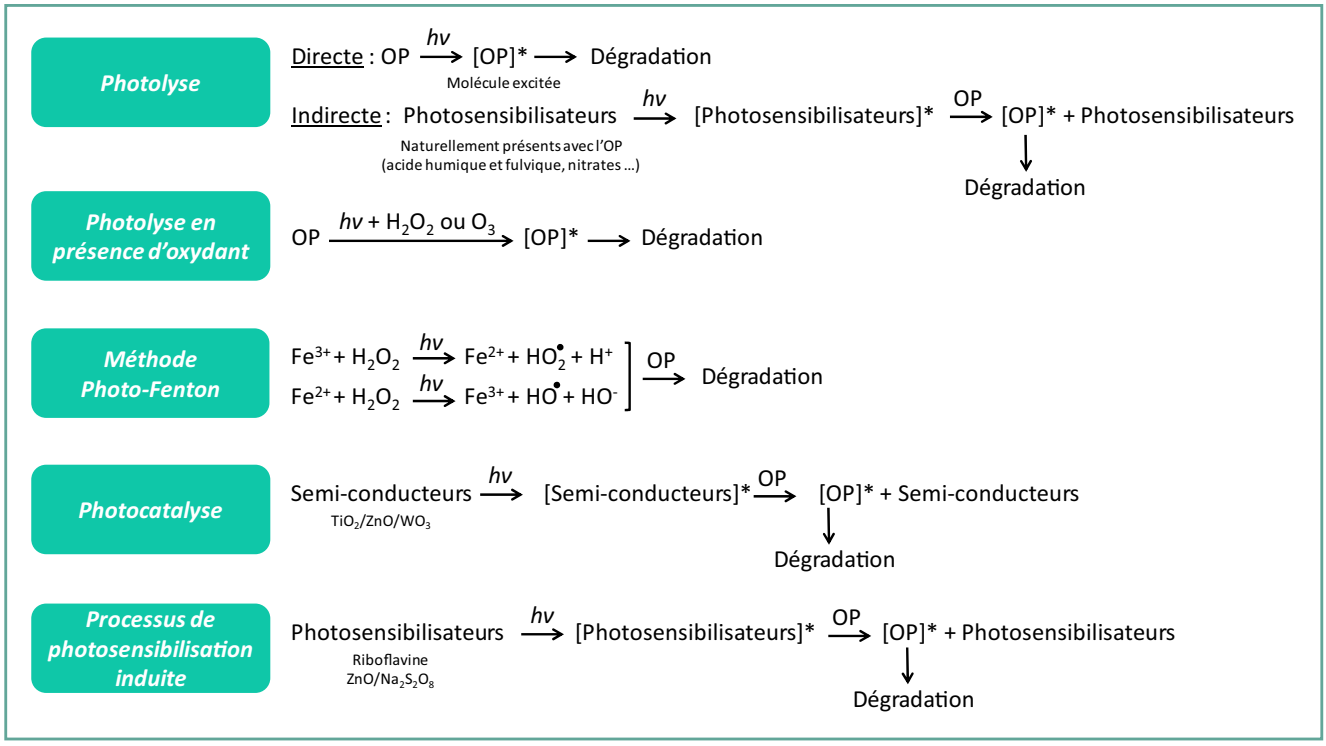


Figure 3. Équations associées aux méthodes photochimiques.
Equations involved in photochemical reactions.

de dégradation des OP présentent le même effet. De plus, le taux de dégradation de la liaison P-F, retrouvée chez le sarin, le cyclosarin ou le soman, est très faible [22].

Méthodes photochimiques

Les méthodes photochimiques sont basées sur l'utilisation du rayonnement lumineux pour dégrader les OP et les substances organiques en général [28]. Ces techniques font parties des processus avancés d'oxydation qui utilisent la forte réactivité des radicaux HO· pour dégrader les polluants [29]. En résumé, ces méthodes peuvent être classées en cinq catégories pour la dégradation des OP au niveau du sol, de l'eau et de l'air (Fig. 3).

Photolyse

La dégradation photolytique du composé ciblé consiste en l'absorption du rayonnement de manière directe et indirecte, conduisant à la destruction du composé. Plusieurs exemples de photolyse d'OP (diazinon, méthylparathion ou quinalphos) ont été traités de manière directe [30—34] et indirecte [35,36].

Photolyse en présence d'oxydant

L'association de la photolyse classique avec des oxydants chimiques comme H_2O_2 et O_3 améliore l'efficacité du processus et semble empêcher la formation de produits défavorables [37].

Méthode photo-Fenton

Cette méthode implique les processus de photo-Fenton, reposant sur la photoréduction de complexe Fe(III) en ions Fe(II) suivie par la réaction de Fenton permettant la formation d'agents oxydants entraînant ainsi l'oxydation des composés organiques [38,39].

Photocatalyse

Elle se réfère à la photo-excitation d'un semi-conducteur tel que le dioxyde de titane (TiO_2), l'oxyde de zinc (ZnO) ou de trioxyde de tungstène (WO_3). Les semi-conducteurs sont des intermédiaires pour la réduction ou l'oxydation des OP. Cette technique présente certaines limites, comme la recombinaison électronique [40—45].

Processus de photosensibilisation induite

Ce processus utilise des sensibilisateurs capables d'absorber le rayonnement lumineux, puis de transférer l'énergie excédentaire à un composé ciblé. Cette technique est utile pour les OP avec une efficacité d'absorption faible [46,47].

Les méthodes photochimiques ont été principalement utilisées pour la décontamination de l'eau [28]. À ce jour, quelques études sur l'air et sur les surfaces solides pour la décontamination des CWNA ont été réalisées [48,49]. Ces méthodes sont faciles à mettre en oeuvre et relativement bon marché. Cependant l'efficacité de ces méthodes dépend de nombreuses variables telles que le débit de l'effluent, les types et les concentrations des contaminants (comme les ions inorganiques).

Pour citer cet article : Poirier L, et al. La décontamination des organophosphorés : vers de nouvelles alternatives. Ann Pharm Fr (2017), http://dx.doi.org/10.1016/j.pharma.2017.01.004

Autres

D'autres techniques de décontamination des OP existent. Ces méthodes restent marginales et nécessiteraient un développement ultérieur. Ci-après est présentée une liste non exhaustive de ces techniques.

Metal-organic framework (MOF)

Les MOF sont des matériaux cristallins, composés d'ions métalliques ou de complexes liés ensemble par des liaisons organiques polydentés. La plupart des MOF sont hautement poreux et leur grande surface spécifique est particulièrement intéressante pour l'adsorption des gaz. De plus les MOF sont basés sur des nœuds métalliques qui pourraient être adaptés pour fonctionner comme une enzyme artificielle [50]. Par exemple, ils pourraient être utilisés pour l'hydrolyse des CWNA par de l'eau en utilisant Cu-BTC [HKUST-1, $Cu_3(C_9H_3O_6)_2$] ou NU-1000 [$Zr_6(\mu_3\text{-}O)_4(\mu_3\text{-}OH)_4(H_2O)_4(OH)_4$] [51,52].

Dégradation par plasma non thermique

Cette technique, également appelée décharge à barrière diélectrique, est une méthode capable de détruire un large éventail d'OP ainsi que d'autres produits chimiques et agents biologiques pathogènes [49]. Cette méthode génère des dérivés réactifs de l'oxygène qui vont ensuite permettre la dégradation des OP dont les produits de dégradation semblent être inoffensifs [53]. Cette technique est utilisée principalement pour la décontamination des eaux usées [54].

Irradiation gamma

Le processus d'irradiation gamma est utilisé pour la dégradation de nombreux polluants. Il fait également partie des processus avancés d'oxydation comme les méthodes photochimiques. L'irradiation gamma permet de dégrader certains OP tels que le chlorpyrifos, le diazinon ou le malathion dans l'eau. Cette technique est également utilisée dans la décontamination de l'eau [29,55,56].

Des enzymes pour la dégradation des organophosphorés

Différentes enzymes issues de plusieurs familles ont été décrites comme étant capables de dégrader les insecticides et ou CWNA organophosphorés. Ci-après les enzymes les plus étudiées sont décrites et un aperçu de leurs structures 3D est présenté sur la Fig. 4.

Organophosphate hydrolase (OPH)

Les OPHs appartiennent aux aryltriphosphate dialkylphosphohydrolases (EC 3.1.8.1), ainsi qu'à la superfamille des amidohydrolases [57,58]. Ces enzymes ont été initialement isolées chez *Brevundimonas diminuta* MG (anciennement *Pseudomonas diminuta*) et *Sphingobium fuliginis* ATCC 27551 (anciennement *Flavobacterium sp.*) [59—62]. Une autre enzyme très proche fut isolée de la bactérie *Agrobacterium radiobacter* P230 [63,64]. De nombreux efforts ont été mis en œuvre pour la caractérisation et l'ingénierie de ces enzymes [65,66]. Les travaux les plus notables sont résumés ci-dessous.

OPH de Brevundimonas diminuta

Cette enzyme de 35 kDa est capable de dégrader un large panel d'insecticides OP, avec des efficacités catalytiques (k_{cat}/K_M) pouvant atteindre $4{,}0 \times 10^7\ M^{-1}s^{-1}$ pour le paraoxon [67]. L'activité de l'enzyme pour dégrader le sarin ou encore le soman a été aussi mise en évidence, bien qu'avec des valeurs de k_{cat}/K_M plus basses par rapport au paraoxon, $8{,}0 \times 10^4\ M^{-1}s^{-1}$ and $9{,}3 \times 10^3\ M^{-1}s^{-1}$ respectivement [68]. La structure 3D de l'apoenzyme est composée d'un repliement en tonneau $(\beta/\alpha)_8$ [69]. Des stratégies d'ingénierie protéique pour améliorer l'activité de l'OPH ont alors été menées [70]. Une approche de mutagenèse a par exemple permis d'obtenir des variants améliorées contre le diisopropylfluorophosphate (DFP) permettant pour la première fois d'augmenter l'hydrolyse des liaisons P-F [71]. D'autres approches ont par ailleurs permis d'améliorer l'efficacité envers le méthylparathion, le chlorpyrifos ou le paraoxon jusqu'à des facteurs d'amélioration de 725 [72,73]. L'évolution dirigée a également permis d'augmenter l'expression hétérologue de l'enzyme chez *E. coli* de plus de 20 fois [74] et d'augmenter la stéréosélectivité de l'enzyme envers les énantiomères d'OP les plus toxiques [75]. Des approches computationnelles couplées à des expériences de mutagenèse ont ainsi permis d'atteindre des efficacités catalytiques de $8{,}3 \times 10^4\ M^{-1}s^{-1}$ à l'encontre de l'énantiomère S_p du VX [76]. Une autre étude à par ailleurs permis d'obtenir un second variant très efficace pour la dégradation du VX amélioré de 230 fois pour la dégradation du VX racémique [77]. Pour conclure, ces résultats mettent en évidence que la phosphotriestérase de *B. diminuta* est un bon candidat, qui peut être amélioré avec des stratégies d'ingénierie enzymatique, pour une décontamination catalytique des OP.

OPH de *Sphingobium fuliginis*

S. fuliginis (ATCC 27551) a été isolée de l'eau d'une rizière et est capable de dégrader le diazinon et le parathion [59] ainsi qu'un certain nombre d'autres OP [78]. L'expression recombinante de l'enzyme OPH de *S. fuliginis* a d'abord été étudiée chez *Streptomyces lividans* [79] permettant de la sécréter de façon soluble à hauteur du milligramme [80,81]. La fabrication de solutions de décontamination des OP a été envisagée, utilisant l'OPH recombinante qui est stable en stockage à long terme après lyophilisation en présence de tréhalose avec une activité accrue en présence de sodium carboxyl polyoxyéthylène tridécyl éther à 0,01 % [82]. La capacité de l'enzyme native à discriminer les énantiomères de certains OP est limitée [83]. Des stratégies d'ingénierie protéique ont donc été considérées pour améliorer cette capacité [70]. Un variant capable d'hydrolyser un analogue chromogénique du stéréoisomère le plus toxique du soman a été produit, environ trois plus efficacement que l'enzyme sauvage [84]. D'autres travaux de mutagenèse ont permis de générer des variants avec des activités améliorées pour le demeton-S methyl, le malathion ou encore le DFP [85,86]. L'utilisation de l'ingénierie protéique a aussi été considérée pour améliorer la dégradation des CWNA [87,88]. Ainsi un

Pour citer cet article : Poirier L, et al. La décontamination des organophosphorés : vers de nouvelles alternatives. Ann Pharm Fr (2017), http://dx.doi.org/10.1016/j.pharma.2017.01.004

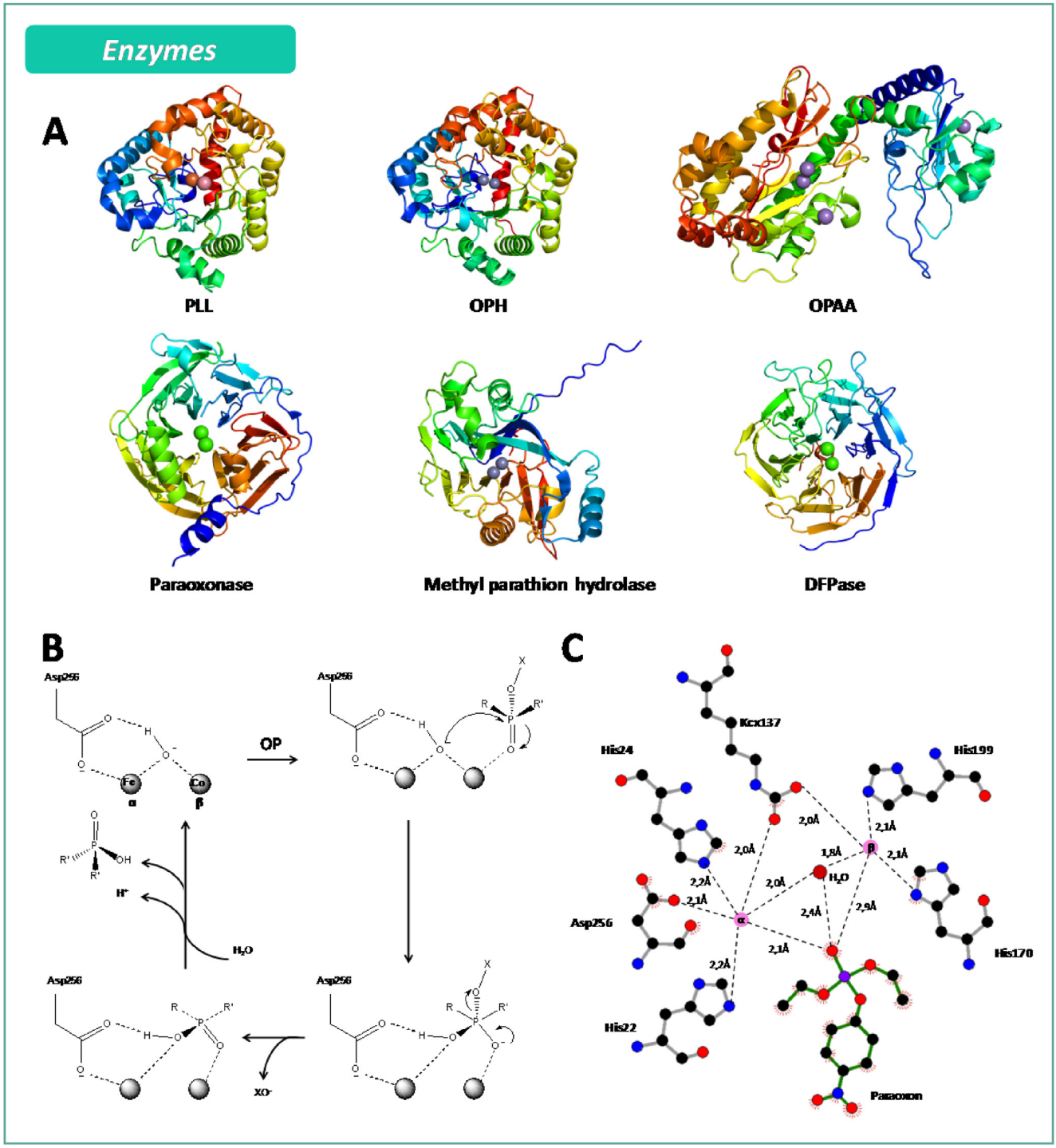


Figure 4. A. Structures tridimensionnelles des principales familles d'enzymes actives pour la décontamination des OP. La PLL *Sso*Pox de *S. solfataricus* (pdb: 2vc5), l'organophosphate hydrolase de *B. diminuta* (pdb: 1dpm), l'organophosphate anhydrolase/prolidase OPAA d'*Alteromonas* sp. (pdb: 3l7g), la serum paraoxonase PON1 (pdb: 1v04), la methyl parathion hydrolase OPHC2 de *P. pseudoalcaligenes* (pdb: 4le6) et la DFPase de *Lolio vulgaris* (pdb: 1e1a) sont ainsi représentées. B. Exemple du mécanisme catalytique de l'enzyme *Sso*Pox [179]. C. Projection du site actif de *Sso*Pox modélisé avec le paraoxon.

A. 3D structures of major decontaminating enzymes. PLL SsoPox from S. solfataricus (pdb: 2vc5), organophosphate hydrolase from B. diminuta (pdb: 1dpm), organophosphate anhydrolase/prolidase OPAA from Alteromonas sp. (pdb: 3l7g), serum paraoxonase PON1 (pdb: 1v04), methyl parathion hydrolase OPHC2 from P. pseudoalcaligenes (pdb: 4le6) and DFPase from Lolio vulgaris (pdb: 1e1a) are presented. B. Example of SsoPox catalytic mechanism [179]. C. 2D projection of SsoPox enzyme docked with paraoxon.

variant 150 fois plus efficace que l'enzyme sauvage, pour l'hydrolyse du VX, a été obtenu.

OPH d'*Agrobacterium radiobacter* (OpdA)

La souche bactérienne *A. radiobacter* P230 exprimant l'enzyme OpdA est capable d'hydrolyser des insecticides OP. La structure de OpdA a été résolue et a permis de mettre en évidence des similarités avec le mécanisme de certaines métallophosphoestérases [89]. L'ingénierie protéique a été utilisée pour améliorer la dégradation des insecticides OP. Une approche rationnelle a permis d'identifier des résidus, impliqués dans la stéréospécificité de l'enzyme, permettant d'obtenir un variant montrant des améliorations d'activité catalytique de 480 fois et 8 fois, respectivement, pour les stéréoisomères *Z* et *E* du chlorfenvinphos. Le potentiel d'OpdA pour dégrader les CWNA a aussi été considéré. L'enzyme hydrolyse le cyclosarin et le soman avec une efficacité de $3{,}9 \times 10^2\,M^{-1}s^{-1}$ et $5{,}8 \times 10^2\,M^{-1}s^{-1}$. Néanmoins, le VX n'est que très faiblement hydrolysé, le k_{cat}/K_M est en effet de $4{,}5\,M^{-1}s^{-1}$ [90]. Trois variants d'OpdA montrent des k_{cat}/K_M allant jusqu'à $1{,}7 \times 10^5\,M^{-1}s^{-1}$ pour le tabun. En revanche, le soman n'est que très peu hydrolysé [91].

Exemples d'utilisation des OPH pour la décontamination des OP

Dans la mesure où les OPH sont des biocatalyseurs efficaces, leur utilisation dans un objectif de décontamination a été envisagée et des stratégies d'immobilisation ont été étudiées. Du trityl-agarose a été utilisé pour l'immobilisation permettant ainsi de maintenir la capacité de l'enzyme à hydrolyser des insecticides OP [92]. De plus, la thermostabilité de l'enzyme immobilisée a été améliorée six fois en comparaison à la forme libre à 55 °C. Un processus d'immobilisation sur nylon a aussi été décrit [93]. Le K_M a été augmenté de 5—6 fois par rapport à l'enzyme soluble, cependant la vitesse maximale d'hydrolyse est réduite à moins de 10 %. Le stockage à long terme est aussi amélioré pour l'enzyme immobilisée. Une autre étude a permis d'immobiliser l'enzyme dans une éponge décontaminante [94]. La phosphotriestérase est alors liée de façon covalente avec une mousse de polyuréthane [95]. La stabilité de l'enzyme est augmentée de façon importante ce qui a suscité un vif intérêt pour la décontamination à large échelle des agents chimiques de guerre [96—98]. Cependant, des limitations technologiques dues à des activités insuffisantes des OPH pour la dégradation des OP les plus toxiques sont apparues [99]. Une immobilisation couplée à une expression en surface a été considérée pour développer un système de décontamination à bas prix [72,100—103]. Récemment, l'OpdA immobilisée de façon covalente sur des textiles de polyester a été reportée offrant un certain nombre de perspectives pour la décontamination environnementale [104]. D'autres exemples d'immobilisation d'OPH sur des nanostructures de fibrilles amyloïdes ou des blocs de copolymères amphiphiles ont été décrit [105,106], ainsi qu'une approche originale consistant à immobiliser l'OPH sur des membranes composées de nanotubes de carbone [107].

DFPase de *Loligo vulgaris*

Une attention spéciale a été apportée à la diisopropylfluorophosphate fluorohydrolase (DFPase, EC 3.1.8.2) issue de *L. vulgaris*. Cette enzyme, issue d'un calmar, hydrolyse efficacement le DFP et le tabun [108,109]. Sa structure 3D a été résolue et consiste en un repliement en hélice de bateau [110,111]. Des études enzymatiques et des expériences de mutagenèse dirigée ont permis de résoudre le mécanisme réactionnel de l'enzyme et d'identifier les résidus essentiels du site actif [110—113]. La production hétérologue de l'enzyme a été réalisée avec un système d'expression chez *E. coli*, une large quantité d'enzyme soluble a été obtenue puis purifiée en utilisant une extension poly-histidine. L'enzyme produite est stable un an à 4 °C [114].

Organophosphate acid anhydrolases (OPAA) et prolidases

Un isolat, provenant d'une bactérie modérément halophile appartenant aux *Alteromonas*, capable d'hydrolyser un certain nombre d'OP a été décrit [115]. À partir de cet extrait, l'enzyme majoritaire OPAA-2, a été purifiée et caractérisée comme un polypeptide de 60 kDa. Cette enzyme est capable d'hydrolyser le DFP ($k_{cat}/K_M = 7{,}7 \times 10^4\,M^{-1}s^{-1}$) ainsi que les agents chimiques de type phosphofluoridate comme le sarin ($k_{cat}/K_M = 2{,}8 \times 10^5\,M^{-1}s^{-1}$), le soman ($k_{cat}/K_M = 6{,}1 \times 10^4\,M^{-1}s^{-1}$) ou le cyclosarin ($k_{cat}/K_M = 9{,}6 \times 10^5\,M^{-1}s^{-1}$). En revanche, elle est faiblement active sur le paraoxon [65,116]. Une attention particulière a été apportée aux souches *Alteromonas* qui ont été criblées pour leur activité d'hydrolyse des OP [117,118]. Beaucoup de gènes codants pour des OPAA ont été identifiés et les enzymes se sont révélées étroitement liées aux prolidases (EC 3.4.13.9). Leur activité de promiscuité permettant à ces enzymes d'hydrolyser des dipeptides avec des prolines en C-terminal (Xaa-Pro) a ainsi été mise en évidence [116,119]. Néanmoins, les OPAA sont particulièrement efficaces pour hydrolyser les OP et elles sont aussi capables de dégrader les agents de guerre de type G. Leur production à large échelle a été démontrée [120—122]. Les substrats et la spécificité stéréochimique d'OPAA, issue de la souche JDS6.5 d'*Alteromonas* sp., ont été analysés et une préférence pour les énantiomères S_p a été mise en évidence [123]. La structure de l'enzyme révèle deux domaines distincts N- et C-terminal. Le domaine C-terminal contient des cations divalent Mn^{2+} et montre un repliement en pain pita [124]. Ce travail a mis en évidence la double activité des OPAA comme prolidase et phosphotriestérase [125]. Les prolidases issues d'organismes hyperthermophiles ont été étudiées notamment celles provenant des souches de *Pyrococcus* sp. Les enzymes venant de *Pyrococcus furiosus* ou *Pyrococcus horikoshii* [126—128], semblent particulièrement intéressantes pour le développement de solutions de décontaminations. Afin d'améliorer leur activité, des stratégies d'ingénierie par mutagenèse aléatoire ont été utilisées permettant d'obtenir des variants efficaces contre les agents chimiques de guerre sur une large gamme de températures [128,129]. L'activité double prolidase/OPAA a aussi été observée pour des prolidases d'origine humaine [130—133]. Ceci est particulièrement intéressant car les

Pour citer cet article : Poirier L, et al. La décontamination des organophosphorés : vers de nouvelles alternatives. Ann Pharm Fr (2017), http://dx.doi.org/10.1016/j.pharma.2017.01.004

enzymes humaines sont extrêmement attrayantes pour le développement de biodécontaminants catalytiques.

Paraoxonase

Une autre classe d'enzyme d'origine humaine, nommée paraoxonase (PON1, EC 3.1.8.1.), a un intérêt considérable. Depuis les premiers rapports décrivant la capacité d'une estérase du sérum de mammifère à dégrader le paraoxon [134] et les agents chimiques de guerre [135,136], de nombreuses études ont été menées [137]. La PON1 est capable d'hydrolyser un large spectre d'insecticides OP [138—140]. Les PON issues de séra de lapin et humain ont été purifiées et ne diffèrent qu'au niveau de la séquence protéique terminale [139,141]. Cependant, la PON1 humaine reste difficile à purifier à partir du plasma et son expression hétérologue ne permet pas d'atteindre des rendements élevés. Les infections par baculovirus et adénovirus de la larve de *Trichoplusia ni* ont toutefois permis la production en grande quantité de la HuPON1 recombinante [142,143]. L'ingénierie d'enzyme a par la suite été utilisée pour obtenir des variants de la PON plus efficaces. Plusieurs études ont ainsi permis de décrypter le rôle des déterminants moléculaires de la catalyse [144,145]. Une description complète du site actif de PON1 a été obtenue en résolvant la structure 3D d'un variant de PON1 recombinante (rePON1-G2E6) exprimé dans *E. coli* et obtenu par évolution dirigée [146,147]. La PON1 des mammifères est plus efficace pour la détoxification du soman et du cyclosarin que l'OPH de *B. diminuta* et la DFPase de *Lolio vulgaris*. Des variants de PON1 ont été améliorés de 10 à 380 fois pour la dégradation du cyclosarin, du soman, du DFP, du parathiol ainsi que du chlorpyrifios-oxon [148]. La spécificité de PON1 vers les isomères *R*p d'analogues fluorogéniques d'agents chimiques de guerre a été mise en évidence [149]. Des expériences d'évolution dirigée ont été réalisées pour améliorer l'efficacité de PON1 pour la dégradation des agents G [150]. Une stratégie d'évolution alliant mutagenèse rationnelle et aléatoire a permis d'isoler un variant 10 000 fois plus actif que l'enzyme sauvage pour dégrader l'analogue du S_p-cyclosarin. Des améliorations notables ont ainsi été obtenues pour la décontamination des agents G, cependant l'hydrolyse des agents V reste problématique. Des expériences in silico ont été utilisées pour mieux comprendre le mécanisme d'hydrolyse du VX par les PON1 et ainsi ouvrir de nouvelles perspectives pour l'ingénierie protéique [151]. Des variants de la PON1 humaine ont été construits et montrent une augmentation de deux fois l'activité catalytique par rapport à l'enzyme sauvage [152]. En outre, les PON ont été également étudiées dans le cadre de la biologie évolutive. Des stratégies originales utilisant par exemple le retour aux formes ancestrales ou consensus ainsi que la dérive génétique neutre ont été employées pour faire évoluer la PON1 de façon non conventionnelle [153—156]. Bien que rarement étudiée, la paraoxonase PON3 a également été purifiée [157,158] puis modifiée par évolution dirigée. L'efficacité catalytique des mutants recombinants de PON3 a été améliorée jusqu'à 240 fois pour le paraoxon [147]. L'activité et la stabilité de PON3 ont de plus été modulées en combinant du brassage génétique et de la mutagenèse basée sur des analyses phylogéniques [154].

Méthylparathion hydrolase

La méthylparathion hydrolase (MPH, EC 3.1.8.1) est une aryldialkylphosphatase appartenant à la famille des métallo-β-lactamases. La structure 3D a été résolue et met en évidence une enzyme dimérique dont chaque sous-unité comporte un centre binucléaire hybride avec du zinc et le métal β le plus exposé au solvant peut être remplacé par du cadmium lorsque celui-ci est présent en solution [159]. Curieusement la MPH est homologue d'autres métallo-β-lactamases mais elle ne présente pas de similarité avec les phosphotriestérases. Une MPH recombinante exprimée chez *E. coli* a été caractérisée et est active sur le méthylparathion ainsi que d'autres insecticides comme le malathion ou le dichlorvos [160]. Une mutagenèse aléatoire de la MPH issue de *Pseudomonas stutzeri*, a permis d'améliorer de 5 fois l'hydrolyse du chlorpyrifos [161]. Une autre MPH, nommée OPHC2, a été identifiée chez la souche C2-1 de *Pseudomonas pseudoalcaligenes* [162] et la souche SMSP-1 de *Stenotrophomonas* sp. [163]. OPHC2 de *P. pseudoalcaligenes* a été caractérisée et sa structure 3D résolue [164,165]. Récemment une enzyme analogue de OPHC2, nommée *Po*OPH provenant de *Pseudomonas oleovorans*, a été découverte [166]. Cette enzyme présente des activités lactonases et arylesterase ainsi qu'une activité de promiscuité OPH. Un variant de $PoOPH_{M2}$ a été construit et son activité améliorée de 7 et 106 fois contre le méthylparathion et l'éthylparaoxon respectivement.

Phosphotriesterase-like lactonase

Parmi les enzymes capables de dégrader les OP, les *phosphotriesterase-like lactonases* (PLL) constituent une famille de protéine prometteuse, proche des phosphotriesterases bactériennes [167,168]. Les PLL sont des lactonases naturelles catalysant l'hydrolyse des *N*-acyl-homoserine lactones (AHL) impliquées dans le système de *quorum* sensing présent chez un certain nombre de bactéries et possèdent de plus une activité de promiscuité OPH [169,170]. Les lactones jouent un rôle physiologique important chez les bactéries compte-tenu de leur implication dans le quorum sensing. Les OP, quant à eux, ont été introduits dans l'environnement depuis seulement quelques décennies comme insecticides, il est probable que l'activité phosphotriestérase des PLL ait émergée à partir d'une lactonase possédant une activité de promiscuité envers les OP probablement pour les utiliser comme source de phosphate dont la disponibilité est limitée dans la nature. Les phosphotriestérases modernes ont donc probablement évoluées à partir d'un ancêtre lactonase ayant perdu sa capacité à hydrolyser les AHL au bénéfice d'une meilleure dégradation des OP parfois proche de la perfection catalytique. Une reconstruction de l'ancêtre de l'OPH de *B. diminuta* a permis de restaurer l'activité lactonase, apportant une preuve expérimentale du lien évolutif entre ces deux activités enzymatiques [171]. Les PLL ont été isolées à partir de différents hôtes comprenant des bactéries hyperthermophiles [172,173], ou des archées [165,174—177]. Ces enzymes font preuve d'une remarquable stabilité à la température, au pH, aux détergents, aux solvants ainsi qu'au stockage, offrant de bonnes perspectives d'utilisations pour la décontamination externe des OP. Une attention particulière a été portée à l'enzyme *Sso*Pox issue

Pour citer cet article : Poirier L, et al. La décontamination des organophosphorés : vers de nouvelles alternatives. Ann Pharm Fr (2017), http://dx.doi.org/10.1016/j.pharma.2017.01.004

de l'archée *Sulfolobus solfataricus*, et les principaux travaux sont résumés ci-après.

SsoPox : un candidat prometteur pour la bioremédiation après contamination par des OP

Une enzyme robuste issue d'une archée hyperthermophile

L'archée *Sulfolobus solfataricus* a été découverte dans les solfatares du Vésuve et possède un gène homologue à celui codant pour la PTE de *B. diminuta*. L'enzyme correspondante a été exprimée et son activité phosphotriestérase, bien que faible, a été mise en évidence. Parmi les substrats hydrolysés on retrouve le paraoxon, c'est pourquoi cette enzyme a été nommée : *S. solftataricus* Paraoxonase [174]. *Sso*Pox hydrolyse efficacement un certain nombre de lactones, parmi lesquelles les *N*-acyl homoserine lactones, qui sont des molécules connues pour leur implication dans la communication bactérienne (*quorum* sensing). En raison de ses origines hyperthermophiles, l'enzyme fait preuve d'une extrême stabilité à la température, elle est active de 10—100 °C, avec une impressionnante température de dénaturation à 106 °C ainsi qu'une grande résistance à la dénaturation par l'urée. Elle est également tolérante aux solvants, à la stérilisation et possède une longue durée de vie [178]. De plus, *Sso*Pox est active sur une large gamme de pH comprise entre pH 5,0 et 9,0 [174]. *Sso*Pox a été cristallisée et sa structure 3D résolue sous la forme *apo* et en complexe [179,180]. La structure montre un repliement en tonneau $(\beta/\alpha)_8$ déformé proche des structures des OPH mésophiles trouvées chez *B. diminuta* et *A. radiobacter*.

Les différences majeures entre *Sso*Pox et les OPH résultent d'un raccourcissement de la boucle 7 ainsi que des deux extrémités de la chaîne polypeptidique. L'arrangement de la boucle 8 est aussi différent entre les structures. Enfin, une boucle additionnelle est observée pour la structure de *Sso*Pox. Ces changements conformationnels sont probablement impliqués dans la stabilité globale de l'enzyme soit en rigidifiant la structure soit en favorisant la formation de dimère. Une analyse des déterminants structurels de *Sso*Pox par rapport à ses homologues mésophiles a été réalisée [181]. Le réseau salin de surface et une structure quaternaire dense contribuent à cette stabilité. La forte similarité des structures et le faible pourcentage d'identité entre les séquences de ces enzymes suggèrent qu'il est possible de trouver un compromis entre activité et stabilité. À partir de ses observations, l'idée est venue de combiner l'incroyable stabilité structurelle de cette enzyme avec l'efficacité catalytique de la PTE de *B. diminuta* en transférant son site actif dans la structure de *Sso*Pox.

Amélioration de l'activité phosphotriestérase de *Sso*Pox

Des stratégies d'ingénierie protéique ont été considérées dans le but d'améliorer le potentiel de l'enzyme pour la décontamination des OP. En effet, une stabilité élevée confère généralement une tolérance aux mutations accrue [182]. Les structures hyperthermophiles sont habituellement de bons candidats pour l'évolution, leur grande stabilité leur permettant de minimiser l'impact délétère de certaines mutations. Une grande diversité de mutations peut ainsi être générée sans effet drastique sur la fonctionnalité de la protéine. En outre, la promiscuité de substrat a été identifiée comme une origine potentielle pour les divergences fonctionnelles qui pourraient être utilisées comme point de départ de stratégies évolutives [183].

Les phosphotriestérases mésophiles ont probablement émergé à partir des PLLs. Leurs séquences et structures respectives ont donc été comparées permettant l'identification de résidus probablement impliqués dans l'amélioration de l'activité phosphotriestérase. Une banque de données mutationnelle listant les substitutions potentiellement bénéfiques pour l'activité phosphotriestérase a été générée [184,185].

Cette base de données combinée à une analyse structurale in silico a été utilisée comme point de départ pour l'ingénierie sur *Sso*Pox pour la dégradation des OP. Des variants présentant des améliorations d'activité jusqu'à 2000 fois pour certains pesticides et un champ d'action élargi ont été obtenus (données non publiées). Les mutations R223H et Y97W sont également connues pour affecter l'activité phosphotriestérase [179]. Le remplacement du résidu W263 a aussi été étudié [186]. Ce résidu est localisé dans le site actif et est impliqué dans la flexibilité conformationnelle de l'enzyme, jouant un rôle prépondérant dans sa promiscuité de substrat. Une mutagenèse à saturation a été réalisée sur cette position en utilisant des amorces dégénérées. Deux sous-ensembles de mutations se distinguent favorisant soit l'activité lactonase soit phosphotriestérase. Pour cette dernière les variants W263F, W263L et W263M sont particulièrement intéressants. *Sso*Pox et ses variants sont actifs sur un large panel d'OP, dont des insecticides (ex. paraoxon, parathion, malathion...) et des analogues d'agents neurotoxiques de guerre (IMP-, PinP- et CMP-coumarin). La stimulation de l'activité de *Sso*Pox par des détergents anioniques à température ambiante a aussi été mise en évidence ce qui s'avère extrêmement intéressant pour la décontamination externe car cela peut améliorer la décontamination de surfaces par action mécanique [186]. Des expériences d'ingénierie sur *Sso*Pox sont en cours dans le but d'obtenir un catalyseur stable, efficace et capable de dégrader un large spectre d'OP.

Conclusion

Les méthodes de décontamination des OP ont été étudiées de façon exhaustive au cours des dernières décennies. Des méthodes physicochimiques efficaces comme l'hypochlorite et l'hydroxyde de sodium ont émergé pour la décontamination externe ou la destruction des stocks. Cependant, ces méthodes sont les plus souvent agressives et sont incompatibles avec la décontamination des personnes ou du matériel sensible.

D'autres méthodes ont été développées telles que le RSDL ou la terre à foulon. Bien que la RSDL soit efficace pour décontaminer la peau à l'échelle individuelle, cette technique n'est pas applicable sur les yeux ni les blessures et reste difficilement envisageable en cas de contamination

Pour citer cet article : Poirier L, et al. La décontamination des organophosphorés : vers de nouvelles alternatives. Ann Pharm Fr (2017), http://dx.doi.org/10.1016/j.pharma.2017.01.004

de masse. La terre à foulon fait preuve d'une bonne adsorption topique des contaminants, mais n'est pas capable de dégrader les OP. Son utilisation peut cependant générer des poussières toxiques pendant le processus de décontamination, rendant cette technique inappropriée à grande échelle.

Des méthodes photochimiques sont également en développement pour la minéralisation des OP dans un milieu environnemental mais ne sont pas envisageables pour la décontamination des personnes. D'autres stratégies comme les CD sont donc envisagées comme biodécontaminant. Néanmoins leur action stœchiométrique (ou faiblement catalytiques) pose un problème de compétitivité. Ainsi les enzymes bioépuratrices suscitent un intérêt grandissant. En effet, l'utilisation d'enzymes est attrayante car elles offrent une décontamination des OP catalytique, non corrosive et non toxique et sans danger pour l'environnement. L'ingénierie protéique a été utilisée pour améliorer les efficacités catalytiques des enzymes recombinantes. La stabilité et les coûts de production des enzymes peuvent cependant poser problème. La découverte d'enzymes hautement résistantes et capables de dégrader les OP comme *Sso*Pox ouvre de nouvelles perspectives. Par ailleurs, les enzymes sont aussi utilisables comme épurateurs catalytiques dans le pré-traitement et le traitement des intoxications aux OP [187]. L'utilisation des techniques d'ingénierie enzymatique devrait permettre à moyen terme de mettre au point des biocatalyseurs compétitifs et efficaces pour le traitement des intoxications et la bioremédiation consécutive à l'épandage d'insecticides et d'agents de guerre OP.

Remerciements

Ce travail a été réalisé dans le cadre d'un contrat DGA-PEA (DANUBE).

P.J. et L.P. sont des doctorants financés par la Direction générale de l'armement (DGA).

Déclaration de liens d'intérêts

M.E., D.D. et E.C. : intérêts financiers dans l'entreprise Gene&GreenTK.

M.E. et E.C. ont un brevet WO2014167140 A1 licencié à Gene&GreenTK.

Références

[1] Szinicz L. History of chemical and biological warfare agents. Toxicology 2005;214:167—81, http://dx.doi.org/10.1016/j.tox.2005.06.011.

[2] Gupta RC. Handbook of toxicology of chemical warfare agents. Academic Press; 2009.

[3] Organisation for the prohibition of chemical weapons. Convention on the prohibition of the development, production, stockpiling and use of chemical weapons and on their destruction. 3rd ed. Hague: The Technical Secretariat of the Organisation for the Prohibition of Chemical Weapons; 2005.

[4] Jaipieam S, Visuthismajarn P, Sutheravut P, Siriwong W, Thoumsang S, Borjan M, et al. Organophosphate pesticide residues in drinking water from artesian wells and health risk assessment of agricultural communities, Thailand. Hum Ecol Risk Assess Int J 2009;15:1304—16, http://dx.doi.org/10.1080/10807030903306984.

[5] Gunnell D, Eddleston M, Phillips MR, Konradsen F. The global distribution of fatal pesticide self-poisoning: systematic review. BMC Public Health 2007;7:357, http://dx.doi.org/10.1186/1471-2458-7-357.

[6] Patel V, Ramasundarahettige C, Vijayakumar L, Thakur J, Gajalakshmi V, Gururaj G, et al. Suicide mortality in India: a nationally representative survey. Lancet 2012;379:2343—51, http://dx.doi.org/10.1016/S0140-6736(12)60606-0.

[7] Zwiener RJ, Ginsburg CM. Organophosphate and carbamate poisoning in infants and children. Pediatrics 1988;81:121—6.

[8] Lessenger JE, Reese BE. Rational use of cholinesterase activity testing in pesticide poisoning. J Am Board Fam Pract 1999;12:307—14, http://dx.doi.org/10.3122/jabfm.12.4.307.

[9] Beauregard G, Lum J, Roufogalis BD. Effect of histidine modification on the aging of organophosphate-inhibited acetylcholinesterase. Biochem Pharmacol 1981;30:2915—20, http://dx.doi.org/10.1016/0006-2952(81)90252-5.

[10] Tuorinsky SD, Caneva DC, Sidell FR. Triage of chemical casualties. In: Chemical aspects of chemical warfare. Washington DC: Walter Reed Army Medical Center Borden Institute; 2009. p. 511—26.

[11] Singh B, Prasad GK, Pandey KS, Danikhel RK, Vijayaraghavan R. Decontamination of chemical warfare agents (review article). Def Sci J 2010;60:428—41, http://dx.doi.org/10.14429/dsj.60.487.

[12] Khan A, Kotta S, Ansari S, Ali J, Sharma R. Recent advances in decontamination of chemical warfare agents. Def Sci J 2013;63:487—96, http://dx.doi.org/10.14429/dsj.63.2882.

[13] Braue Jr EH, Smith KH, Doxzon BF, Lumpkin HL, Clarkson ED. Evaluation of RSDL, M291 SDK, 0.5 % bleach, 1 % soapy water and SERPACWA. Part 2. Challenge with Soman. Army Medical Research Institute of Chemical Defense Aberdeen Proving Ground MD: DTIC Document: ADA539735; 2010.

[14] Braue Jr EH, Smith KH, Doxzon BF, Lumpkin HL, Clarkson ED. Evaluation of RSDL, M291 SDK, 0.5 % bleach, 1 % soapy water and SERPACWA. Part 1. Challenge with VX. Army Medical Research Institute of Chemical Defense Aberdeen Proving Ground MD: DTIC Document: ADA525186; 2010.

[15] Bannard RAB, Casselman AA, Purdon JG, Bovenkamp JW. Broad spectrum chemical decontaminant system; 1991 [Patent US 5:075, 297].

[16] Elsinghorst PW, Worek F, Koller M. Detoxification of organophosphorus pesticides and nerve agents through RSDL: efficacy evaluation by 31P NMR spectroscopy. Toxicol Lett 2015;233:207—13, http://dx.doi.org/10.1016/j.toxlet.2014.12.004.

[17] Taysse L, Daulon S, Delamanche S, Bellier B, Breton P. Skin decontamination of mustards and organophosphates: comparative efficiency of RSDL and Fuller's earth in domestic swine. Hum Exp Toxicol 2007;26:135—41.

[18] Sambrook MR, Notman S. Supramolecular chemistry and chemical warfare agents: from fundamentals of recognition to catalysis and sensing. Chem Soc Rev 2013;42:9251, http://dx.doi.org/10.1039/c3cs60230c.

[19] Désiré B, Saint-André S. Interaction of soman with beta-cyclodextrin. Fundam Appl Toxicol 1986;7:646—57.

[20] Désiré B, Saint-André S. Inactivation of sarin and soman by cyclodextrins in vitro. Experientia 1987;43:395—7.

[21] Masurier N, Lafont O, Estour F. Les cyclodextrines substituées : un exemple de catalyseurs biomimétiques. Ann Pharm Fr 2007;65:126—33, http://dx.doi.org/10.1016/S0003-4509(07)90026-7.

Pour citer cet article : Poirier L, et al. La décontamination des organophosphorés : vers de nouvelles alternatives. Ann Pharm Fr (2017), http://dx.doi.org/10.1016/j.pharma.2017.01.004

[22] Hoskin FC, Steeves DM, Walker JE. Substituted cyclodextrin as a model for a squid enzyme that hydrolyzes the nerve gas soman. Biol Bull 1999;197:284—5.
[23] Letort S, Mathiron D, Grel T, Albaret C, Daulon S, Djedaïni-Pilard F, et al. The first 2 ^{IB},3 ^{IA} -heterodifunctionalized β-cyclodextrin derivatives as artificial enzymes. Chem Commun 2015;51:2601—4, http://dx.doi.org/10.1039/C4CC09189B.
[24] Wille T, Tenberken O, Reiter G, Müller S, Le Provost R, Lafont O, et al. Detoxification of nerve agents by a substituted β-cyclodextrin: application of a modified biological assay. Toxicology 2009;265:96—100, http://dx.doi.org/10.1016/j.tox.2009.09.018.
[25] Kalakuntla RK, Wille T, Le Provost R, Letort S, Reiter G, Müller S, et al. New modified β-cyclodextrin derivatives as detoxifying agents of chemical warfare agents (I). Synthesis and preliminary screening: evaluation of the detoxification using a half-quantitative enzymatic assay. Toxicol Lett 2013;216:200—5, http://dx.doi.org/10.1016/j.toxlet.2012.11.020.
[26] Masurier N, Estour F, Froment M-T, Lefèvre B, Debouzy J-C, Brasme B, et al. Synthesis of 2-substituted β-cyclodextrin derivatives with a hydrolytic activity against the organophosphorylester paraoxon. Eur J Med Chem 2005;40:615—23, http://dx.doi.org/10.1016/j.ejmech.2005.02.008.
[27] Estour F, Letort S, Müller S, Kalakuntla RK, Le Provost R, Wille T, et al. Functionalized cyclodextrins bearing an alpha nucleophile — A promising way to degrade nerve agents. Chem Biol Interact 2013;203:202—7, http://dx.doi.org/10.1016/j.cbi.2012.10.020.
[28] Reddy PVL, Kim K-H. A review of photochemical approaches for the treatment of a wide range of pesticides. J Hazard Mater 2015;285:325—35, http://dx.doi.org/10.1016/j.jhazmat.2014.11.036.
[29] Hossain MS, Fakhruddin ANM, Chowdhury MAZ, Alam MK. Degradation of chlorpyrifos, an organophosphorus insecticide in aqueous solution with gamma irradiation and natural sunlight. J Environ Chem Eng 2013;1:270—4, http://dx.doi.org/10.1016/j.jece.2013.05.006.
[30] Wan HB, Wong MK, Mok CY. Comparative study on the quantum yields of direct photolysis of organophosphorus pesticides in aqueous solution. J Agric Food Chem 1994;42:2625—30, http://dx.doi.org/10.1021/jf00047a046.
[31] Sinderhauf K, Schwack W. Photolysis experiments on phosmet, an organophosphorus insecticide. J Agric Food Chem 2003;51:5990—5, http://dx.doi.org/10.1021/jf034253y.
[32] Gonçalves C, Dimou A, Sakkas V, Alpendurada MF, Albanis TA. Photolytic degradation of quinalphos in natural waters and on soil matrices under simulated solar irradiation. Chemosphere 2006;64:1375—82, http://dx.doi.org/10.1016/j.chemosphere.2005.12.020.
[33] Segal-Rosenheimer M, Dubowski Y. Photolysis of methyl parathion thin films: products, kinetics and quantum yields under different atmospheric conditions. J Photochem Photobiol Chem 2010;209:193—202, http://dx.doi.org/10.1016/j.jphotochem.2009.11.014.
[34] Muñoz A, Person AL, Calvé SL, Mellouki A, Borrás E, Daële V, et al. Studies on atmospheric degradation of diazinon in the EUPHORE simulation chamber. Chemosphere 2011;85:724—30, http://dx.doi.org/10.1016/j.chemosphere.2011.06.044.
[35] Lam MW, Tantuco K, Mabury SA. PhotoFate: a new approach in accounting for the contribution of indirect photolysis of pesticides and pharmaceuticals in surface waters. Environ Sci Technol 2003;37:899—907, http://dx.doi.org/10.1021/es025902+.
[36] Garbin JR, Milori DMBP, Simões ML, da Silva WTL, Neto LM. Influence of humic substances on the photolysis of aqueous pesticide residues. Chemosphere 2007;66:1692—8, http://dx.doi.org/10.1016/j.chemosphere.2006.07.017.
[37] Wu C, Linden KG. Phototransformation of selected organophosphorus pesticides: Roles of hydroxyl and carbonate radicals. Water Res 2010;44:3585—94, http://dx.doi.org/10.1016/j.watres.2010.04.011.
[38] Kim S-M, Vogelpohl A. Degradation of organic pollutants by the photo-Fenton-process. Chem Eng Technol 1998:187—91.
[39] Ikehata K, El-Din MG. Aqueous pesticide degradation by hydrogen peroxide/ultraviolet irradiation and Fenton-type advanced oxidation processes: a review. J Environ Eng Sci 2006;5:81—135, http://dx.doi.org/10.1139/S05-046.
[40] Balkaya N. A study of optimal experimental conditions in the photocatalytic degradation of an organophosphorous insecticide. Environ Technol 1999;20:617—23, http://dx.doi.org/10.1080/09593332008616856.
[41] Konstantinou IK, Sakellarides TM, Sakkas VA, Albanis TA. Photocatalytic degradation of selected s-Triazine herbicides and organophosphorus insecticides over aqueous TiO2 suspensions. Environ Sci Technol 2001;35:398—405, http://dx.doi.org/10.1021/es001271c.
[42] Li L, Wu Q, Guo Y, Hu C. Nanosize and bimodal porous polyoxotungstate—anatase TiO2 composites: preparation and photocatalytic degradation of organophosphorus pesticide using visible-light excitation. Microporous Mesoporous Mater 2005;87:1—9, http://dx.doi.org/10.1016/j.micromeso.2005.07.035.
[43] Evgenidou E, Konstantinou I, Fytianos K, Albanis T. Study of the removal of dichlorvos and dimethoate in a titanium dioxide mediated photocatalytic process through the examination of intermediates and the reaction mechanism. J Hazard Mater 2006;137:1056—64, http://dx.doi.org/10.1016/j.jhazmat.2006.03.042.
[44] Chen H, Shen M, Chen R, Dai K, Peng T. Photocatalytic degradation of commercial methyl parathion in aqueous suspension containing La-doped TiO2 nanoparticles. Environ Technol 2011;32:1515—22, http://dx.doi.org/10.1080/09593330.2010.543927.
[45] Jonidi-Jafari A, Shirzad-Siboni M, Yang J-K, Naimi-Joubani M, Farrokhi M. Photocatalytic degradation of diazinon with illuminated ZnO—TiO2 composite. J Taiwan Inst Chem Eng 2015;50:100—7, http://dx.doi.org/10.1016/j.jtice.2014.12.020.
[46] Kamiya M, Kameyama K. Effects of selected metal ions on photodegradation of organophosphorus pesticides sensitized by humic acids. Chemosphere 2001;45:231—5, http://dx.doi.org/10.1016/S0045-6535(00)00573-7.
[47] Nowakowska M, Sterzel M, Zapotoczny S, Kot E. Photosensitized degradation of ethyl parathion pesticide in aqueous solution of anthracene modified photoactive dextran. Appl Catal B Environ 2005;57:1—8, http://dx.doi.org/10.1016/j.apcatb.2004.10.002.
[48] Zuo G-M, Cheng Z-X, Li G-W, Shi W-P, Miao T. Study on photolytic and photocatalytic decontamination of air polluted by chemical warfare agents (CWAs). Chem Eng J 2007;128:135—40, http://dx.doi.org/10.1016/j.cej.2006.10.006.
[49] Kim SH, Kim JH, Kang B-K. Decomposition reaction of organophosphorus nerve agents on solid surfaces with atmospheric radio frequency plasma generated gaseous species. Langmuir 2007;23:8074—8, http://dx.doi.org/10.1021/la700692t.
[50] Lee J, Farha OK, Roberts J, Scheidt KA, Nguyen ST, Hupp JT. Metal—organic framework materials as catalysts. Chem Soc Rev 2009;38:1450, http://dx.doi.org/10.1039/b807080f.
[51] DeCoste JB, Peterson GW. Metal—organic frameworks for air purification of toxic chemicals. Chem Rev 2014;114:5695—727, http://dx.doi.org/10.1021/cr4006473.
[52] Mondloch JE, Katz MJ, Isley III WC, Ghosh P, Liao P, Bury W, et al. Destruction of chemical warfare agents

Pour citer cet article : Poirier L, et al. La décontamination des organophosphorés : vers de nouvelles alternatives. Ann Pharm Fr (2017), http://dx.doi.org/10.1016/j.pharma.2017.01.004

using metal–organic frameworks. Nat Mater 2015;14:512–6, http://dx.doi.org/10.1038/nmat4238.
[53] Bai Y, Chen J, Yang Y, Guo L, Zhang C. Degradation of organophosphorus pesticide induced by oxygen plasma: effects of operating parameters and reaction mechanisms. Chemosphere 2010;81:408–14, http://dx.doi.org/10.1016/j.chemosphere.2010.06.071.
[54] Hu Y, Bai Y, Yu H, Zhang C, Chen J. Degradation of selected organophosphate pesticides in wastewater by dielectric barrier discharge plasma. Bull Environ Contam Toxicol 2013;91:314–9, http://dx.doi.org/10.1007/s00128-013-1048-x.
[55] Basfar AA, Mohamed KA, Al-Abduly AJ, Al-Kuraiji TS, Al-Shahrani AA. Degradation of diazinon contaminated waters by ionizing radiation. Radiat Phys Chem 2007;76:1474–9, http://dx.doi.org/10.1016/j.radphyschem.2007.02.055.
[56] Mohamed KA, Basfar AA, Al-Kahtani HA, Al-Hamad KS. Radiolytic degradation of malathion and lindane in aqueous solutions. Radiat Phys Chem 2009;78:994–1000, http://dx.doi.org/10.1016/j.radphyschem.2009.06.003.
[57] Schomburg PDD, Stephan DD. Aryldialkylphosphatase. In: Schomburg PDD, Stephan DD, editors. Enzyme Handbook 15. Berlin; Heidelberg: Springer; 1998. p. 201–6.
[58] Seibert CM, Raushel FM. Structural and catalytic diversity within the amidohydrolase superfamily. Biochemistry (Mosc) 2005;44:6383–91, http://dx.doi.org/10.1021/bi047326v.
[59] Sethunathan N, Yoshida T. A *Flavobacterium* sp. that degrades diazinon and parathion. Can J Microbiol 1973;19:873–5, http://dx.doi.org/10.1139/m73-138.
[60] Serdar CM, Gibson DT, Munnecke DM, Lancaster JH. Plasmid involvement in parathion hydrolysis by *Pseudomonas diminuta*. Appl Environ Microbiol 1982;44:246–9.
[61] Mulbry WW, Karns JS, Kearney PC, Nelson JO, McDaniel CS, Wild JR. Identification of a plasmid-borne parathion hydrolase gene from *Flavobacterium* sp. by southern hybridization with opd from *Pseudomonas diminuta*. Appl Environ Microbiol 1986;51:926–30.
[62] Harper LL, McDaniel CS, Miller CE, Wild JR. Dissimilar plasmids isolated from *Pseudomonas diminuta* MG and a *Flavobacterium* sp. (ATCC 27551) contain identical opd genes. Appl Environ Microbiol 1988;54:2586–9.
[63] Horne I, Sutherland TD, Harcourt RL, Russell RJ, Oakeshott JG. Identification of an opd (organophosphate degradation) gene in an *Agrobacterium* isolate. Appl Environ Microbiol 2002;68:3371–6, http://dx.doi.org/10.1128/AEM.68.7.3371-3376.2002.
[64] Horne I, Qiu X, Russell RJ, Oakeshott JG. The phosphotriesterase gene opdA in *Agrobacterium radiobacter* P230 is transposable. FEMS Microbiol Lett 2003;222:1–8, http://dx.doi.org/10.1016/S0378-1097(03)00211-8.
[65] Theriot CM, Grunden AM. Hydrolysis of organophosphorus compounds by microbial enzymes. Appl Microbiol Biotechnol 2010;89:35–43, http://dx.doi.org/10.1007/s00253-010-2807-9.
[66] Wales ME, Reeves TE. Organophosphorus hydrolase as an in vivo catalytic nerve agent bioscavenger. Drug Test Anal 2012;4:271–81, http://dx.doi.org/10.1002/dta.381.
[67] Dumas DP, Caldwell SR, Wild JR, Raushel FM. Purification and properties of the phosphotriesterase from *Pseudomonas diminuta*. J Biol Chem 1989;264:19659–65.
[68] Dumas DP, Durst HD, Landis WG, Raushel FM, Wild JR. Inactivation of organophosphorus nerve agents by the phosphotriesterase from *Pseudomonas diminuta*. Arch Biochem Biophys 1990;277:155–9, http://dx.doi.org/10.1016/0003-9861(90)90564-F.
[69] Benning MM, Kuo JM, Raushel FM, Holden HM. Three-dimensional structure of phosphotriesterase: an enzyme capable of detoxifying organophosphate nerve agents. Biochemistry (Mosc) 1994;33:15001–7, http://dx.doi.org/10.1021/bi00254a008.
[70] Iyer R, Iken B. Protein engineering of representative hydrolytic enzymes for remediation of organophosphates. Biochem Eng J 2015;94:134–44, http://dx.doi.org/10.1016/j.bej.2014.11.010.
[71] Watkins LM, Mahoney HJ, McCulloch JK, Raushel FM. Augmented hydrolysis of diisopropyl fluorophosphate in engineered mutants of phosphotriesterase. J Biol Chem 1997;272:25596–601, http://dx.doi.org/10.1074/jbc.272.41.25596.
[72] Cho CM-H, Mulchandani A, Chen W. Bacterial cell surface display of organophosphorus hydrolase for selective screening of improved hydrolysis of organophosphate nerve agents. Appl Environ Microbiol 2002;68:2026–30, http://dx.doi.org/10.1128/AEM.68.4.2026-2030.2002.
[73] Cho CM-H, Mulchandani A, Chen W. Altering the substrate specificity of organophosphorus hydrolase for enhanced hydrolysis of chlorpyrifos. Appl Environ Microbiol 2004;70:4681–5, http://dx.doi.org/10.1128/AEM.70.8.4681-4685.2004.
[74] Roodveldt C, Tawfik DS. Directed evolution of phosphotriesterase from *Pseudomonas diminuta* for heterologous expression in *Escherichia coli* results in stabilization of the metal-free state. Protein Eng Des Sel 2005;18:51–8, http://dx.doi.org/10.1093/protein/gzi005.
[75] Chen-Goodspeed M, Sogorb MA, Wu F, Raushel FM. Enhancement, relaxation, and reversal of the stereoselectivity for phosphotriesterase by rational evolution of active site residues. Biochemistry (Mosc) 2001;40:1332–9, http://dx.doi.org/10.1021/bi001549d.
[76] Cherny I, Greisen P, Ashani Y, Khare SD, Oberdorfer G, Leader H, et al. Engineering V-type nerve agents detoxifying enzymes using computationally focused libraries. ACS Chem Biol 2013;8:2394–403, http://dx.doi.org/10.1021/cb4004892.
[77] Bigley AN, Xu C, Henderson TJ, Harvey SP, Raushel FM. Enzymatic neutralization of the chemical warfare agent VX: evolution of phosphotriesterase for phosphorothiolate hydrolysis. J Am Chem Soc 2013;135:10426–32, http://dx.doi.org/10.1021/ja402832.
[78] Brown KA. Phosphotriesterases of *Flavobacterium* sp. Soil Biol Biochem 1980;12:105–12, http://dx.doi.org/10.1016/0038-0717(80)90044-9.
[79] Rowland SS, Speedie MK, Pogell BM. Purification and characterization of a secreted recombinant phosphotriesterase (parathion hydrolase) from *Streptomyces lividans*. Appl Environ Microbiol 1991;57:440–4.
[80] Steiert JG, Pogell BM, Speedie MK, Laredo J. A gene coding for a membrane–bound hydrolase is expressed as a secreted, soluble enzyme in *Streptomyces Lividans*. Nat Biotechnol 1989;7:65–8, http://dx.doi.org/10.1038/nbt0189-65.
[81] Rowland SS, Zulty JJ, Sathyamoorthy M, Pogell BM, Speedie MK. The effect of signal sequences on the efficiency of secretion of a heterologous phosphotriesterase by *Streptomyces lividans*. Appl Microbiol Biotechnol 1992;38:94–100, http://dx.doi.org/10.1007/BF00169426.
[82] Sode K, Nakamura H. Compatibility of phosphotriesterase from *Flavobacterium* sp. with detergents. Biotechnol Lett 1997;19:1239–42, http://dx.doi.org/10.1023/A:1018402407802.
[83] Ohuchi S, Nakamura H, Sligiura H, Narita M, Sode K. An optical resolution of racemic organophosphorous esters by phosphotriesterase-catalyzing hydrolysis. Appl Biochem Biotechnol 1997;63–65:659–65, http://dx.doi.org/10.1007/BF02920464.
[84] Hill CM, Li W-S, Thoden JB, Holden HM, Raushel FM. Enhanced degradation of chemical warfare agents through molecular engineering of the phosphotriesterase

Pour citer cet article : Poirier L, et al. La décontamination des organophosphorés : vers de nouvelles alternatives. Ann Pharm Fr (2017), http://dx.doi.org/10.1016/j.pharma.2017.01.004

active site. J Am Chem Soc 2003;125:8990—1, http://dx.doi.org/10.1021/ja0358798.
[85] Gopal S, Rastogi V, Ashman W, Mulbry W. Mutagenesis of organophosphorus hydrolase to enhance hydrolysis of the nerve agent VX. Biochem Biophys Res Commun 2000;279:516—9, http://dx.doi.org/10.1006/bbrc.2000.4004.
[86] Schofield DA, DiNovo AA. Generation of a mutagenized organophosphorus hydrolase for the biodegradation of the organophosphate pesticides malathion and demeton-S. J Appl Microbiol 2010;109:548—57, http://dx.doi.org/10.1111/j.1365-2672.2010.04672.x.
[87] Jeong Y-S, Choi JM, Kyeong H-H, Choi J-Y, Kim E-J, Kim H-S. Rational design of organophosphorus hydrolase with high catalytic efficiency for detoxifying a V-type nerve agent. Biochem Biophys Res Commun 2014;449:263—7, http://dx.doi.org/10.1016/j.bbrc.2014.04.155.
[88] Nakayama K, Ishikawa S, Kawahara K, Ohmori T, Seto Y. Improvement of organophosphorus hydrolase activity toward nerve agents by amino acid substitutions. Forensic Toxicol 2014, http://dx.doi.org/10.1007/s11419-013-0223-4.
[89] Jackson C, Kim H-K, Carr PD, Liu J-W, Ollis DL. The structure of an enzyme—product complex reveals the critical role of a terminal hydroxide nucleophile in the bacterial phosphotriesterase mechanism. Biochim Biophys Acta 2005;1752:56—64, http://dx.doi.org/10.1016/j.bbapap.2005.06.008.
[90] Wille T, Scott C, Thiermann H, Worek F. Detoxification of G- and V-series nerve agents by the phosphotriesterase OpdA. Biocatal Biotransformation 2012;30:203—8, http://dx.doi.org/10.3109/10242422.2012.661724.
[91] Dawson RM, Pantelidis S, Rose HR, Kotsonis SE. Degradation of nerve agents by an organophosphate-degrading agent (OpdA). J Hazard Mater 2008;157:308—14, http://dx.doi.org/10.1016/j.jhazmat.2007.12.099.
[92] Caldwell SR, Raushel FM. Detoxification of organophosphate pesticides using an immobilized phosphotriesterase from *Pseudomonas diminuta*. Biotechnol Bioeng 1991;37:103—9, http://dx.doi.org/10.1002/bit.260370203.
[93] Caldwell SR, Raushel FM. Detoxification of organophosphate pesticides using a nylon based immobilized phosphotriesterase from *Pseudomonas diminuta*. Appl Biochem Biotechnol 1991;31:59—73, http://dx.doi.org/10.1007/BF02922126.
[94] Havens PL, Rase HF. Reusable immobilized enzyme/polyurethane sponge for removal and detoxification of localized organophosphate pesticide spills. Ind Eng Chem Res 1993;32:2254—8, http://dx.doi.org/10.1021/ie00022a009.
[95] LeJeune KE, Russell AJ. Covalent binding of a nerve agent hydrolyzing enzyme within polyurethane foams. Biotechnol Bioeng 1996;51:450—7 [doi:10.1002/(SICI)1097-0290(19960820)51:4<450::AID-BIT8>3.0.CO;2-H].
[96] LeJeune KE, Mesiano AJ, Bower SB, Grimsley JK, Wild JR, Russell AJ. Dramatically stabilized phosphotriesterase—polymers for nerve agent degradation. Biotechnol Bioeng 1997;54:105—14 [doi:10.1002/(SICI)1097-0290(19970420)54:2<105::AID-BIT2>3.0.CO;2-P].
[97] LeJeune KE, Wild JR, Russell AJ. Nerve agents degraded by enzymatic foams. Nature 1998;395:27—8, http://dx.doi.org/10.1038/25634.
[98] LeJeune KE, Russell AJ. Biocatalytic nerve agent detoxification in fire fighting foams. Biotechnol Bioeng 1999;62:659—65 [doi:10.1002/(SICI)1097-0290(19990320)62:6<659::AID-BIT5>3.0.CO;2-N].
[99] Donarski WJ, Dumas DP, Heitmeyer DP, Lewis VE, Raushel FM. Structure-activity relationships in the hydrolysis of substrates by the phosphotriesterase from *Pseudomonas diminuta*. Biochemistry (Mosc) 1989;28:4650—5, http://dx.doi.org/10.1021/bi00437a021.
[100] Richins RD, Kaneva I, Mulchandani A, Chen W. Biodegradation of organophosphorus pesticides by surface-expressed organophosphorus hydrolase. Nat Biotechnol 1997;15:984—7, http://dx.doi.org/10.1038/nbt1097-984.
[101] Chen W, Richins RD, Mulchandani P, Kaneva I, Mulchandani A. Biodegradation of organophosphorus nerve agents by surface-expressed organophosphorus hydrolase. In: Zwanenburg B, Mikołajczyk M, Kiełbasiński P, editors. Enzym. Action. Netherlands: Springer; 2000. p. 211—21.
[102] Richins RD, Mulchandani A, Chen W. Expression, immobilization, and enzymatic characterization of cellulose-binding domain-organophosphorus hydrolase fusion enzymes. Biotechnol Bioeng 2000;69:591—6 [doi:10.1002/1097-0290(20000920)69:6<591::AID-BIT2>3.0.CO;2-X].
[103] Mansee AH, Chen W, Mulchandani A. Detoxification of the organophosphate nerve agent coumaphos using organophosphorus hydrolase immobilized on cellulose materials. J Ind Microbiol Biotechnol 2005;32:554—60, http://dx.doi.org/10.1007/s10295-005-0059-y.
[104] Gao Y, Truong YB, Cacioli P, Butler P, Kyratzis IL. Bioremediation of pesticide contaminated water using an organophosphate-degrading enzyme-immobilized on nonwoven polyester textiles. Enzyme Microb Technol 2014;54:38—44, http://dx.doi.org/10.1016/j.enzmictec.2013.10.001.
[105] Raynes JK, Pearce FG, Meade SJ, Gerrard JA. Immobilization of organophosphate hydrolase on an amyloid fibril nanoscaffold: towards bioremediation and chemical detoxification. Biotechnol Prog 2011;27:360—7, http://dx.doi.org/10.1002/btpr.518.
[106] Suthiwangcharoen N, Nagarajan R. Enhancing enzyme stability by construction of polymer—enzyme conjugate micelles for decontamination of organophosphate agents. Biomacromolecules 2014;15:1142—52, http://dx.doi.org/10.1021/bm401531d.
[107] Mechrez G, Krepker MA, Harel Y, Lellouche J-P, Segal E. Biocatalytic carbon nanotube paper: a ''one-pot'' route for fabrication of enzyme-immobilized membranes for organophosphate bioremediation. J Mater Chem B 2014;2:915, http://dx.doi.org/10.1039/c3tb21439g.
[108] Hoskin FCG. Diisopropylphosphorofluoridate and tabun: enzymatic hydrolysis and nerve function. Science 1971;172:1243—5, http://dx.doi.org/10.1126/science.172.3989.1243.
[109] Hoskin FC, Roush AH. Hydrolysis of nerve gas by squid-type diisopropyl phosphorofluoridate hydrolyzing enzyme on agarose resin. Science 1982;215:1255—7, http://dx.doi.org/10.1126/science.7058344.
[110] Scharff EI, Koepke J, Fritzsch G, Lücke C, Rüterjans H. Crystal structure of diisopropylfluorophosphatase from *Loligo vulgaris*. Structure 2001;9:493—502, http://dx.doi.org/10.1016/S0969-2126(01)00610-4.
[111] Scharff EI, Lücke C, Fritzsch G, Koepke J, Hartleib J, Dierl S, et al. Crystallization and preliminary X-ray crystallographic analysis of DFPase from *Loligo vulgaris*. Acta Crystallogr D Biol Crystallogr 2001;57:148—9, http://dx.doi.org/10.1107/S0907444900014232.
[112] Hartleib J, Rüterjans H. Insights into the reaction mechanism of the diisopropyl fluorophosphatase from *Loligo vulgaris* by means of kinetic studies, chemical modification and site-directed mutagenesis. Biochim Biophys Acta 2001;1546:312—24, http://dx.doi.org/10.1016/S0167-4838(01)00153-4.
[113] Katsemi V, Lücke C, Koepke J, Löhr F, Maurer S, Fritzsch G, et al. Mutational and structural studies of the diisopropylfluorophosphatase from Loligo vulgaris shed new light on the catalytic mechanism of the enzyme. Biochemistry (Mosc) 2005;44:9022—33, http://dx.doi.org/10.1021/bi0500675.

Pour citer cet article : Poirier L, et al. La décontamination des organophosphorés : vers de nouvelles alternatives. Ann Pharm Fr (2017), http://dx.doi.org/10.1016/j.pharma.2017.01.004

[114] Hartleib J, Rüterjans H. High-yield expression, purification, and characterization of the recombinant diisopropylfluorophosphatase from *Loligo vulgaris*. Protein Expr Purif 2001;21:210—9, http://dx.doi.org/10.1006/prep.2000.1360.

[115] DeFrank JJ, Cheng TC. Purification and properties of an organophosphorus acid anhydrase from a halophilic bacterial isolate. J Bacteriol 1991;173:1938—43.

[116] Cheng TC, Harvey SP, Chen GL. Cloning and expression of a gene encoding a bacterial enzyme for decontamination of organophosphorus nerve agents and nucleotide sequence of the enzyme. Appl Environ Microbiol 1996;62:1636—41.

[117] DeFrank JJ, Beaudry WT, Cheng T-C, Harvey SP, Stroup AN, Szafraniec LL. Screening of halophilic bacteria and *Alteromonas* species for organophosphorus hydrolyzing enzyme activity. Chem Biol Interact 1993;87:141—8, http://dx.doi.org/10.1016/0009-2797(93)90035-W.

[118] Cheng T-C, Harvey SP, Stroup AN. Purification and properties of a highly active organophosphorus acid anhydrolase from *Alteromonas undina*. Appl Environ Microbiol 1993;59:3138—40.

[119] Cheng T, Liu L, Wang B, Wu J, DeFrank JJ, Anderson DM, et al. Nucleotide sequence of a gene encoding an organophosphorus nerve agent degrading enzyme from *Alteromonas haloplanktis*. J Ind Microbiol Biotechnol 1997;18:49—55, http://dx.doi.org/10.1038/sj.jim.2900358.

[120] Cheng T-C, Rastogi VK, Defrank JJ, Sawiris GP. G-type nerve agent decontamination by *Alteromonas* prolidase. Ann N Y Acad Sci 1998;864:253—8, http://dx.doi.org/10.1111/j.1749-6632.1998.tb10316.x.

[121] Cheng T, DeFrank JJ, Rastogi VK. *Alteromonas* prolidase for organophosphorus G-agent decontamination. Chem Biol Interact 1999;119—120:455—62, http://dx.doi.org/10.1016/S0009-2797(99)00058-7.

[122] Cheng T-C, Defrank JJ. Hydrolysis of organophosphorus compounds by bacterial prolidases. In: Zwanenburg B, Mikołajczyk M, Kiełbasiński P, editors. Enzym. Action. Netherlands: Springer; 2000. p. 243—61.

[123] Hill CM, Wu F, Cheng T-C, DeFrank JJ, Raushel FM. Substrate and stereochemical specificity of the organophosphorus acid anhydrolase from *Alteromonas* sp. JD6.5 toward p-nitrophenyl phosphotriesters. Bioorg Med Chem Lett 2000;10:1285—8, http://dx.doi.org/10.1016/S0960-894X(00)00213-4.

[124] Vyas NK, Nickitenko A, Rastogi VK, Shah SS, Quiocho FA. Structural insights into the dual activities of the nerve agent degrading organophosphate anhydrolase/prolidase. Biochemistry (Mosc) 2010;49:547—59, http://dx.doi.org/10.1021/bi9011989.

[125] Štěpánková A, Dušková J, Skálová T, Hašek J, Koval' T, Østergaard LH, et al. Organophosphorus acid anhydrolase from *Alteromonas macleodii*: structural study and functional relationship to prolidases. Acta Crystallograph Sect F Struct Biol Cryst Commun 2013;69:346—54, http://dx.doi.org/10.1107/S1744309113002674.

[126] Maher MJ, Ghosh M, Grunden AM, Menon AL, Adams MWW, Freeman HC, et al. Structure of the prolidase from *Pyrococcus furiosus*. Biochemistry (Mosc) 2004;43:2771—83, http://dx.doi.org/10.1021/bi0356451.

[127] Theriot CM, Tove SR, Grunden AM. Characterization of two proline dipeptidases (prolidases) from the hyperthermophilic archaeon *Pyrococcus horikoshii*. Appl Microbiol Biotechnol 2009;86:177—88, http://dx.doi.org/10.1007/s00253-009-2235-x.

[128] Theriot CM, Du X, Tove SR, Grunden AM. Improving the catalytic activity of hyperthermophilic *Pyrococcus* prolidases for detoxification of organophosphorus nerve agents over a broad range of temperatures. Appl Microbiol Biotechnol 2010;87:1715—26, http://dx.doi.org/10.1007/s00253-010-2614-3.

[129] Theriot CM, Semcer RL, Shah SS, Grunden AM. Improving the catalytic activity of hyperthermophilic *Pyrococcus horikoshii* prolidase for detoxification of organophosphorus nerve agents over a broad range of temperatures. Archaea 2011;2011:e565127, http://dx.doi.org/10.1155/2011/565127.

[130] Wang S-H, Liu M, Chi M-G, Wang Q-D, Sun M-J. Production of human liver prolidase by *Saccharomyces cerevisiae* as host cells. Acta Pharmacol Sin 2004;25:794—800.

[131] Wang SH, Zhi QW, Sun MJ. Dual activities of human prolidase. Toxicol In Vitro 2006;20:71—7, http://dx.doi.org/10.1016/j.tiv.2005.06.003.

[132] diTargiani RC, Chandrasekaran L, Belinskaya T, Saxena A. In search of a catalytic bioscavenger for the prophylaxis of nerve agent toxicity. Chem Biol Interact 2010;187:349—54, http://dx.doi.org/10.1016/j.cbi.2010.02.021.

[133] Costante M, Biggemann L, Alamneh Y, Soojhawon I, Short R, Nigam S, et al. Hydrolysis potential of recombinant human skin and kidney prolidase against diisopropylfluorophosphate and sarin by in vitro analysis. Toxicol In Vitro 2012;26:182—8, http://dx.doi.org/10.1016/j.tiv.2011.11.006.

[134] Aldridge WN. Serum esterases. 2. An enzyme hydrolysing diethyl p-nitrophenyl phosphate (E 600) and its identity with the A-esterase of mammalian sera. Biochem J 1953;53:117—24.

[135] Broomfield CA, Ford KW. Hydrolysis of nerve gases by plasma enzymes. In: Proc 3rd Int Meet Cholinesterases Gd-Motte. 1991. p. 161.

[136] Davies HG, Richter RJ, Keifer M, Broomfield CA, Sowalla J, Furlong CE. The effect of the human serum paraoxonase polymorphism is reversed with diazoxon, soman and sarin. Nat Genet 1996;14:334—6, http://dx.doi.org/10.1038/ng1196-334.

[137] Rochu D, Chabrière E, Masson P. Human paraoxonase: a promising approach for pre-treatment and therapy of organophosphorus poisoning. Toxicology 2007;233:47—59, http://dx.doi.org/10.1016/j.tox.2006.08.037.

[138] Mackness MI, Arrol S, Durrington PN. Substrate specificity of human serum paraoxonase. Biochem Soc Trans 1991;19:304S.

[139] Furlong CE, Richter RJ, Chapline C, Crabb JW. Purification of rabbit and human serum paraoxonase. Biochemistry (Mosc) 1991;30:10133—40, http://dx.doi.org/10.1021/bi00106a009.

[140] Li WF, Furlong CE, Costa LG. Paraoxonase protects against chlorpyrifos toxicity in mice. Toxicol Lett 1995;76:219—26, http://dx.doi.org/10.1016/0378-4274(95)80006-Y.

[141] Gan KN, Smolen A, Eckerson HW, Du BNL. Purification of human serum paraoxonase/arylesterase. Evidence for one esterase catalyzing both activities. Drug Metab Dispos 1991;19:100—6.

[142] Otto TC, Kasten SA, Kovaleva E, Liu Z, Buchman G, Tolosa M, et al. Purification and characterization of functional human paraoxonase-1 expressed in *Trichoplusia ni larvae*. Chem Biol Interact 2010;187:388—92, http://dx.doi.org/10.1016/j.cbi.2010.02.022.

[143] Hodgins SM, Kasten SA, Harrison J, Otto TC, Oliver ZP, Rezk P, et al. Assessing protection against OP pesticides and nerve agents provided by wild-type HuPON1 purified from *Trichoplusia ni larvae* or induced via adenoviral infection. Chem Biol Interact 2013;203:177—80, http://dx.doi.org/10.1016/j.cbi.2012.10.015.

[144] Josse D, Xie W, Masson P, Lockridge O. Human serum paraoxonase (PON1): identification of essential amino acid residues by group-selective labelling and site-directed mutagenesis. Chem Biol Interact 1999;119—120:71—8, http://dx.doi.org/10.1016/S0009-2797(99)00015-0.

Pour citer cet article : Poirier L, et al. La décontamination des organophosphorés : vers de nouvelles alternatives. Ann Pharm Fr (2017), http://dx.doi.org/10.1016/j.pharma.2017.01.004

[145] Josse D, Xie W, Renault F, Rochu D, Schopfer LM, Masson P, et al. Identification of residues essential for human paraoxonase (PON1) arylesterase/organophosphatase activities. Biochemistry (Mosc) 1999;38:2816—25, http://dx.doi.org/10.1021/bi982281h.
[146] Harel M, Aharoni A, Gaidukov L, Brumshtein B, Khersonsky O, Meged R, et al. Structure and evolution of the serum paraoxonase family of detoxifying and antiatherosclerotic enzymes. Nat Struct Mol Biol 2004;11:412—9, http://dx.doi.org/10.1038/nsmb767.
[147] Aharoni A, Gaidukov L, Yagur S, Toker L, Silman I, Tawfik DS. Directed evolution of mammalian paraoxonases PON1 and PON3 for bacterial expression and catalytic specialization. Proc Natl Acad Sci U S A 2004;101:482—7, http://dx.doi.org/10.1073/pnas.2536901100.
[148] Amitai G, Gaidukov L, Adani R, Yishay S, Yacov G, Kushnir M, et al. Enhanced stereoselective hydrolysis of toxic organophosphates by directly evolved variants of mammalian serum paraoxonase. FEBS J 2006;273:1906—19, http://dx.doi.org/10.1111/j.1742-4658.2006.05198.x.
[149] Ashani Y, Gupta RD, Goldsmith M, Silman I, Sussman JL, Tawfik DS, et al. Stereo-specific synthesis of analogs of nerve agents and their utilization for selection and characterization of paraoxonase (PON1) catalytic scavengers. Chem Biol Interact 2010;187:362—9, http://dx.doi.org/10.1016/j.cbi.2010.02.039.
[150] Gupta RD, Goldsmith M, Ashani Y, Simo Y, Mullokandov G, Bar H, et al. Directed evolution of hydrolases for prevention of G-type nerve agent intoxication. Nat Chem Biol 2011;7:120—5, http://dx.doi.org/10.1038/nchembio.510.
[151] Peterson MW, Fairchild SZ, Otto TC, Mohtashemi M, Cerasoli DM, Chang WE. VX hydrolysis by human serum paraoxonase 1: a comparison of experimental and computational results. PLoS One 2011;6:e20335, http://dx.doi.org/10.1371/journal.pone.0020335.
[152] Kirby SD, Norris JR, Richard Smith J, Bahnson BJ, Cerasoli DM. Human paraoxonase double mutants hydrolyze V and G class organophosphorus nerve agents. Chem Biol Interact 2013;203:181—5, http://dx.doi.org/10.1016/j.cbi.2012.10.023.
[153] Amitai G, Gupta RD, Tawfik DS. Latent evolutionary potentials under the neutral mutational drift of an enzyme. HFSP J 2007;1:67—78, http://dx.doi.org/10.2976/1.2739115/10.2976/1.
[154] Khersonsky O, Rosenblat M, Toker L, Yacobson S, Hugenmatter A, Silman I, et al. Directed evolution of serum paraoxonase PON3 by family shuffling and ancestor/consensus mutagenesis, and its biochemical characterization. Biochemistry (Mosc) 2009;48:6644—54, http://dx.doi.org/10.1021/bi900583y.
[155] Alcolombri U, Elias M, Tawfik DS. Directed evolution of sulfotransferases and paraoxonases by ancestral libraries. J Mol Biol 2011;411:837—53, http://dx.doi.org/10.1016/j.jmb.2011.06.037.
[156] Bar-Rogovsky H, Hugenmatter A, Tawfik DS. The evolutionary origins of detoxifying enzymes: the mammalian serum paraoxonases (PONs) relate to bacterial homoserine lactonases. J Biol Chem 2013;288:23914—27, http://dx.doi.org/10.1074/jbc.M112.427922.
[157] Draganov DI, Stetson PL, Watson CE, Billecke SS, Du BNL. Rabbit serum paraoxonase 3 (PON3) is a high density lipoprotein-associated lactonase and protects low density lipoprotein against oxidation. J Biol Chem 2000;275:33435—42, http://dx.doi.org/10.1074/jbc.M004543200.
[158] Reddy ST, Wadleigh DJ, Grijalva V, Ng C, Hama S, Gangopadhyay A, et al. Human paraoxonase-3 is an HDL-associated enzyme with biological activity similar to paraoxonase-1 protein but is not regulated by oxidized lipids. Arterioscler Thromb Vasc Biol 2001;21:542—7, http://dx.doi.org/10.1161/01.ATV.21.4.542.
[159] Dong Y-J, Bartlam M, Sun L, Zhou Y-F, Zhang Z-P, Zhang C-G, et al. Crystal structure of methyl parathion hydrolase from *Pseudomonas* sp. WBC-3. J Mol Biol 2005;353:655—63, http://dx.doi.org/10.1016/j.jmb.2005.08.057.
[160] Yang J, Yang C, Jiang H, Qiao C. Overexpression of methyl parathion hydrolase and its application in detoxification of organophosphates. Biodegradation 2008;19:831—9, http://dx.doi.org/10.1007/s10532-008-9186-2.
[161] Xie J, Zhao Y, Zhang H, Liu Z, Lu Z. Improving methyl parathion hydrolase to enhance its chlorpyrifos-hydrolysing efficiency. Lett Appl Microbiol 2014;58:53—9, http://dx.doi.org/10.1111/lam.12155.
[162] Ningfeng W, Minjie D, Guoyi L, Xiaoyu C, Bin Y, Yunliu F. Cloning and expression of ophc2, a new organphosphorus hydrolase gene. Chin Sci Bull 2004;49:1245—9, http://dx.doi.org/10.1360/04wc0146.
[163] Shen Y, Lu P, Mei H, Yu H, Hong Q, Li S. Isolation of a methyl parathion-degrading strain *Stenotrophomonas* sp. SMSP-1 and cloning of the ophc2 gene. Biodegradation 2010;21:785—92, http://dx.doi.org/10.1007/s10532-010-9343-2.
[164] Gotthard G, Hiblot J, Gonzalez D, Chabrière E, Elias M. Crystallization and preliminary X-ray diffraction analysis of the organophosphorus hydrolase OPHC2 from *Pseudomonas pseudoalcaligenes*. Acta Crystallograph Sect F Struct Biol Cryst Commun 2013;69:73—6, http://dx.doi.org/10.1107/S174430911205049X.
[165] Gotthard G, Hiblot J, Gonzalez D, Elias M, Chabriere E. Structural and enzymatic characterization of the phosphotriesterase OPHC2 from *Pseudomonas pseudoalcaligenes*. PLoS One 2013;8:e77995, http://dx.doi.org/10.1371/journal.pone.0077995.
[166] Luo X-J, Kong X-D, Zhao J, Chen Q, Zhou J, Xu J-H. Switching a newly discovered lactonase into an efficient and thermostable phosphotriesterase by simple double mutations His250Ile/Ile263Trp. Biotechnol Bioeng 2014;111:1920—30, http://dx.doi.org/10.1002/bit.25272.
[167] Afriat L, Roodveldt C, Manco G, Tawfik DS. The latent promiscuity of newly identified microbial lactonases is linked to a recently diverged phosphotriesterase†. Biochemistry (Mosc) 2006;45:13677—86, http://dx.doi.org/10.1021/bi061268r.
[168] Draganov DI. Lactonases with oragnophosphatase activity: structural and evolutionary perspectives. Chem Biol Interact 2010;187:370—2, http://dx.doi.org/10.1016/j.cbi.2010.01.039.
[169] Bzdrenga J, Daudé D, Rémy B, Jacquet P, Plener L, Elias M, et al. Biotechnological applications of quorum quenching enzymes. Chem Biol Interact 2016, http://dx.doi.org/10.1016/j.cbi.2016.05.028 [in press].
[170] Rémy B, Plener L, Elias M, Daudé D, Chabrière E. Des enzymes pour bloquer la communication bactérienne, une alternative aux antibiotiques ? Ann Pharm Fr 2016;74:413—20, http://dx.doi.org/10.1016/j.pharma.2016.06.005.
[171] Afriat-Jurnou L, Jackson CJ, Tawfik DS. Reconstructing a missing link in the evolution of a recently diverged phosphotriesterase by active site loop remodeling. Biochemistry (Mosc) 2012;51:6047—55, http://dx.doi.org/10.1021/bi300694t.
[172] Xiang DF, Kolb P, Fedorov AA, Meier MM, Fedorov LV, Nguyen TT, et al. Functional annotation and three-dimensional structure of Dr0930 from Deinococcus radiodurans, a close relative of phosphotriesterase in the amidohydrolase superfamily. Biochemistry (Mosc) 2009;48:2237—47, http://dx.doi.org/10.1021/bi802274f.
[173] Zhang Y, An J, Ye W, Yang G, Qian Z-G, Chen H-F, et al. Enhancing the promiscuous phosphotriesterase activity of a thermostable lactonase (GkaP) for

Pour citer cet article : Poirier L, et al. La décontamination des organophosphorés : vers de nouvelles alternatives. Ann Pharm Fr (2017), http://dx.doi.org/10.1016/j.pharma.2017.01.004

the efficient degradation of organophosphate pesticides. Appl Environ Microbiol 2012;78:6647—55, http://dx.doi.org/10.1128/AEM.01122-12.

[174] Merone L, Mandrich L, Rossi M, Manco G. A thermostable phosphotriesterase from the archaeon *Sulfolobus solfataricus*: cloning, overexpression and properties. Extremophiles 2005;9:297—305, http://dx.doi.org/10.1007/s00792-005-0445-4.

[175] Hiblot J, Gotthard G, Chabriere E, Elias M. Structural and enzymatic characterization of the lactonase SisLac from *Sulfolobus islandicus*. PLoS One 2012;7:e47028, http://dx.doi.org/10.1371/journal.pone.0047028.

[176] Bzdrenga J, Hiblot J, Gotthard G, Champion C, Elias M, Chabriere E. SacPox from the thermoacidophilic crenarchaeon *Sulfolobus acidocaldarius* is a proficient lactonase. BMC Res Notes 2014;7:333, http://dx.doi.org/10.1186/1756-0500-7-333.

[177] Kallnik V, Bunescu A, Sayer C, Bräsen C, Wohlgemuth R, Littlechild J, et al. Characterization of a phosphotriesterase-like lactonase from the hyperthermoacidophilic crenarchaeon *Vulcanisaeta moutnovskia*. J Biotechnol 2014;190:11—7, http://dx.doi.org/10.1016/j.jbiotec.2014.04.026.

[178] Elias M, Dupuy J, Merone L, Lecomte C, Rossi M, Masson P, et al. Crystallization and preliminary X-ray diffraction analysis of the hyperthermophilic *Sulfolobus solfataricus* phosphotriesterase. Acta Crystallograph Sect F Struct Biol Cryst Commun 2007;63:553—5, http://dx.doi.org/10.1107/S1744309107023512.

[179] Rémy B, Plener L, Poirier L, Elias M, Daudé D, Chabrière E. Harnessing hyperthermostable lactonase from *Sulfolobus solfataricus* for biotechnological applications. Sci Rep 2016:6, http://dx.doi.org/10.1038/srep37780.

[180] Elias M, Dupuy J, Merone L, Mandrich L, Porzio E, Moniot S, et al. Structural basis for natural lactonase and promiscuous phosphotriesterase activities. J Mol Biol 2008;379:1017—28, http://dx.doi.org/10.1016/j.jmb.2008.04.022.

[181] Vecchio P, Elias M, Merone L, Graziano G, Dupuy J, Mandrich L, et al. Structural determinants of the high thermal stability of SsoPox from the hyperthermophilic archaeon *Sulfolobus solfataricus*. Extremophiles 2009;13:461—70, http://dx.doi.org/10.1007/s00792-009-0231-9.

[182] Tokuriki N, Tawfik DS. Stability effects of mutations and protein evolvability. Curr Opin Struct Biol 2009;19:596—604, http://dx.doi.org/10.1016/j.sbi.2009.08.003.

[183] Khersonsky O, Roodveldt C, Tawfik DS. Enzyme promiscuity: evolutionary and mechanistic aspects. Curr Opin Chem Biol 2006;10:498—508, http://dx.doi.org/10.1016/j.cbpa.2006.08.011.

[184] Chabriere E, Elias M, Hiblot J, Raoult D. Sulfolobal phosphotriesterase-like (pll) lactonases activity having enhanced properties and the uses thereof. WO/2014/167140; 2014 https://patentscope.wipo.int/search/en/detail.jsf?docId=WO2014167140.

[185] Chabriere E, Elias M, Hiblot J, Raoult D. Vulcanisaetal phosphotriesterase-like lactonases (pll) having enhanced properties and the uses thereof. WO/2015/014971; 2015 https://patentscope.wipo.int/search/en/detail.jsf?docId=WO2015014971.

[186] Hiblot J, Gotthard G, Chabriere E, Elias M. Characterisation of the organophosphate hydrolase catalytic activity of SsoPox. Sci Rep 2012:2, http://dx.doi.org/10.1038/srep00779.

[187] Masson P, Lushchekina SV. Emergence of catalytic bioscavengers against organophosphorus agents. Chem Biol Interact 2016, http://dx.doi.org/10.1016/j.cbi.2016.02.010.

[188] Müller S, Koller M, Le Provost R, Lafont O, Estour F, Wille T, et al. In vitro detoxification of cyclosarin (GF) by modified cyclodextrins. Toxicol Lett 2011;200:53—8, http://dx.doi.org/10.1016/j.toxlet.2010.10.014.

[189] Rougier NM, Cruickshank DL, Vico RV, Bourne SA, Caira MR, Buján EI, et al. Effect of cyclodextrins on the reactivity of fenitrothion. Carbohydr Res 2011;346:322—7, http://dx.doi.org/10.1016/j.carres.2010.06.016.

Pour citer cet article : Poirier L, et al. La décontamination des organophosphorés : vers de nouvelles alternatives. Ann Pharm Fr (2017), http://dx.doi.org/10.1016/j.pharma.2017.01.004

V. Références

V. Références

(1) Tokuriki, N., and Tawfik, D. S. (2009) Protein Dynamism and Evolvability. *Science 324*, 203–207.
(2) Cooper, G. M. (2000) The Central Role of Enzymes as Biological Catalysts.
(3) Humble, M. S., and Berglund, P. (2011) Biocatalytic Promiscuity. *Eur. J. Org. Chem. 2011*, 3391–3401.
(4) Tawfik, O. K. and D. S. (2010) Enzyme Promiscuity: A Mechanistic and Evolutionary Perspective. *Annu. Rev. Biochem. 79*, 471–505.
(5) Campbell, E., Kaltenbach, M., Correy, G. J., Carr, P. D., Porebski, B. T., Livingstone, E. K., Afriat-Jurnou, L., Buckle, A. M., Weik, M., Hollfelder, F., Tokuriki, N., and Jackson, C. J. (2016) The role of protein dynamics in the evolution of new enzyme function. *Nat. Chem. Biol. 12*, 944–950.
(6) Ashraf, M. A., and Sarfraz, M. (2016) Biology and evolution of life science. *Saudi J. Biol. Sci. 23*, S1–S5.
(7) Palumbi, S. R. (2001) Humans as the world's greatest evolutionary force. *Science 293*, 1786–1790.
(8) Vieille, C., and Zeikus, G. J. (2001) Hyperthermophilic Enzymes: Sources, Uses, and Molecular Mechanisms for Thermostability. *Microbiol. Mol. Biol. Rev. 65*, 1–43.
(9) Elias, M., Wieczorek, G., Rosenne, S., and Tawfik, D. S. (2014) The universality of enzymatic rate–temperature dependency. *Trends Biochem. Sci. 39*, 1–7.
(10) Rémy, B., Plener, L., Poirier, L., Elias, M., Daudé, D., and Chabrière, E. (2016) Harnessing hyperthermostable lactonase from Sulfolobus solfataricus for biotechnological applications. *Sci. Rep. 6*.
(11) Park, T.-H., Choi, K.-W., Park, C.-S., Lee, S.-B., Kang, H.-Y., Shon, K.-J., Park, J.-S., and Cha, J. (2005) Substrate specificity and transglycosylation catalyzed by a thermostable β-glucosidase from marine hyperthermophile Thermotoga neapolitana. *Appl. Microbiol. Biotechnol. 69*, 411–422.
(12) Li, W. F., Zhou, X. X., and Lu, P. (2005) Structural features of thermozymes. *Biotechnol. Adv. 23*, 271–281.
(13) Afriat, L., Roodveldt, C., Manco, G., and Tawfik, D. S. (2006) The Latent Promiscuity of Newly Identified Microbial Lactonases Is Linked to a Recently Diverged Phosphotriesterase †. *Biochemistry (Mosc.) 45*, 13677–13686.
(14) Kallnik, V., Bunescu, A., Sayer, C., Bräsen, C., Wohlgemuth, R., Littlechild, J., and Siebers, B. (2014) Characterization of a phosphotriesterase-like lactonase from the hyperthermoacidophilic crenarchaeon Vulcanisaeta moutnovskia. *J. Biotechnol. 190*, 11–17.
(15) Mohapatra, P. K., and Pattanaik, S. (2013) Origin, evolution and diversity of phosphotriesterases-an organophosphate degrading enzyme. *Development 25*, 27.
(16) Bzdrenga, J., Daudé, D., Rémy, B., Jacquet, P., Plener, L., Elias, M., and Chabrière, E. (2016) Biotechnological applications of quorum quenching enzymes. *Chem. Biol. Interact.*
(17) DeLano, W. L. (2002) The PyMOL Molecular Graphics System. *DeLano Sci. San Carlos CA USA*.
(18) Elias, M., Dupuy, J., Merone, L., Mandrich, L., Porzio, E., Moniot, S., Rochu, D., Lecomte, C., Rossi, M., Masson, P., Manco, G., and Chabriere, E. (2008) Structural Basis for Natural Lactonase and Promiscuous Phosphotriesterase Activities. *J. Mol. Biol. 379*, 1017–1028.
(19) Hiblot, J., Bzdrenga, J., Champion, C., Chabriere, E., and Elias, M. (2015) Crystal structure of VmoLac, a tentative quorum quenching lactonase from the extremophilic crenarchaeon Vulcanisaeta moutnovskia. *Sci. Rep. 5*, 8372.
(20) Gotthard, G. (2013) Caractérisation structurale d'enzymes hydrolysant les organophosphorés et rationalisation de leur amélioration en vue d'applications biotechnologiques. Aix Marseille Université.
(21) Merone, L., Mandrich, L., Rossi, M., and Manco, G. (2005) A thermostable phosphotriesterase from the archaeon Sulfolobus solfataricus: cloning, overexpression and properties. *Extremophiles 9*, 297–305.
(22) Hiblot, J., Gotthard, G., Chabriere, E., and Elias, M. (2012) Characterisation of the organophosphate hydrolase catalytic activity of SsoPox. *Sci. Rep. 2*.
(23) Hiblot, J., Gotthard, G., Elias, M., and Chabriere, E. (2013) Differential active site loop conformations mediate promiscuous activities in the lactonase SsoPox. *PloS One 8*, e75272.
(24) Petroianu, G. A. (2010) History of organophosphate synthesis: the very early days. *Pharm.- Int. J. Pharm. Sci. 65*, 306–311.
(25) Worek, F., Wille, T., Koller, M., and Thiermann, H. (2016) Toxicology of organophosphorus compounds in view of an increasing terrorist threat. *Arch. Toxicol. 90*, 2131–2145.
(26) Soltaninejad, K., and Shadnia, S. (2014) History of the Use and Epidemiology of Organophosphorus Poisoning, in *Basic and Clinical Toxicology of Organophosphorus Compounds* (Balali-Mood, M., and Abdollahi, M., Eds.), pp 25–43. Springer London, London.

(27) Sirin, G. S., Zhou, Y., Lior-Hoffmann, L., Wang, S., and Zhang, Y. (2012) Aging Mechanism of Soman Inhibited Acetylcholinesterase. *J. Phys. Chem. B 116*, 12199–12207.
(28) Schindler, B. K., Koslitz, S., Weiss, T., Broding, H. C., Brüning, T., and Bünger, J. (2014) Exposure of aircraft maintenance technicians to organophosphates from hydraulic fluids and turbine oils: A pilot study. *Int. J. Hyg. Environ. Health 217*, 34–37.
(29) Hardos, J. E., Whitehead, L. W., Han, I., Ott, D. K., and Waller, D. K. (2016) Depression Prevalence and Exposure to Organophosphate Esters in Aircraft Maintenance Workers. *Aerosp. Med. Hum. Perform. 87*, 712–717.
(30) Quinn, D. M. (1987) Acetylcholinesterase: enzyme structure, reaction dynamics, and virtual transition states. *Chem. Rev. 87*, 955–979.
(31) Gorecki, L., Korabecny, J., Musilek, K., Nepovimova, E., Malinak, D., Kucera, T., Dolezal, R., Jun, D., Soukup, O., and Kuca, K. (2017) Progress in acetylcholinesterase reactivators and in the treatment of organophosphorus intoxication: a patent review (2006–2016). *Expert Opin. Ther. Pat.* 1–15.
(32) Zhang, Y., Kua, J., and McCammon, J. A. (2002) Role of the Catalytic Triad and Oxyanion Hole in Acetylcholinesterase Catalysis: An ab initio QM/MM Study. *J. Am. Chem. Soc. 124*, 10572–10577.
(33) Silman, I., and Sussman, J. L. (2008) Acetylcholinesterase: How is structure related to function? *Chem. Biol. Interact. 175*, 3–10.
(34) Millard, C. B., Kryger, G., Ordentlich, A., Greenblatt, H. M., Harel, M., Raves, M. L., Segall, Y., Barak, D., Shafferman, A., Silman, I., and Sussman, J. L. (1999) Crystal Structures of Aged Phosphonylated Acetylcholinesterase: Nerve Agent Reaction Products at the Atomic Level †,‡. *Biochemistry (Mosc.) 38*, 7032–7039.
(35) Soreq, H., and Seidman, S. (2001) Acetylcholinesterase—new roles for an old actor. *Nat. Rev. Neurosci. 2*, 294–302.
(36) Dvir, H., Silman, I., Harel, M., Rosenberry, T. L., and Sussman, J. L. (2010) Acetylcholinesterase: From 3D structure to function. *Chem. Biol. Interact. 187*, 10–22.
(37) Shafferman, A., Ordentlich, A., Barak, D., Stein, D., Ariel, N., and Velan, B. (1996) Aging of phosphylated human acetylcholinesterase: catalytic processes mediated by aromatic and polar residues of the active centre. *Biochem. J. 318*, 833–840.
(38) Eddleston, M., Buckley, N. A., Eyer, P., and Dawson, A. H. (2008) Management of acute organophosphorus pesticide poisoning. *The Lancet 371*, 597–607.
(39) Vonescha, M. A., Nachonb, F., and Burnatc, P. (2011) Actions et efficacités des différentes oximes dans le traitement de l'intoxication par les neurotoxiques organophosphorés. *Med Armées 39*, 445–452.
(40) Buckley, N. A., Eddleston, M., Li, Y., Bevan, M., and Robertson, J. (2011) Oximes for acute organophosphate pesticide poisoning, in *Cochrane Database of Systematic Reviews* (The Cochrane Collaboration, Ed.). John Wiley & Sons, Ltd, Chichester, UK.
(41) Nurulain, S. (2011) Efficacious Oxime for Organophosphorus Poisoning: A Minireview. *Trop. J. Pharm. Res. 10*.
(42) Lenz, D. E., Yeung, D., Smith, J. R., Sweeney, R. E., Lumley, L. A., and Cerasoli, D. M. (2007) Stoichiometric and catalytic scavengers as protection against nerve agent toxicity: a mini review. *Toxicology 233*, 31–39.
(43) Masson, P., and Lockridge, O. (2010) Butyrylcholinesterase for protection from organophosphorus poisons: Catalytic complexities and hysteretic behavior. *Arch. Biochem. Biophys. 494*, 107–120.
(44) Miller, M. B., and Bassler, B. L. (2001) Quorum sensing in bacteria. *Annu. Rev. Microbiol. 55*, 165–199.
(45) Waters, C. M., and Bassler, B. L. (2005) Quorum sensing: cell-to-cell communication in bacteria. *Annu Rev Cell Dev Biol 21*, 319–346.
(46) Williams, P. (2007) Quorum sensing, communication and cross-kingdom signalling in the bacterial world. *Microbiology 153*, 3923–3938.
(47) Deng, Y., Wu, J., Tao, F., and Zhang, L.-H. (2011) Listening to a New Language: DSF-Based Quorum Sensing in Gram-Negative Bacteria. *Chem. Rev. 111*, 160–173.
(48) McGrath, S., Wade, D. S., and Pesci, E. C. (2004) Dueling quorum sensing systems in Pseudomonas aeruginosa control the production of the Pseudomonas quinolone signal (PQS). *FEMS Microbiol. Lett. 230*, 27–34.
(49) Reading, N. C., and Sperandio, V. (2006) Quorum sensing: the many languages of bacteria. *FEMS Microbiol. Lett. 254*, 1–11.
(50) LaSarre, B., and Federle, M. J. (2013) Exploiting Quorum Sensing To Confuse Bacterial Pathogens. *Microbiol. Mol. Biol. Rev. 77*, 73–111.
(51) Schauder, S., Shokat, K., Surette, M. G., and Bassler, B. L. (2001) The LuxS family of bacterial autoinducers: biosynthesis of a novel quorum-sensing signal molecule. *Mol. Microbiol. 41*, 463–476.

(52) Ali, L., Goraya, M., Arafat, Y., Ajmal, M., Chen, J.-L., and Yu, D. (2017) Molecular Mechanism of Quorum-Sensing in Enterococcus faecalis: Its Role in Virulence and Therapeutic Approaches. *Int. J. Mol. Sci. 18*, 960.
(53) Bassler, B. L. (2002) Small talk: cell-to-cell communication in bacteria. *Cell 109*, 421–424.
(54) Verbeke, F., De Craemer, S., Debunne, N., Janssens, Y., Wynendaele, E., Van de Wiele, C., and De Spiegeleer, B. (2017) Peptides as Quorum Sensing Molecules: Measurement Techniques and Obtained Levels In vitro and In vivo. *Front. Neurosci. 11*.
(55) Eberl, L., and Riedel, K. (2011) Mining quorum sensing regulated proteins - Role of bacterial cell-to-cell communication in global gene regulation as assessed by proteomics. *PROTEOMICS 11*, 3070–3085.
(56) Lee, J., and Zhang, L. (2015) The hierarchy quorum sensing network in Pseudomonas aeruginosa. *Protein Cell 6*, 26–41.
(57) Mathesius, U., Mulders, S., Gao, M., Teplitski, M., Caetano-Anollés, G., Rolfe, B. G., and Bauer, W. D. (2003) Extensive and specific responses of a eukaryote to bacterial quorum-sensing signals. *Proc. Natl. Acad. Sci. 100*, 1444–1449.
(58) González, J. F., and Venturi, V. (2013) A novel widespread interkingdom signaling circuit. *Trends Plant Sci. 18*, 167–174.
(59) Papenfort, K., and Bassler, B. L. (2016) Quorum sensing signal–response systems in Gram-negative bacteria. *Nat. Rev. Microbiol. 14*, 576–588.
(60) Zhu, J., and Kaufmann, G. F. (2013) Quo vadis quorum quenching? *Curr. Opin. Pharmacol. 13*, 688–698.
(61) O'Loughlin, C. T., Miller, L. C., Siryaporn, A., Drescher, K., Semmelhack, M. F., and Bassler, B. L. (2013) A quorum-sensing inhibitor blocks Pseudomonas aeruginosa virulence and biofilm formation. *Proc. Natl. Acad. Sci. 110*, 17981–17986.
(62) Fetzner, S. (2015) Quorum quenching enzymes. *J. Biotechnol. 201*, 2–14.
(63) Dobretsov, S., Teplitski, M., and Paul, V. (2009) Mini-review: quorum sensing in the marine environment and its relationship to biofouling. *Biofouling 25*, 413–427.
(64) Theriot, C. M., and Grunden, A. M. (2011) Hydrolysis of organophosphorus compounds by microbial enzymes. *Appl. Microbiol. Biotechnol. 89*, 35–43.
(65) Roodveldt, C., and Tawfik, D. S. (2005) Directed evolution of phosphotriesterase from Pseudomonas diminuta for heterologous expression in Escherichia coli results in stabilization of the metal-free state. *Protein Eng. Des. Sel. 18*, 51–58.
(66) Donarski, W. J., Dumas, D. P., Heitmeyer, D. P., Lewis, V. E., and Raushel, F. M. (1989) Structure-activity relationships in the hydrolysis of substrates by the phosphotriesterase from Pseudomonas diminuta. *Biochemistry (Mosc.) 28*, 4650–4655.
(67) Hiblot, J., Gotthard, G., Elias, M., and Chabriere, E. (2013) Differential Active Site Loop Conformations Mediate Promiscuous Activities in the Lactonase SsoPox. *PLoS ONE* (Rodrigues-Lima, F., Ed.) *8*, e75272.
(68) Wolfenden, R. (2011) Benchmark Reaction Rates, the Stability of Biological Molecules in Water, and the Evolution of Catalytic Power in Enzymes. *Annu. Rev. Biochem. 80*, 645–667.
(69) Singh, R. K., Tiwari, M. K., Singh, R., and Lee, J.-K. (2013) From Protein Engineering to Immobilization: Promising Strategies for the Upgrade of Industrial Enzymes. *Int. J. Mol. Sci. 14*, 1232–1277.
(70) Bar-Even, A., Noor, E., Savir, Y., Liebermeister, W., Davidi, D., Tawfik, D. S., and Milo, R. (2011) The Moderately Efficient Enzyme: Evolutionary and Physicochemical Trends Shaping Enzyme Parameters. *Biochemistry (Mosc.) 50*, 4402–4410.
(71) Tokuriki, N., Jackson, C. J., Afriat-Jurnou, L., Wyganowski, K. T., Tang, R., and Tawfik, D. S. (2012) Diminishing returns and tradeoffs constrain the laboratory optimization of an enzyme. *Nat. Commun. 3*, 1257.
(72) Burton, S. G., Cowan, D. A., and Woodley, J. M. (2002) The search for the ideal biocatalyst. *Nat. Biotechnol. 20*, 37–45.
(73) Gupta, R. D., and Tawfik, D. S. (2008) Directed enzyme evolution via small and effective neutral drift libraries. *Nat. Methods 5*, 939–942.
(74) Bommarius, A. S. (2015) Biocatalysis: A Status Report. *Annu. Rev. Chem. Biomol. Eng. 6*, 319–345.
(75) Currin, A., Swainston, N., Day, P. J., and Kell, D. B. (2015) Synthetic biology for the directed evolution of protein biocatalysts: navigating sequence space intelligently. *Chem Soc Rev 44*, 1172–1239.
(76) Reetz, M. T. (2016) Directed Evolution of Selective Enzymes: Catalysts for Organic Chemistry and Biotechnology. Wiley-VCH Verlag GmbH & Co. KGaA, Weinheim, Germany.
(77) Alcalde, M. (Ed.). (2017) Directed Enzyme Evolution: Advances and Applications. Springer International Publishing, Cham.
(78) Hiblot, J., Gotthard, G., Elias, M., and Chabriere, E. (2013) Differential Active Site Loop Conformations Mediate Promiscuous Activities in the Lactonase SsoPox. *PLoS ONE* (Rodrigues-Lima, F., Ed.) *8*, e75272.

(79) Reetz, M. T. (2011) Laboratory Evolution of Stereoselective Enzymes: A Prolific Source of Catalysts for Asymmetric Reactions. *Angew. Chem. Int. Ed. 50*, 138–174.
(80) Daudé, D., Topham, C. M., Remaud-Siméon, M., and André, I. (2013) Probing impact of active site residue mutations on stability and activity of *Neisseria polysaccharea* amylosucrase: Probing Impact of Active Site Residue Mutations. *Protein Sci. 22*, 1754–1765.
(81) Alcolombri, U., Elias, M., and Tawfik, D. S. (2011) Directed Evolution of Sulfotransferases and Paraoxonases by Ancestral Libraries. *J. Mol. Biol. 411*, 837–853.
(82) Gonzalez, D., Hiblot, J., Darbinian, N., Miller, J. C., Gotthard, G., Amini, S., Chabriere, E., and Elias, M. (2014) Ancestral mutations as a tool for solubilizing proteins: The case of a hydrophobic phosphate-binding protein. *FEBS Open Bio 4*, 121–127.
(83) Hawwa, R., Larsen, S. D., Ratia, K., and Mesecar, A. D. (2009) Structure-Based and Random Mutagenesis Approaches Increase the Organophosphate-Degrading Activity of a Phosphotriesterase Homologue from Deinococcus radiodurans. *J. Mol. Biol. 393*, 36–57.
(84) Herman, A., and Tawfik, D. S. (2007) Incorporating Synthetic Oligonucleotides via Gene Reassembly (ISOR): a versatile tool for generating targeted libraries. *Protein Eng. Des. Sel. 20*, 219–226.
(85) Rochu, D., Chabrière, E., and Masson, P. (2007) Human paraoxonase: A promising approach for pre-treatment and therapy of organophosphorus poisoning. *Toxicology 233*, 47–59.
(86) Krieger, R. (2001) Handbook of Pesticide Toxicology, Two-Volume Set: Principles and Agents. Academic Press.
(87) Gupta, R. C. (2009) Handbook of Toxicology of Chemical Warfare Agents. Academic Press.
(88) Sapozhnikova, Y., Zubcov, N., Hungerford, S., Roy, L. A., Boicenco, N., Zubcov, E., and Schlenk, D. (2005) Evaluation of pesticides and metals in fish of the Dniester River, Moldova. *Chemosphere 60*, 196–205.
(89) Sapozhnikova, Y., Bawardi, O., and Schlenk, D. (2004) Pesticides and PCBs in sediments and fish from the Salton Sea, California, USA. *Chemosphere 55*, 797–809.
(90) LeJeune, K. E., Wild, J. R., and Russell, A. J. (1998) Nerve agents degraded by enzymatic foams. *Nature 395*, 27–28.
(91) Jacquet, P., Daudé, D., Bzdrenga, J., Masson, P., Elias, M., and Chabrière, E. (2016) Current and emerging strategies for organophosphate decontamination: special focus on hyperstable enzymes. *Environ. Sci. Pollut. Res.* 1–19.
(92) Poirier, L., Jacquet, P., Elias, M., Daudé, D., and Chabrière, E. (2017) Decontamination of organophosphorus compounds: Towards new alternatives. *Ann. Pharm. Fr.*
(93) Afriat, L., Roodveldt, C., Manco, G., and Tawfik, D. S. (2006) The Latent Promiscuity of Newly Identified Microbial Lactonases Is Linked to a Recently Diverged Phosphotriesterase†. *Biochemistry (Mosc.) 45*, 13677–13686.
(94) Dumas, D. P., Caldwell, S. R., Wild, J. R., and Raushel, F. M. (1989) Purification and properties of the phosphotriesterase from Pseudomonas diminuta. *J. Biol. Chem. 264*, 19659–19665.
(95) Seibert, C. M., and Raushel, F. M. (2005) Structural and Catalytic Diversity within the Amidohydrolase Superfamily†. *Biochemistry (Mosc.) 44*, 6383–6391.
(96) Roodveldt, C., and Tawfik, D. S. (2005) Shared Promiscuous Activities and Evolutionary Features in Various Members of the Amidohydrolase Superfamily. *Biochemistry (Mosc.) 44*, 12728–12736.
(97) Hiblot, J., Gotthard, G., Chabriere, E., and Elias, M. (2012) Structural and Enzymatic characterization of the lactonase SisLac from Sulfolobus islandicus. *PLoS ONE* (Rodrigues-Lima, F., Ed.) *7*, e47028.
(98) Porzio, E., Merone, L., Mandrich, L., Rossi, M., and Manco, G. (2007) A new phosphotriesterase from Sulfolobus acidocaldarius and its comparison with the homologue from Sulfolobus solfataricus. *Biochimie 89*, 625–636.
(99) Merone, L., Mandrich, L., Rossi, M., and Manco, G. (2005) A thermostable phosphotriesterase from the archaeon Sulfolobus solfataricus: cloning, overexpression and properties. *Extremophiles 9*, 297–305.
(100) Hawwa, R., Aikens, J., Turner, R. J., Santarsiero, B. D., and Mesecar, A. D. (2009) Structural basis for thermostability revealed through the identification and characterization of a highly thermostable phosphotriesterase-like lactonase from Geobacillus stearothermophilus. *Arch. Biochem. Biophys. 488*, 109–120.
(101) Xiang, D. F., Patskovsky, Y., Xu, C., Meyer, A. J., Sauder, J. M., Burley, S. K., Almo, S. C., and Raushel, F. M. (2009) Functional Identification of Incorrectly Annotated Prolidases from the Amidohydrolase Superfamily of Enzymes. *Biochemistry (Mosc.) 48*, 3730–3742.
(102) Chow, J. Y., Xue, B., Lee, K. H., Tung, A., Wu, L., Robinson, R. C., and Yew, W. S. (2010) Directed Evolution of a Thermostable Quorum-quenching Lactonase from the Amidohydrolase Superfamily. *J. Biol. Chem. 285*, 40911–40920.

(103) Hiblot, J., Gotthard, G., Champion, C., Chabriere, E., and Elias, M. (2013) Crystallization and preliminary X-ray diffraction analysis of the lactonase VmoLac from Vulcanisaeta moutnovskia. *Acta Crystallograph. Sect. F Struct. Biol. Cryst. Commun. 69*, 1235–1238.
(104) Hiblot, J., Bzdrenga, J., Champion, C., Chabriere, E., and Elias, M. (2015) Crystal structure of VmoLac, a tentative quorum quenching lactonase from the extremophilic crenarchaeon Vulcanisaeta moutnovskia. *Sci. Rep. 5*, 8372.
(105) Bzdrenga, J., Hiblot, J., Gotthard, G., Champion, C., Elias, M., and Chabriere, E. (2014) SacPox from the thermoacidophilic crenarchaeon Sulfolobus acidocaldarius is a proficient lactonase. *BMC Res. Notes 7*, 333.
(106) Rémy, B., Plener, L., Elias, M., Daudé, D., and Chabrière, E. (2016) Des enzymes pour bloquer la communication bactérienne, une alternative aux antibiotiques ? *Ann. Pharm. Fr.*
(107) Vieille, C., and Zeikus, G. J. (2001) Hyperthermophilic Enzymes: Sources, Uses, and Molecular Mechanisms for Thermostability. *Microbiol. Mol. Biol. Rev. 65*, 1–43.
(108) Elias, M., Dupuy, J., Merone, L., Mandrich, L., Porzio, E., Moniot, S., Rochu, D., Lecomte, C., Rossi, M., Masson, P., Manco, G., and Chabriere, E. (2008) Structural Basis for Natural Lactonase and Promiscuous Phosphotriesterase Activities. *J. Mol. Biol. 379*, 1017–1028.
(109) Hoque, M. A., Zhang, Y., Chen, L., Yang, G., Khatun, M. A., Chen, H., Hao, L., and Feng, Y. (2017) Stepwise Loop Insertion Strategy for Active Site Remodeling to Generate Novel Enzyme Functions. *ACS Chem. Biol.*
(110) Meier, M. M., Rajendran, C., Malisi, C., Fox, N. G., Xu, C., Schlee, S., Barondeau, D. P., Höcker, B., Sterner, R., and Raushel, F. M. (2013) Molecular Engineering of Organophosphate Hydrolysis Activity from a Weak Promiscuous Lactonase Template. *J. Am. Chem. Soc. 135*, 11670–11677.
(111) Elias, M., Dupuy, J., Merone, L., Lecomte, C., Rossi, M., Masson, P., Manco, G., and Chabriere, E. (2007) Crystallization and preliminary X-ray diffraction analysis of the hyperthermophilic *Sulfolobus solfataricus* phosphotriesterase. *Acta Crystallograph. Sect. F Struct. Biol. Cryst. Commun. 63*, 553–555.
(112) Del Giudice, I., Coppolecchia, R., Merone, L., Porzio, E., Carusone, T. M., Mandrich, L., Worek, F., and Manco, G. (2016) An efficient thermostable organophosphate hydrolase and its application in pesticide decontamination. *Biotechnol. Bioeng. 113*, 724–734.
(113) Rémy, B., Plener, L., Poirier, L., Elias, M., Daudé, D., and Chabrière, E. (2016) Harnessing hyperthermostable lactonase from Sulfolobus solfataricus for biotechnological applications. *Sci. Rep. 6*.
(114) Vecchio, P. D., Elias, M., Merone, L., Graziano, G., Dupuy, J., Mandrich, L., Carullo, P., Fournier, B., Rochu, D., Rossi, M., Masson, P., Chabriere, E., and Manco, G. (2009) Structural determinants of the high thermal stability of SsoPox from the hyperthermophilic archaeon Sulfolobus solfataricus. *Extremophiles 13*, 461–470.
(115) Afriat-Jurnou, L., Jackson, C. J., and Tawfik, D. S. (2012) Reconstructing a Missing Link in the Evolution of a Recently Diverged Phosphotriesterase by Active-Site Loop Remodeling. *Biochemistry (Mosc.) 51*, 6047–6055.
(116) Jackson, C. J., Carr, P. D., Kim, H.-K., Liu, J.-W., Herrald, P., Mitić, N., Schenk, G., Smith, C. A., and Ollis, D. L. (2006) Anomalous scattering analysis of Agrobacterium radiobacter phosphotriesterase: the prominent role of iron in the heterobinuclear active site. *Biochem. J. 397*, 501.
(117) Tawfik, D. S. (2014) Accuracy-rate tradeoffs: how do enzymes meet demands of selectivity and catalytic efficiency? *Curr. Opin. Chem. Biol. 21*, 73–80.
(118) Xiang, D. F., Kolb, P., Fedorov, A. A., Meier, M. M., Fedorov, E. V., Nguyen, T. T., Sterner, R., Almo, S. C., Shoichet, B. K., and Raushel, F. M. (2009) Functional Annotation and Three-Dimensional Structure of Dr0930 from Deinococcus radiodurans: A Close Relative of Phosphotriesterase in the Amidohydrolase Superfamily. *Biochemistry (Mosc.) 48*, 2237–2247.
(119) Dellus-Gur, E., Elias, M., Caselli, E., Prati, F., Salverda, M. L. M., de Visser, J. A. G. M., Fraser, J. S., and Tawfik, D. S. (2015) Negative Epistasis and Evolvability in TEM-1 β-Lactamase—The Thin Line between an Enzyme's Conformational Freedom and Disorder. *J. Mol. Biol. 427*, 2396–2409.
(120) Reetz, M. T. (2013) The Importance of Additive and Non-Additive Mutational Effects in Protein Engineering. *Angew. Chem. Int. Ed. 52*, 2658–2666.
(121) Campbell, E., Kaltenbach, M., Correy, G. J., Carr, P. D., Porebski, B. T., Livingstone, E. K., Afriat-Jurnou, L., Buckle, A. M., Weik, M., Hollfelder, F., Tokuriki, N., and Jackson, C. J. (2016) The role of protein dynamics in the evolution of new enzyme function. *Nat. Chem. Biol. 12*, 944–950.
(122) Dellus-Gur, E., Toth-Petroczy, A., Elias, M., and Tawfik, D. S. (2013) What Makes a Protein Fold Amenable to Functional Innovation? Fold Polarity and Stability Trade-offs. *J. Mol. Biol. 425*, 2609–2621.
(123) Guendouze, A., Plener, L., Bzdrenga, J., Jacquet, P., Rémy, B., Elias, M., Lavigne, J.-P., Daudé, D., and Chabriere, E. (2017) Effect of quorum quenching lactonase in clinical isolates of Pseudomonas aeruginosa and comparison with quorum sensing inhibitors. *Front. Microbiol. 8*.
(124) Emsley, P., and Cowtan, K. (2004) *Coot* : model-building tools for molecular graphics. *Acta Crystallogr. D Biol. Crystallogr. 60*, 2126–2132.

(125) Kabsch, W. (1993) Automatic processing of rotation diffraction data from crystals of initially unknown symmetry and cell constants. *J. Appl. Crystallogr. 26*, 795–800.
(126) McCoy, A. J., Grosse-Kunstleve, R. W., Adams, P. D., Winn, M. D., Storoni, L. C., and Read, R. J. (2007) *Phaser* crystallographic software. *J. Appl. Crystallogr. 40*, 658–674.
(127) Vagin, A., and Teplyakov, A. (2000) An approach to multi-copy search in molecular replacement. *Acta Crystallogr. D Biol. Crystallogr. 56*, 1622–1624.
(128) Murshudov, G. N., Vagin, A. A., and Dodson, E. J. (1997) Refinement of Macromolecular Structures by the Maximum-Likelihood Method. *Acta Crystallogr. D Biol. Crystallogr. 53*, 240–255.
(129) Kaltenbach, M., Jackson, C. J., Campbell, E. C., Hollfelder, F., and Tokuriki, N. (2015) Reverse evolution leads to genotypic incompatibility despite functional and active site convergence. *Elife 4*, e06492.
(130) Roodveldt, C., and Tawfik, D. S. (2005) Shared Promiscuous Activities and Evolutionary Features in Various Members of the Amidohydrolase Superfamily †. *Biochemistry (Mosc.) 44*, 12728–12736.
(131) Pandya, C., Farelli, J. D., Dunaway-Mariano, D., and Allen, K. N. (2014) Enzyme Promiscuity: Engine of Evolutionary Innovation. *J. Biol. Chem. 289*, 30229–30236.
(132) O'Brien, P. J., and Herschlag, D. (1999) Catalytic promiscuity and the evolution of new enzymatic activities. *Chem. Biol. 6*, R91–R105.
(133) Babtie, A., Tokuriki, N., and Hollfelder, F. (2010) What makes an enzyme promiscuous? *Curr. Opin. Chem. Biol. 14*, 200–207.
(134) DePristo, M. A. (2007) The subtle benefits of being promiscuous: Adaptive evolution potentiated by enzyme promiscuity. *HFSP J. 1*, 94–98.
(135) Aharoni, A., Gaidukov, L., Khersonsky, O., Gould, S. M., Roodveldt, C., and Tawfik, D. S. (2005) The "evolvability" of promiscuous protein functions. *Nat. Genet. 37*, 73–76.
(136) Amitai, G., Gupta, R. D., and Tawfik, D. S. (2007) Latent evolutionary potentials under the neutral mutational drift of an enzyme. *HFSP J. 1*, 67–78.
(137) Wroe, R., Chan, H. S., and Bornberg-Bauer, E. (2007) A structural model of latent evolutionary potentials underlying neutral networks in proteins. *HFSP J. 1*, 79–87.
(138) Bornscheuer, U. T., and Kazlauskas, R. J. (2004) Catalytic Promiscuity in Biocatalysis: Using Old Enzymes to Form New Bonds and Follow New Pathways. *Angew. Chem. Int. Ed. 43*, 6032–6040.
(139) Elias, M., and Tawfik, D. S. (2011) Divergence and Convergence in Enzyme Evolution: Parallel Evolution of Paraoxonases from Quorum-quenching Lactonases. *J. Biol. Chem. 287*, 11–20.
(140) Naqvi, T., Warden, A. C., French, N., Sugrue, E., Carr, P. D., Jackson, C. J., and Scott, C. (2014) A 5000-Fold Increase in the Specificity of a Bacterial Phosphotriesterase for Malathion through Combinatorial Active Site Mutagenesis. *PLoS ONE 9*, e94177.
(141) Cherny, I., Greisen, P., Ashani, Y., Khare, S. D., Oberdorfer, G., Leader, H., Baker, D., and Tawfik, D. S. (2013) Engineering V-Type Nerve Agents Detoxifying Enzymes Using Computationally Focused Libraries. *ACS Chem. Biol. 8*, 2394–2403.
(142) Bigley, A. N., Xu, C., Henderson, T. J., Harvey, S. P., and Raushel, F. M. (2013) Enzymatic Neutralization of the Chemical Warfare Agent VX: Evolution of Phosphotriesterase for Phosphorothiolate Hydrolysis. *J. Am. Chem. Soc. 135*, 10426–10432.
(143) Tsai, P.-C., Fox, N., Bigley, A. N., Harvey, S. P., Barondeau, D. P., and Raushel, F. M. (2012) Enzymes for the Homeland Defense: Optimizing Phosphotriesterase for the Hydrolysis of Organophosphate Nerve Agents. *Biochemistry (Mosc.) 51*, 6463–6475.
(144) Tsai, P.-C., Bigley, A., Li, Y., Ghanem, E., Cadieux, C. L., Kasten, S. A., Reeves, T. E., Cerasoli, D. M., and Raushel, F. M. (2010) Stereoselective Hydrolysis of Organophosphate Nerve Agents by the Bacterial Phosphotriesterase. *Biochemistry (Mosc.) 49*, 7978–7987.
(145) Hill, C. M., Li, W.-S., Thoden, J. B., Holden, H. M., and Raushel, F. M. (2003) Enhanced Degradation of Chemical Warfare Agents through Molecular Engineering of the Phosphotriesterase Active Site. *J. Am. Chem. Soc. 125*, 8990–8991.
(146) Ghanem, E., and Raushel, F. (2005) Detoxification of organophosphate nerve agents by bacterial phosphotriesterase. *Toxicol. Appl. Pharmacol. 207*, 459–470.
(147) Worek, F., Seeger, T., Goldsmith, M., Ashani, Y., Leader, H., Sussman, J. S., Tawfik, D., Thiermann, H., and Wille, T. (2014) Efficacy of the rePON1 mutant IIG1 to prevent cyclosarin toxicity in vivo and to detoxify structurally different nerve agents in vitro. *Arch. Toxicol.*
(148) Tokuriki, N., Stricher, F., Serrano, L., and Tawfik, D. S. (2008) How Protein Stability and New Functions Trade Off. *PLOS Comput Biol 4*, e1000002.
(149) Tokuriki, N., and Tawfik, D. S. (2009) Stability effects of mutations and protein evolvability. *Curr. Opin. Struct. Biol. 19*, 596–604.

(150) Bloom, J. D., Labthavikul, S. T., Otey, C. R., and Arnold, F. H. (2006) Protein stability promotes evolvability. *Proc. Natl. Acad. Sci. 103*, 5869–5874.
(151) Tokuriki, N., and Tawfik, D. S. (2009) Chaperonin overexpression promotes genetic variation and enzyme evolution. *Nature 459*, 668–673.
(152) Hiblot, J., Gotthard, G., Chabriere, E., and Elias, M. (2012) Characterisation of the organophosphate hydrolase catalytic activity of SsoPox. *Sci. Rep. 2*.
(153) Merone, L., Mandrich, L., Rossi, M., and Manco, G. (2005) A thermostable phosphotriesterase from the archaeon Sulfolobus solfataricus: cloning, overexpression and properties. *Extremophiles 9*, 297–305.
(154) Hiblot, J., Gotthard, G., Elias, M., and Chabriere, E. (2013) Differential Active Site Loop Conformations Mediate Promiscuous Activities in the Lactonase SsoPox. *PLoS ONE 8*, e75272.
(155) Merone, L., Mandrich, L., Porzio, E., Rossi, M., Müller, S., Reiter, G., Worek, F., and Manco, G. (2010) Improving the promiscuous nerve agent hydrolase activity of a thermostable archaeal lactonase. *Bioresour. Technol. 101*, 9204–9212.
(156) Briseño-Roa, L., Hill, J., Notman, S., Sellers, D., Smith, A. P., Timperley, C. M., Wetherell, J., Williams, N. H., Williams, G. R., Fersht, A. R., and Griffiths, A. D. (2006) Analogues with Fluorescent Leaving Groups for Screening and Selection of Enzymes That Efficiently Hydrolyze Organophosphorus Nerve Agents. *J. Med. Chem. 49*, 246–255.
(157) Ellman, G. L., Courtney, K. D., Andres, V., and Featherstone, R. M. (1961) A new and rapid colorimetric determination of acetylcholinesterase activity. *Biochem. Pharmacol. 7*, 88IN191–9095.
(158) Goldsmith, M., Ashani, Y., Simo, Y., Ben-David, M., Leader, H., Silman, I., Sussman, J. L., and Tawfik, D. S. (2012) Evolved Stereoselective Hydrolases for Broad-Spectrum G-Type Nerve Agent Detoxification. *Chem. Biol. 19*, 456–466.
(159) Geders, T. W., Gustafson, K., and Finzel, B. C. (2012) Use of differential scanning fluorimetry to optimize the purification and crystallization of PLP-dependent enzymes. *Acta Crystallograph. Sect. F Struct. Biol. Cryst. Commun. 68*, 596–600.
(160) Kaltenbach, M., Jackson, C. J., Campbell, E. C., Hollfelder, F., and Tokuriki, N. (2015) Reverse evolution leads to genotypic incompatibility despite functional and active site convergence. *eLife 4*, e06492.
(161) Briseno-Roa, L., Oliynyk, Z., Timperley, C. M., Griffiths, A. D., and Fersht, A. R. (2010) Highest paraoxonase turnover rate found in a bacterial phosphotriesterase variant. *Protein Eng. Des. Sel. 24*, 209–211.
(162) Briseno-Roa, L., Timperley, C. M., Griffiths, A. D., and Fersht, A. R. (2010) Phosphotriesterase variants with high methylphosphonatase activity and strong negative trade-off against phosphotriesters. *Protein Eng. Des. Sel. 24*, 151–159.
(163) Fields, P. A. (2001) Protein function at thermal extremes: balancing stability and flexibility. *Comp. Biochem. Physiol. A. Mol. Integr. Physiol. 129*, 417–431.
(164) Llop, S., Julvez, J., Fernandez-Somoano, A., Santa Marina, L., Vizcaino, E., Iñiguez, C., Lertxundi, N., Gascón, M., Rebagliato, M., and Ballester, F. (2013) Prenatal and postnatal insecticide use and infant neuropsychological development in a multicenter birth cohort study. *Environ. Int. 59*, 175–182.
(165) Jaipieam, S., Visuthismajarn, P., Sutheravut, P., Siriwong, W., Thoumsang, S., Borjan, M., and Robson, M. (2009) Organophosphate Pesticide Residues in Drinking Water from Artesian Wells and Health Risk Assessment of Agricultural Communities, Thailand. *Hum. Ecol. Risk Assess. Int. J. 15*, 1304–1316.
(166) Beauregard, G., Lum, J., and Roufogalis, B. D. (1981) Effect of histidine modification on the aging of organophosphate-inhibited acetylcholinesterase. *Biochem. Pharmacol. 30*, 2915–2920.
(167) Zwiener, R. J., and Ginsburg, C. M. (1988) Organophosphate and Carbamate Poisoning in Infants and Children. *Pediatrics 81*, 121–126.
(168) Lessenger, J. E., and Reese, B. E. (1999) Rational Use of Cholinesterase Activity Testing in Pesticide Poisoning. *J. Am. Board Fam. Pract. 12*, 307–314.
(169) De Silva, H. J., Samarawickrema, N. A., and Wickremasinghe, A. R. (2006) Toxicity due to organophosphorus compounds: what about chronic exposure? *Trans. R. Soc. Trop. Med. Hyg. 100*, 803–806.
(170) Ray, D. E., and Richards, P. G. (2001) The potential for toxic effects of chronic, low-dose exposure to organophosphates. *Toxicol. Lett. 120*, 343–351.
(171) Maxwell, D. M., Brecht, K. M., Koplovitz, I., and Sweeney, R. E. (2006) Acetylcholinesterase inhibition: does it explain the toxicity of organophosphorus compounds? *Arch. Toxicol. 80*, 756–760.
(172) Costa, L. G. (2006) Current issues in organophosphate toxicology. *Clin. Chim. Acta 366*, 1–13.
(173) Hiblot, J., Gotthard, G., Chabriere, E., and Elias, M. (2012) Characterisation of the organophosphate hydrolase catalytic activity of SsoPox. *Sci. Rep. 2*.

(174) Del Giudice, I., Coppolecchia, R., Merone, L., Porzio, E., Carusone, T. M., Mandrich, L., Worek, F., and Manco, G. (2016) An efficient thermostable organophosphate hydrolase and its application in pesticide decontamination. *Biotechnol. Bioeng. 113*, 724–734.
(175) Vitola, G., Mazzei, R., Fontananova, E., Porzio, E., Manco, G., Gaeta, S. N., and Giorno, L. (2016) Polymeric biocatalytic membranes with immobilized thermostable phosphotriesterase. *J. Membr. Sci. 516*, 144–151.
(176) Singh, B. K., and Walker, A. (2006) Microbial degradation of organophosphorus compounds. *FEMS Microbiol. Rev. 30*, 428–471.
(177) Conti, F., Abnave, P., and Ghigo, E. (2014) Unconventional animal models: a booster for new advances in host—pathogen interactions. *Front. Cell. Infect. Microbiol. 4*.
(178) Torre, C., and Ghigo, É. (2015) Planaria: an immortal worm to clarify human immune response. *Médecine Sci. MS 31*, 20–22.
(179) Hagstrom, D., Cochet-Escartin, O., Zhang, S., Khuu, C., and Collins, E.-M. S. (2015) Freshwater Planarians as an Alternative Animal Model for Neurotoxicology. *Toxicol. Sci. 147*, 270–285.
(180) Hagstrom, D., Cochet-Escartin, O., and Collins, E.-M. S. (2016) Planarian brain regeneration as a model system for developmental neurotoxicology. *Regeneration 3*, 65–77.
(181) Hagstrom, D., Hirokawa, H., Zhang, L., Radic, Z., Taylor, P., and Collins, E.-M. S. (2016) Planarian cholinesterase: in vitro characterization of an evolutionarily ancient enzyme to study organophosphorus pesticide toxicity and reactivation. *Arch. Toxicol.* 1–11.
(182) Rodríguez, H. H., Espinoza-Navarro, O., Silva, I., Needham, D., Castro, M. E., Sarabia, L., Inostroza, J., and Jimenez, L. (2010) The effect of paraoxon on spermatogenesis in Dugesia gonocephala from the Chilean Altiplano: proliferation and apoptosis. *Environ. Sci. Pollut. Res. 18*, 497–502.
(183) Villar, D., Li, M. H., and Schaeffer, D. J. (1993) Toxicity of organophosphorus pesticides to Dugesia dorotocephala. *Bull. Environ. Contam. Toxicol. 51*, 80–87.
(184) Villar, D., González, M., Gualda, M. J., and Schaeffer, D. J. (1994) Effects of organophosphorus insecticides on Dugesia tigrina: Cholinesterase activity and head regeneration. *Bull. Environ. Contam. Toxicol. 52*, 319–324.
(185) Pezzementi, L., Nachon, F., and Chatonnet, A. (2011) Evolution of Acetylcholinesterase and Butyrylcholinesterase in the Vertebrates: An Atypical Butyrylcholinesterase from the Medaka Oryzias latipes. *PLOS ONE 6*, e17396.
(186) Pezzementi, L., and Chatonnet, A. (2010) Evolution of cholinesterases in the animal kingdom. *Chem. Biol. Interact. 187*, 27–33.
(187) Sanders, M., Mathews, B., Sutherland, D., Soong, W., Giles, H., and Pezzementi, L. (1996) Biochemical and molecular characterization of acetylcholinesterase from the hagfish Myxine glutinosa. *Comp. Biochem. Physiol. B Biochem. Mol. Biol. 115*, 97–109.
(188) Chatonnet, A., and Lockridge, O. (1989) Comparison of butyrylcholinesterase and acetylcholinesterase. *Biochem. J. 260*, 625–634.
(189) Reddien, P. W., Newmark, P. A., and Sánchez Alvarado, A. (2008) Gene nomenclature guidelines for the planarian Schmidtea mediterranea. *Dev. Dyn. Off. Publ. Am. Assoc. Anat. 237*, 3099–3101.
(190) Grudniewska, M., Mouton, S., Simanov, D., Beltman, F., Grelling, M., Mulder, K. de, Arindrarto, W., Weissert, P. M., Elst, S. van der, and Berezikov, E. (2016) Transcriptional signatures of somatic neoblasts and germline cells in Macrostomum lignano. *eLife 5*, e20607.
(191) Jones, D. T., Taylor, W. R., and Thornton, J. M. (1992) The rapid generation of mutation data matrices from protein sequences. *Bioinformatics 8*, 275–282.
(192) Kumar, S., Stecher, G., and Tamura, K. (2016) MEGA7: Molecular Evolutionary Genetics Analysis Version 7.0 for Bigger Datasets. *Mol. Biol. Evol. 33*, 1870–1874.
(193) Ellman, G. L., Courtney, K. D., Andres, V., and Featherstone, R. M. (1961) A new and rapid colorimetric determination of acetylcholinesterase activity. *Biochem. Pharmacol. 7*, 88–95.
(194) Fukuto, T. R. (1990) Mechanism of action of organophosphorus and carbamate insecticides. *Environ. Health Perspect. 87*, 245–254.
(195) Mutch, E., Blain, P. G., and Williams, F. M. (1999) The role of metabolism in determining susceptibility to parathion toxicity in man. *Toxicol. Lett. 107*, 177–187.
(196) Jokanović, M. (2001) Biotransformation of organophosphorus compounds. *Toxicology 166*, 139–160.
(197) Nishimura, K., Kitamura, Y., Taniguchi, T., and Agata, K. (2010) Analysis of motor function modulated by cholinergic neurons in planarian Dugesia japonica. *Neuroscience 168*, 18–30.
(198) Ren, D., Sims, J. J., and Wood, T. K. (2001) Inhibition of biofilm formation and swarming of Escherichia coli by (5Z)-4-bromo-5-(bromomethylene)-3-butyl-2(5H)-furanone. *Environ. Microbiol. 3*, 731–736.
(199) Ueda, A., Attila, C., Whiteley, M., and Wood, T. K. (2009) Uracil influences quorum sensing and biofilm formation in Pseudomonas aeruginosa and fluorouracil is an antagonist. *Microb. Biotechnol. 2*, 62–74.

(200) Stover, C. K., Pham, X. Q., Erwin, A. L., Mizoguchi, S. D., Warrener, P., Hickey, M. J., Brinkman, F. S. L., Hufnagle, W. O., Kowalik, D. J., Lagrou, M., Garber, R. L., Goltry, L., Tolentino, E., Westbrock-Wadman, S., Yuan, Y., Brody, L. L., Coulter, S. N., Folger, K. R., Kas, A., Larbig, K., Lim, R., Smith, K., Spencer, D., Wong, G. K.-S., Wu, Z., Paulsen, I. T., Reizer, J., Saier, M. H., Hancock, R. E. W., Lory, S., and Olson, M. V. (2000) Complete genome sequence of Pseudomonas aeruginosa PAO1, an opportunistic pathogen. *Nature 406*, 959–964.
(201) Driscoll, J. A., Brody, S. L., and Kollef, D. M. H. (2012) The Epidemiology, Pathogenesis and Treatment of Pseudomonas aeruginosa Infections. *Drugs 67*, 351–368.
(202) Sievert, D. M., Ricks, P., Edwards, J. R., Schneider, A., Patel, J., Srinivasan, A., Kallen, A., Limbago, B., and Fridkin, S. (2013) Antimicrobial-Resistant Pathogens Associated with Healthcare-Associated Infections Summary of Data Reported to the National Healthcare Safety Network at the Centers for Disease Control and Prevention, 2009–2010. *Infect. Control Hosp. Epidemiol. 34*, 1–14.
(203) Hentzer, M. (2003) Attenuation of Pseudomonas aeruginosa virulence by quorum sensing inhibitors. *EMBO J. 22*, 3803–3815.
(204) Daniels, R., Vanderleyden, J., and Michiels, J. (2004) Quorum sensing and swarming migration in bacteria. *FEMS Microbiol. Rev. 28*, 261–289.
(205) Whiteley, M., Bangera, M. G., Bumgarner, R. E., Parsek, M. R., Teitzel, G. M., Lory, S., and Greenberg, E. P. (2001) Gene expression in Pseudomonas aeruginosa biofilms. *Nature 413*, 860–864.
(206) Gambello, M. J., and Iglewski, B. H. (1991) Cloning and characterization of the Pseudomonas aeruginosa lasR gene, a transcriptional activator of elastase expression. *J. Bacteriol. 173*, 3000–3009.
(207) Pearson, J. P., Gray, K. M., Passador, L., Tucker, K. D., Eberhard, A., Iglewski, B. H., and Greenberg, E. P. (1994) Structure of the autoinducer required for expression of Pseudomonas aeruginosa virulence genes. *Proc. Natl. Acad. Sci. 91*, 197–201.
(208) Diggle, S. P., Winzer, K., Chhabra, S. R., Worrall, K. E., Cámara, M., and Williams, P. (2003) The Pseudomonas aeruginosa quinolone signal molecule overcomes the cell density-dependency of the quorum sensing hierarchy, regulates rhl-dependent genes at the onset of stationary phase and can be produced in the absence of LasR: PQS regulation of rhl-dependent phenotypes. *Mol. Microbiol. 50*, 29–43.
(209) Lee, J., and Zhang, L. (2014) The hierarchy quorum sensing network in Pseudomonas aeruginosa. *Protein Cell 6*, 26–41.
(210) Brackman, G., and Coenye, T. (2015) Quorum Sensing Inhibitors as Anti-Biofilm Agents. *Curr. Pharm. Des. 21*, 5–11.
(211) Dong, Y.-H., Wang, L.-H., and Zhang, L.-H. (2007) Quorum-quenching microbial infections: mechanisms and implications. *Philos. Trans. R. Soc. Lond. B Biol. Sci. 362*, 1201–1211.
(212) Fetzner, S. (2015) Quorum quenching enzymes. *J. Biotechnol. 201*, 2–14.
(213) Kalia, V. C. (2013) Quorum sensing inhibitors: An overview. *Biotechnol. Adv. 31*, 224–245.
(214) Tang, K., and Zhang, X.-H. (2014) Quorum Quenching Agents: Resources for Antivirulence Therapy. *Mar. Drugs 12*, 3245–3282.
(215) Diggle, S. P., Matthijs, S., Wright, V. J., Fletcher, M. P., Chhabra, S. R., Lamont, I. L., Kong, X., Hider, R. C., Cornelis, P., Cámara, M., and Williams, P. (2007) The Pseudomonas aeruginosa 4-Quinolone Signal Molecules HHQ and PQS Play Multifunctional Roles in Quorum Sensing and Iron Entrapment. *Chem. Biol. 14*, 87–96.
(216) Welsh, M. A., and Blackwell, H. E. (2016) Chemical Genetics Reveals Environment-Specific Roles for Quorum Sensing Circuits in Pseudomonas aeruginosa. *Cell Chem. Biol. 23*, 361–369.
(217) Ciofu, O., Mandsberg, L. F., Bjarnsholt, T., Wassermann, T., and Hoiby, N. (2010) Genetic adaptation of Pseudomonas aeruginosa during chronic lung infection of patients with cystic fibrosis: strong and weak mutators with heterogeneous genetic backgrounds emerge in mucA and/or lasR mutants. *Microbiology 156*, 1108–1119.
(218) Hraiech, S., Hiblot, J., Lafleur, J., Lepidi, H., Papazian, L., Rolain, J.-M., Raoult, D., Elias, M., Silby, M. W., Bzdrenga, J., Bregeon, F., and Chabriere, E. (2014) Inhaled Lactonase Reduces Pseudomonas aeruginosa Quorum Sensing and Mortality in Rat Pneumonia. *PLoS ONE 9*, e107125.
(219) Seng, P., Drancourt, M., Gouriet, F., La Scola, B., Fournier, P., Rolain, J. M., and Raoult, D. (2009) Ongoing Revolution in Bacteriology: Routine Identification of Bacteria by Matrix-Assisted Laser Desorption Ionization Time-of-Flight Mass Spectrometry. *Clin. Infect. Dis. 49*, 543–551.
(220) Hiblot, J., Gotthard, G., Elias, M., and Chabriere, E. (2013) Differential Active Site Loop Conformations Mediate Promiscuous Activities in the Lactonase SsoPox. *PLoS ONE 8*, 1–14.
(221) Hiblot, J., Gotthard, G., Chabriere, E., and Elias, M. (2012) Characterisation of the organophosphate hydrolase catalytic activity of SsoPox. *Sci. Rep. 2*, 779.
(222) Chessa, J.-P., Petrescu, I., Bentahir, M., Van Beeumen, J., and Gerday, C. (2000) Purification, physico-chemical characterization and sequence of a heat labile alkaline metalloprotease isolated from a psychrophilic Pseudomonas species. *Biochim. Biophys. Acta BBA - Protein Struct. Mol. Enzymol. 1479*, 265–274.

(223) Price-Whelan, A., Dietrich, L. E. P., and Newman, D. K. (2007) Pyocyanin alters redox homeostasis and carbon flux through central metabolic pathways in Pseudomonas aeruginosa PA14. *J. Bacteriol. 189*, 6372–6381.
(224) García-Contreras, R., Martínez-Vázquez, M., Guadarrama, N. V., Pañeda, A. G. V., Hashimoto, T., Maeda, T., Quezada, H., and Wood, T. K. (2013) Resistance to the quorum-quenching compounds brominated furanone C-30 and 5-fluorouracil in Pseudomonas aeruginosa clinical isolates. *Pathog. Dis. 68*, 8–11.
(225) García-Contreras, R., Peréz-Eretza, B., Jasso-Chávez, R., Lira-Silva, E., Roldán-Sánchez, J. A., González-Valdez, A., Soberón-Chávez, G., Coria-Jiménez, R., Martínez-Vázquez, M., Alcaraz, L. D., Maeda, T., and Wood, T. K. (2015) High variability in quorum quenching and growth inhibition by furanone C-30 in Pseudomonas aeruginosa clinical isolates from cystic fibrosis patients. *Pathog. Dis. 73*, ftv040.
(226) Lavery, L. A., Armstrong, D. G., Wunderlich, R. P., Mohler, M. J., Wendel, C. S., and Lipsky, B. A. (2006) Risk factors for foot infections in individuals with diabetes. *Diabetes Care 29*, 1288–1293.
(227) Richard, J.-L., Sotto, A., and Lavigne, J.-P. (2011) New insights in diabetic foot infection. *World J. Diabetes 2*, 24–32.
(228) Rastogi, A., Sukumar, S., Hajela, A., Mukherjee, S., Dutta, P., Bhadada, S. K., and Bhansali, A. (2016) The microbiology of diabetic foot infections in patients recently treated with antibiotic therapy: A prospective study from India. *J. Diabetes Complications*.
(229) Hancock, R. E. W., and Speert, D. P. (2000) Antibiotic resistance in Pseudomonas aeruginosa: mechanisms and impact on treatment. *Drug Resist. Updat. 3*, 247–255.
(230) Lauretti, L., Riccio, M. L., Mazzariol, A., Cornaglia, G., Amicosante, G., Fontana, R., and Rossolini, G. M. (1999) Cloning and Characterization of bla VIM, a New Integron-Borne Metallo-β-Lactamase Gene from a Pseudomonas aeruginosa Clinical Isolate. *Antimicrob. Agents Chemother. 43*, 1584–1590.
(231) Poole, K., Krebes, K., McNally, C., and Neshat, S. (1993) Multiple antibiotic resistance in Pseudomonas aeruginosa: evidence for involvement of an efflux operon. *J. Bacteriol. 175*, 7363–7372.
(232) Carmeli Y, Troillet N, Karchmer AW, and Samore MH. (1999) Health and economic outcomes of antibiotic resistance in pseudomonas aeruginosa. *Arch. Intern. Med. 159*, 1127–1132.
(233) Grosso-Becerra, M.-V., Santos-Medellín, C., González-Valdez, A., Méndez, J.-L., Delgado, G., Morales-Espinosa, R., Servín-González, L., Alcaraz, L.-D., and Soberón-Chávez, G. (2014) Pseudomonas aeruginosa clinical and environmental isolates constitute a single population with high phenotypic diversity. *BMC Genomics 15*, 318.
(234) Sethupathy, S., Prasath, K. G., Ananthi, S., Mahalingam, S., Balan, S. Y., and Pandian, S. K. (2016) Proteomic analysis reveals modulation of iron homeostasis and oxidative stress response in Pseudomonas aeruginosa PAO1 by curcumin inhibiting quorum sensing regulated virulence factors and biofilm production. *J. Proteomics 145*, 112–126.
(235) Maeda, T., García-Contreras, R., Pu, M., Sheng, L., Garcia, L. R., Tomás, M., and Wood, T. K. (2012) Quorum quenching quandary: resistance to antivirulence compounds. *ISME J. 6*, 493–501.
(236) García-Contreras, R. (2016) Is Quorum Sensing Interference a Viable Alternative to Treat Pseudomonas aeruginosa Infections? *Front. Microbiol. 7*.
(237) Sunder, A. V., Utari, P. D., Ramasamy, S., van Merkerk, R., Quax, W., and Pundle, A. (2016) Penicillin V acylases from gram-negative bacteria degrade N-acylhomoserine lactones and attenuate virulence in Pseudomonas aeruginosa. *Appl. Microbiol. Biotechnol.* 1–13.
(238) Grover, N., Plaks, J. G., Summers, S. R., Chado, G. R., Schurr, M. J., and Kaar, J. L. (2016) Acylase-containing polyurethane coatings with anti-biofilm activity. *Biotechnol. Bioeng. 113*, 2535–2543.
(239) Ivanova, K., Fernandes, M. M., Francesko, A., Mendoza, E., Guezguez, J., Burnet, M., and Tzanov, T. (2015) Quorum-Quenching and Matrix-Degrading Enzymes in Multilayer Coatings Synergistically Prevent Bacterial Biofilm Formation on Urinary Catheters. *ACS Appl. Mater. Interfaces*.
(240) Tang, K., Su, Y., Brackman, G., Cui, F., Zhang, Y., Shi, X., Coenye, T., and Zhang, X.-H. (2015) MomL, a Novel Marine-Derived N-Acyl Homoserine Lactonase from Muricauda olearia. *Appl. Environ. Microbiol. 81*, 774–782.
(241) Chen, R. (2001) Enzyme engineering: rational redesign versus directed evolution. *Trends Biotechnol. 19*, 13–14.
(242) Goldsmith, M., and Tawfik, D. S. (2013) Enzyme engineering by targeted libraries. *Methods Enzymol. 523*, 257–283.
(243) Davids, T., Schmidt, M., Böttcher, D., and Bornscheuer, U. T. (2013) Strategies for the discovery and engineering of enzymes for biocatalysis. *Curr. Opin. Chem. Biol. 17*, 215–220.
(244) Aboobaker, A. A. (2011) Planarian stem cells: a simple paradigm for regeneration. *Trends Cell Biol. 21*, 304–311.
(245) Goldsmith, M., Aggarwal, N., Ashani, Y., Jubran, H., Greisen, P. J., Ovchinnikov, S., Leader, H., Baker, D., Sussman, J. L., Goldenzweig, A., Fleishman, S. J., and Tawfik, D. S. (2017) Overcoming an optimization plateau in the directed evolution of highly efficient nerve agent bioscavengers. *Protein Eng. Des. Sel. 30*, 333–345.

(246) Tokuriki, N., Jackson, C. J., Afriat-Jurnou, L., Wyganowski, K. T., Tang, R., and Tawfik, D. S. (2012) Diminishing returns and tradeoffs constrain the laboratory optimization of an enzyme. *Nat. Commun. 3*, 1257.
(247) Tsai, P.-C., Fox, N., Bigley, A. N., Harvey, S. P., Barondeau, D. P., and Raushel, F. M. (2012) Enzymes for the Homeland Defense: Optimizing Phosphotriesterase for the Hydrolysis of Organophosphate Nerve Agents. *Biochemistry (Mosc.) 51*, 6463–6475.
(248) Eijsink, V. G. H., Gåseidnes, S., Borchert, T. V., and van den Burg, B. (2005) Directed evolution of enzyme stability. *Biomol. Eng. 22*, 21–30.
(249) Tokuriki, N., and Tawfik, D. S. (2009) Stability effects of mutations and protein evolvability. *Curr. Opin. Struct. Biol. 19*, 596–604.
(250) Akanuma, S., Nakajima, Y., Yokobori, S. -i., Kimura, M., Nemoto, N., Mase, T., Miyazono, K. -i., Tanokura, M., and Yamagishi, A. (2013) Experimental evidence for the thermophilicity of ancestral life. *Proc. Natl. Acad. Sci. 110*, 11067–11072.
(251) Merkl, R., and Sterner, R. (2016) Ancestral protein reconstruction: techniques and applications. *Biol. Chem. 397*, 1–21.
(252) Risso, V. A., Gavira, J. A., Mejia-Carmona, D. F., Gaucher, E. A., and Sanchez-Ruiz, J. M. (2013) Hyperstability and Substrate Promiscuity in Laboratory Resurrections of Precambrian β-Lactamases. *J. Am. Chem. Soc. 135*, 2899–2902.
(253) Gonzalez, D., Hiblot, J., Darbinian, N., Miller, J. C., Gotthard, G., Amini, S., Chabriere, E., and Elias, M. (2014) Ancestral mutations as a tool for solubilizing proteins: The case of a hydrophobic phosphate-binding protein. *FEBS Open Bio 4*, 121–127.
(254) Alcalde, M. (2017) When directed evolution met ancestral enzyme resurrection. *Microb. Biotechnol. 10*, 22–24.
(255) Fischer, S., Arad, A., and Margalit, R. (2005) Lipsome-formulated enzymes for organophosphate scavenging: Butyrylcholinesterase and Demeton-S. *Arch. Biochem. Biophys. 434*, 108–115.
(256) Veronese, F. M., and Pasut, G. (2005) PEGylation, successful approach to drug delivery. *Drug Discov. Today 10*, 1451–1458.
(257) Johansson, M. U., Zoete, V., Michielin, O., and Guex, N. (2012) Defining and searching for structural motifs using DeepView/Swiss-PdbViewer. *BMC Bioinformatics 13*, 173.

Résumé

Les organophosphorés (OPs) sont des composés neurotoxiques qui sont largement et mondialement utilisés comme pesticides. L'utilisation intensive des OPs a conduit à une importante pollution des sols et des effluents agricoles et sont retrouvés jusque dans les aliments. Ces pesticides entrainent chaque année de nombreuses intoxications et sont responsables de 300 000 morts à travers le monde. Les OPs ont également été développés comme agents neurotoxiques de guerre tels que le sarin, tabun ou VX. Actuellement, il n'existe pas de méthode de décontamination externe ou de bioremédiation satisfaisante pour limiter l'impact des OPs, c'est pourquoi l'utilisation d'enzymes est une stratégie attractive. Parmi les enzymes capables de dégrader les OPs, les phosphotriestérases mésophiles (PTEs) sont les plus actives avec des efficacités catalytiques proches de la limite théorique de diffusion. Cependant, ces enzymes sont peu stables ce qui limite leurs applications. Les enzymes hyperthermostables issues d'environnements extrêmes ont donc été considérées. Ainsi l'enzyme *Sso*Pox, isolée de l'archée *Sulfolobus solfataricus* ayant une activité lactonase et une activité de promiscuité phosphotriestérase, a été plus particulièrement étudiée. Contrairement aux PTEs, *Sso*Pox est extrêmement robuste (T_m=106°C) mais son activité phosphotriestérase est en revanche beaucoup plus faible. Une stratégie d'ingénierie protéique a été réalisée afin d'obtenir un compromis entre l'activité de l'enzyme mésophile et la stabilité de *Sso*Pox. En utilisant les similarités structurales entre ces deux enzymes, une base de données mutationnelle détaillant l'ensemble des substitutions bénéfiques potentielles a été réalisée dans l'objectif de transférer le site actif hautement performant d'une PTE bactérienne dans l'architecture hyperstable de *Sso*Pox. Cette stratégie a permis d'obtenir des variants de *Sso*Pox améliorés jusqu'à 2 000 fois par rapport à l'enzyme sauvage. Ces variants ont de plus des spectres d'action élargis tout en maintenant une importante stabilité, et des taux de dégradation extrêmement rapides pour la plupart des OPs. L'efficacité de ces variants a été démontrée *in vivo* chez un modèle animal original, la planaire, un ver plat de l'embranchement des Plathelminthes permettant d'améliorer la survie ainsi que la mobilité et la capacité de régénération. En complément de ce travail sur les organophosphorés, l'efficacité d'un variant de *Sso*Pox à l'activité lactonase améliorée, capable de bloquer la communication de certaines bactéries, a été évalué sur un souchier clinique de *Pseudomonas aeruginosa*.

Abstract

Organophosphates (OPs) are neurotoxic compounds widely used as pesticides around the world. Over the years, utilization of OP led to a considerable environmental contamination of soils and agricultural wastewaters, this pollution is furthermore a major health issue as these insecticides can be found in food. OP are highly toxic and are responsible for 300,000 deaths in the world every year. OPs were also developed as chemical warfare nerve agents such as sarin, tabun or VX. Currently, no satisfying method for external decontamination is available, therefore bioremediation with enzymes is highly appealing. Among OP degrading enzymes, mesophilic phosphotriesterases (PTEs) are the most active biocatalysts with catalytic efficiencies close to the theoretical diffusion limit. However these enzymes are poorly stable what hinders their potential for bioremediation. Hyperthermostable enzymes from extreme environments were thus considered to circumvent this limitation. In particular, *Sso*Pox isolated from the archaeon *Sulfolobus solfataricus*, displaying a lactonase activity and a promiscuous phosphotriesterase activity was deeply investigated. Conversely to PTEs, *Sso*Pox is extremely robust (T_m=106°C) but its activity for OP degradation is from far lower. A protein engineering strategy was started in order to reach a compromise between mesophilic enzyme activity and *Sso*Pox robustness. Using structural similarities between PTEs and *Sso*Pox, a mutational database listing potential beneficial substitutions was designed in order to transfer the highly performant active site of PTE into the hyperstable scaffold of *Sso*Pox. This strategy led to variants displaying up to 2,000-fold increase against OPs as compared to wild-type enzyme. These variants were further showed to have a broader spectrum of action while maintaining a tremendous stability, and a degradation rate below a minute for most OP. The variants efficiency was demonstrated *in vivo* using an original animal model planarian, a flat worm belonging to Platyhelminthes branch and allowed to enhance survival rate as well as mobility and regeneration capacity. In addition to the work on OPs, the efficiency of *Sso*Pox lactonase-enhanced variant able to inhibit the communication of some bacteria was evaluated on clinical strains of *Pseudomonas aeruginosa*.